

55th IEEE Semiconductor Interface Specialists Conference (SISC)  
Tutorial, Dec 11, 2024  
Catamaran Resort Hotel and Spa, San Diego, CA, USA

# Hafnia-Based Ferroelectric FETs and Capacitors for Low-Power Memory and AI Applications: Physical Understanding of Device Operation and Reliability

Shinichi Takagi

The University of Tokyo, Tokyo, Japan





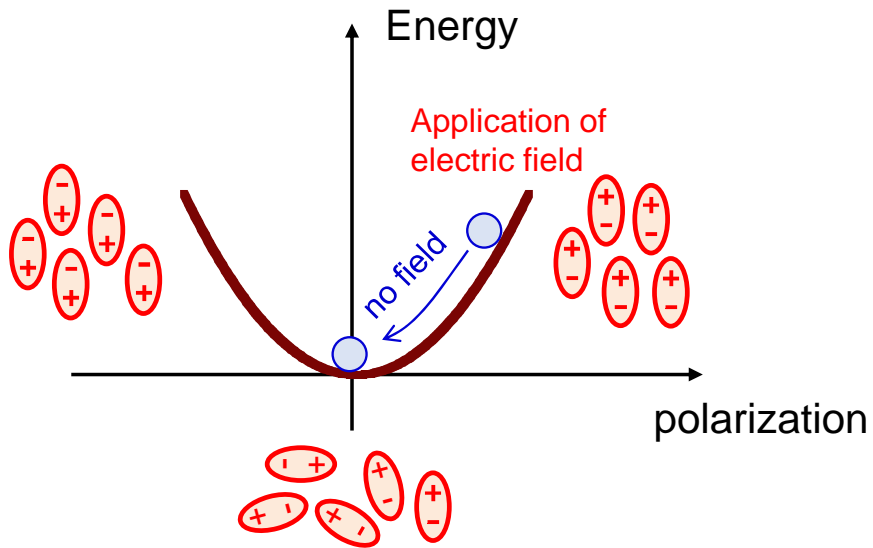
# Outline

- Expectation of HfO<sub>2</sub>-based ferroelectric materials and devices
- FeRAM ~ MFM capacitors
  - FeRAM operation
  - Reliability of MFM capacitor
- FeFET memory
  - FeFET memory operation
  - Understanding of coupling between polarization and carrier traps in FeFET
  - Issues related FeFET memory operation
  - FeFET reliability
- AI applications
  - Expectation of FeFETs for AI applications
  - Physical reservoir computing using FeFETs

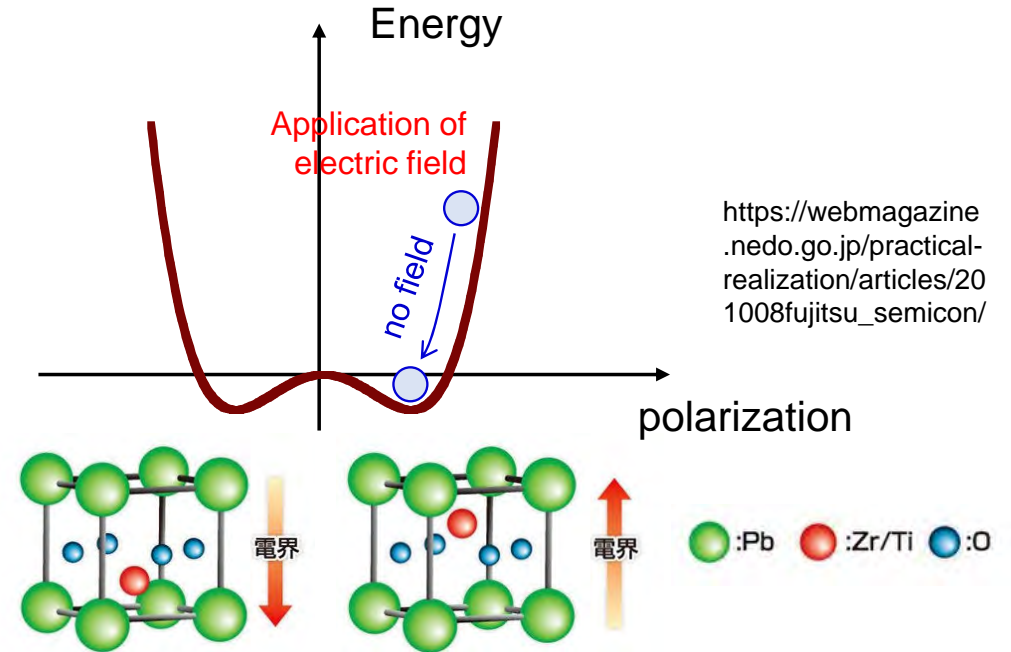
# Expectation of HfO<sub>2</sub>-based ferroelectric materials and devices

# Ferroelectrics

## Paraelectric



## Ferroelectric



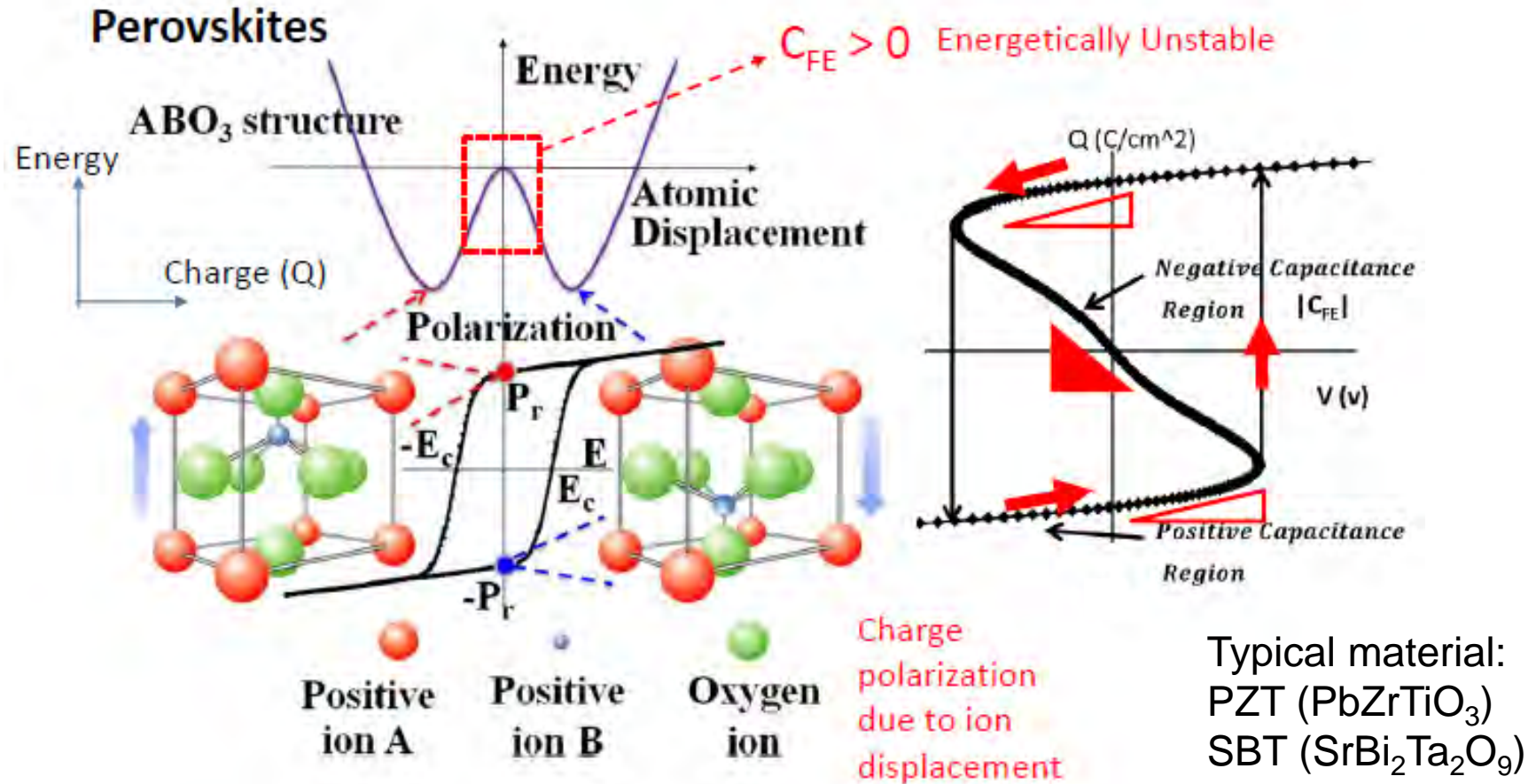
[https://webmagazine.nedo.go.jp/practical-realization/articles/201008fujitsu\\_semicon/](https://webmagazine.nedo.go.jp/practical-realization/articles/201008fujitsu_semicon/)

Ferroelectric = material whose polarization is stable in the absence of an electric field (spontaneous polarization) and whose polarization can be controlled by an external electric field



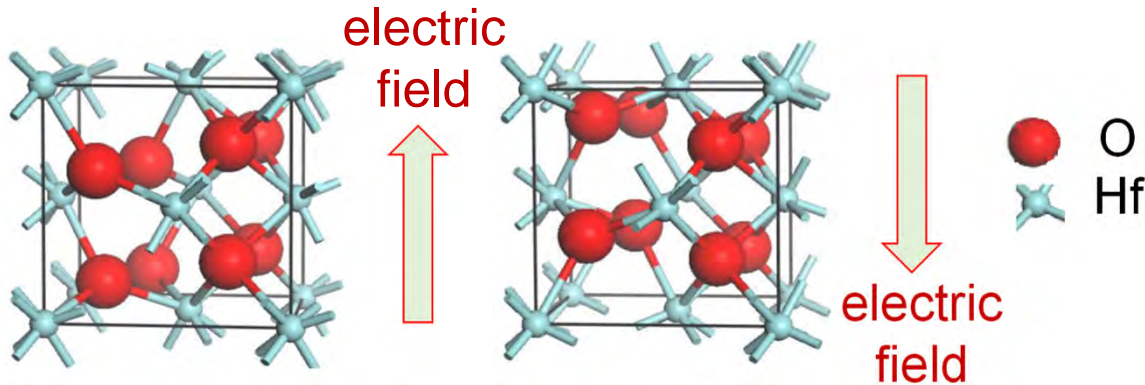
# Electrical characteristics of ferroelectric films

A. Thean, Option beyond FinFETs at 45 nm node, IEDM short course (2016)



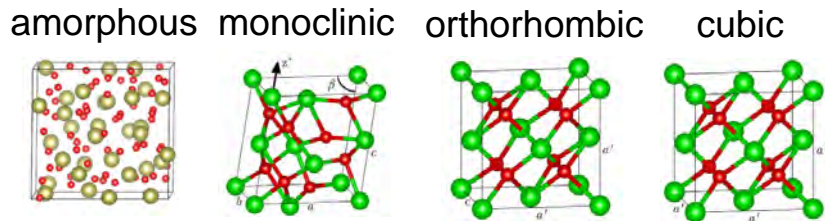
- The stability point of ions is determined by the direction of the electric field
- A change in the position of this stability point of ions causes a large polarization reversal

# HfO<sub>2</sub>-based ferroelectric film



T. S. Börscke *et al.* (NaMLab), *Appl. Phys. Lett.* **99**, 102903 (2011)

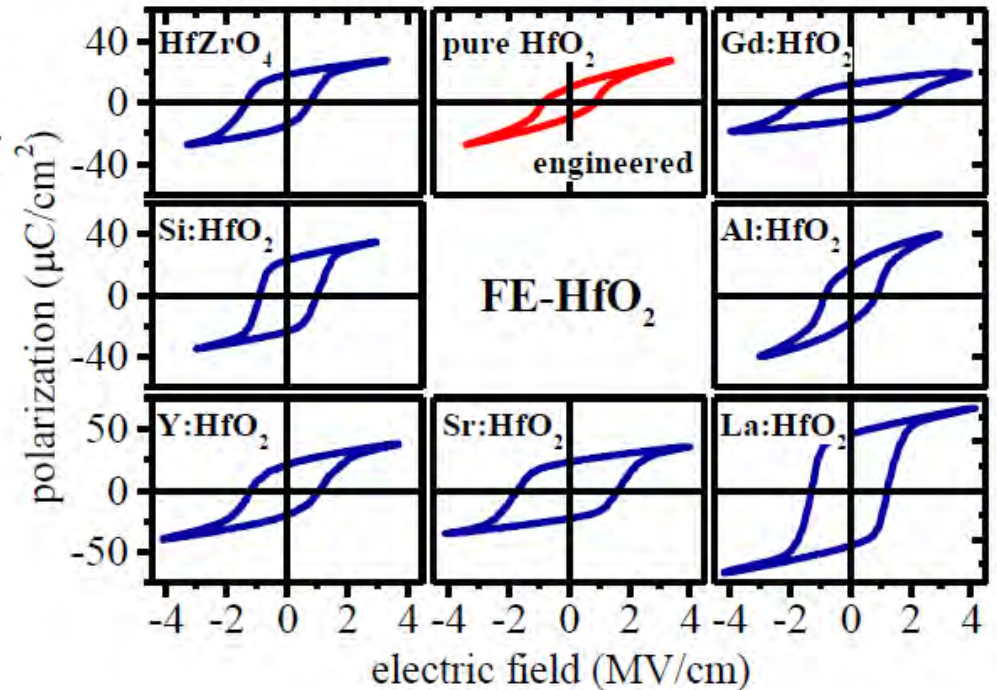
- Discovered in 2011
- Movement of oxygen atoms is the origin of spontaneous polarization



R. Materlik *et al.*, *J. Appl. Phys.* **117**, 134109 (2015)

L. Zhao *et al.*, *Appl. Phys. Lett.* **107**, 013504 (2015)

- Various crystal phases can exist
- Ferroelectricity originates in orthorhombic phase with an asymmetric crystal structure

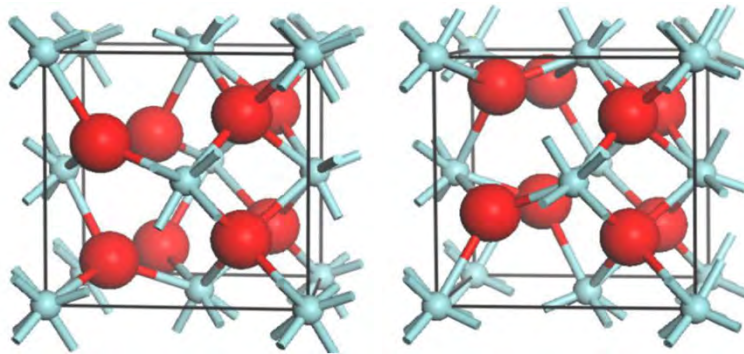


J. Müller *et al.*, *IEDM* (2013); *IEDM Tutorial* (2019)

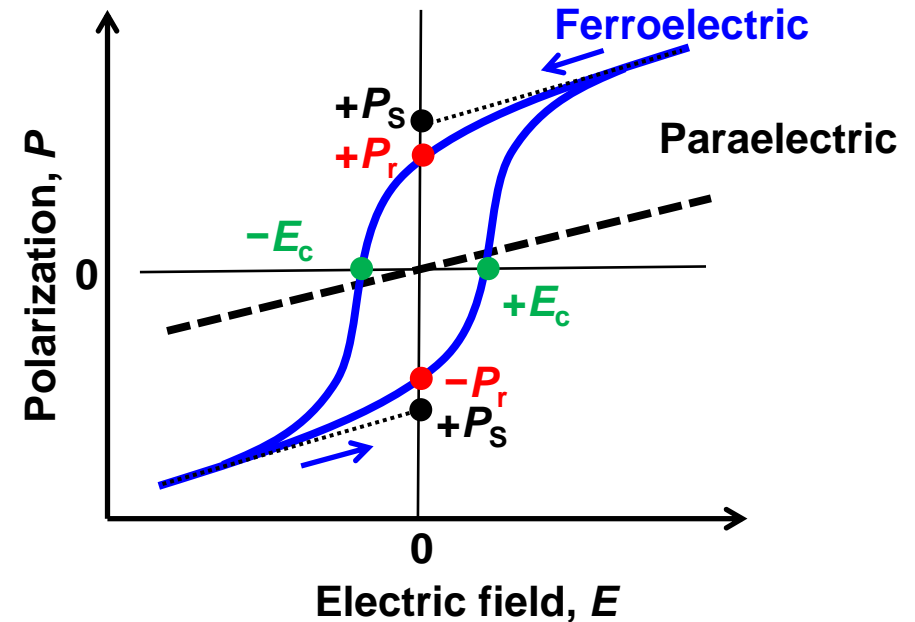
- Ferroelectric crystal phase (orthorhombic-phase) can be stabilized by doping various impurities
- Zr-doped HfO<sub>2</sub> (HZO) exhibits ferroelectricity in a wide range of Zr content

# Comparison of ferroelectric characteristics

Orthorhombic phase



Discovery of doped HfO<sub>2</sub>-based ferroelectric films in 2011 by NamLab group (T.S. Böscke *et al.* *APL* **99** (2011))



	Pb(Zr, Ti) <sub>3</sub>	SrBi <sub>2</sub> Ta <sub>2</sub> O <sub>9</sub>	HfO <sub>2</sub> -based
Film thickness (nm)	50-340	50-130	4-100
Dielectric constant	200	150	30
2Pr (μC/cm <sup>2</sup> )	10-40	10-40	10-40
Ec (kV/cm)	31	90	1000

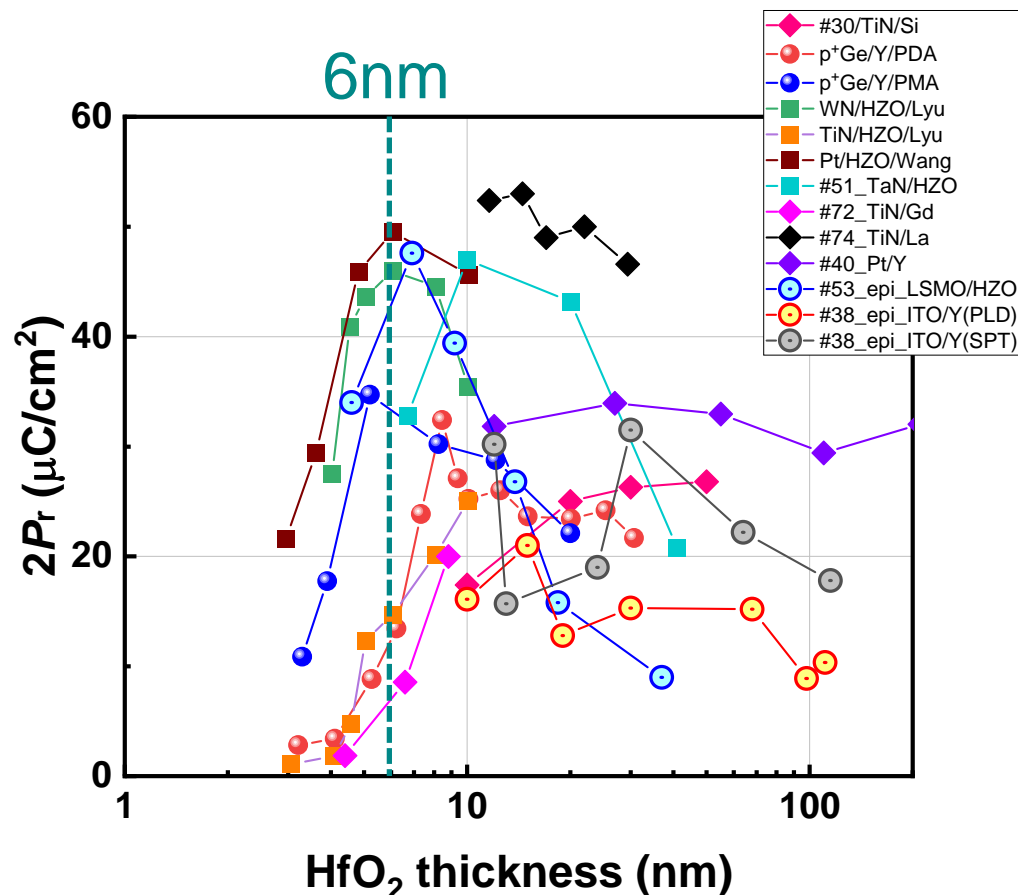
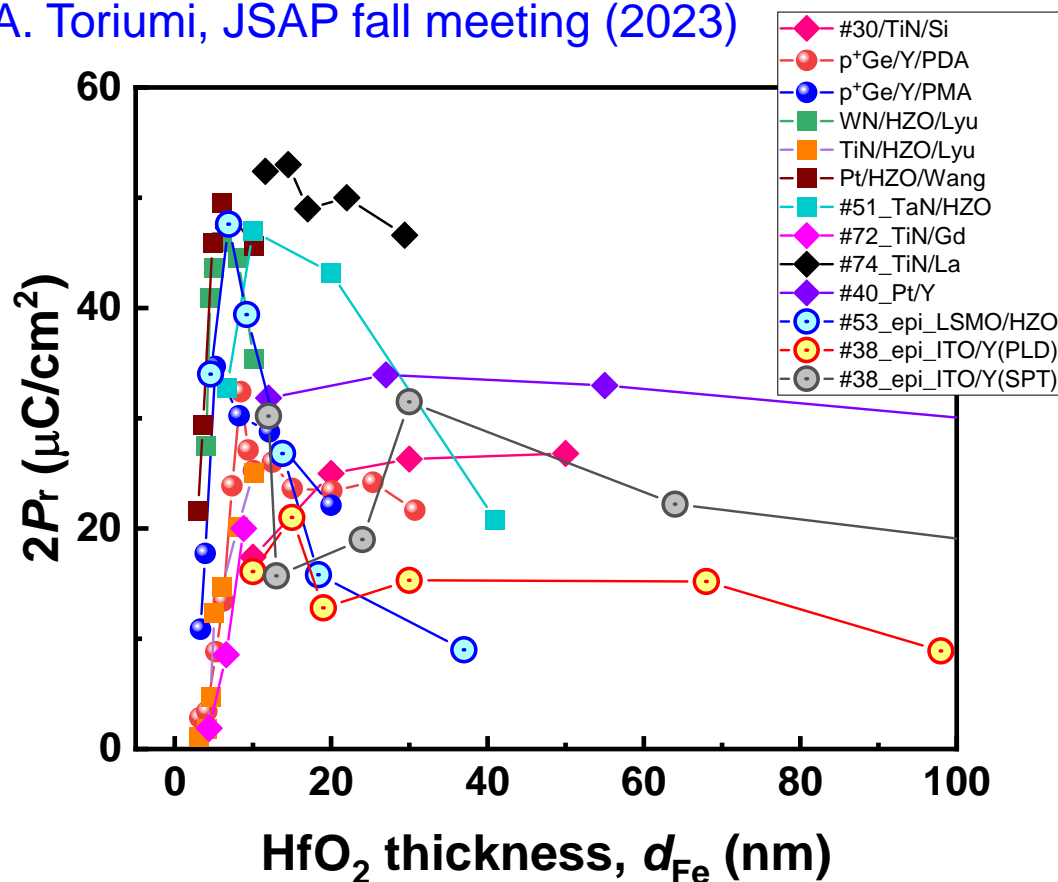
HfO<sub>2</sub>-based materials:

- Higher  $E_c$  → (pros) better retention (cons) high operation voltage, worse reliability
- lower permittivity → (pros) higher ferroelectric field in MFIS



# Impact of film thickness on HfO<sub>2</sub>-based ferroelectric characteristics

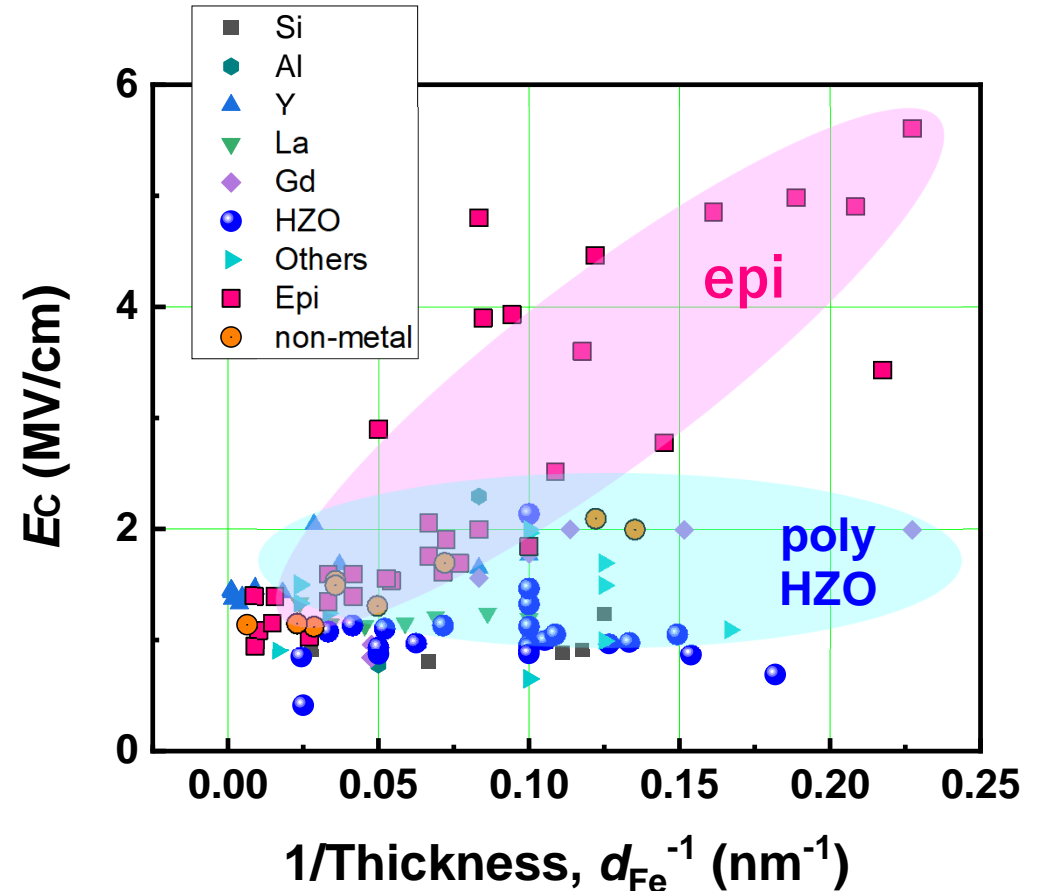
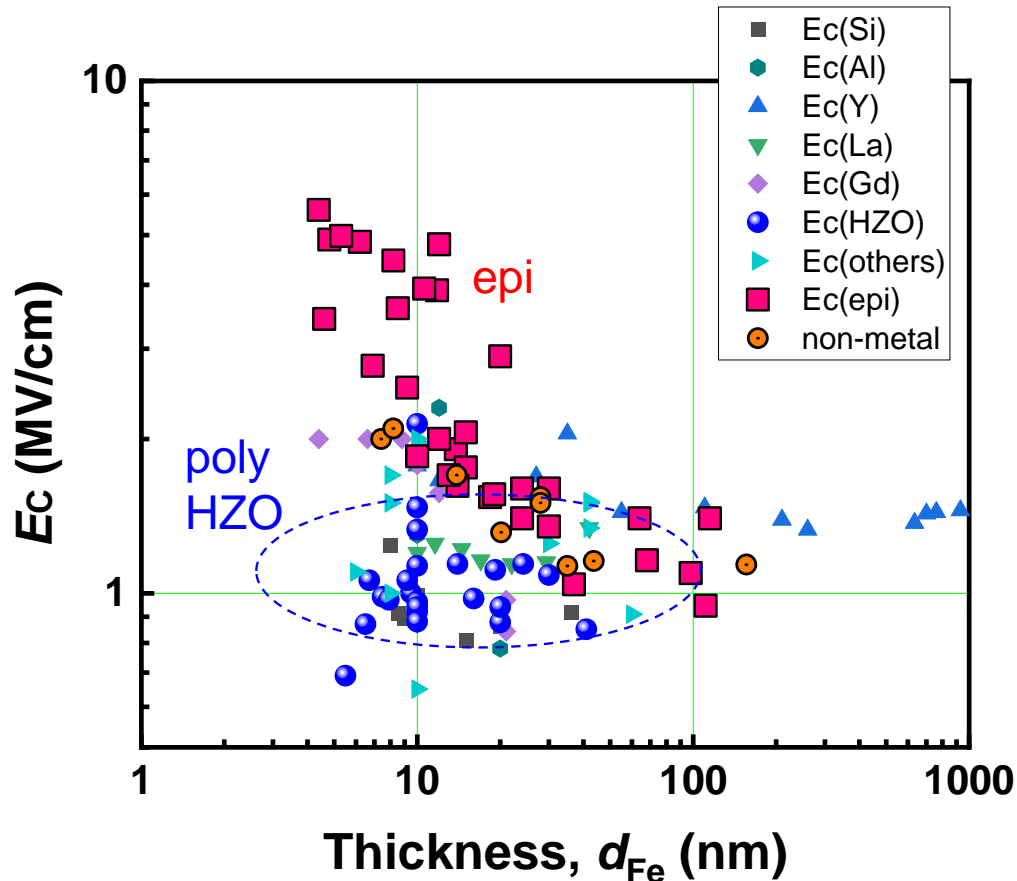
A. Toriumi, JSAP fall meeting (2023)



- Sufficiently high  $2P_r$  can be obtained in thickness less than 10 nm
- $2P_r$  increases with thinner films, has a peak around 6 nm and rapidly decreases down to 3 nm

# Impact of film thickness on HfO<sub>2</sub>-based ferroelectric characteristics

A. Toriumi, JSAP spring meeting (2024)

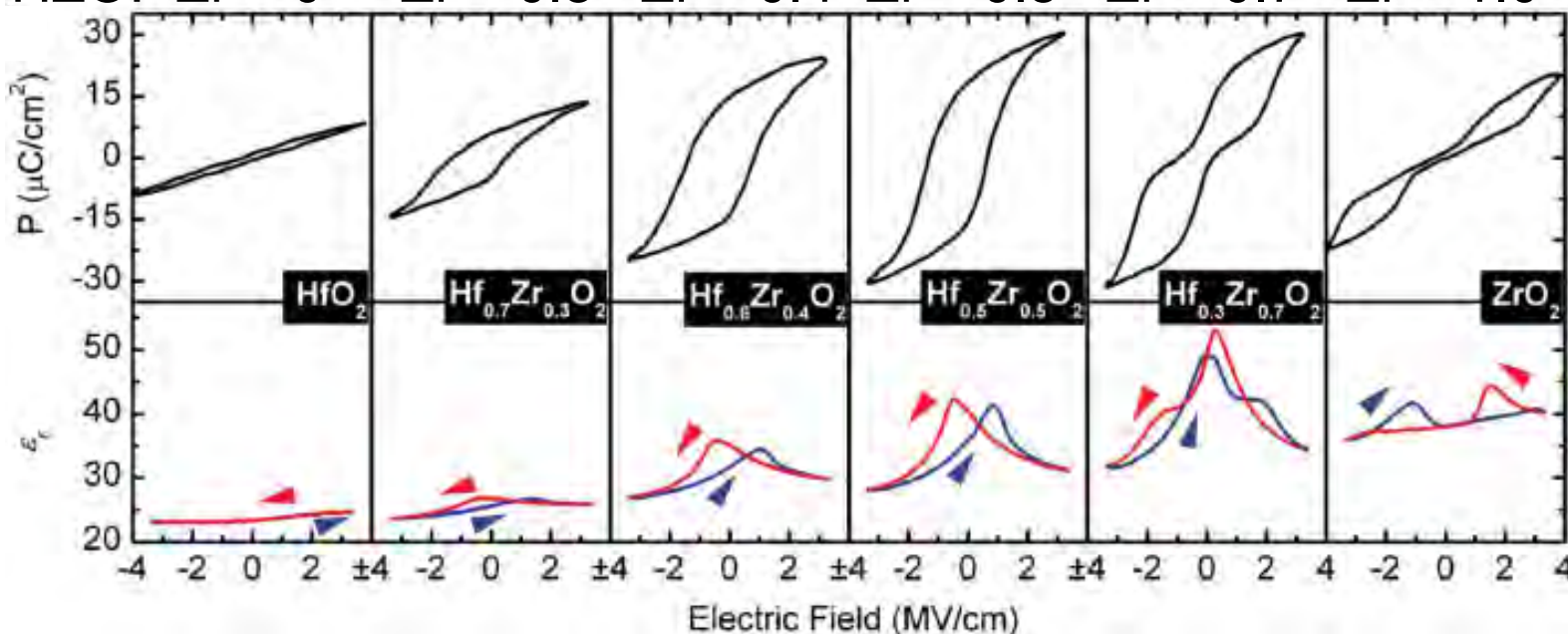


- $E_c$  of poly HZO films (1-2 MV/cm) is almost constant, irrespective of thickness
- $E_c$  of epi HZO films seem to be inversely proportional to thickness

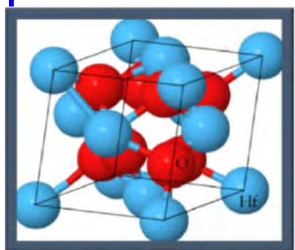
# Control of ferroelectric/anti-ferroelectric properties by Zr content

Müller et al., Nano Lett., 12 (2012) 4318

HZO: Zr = 0    Zr = 0.3    Zr = 0.4    Zr = 0.5    Zr = 0.7    Zr = 1.0



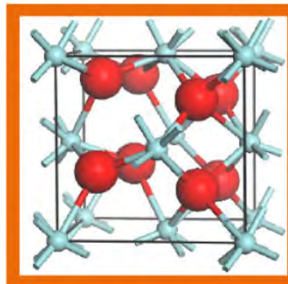
paraelectric



monoclinic

( $P2_1/c$ )  $\epsilon_r \sim 20$

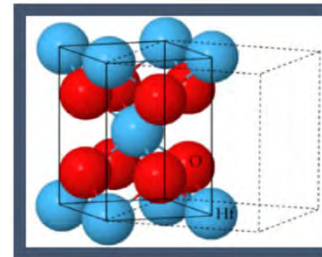
ferroelectric



orthorhombic

( $Pbc2_1$ )  $\epsilon_r \sim 25$

anti-ferroelectric



tetragonal

( $P4_2/nmc$ )  $\epsilon_r \sim 35$

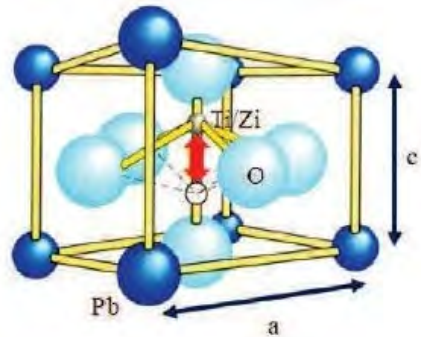
- Ferroelectric/ anti-ferroelectric properties are well controlled by Zr content of  $Hf_{1-x}Zr_xO_2$  (HZO) films
- low and mid Zr contents lead to ferroelectricity due to orthorhombic phase and high Zr contents lead to anti-ferroelectricity due to tetragonal phase



# Comparison between HfO<sub>2</sub>-based and Perovskite ferroelectric films

## Perovskite ferroelectrics

PZT, BTO, SBT, ...



Mass production over 20 years

10~40  $\mu\text{C}/\text{cm}^2$

50~200 nm

Noble metal (difficult to process)

Possible, but not easy

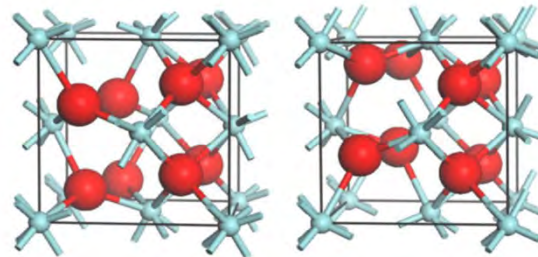
Pb (special fabrication line needed)

Passivation layer needed for protection

## HfO<sub>2</sub>-based ferroelectrics



### Orthorhombic phase



Technology

Polarization (Pr)

Film thickness

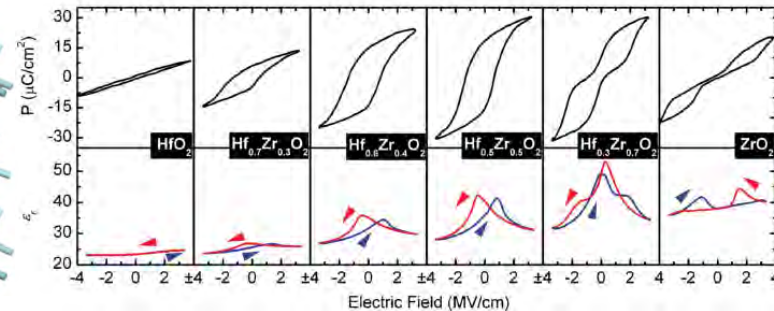
Electrode

3D trench structure

Element

hydrogen tolerance

### HfZrO<sub>2</sub>



First report in 2011, under development

10~40  $\mu\text{C}/\text{cm}^2$

10 nm or less → high scalability

e.g. TiN (easy to process)

Applicable (formed by ALD)

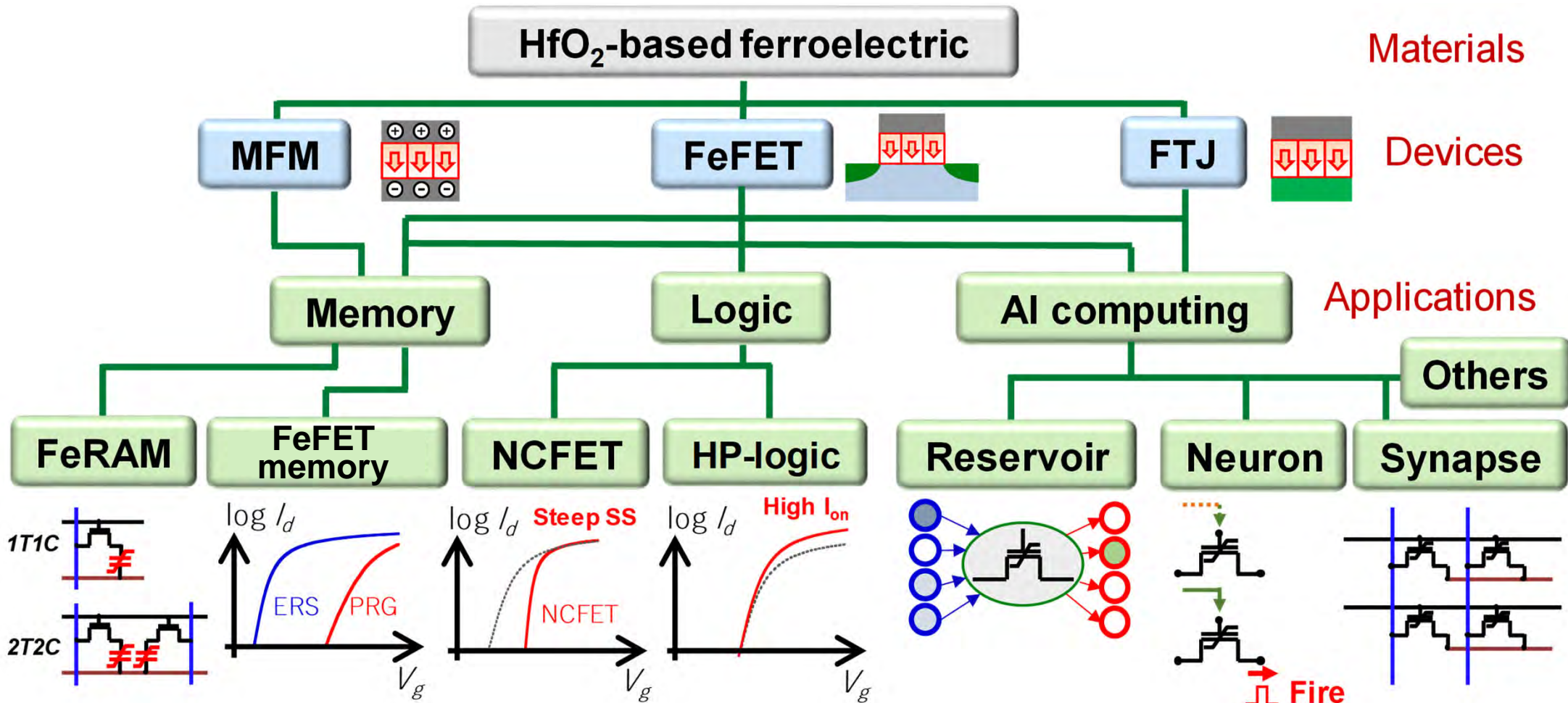
Hf, Zr, Si

Highly resistant

easy fabrication

Easy implementation into Si platform

# A variety of device applications using HfO<sub>2</sub>-based ferroelectrics



- Promising for a variety of applications such as NVDRAM, SRAM, NAND flash etc.

- Polarization-induced higher k expected for logic applications

- Analog memory functions suitable for a variety of AI calculations like multiply-accumulate operation



# Benchmark of ferroelectric memory

	Mainstream Charged based Memories				Emerging Non-volatile Memories					
	SRAM	DRAM	FLASH		PCM	RRAM	STT-MRAM	SOT-MRAM	FeRAM	FeFET
			NOR	NAND						
Cell area	>150F <sup>2</sup>	6F <sup>2</sup>	10F <sup>2</sup>	<4F <sup>2</sup> (3D)	4~50F <sup>2</sup>	4~50F <sup>2</sup>	6~50F <sup>2</sup>	12~100F <sup>2</sup>	6~50F <sup>2</sup>	6~50F <sup>2</sup>
Multi-bit	1	1	2	3-4	2-3	2-3	1	1	1	2-3
Voltage	<1V	<1V	>10V	>10V	<3V	<3V	<1V	<1V	<2V	<3V
Read time	~1ns	~10ns	~50ns	~10μs	<10ns	<10ns	<10ns	~1ns	<100ns	<50ns
Write time	~1ns	~10ns	10μs-1ms	100μs-1ms	~50ns	<100ns	<20ns	<3ns	<100ns	<100ns
Retention	N/A	~64ms	>10y	>10y	>10y	>10y	>1y	>1y	>10y	>1y
Endurance	>1E16	>1E16	~1E5	1E3~1E4	1E6~1E9	1E3~1E9	1E6~1E14	~1E12	1E9~1E12	1E6~1E9
Write Energy (J/bit)	~fJ	~10fJ	100pJ	~10fJ	~10pJ	~pJ	~pJ	~pJ	~100fJ	~fJ

(HfO<sub>2</sub>-based FE is also promising for SN in advanced NAND flash) S. Yu, IEDM short course 2 (2022)

Parameter/NVM	MRAM	FeRAM	FeFET	PCM	RRAM	NAND flash	NOR flash	DRAM
R/W speed	<10 ns	10 ns	100 ns	>100 ns	<10 ns	100 μs	1 μs to 1 s	~10 ns
Endurance	1 × 10 <sup>15</sup>	1 × 10 <sup>15</sup>	1 × 10 <sup>5</sup>	>1 × 10 <sup>8</sup>	1 × 10 <sup>9</sup>	1 × 10 <sup>4</sup>	1 × 10 <sup>6</sup>	1 × 10 <sup>16</sup>
Retention	10 years	10 years	10 years	10 years	10 years	10 years	10 years	64 ms
Energy	2 pJ bit <sup>-1</sup>	50 fJ bit <sup>-1</sup>	<1 fJ bit <sup>-1</sup>	3 pJ bit <sup>-1</sup>	50 pJ bit <sup>-1</sup>	1 nJ bit <sup>-1</sup>	10 nJ bit <sup>-1</sup>	pJ bit <sup>-1</sup>
Cell size	20F <sup>2</sup>	6F <sup>2</sup>	6-10F <sup>2</sup>	5.5F <sup>2</sup>	4F <sup>2</sup>	4F <sup>2</sup>	10F <sup>2</sup>	6F <sup>2</sup>

T. Schenk et al., *Rep. Prog. Phys.* **83**, 086501 (2020)

- Low energy consumption is an advantage for ferroelectric memory because of writing by voltage<sub>13</sub>

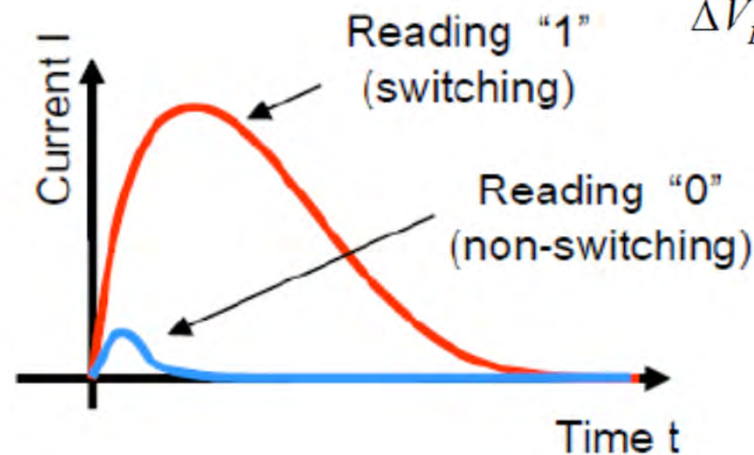
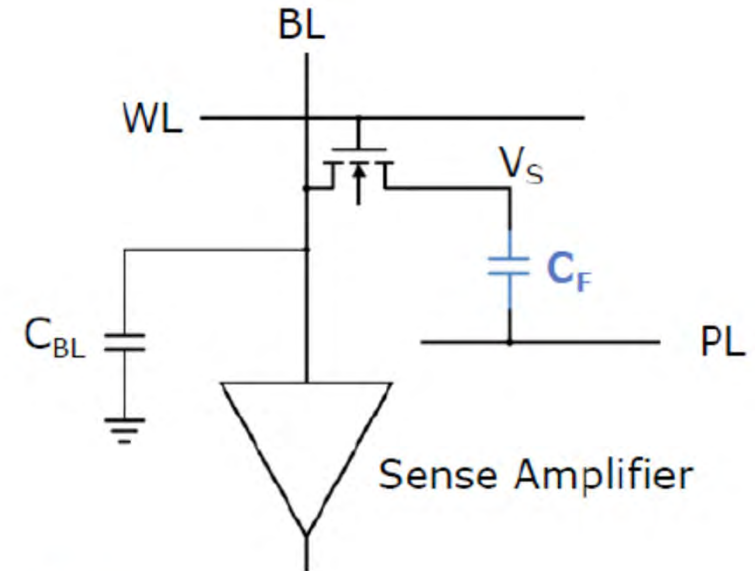
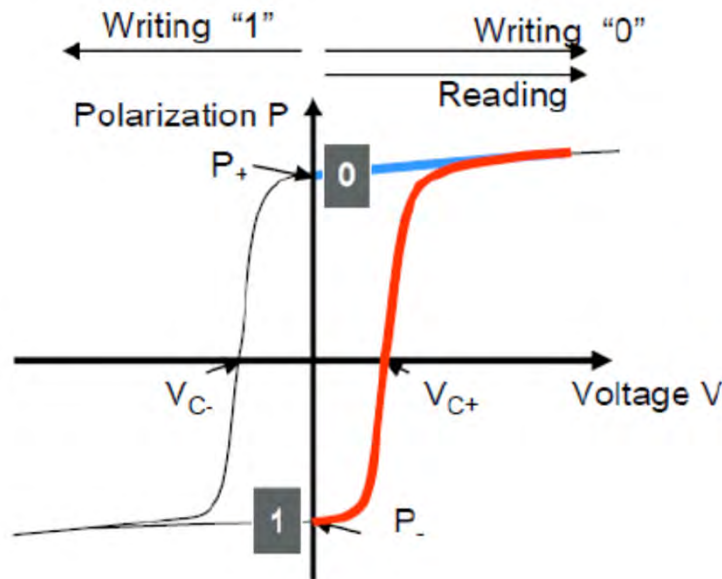
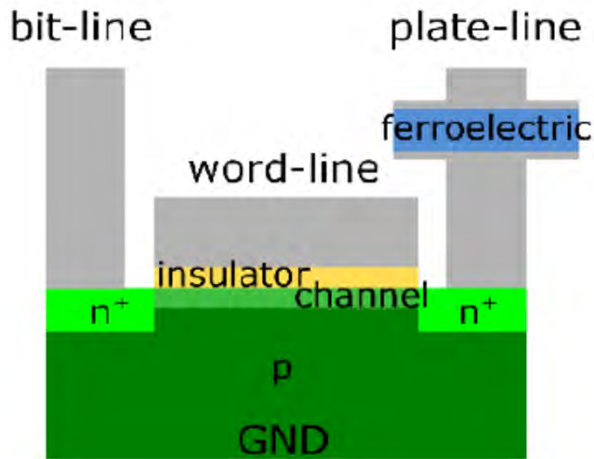


FeRAM ~ MFM capacitors

# FeRAM operation

# Operation of FeRAM

## 1T1C memory cell



$$\Delta V_{BL} ("0") \approx 0 \quad \Delta V_{BL} ("1") = \frac{2P_r \cdot A}{C_F + C_{BL}}$$

- Polarization orientation used for memory storage
- Destructive readout -> re-write necessary
- Memory window (sensing margin) in FRAM can be improved by increasing capacitor area  $A$  and remanent polarization  $P_r$  as well as w/  $P_r/P_s$  ratio getting closer to unity

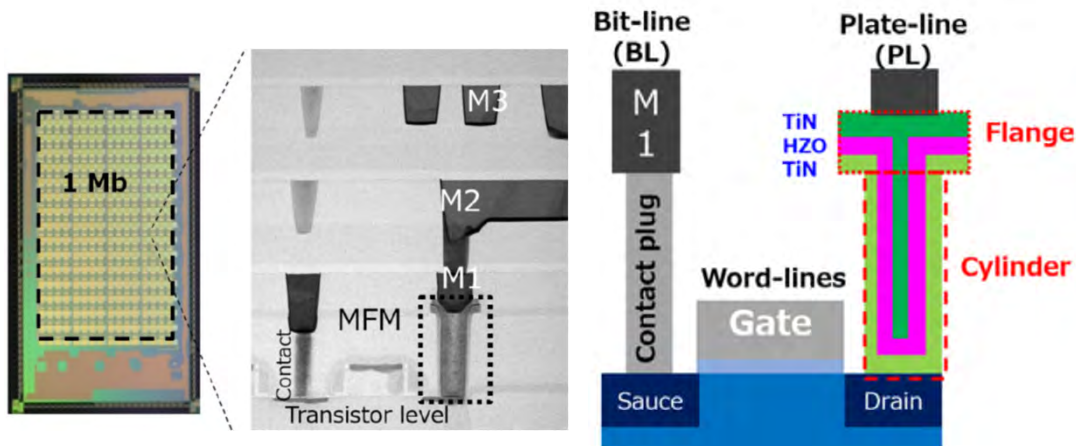
U. Schroeder, VLSI symp. short course (2020)



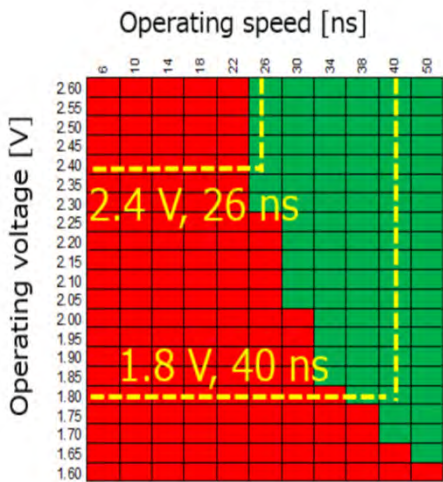
# Recent Progress of HZO FeRAM – 1Mb 3D FeRAM, 32 Gb NVDRAM

## 1Mb 3D 1T/1C FeRAM

J. Okuno et al. (Sony), IEDM (2023) 11-7



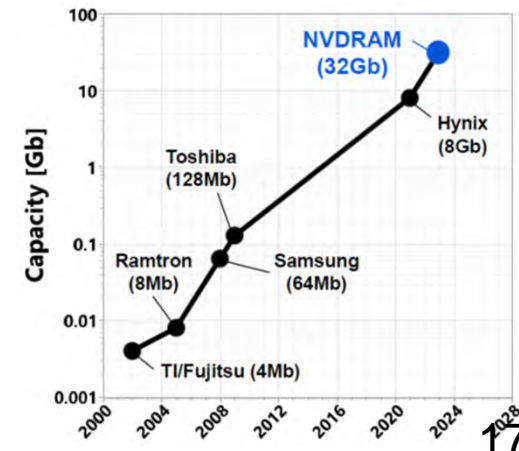
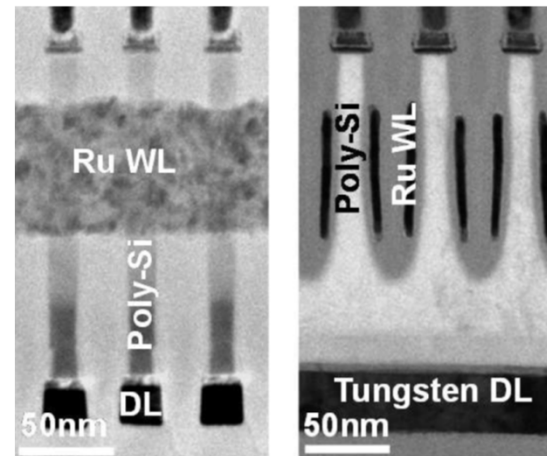
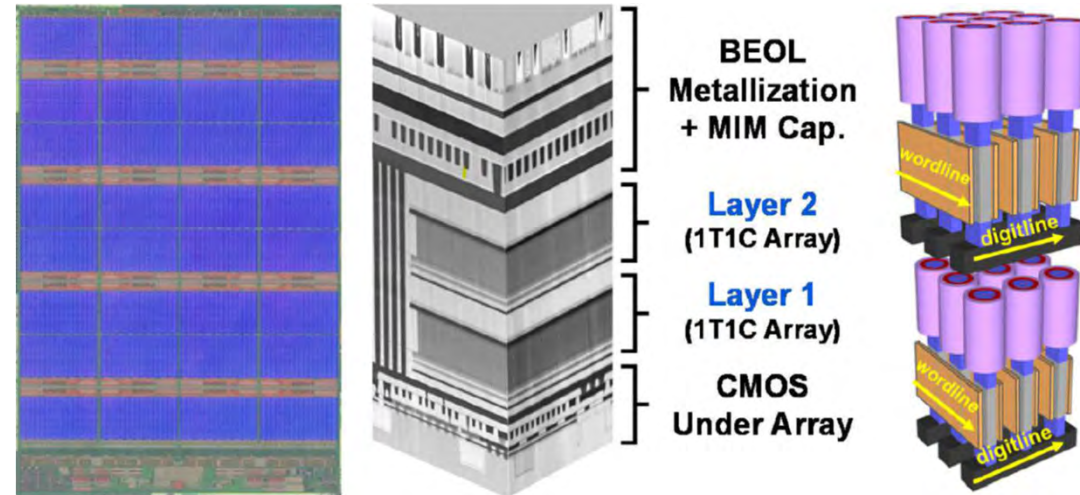
### Sense



Device	IEDM'23 [This Work]	
Capacity	1 Mb	
MFM type	3D	
MFM size [ $\mu\text{m}^2$ ]	0.028	
Ferro. film [nm]	HZO 6 nm	
Write voltage [V]	1.8	2.4
Retention	85°C, $>10^6$ sec	85°C, $>10$ year
Endurance <sup>*without refresh</sup> [cycles]	$10^{11}$	$10^{12}$

## 32Gb 3D Stacked Non-volatile DRAM

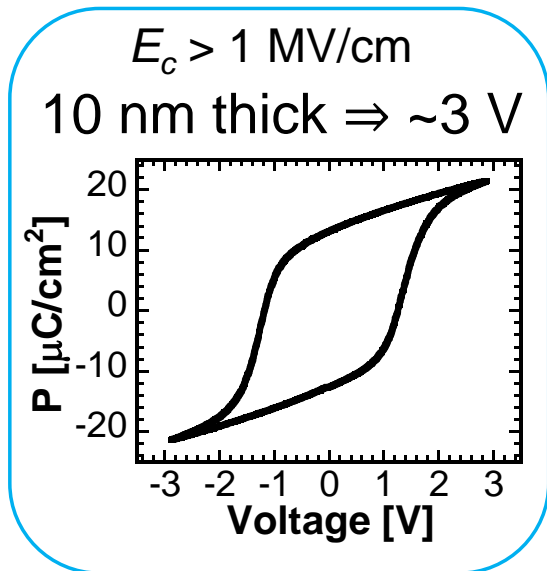
N. Ramaswamy et al. (Micron), IEDM (2023) 15-7



# Critical issues of HZO MFM capacitors for FeRAM application

## Challenge #1

Low operating voltage



- High polarization reversal voltage due to high  $E_c$  in HZO  $\rightarrow$  difficulty in low voltage operation, needed for FeRAM embedded with advanced logic

High  $2P_r$

10~50  $\mu\text{C}/\text{cm}^2$

Requirements for advanced FeRAM applications

Low annealing temperature compatible BEOL

400~500°C for  $\text{Hf}_{0.5}\text{Zr}_{0.5}\text{O}_2$   
( $<400^\circ\text{C}$  is more desired)

## Challenge #2

High retention

High endurance and reliability

Impact is not too clear

PZT  $> 10^{13}$  to  $10^{17}$  cycles  
 $\text{HfO}_2$   $10^6 \sim 10^9$  to  $10^{11}$  cycles

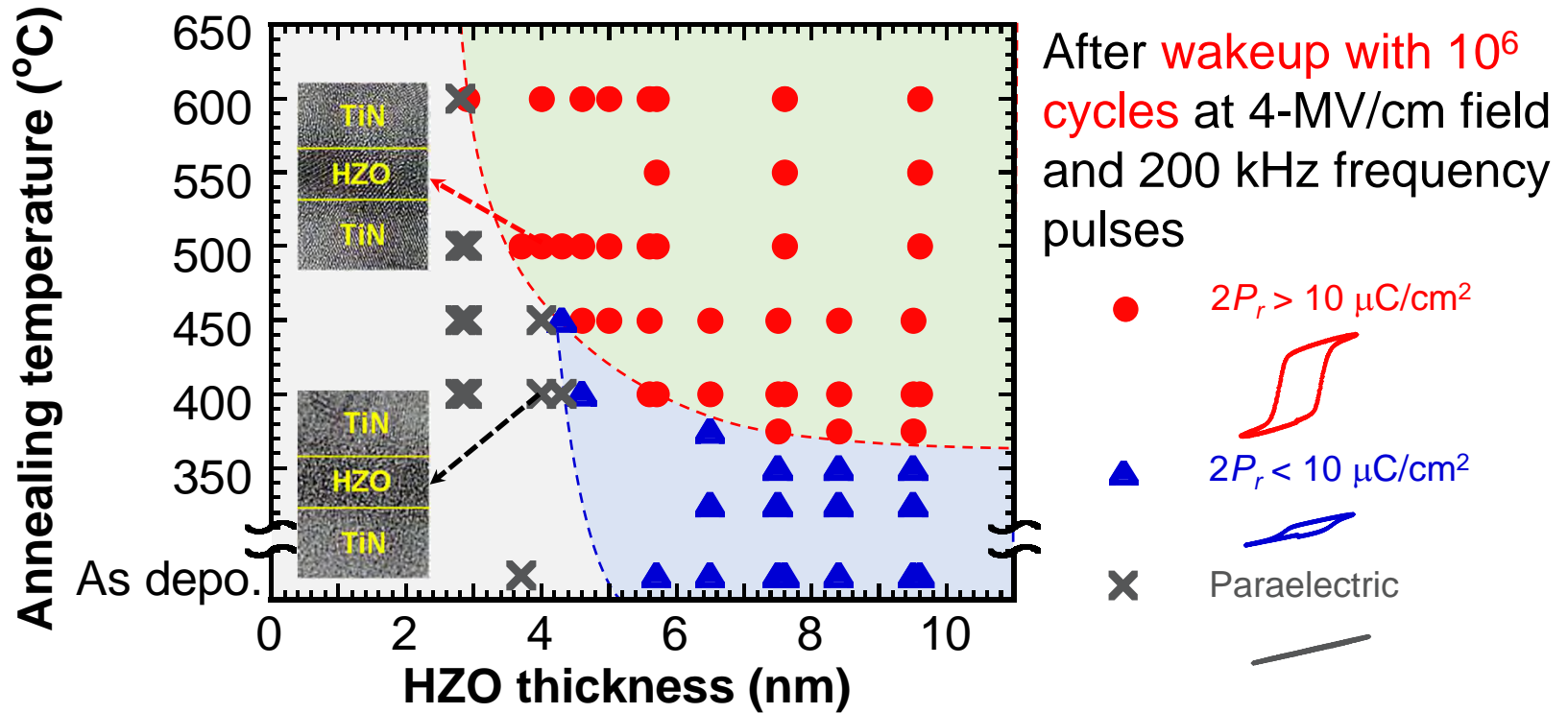
- further improvement in endurance needed for  $\text{HfO}_2$ -based ferroelectrics

**$\rightarrow$  Expectation to HZO thickness scaling**

# Relationship between HZO thickness and crystallization temperature

K. Toprasertpong et al., ACS Appl. Mater. Interfaces **14**, 51137 (2022)

- Highly-doped Si sub.
  - TiN by sputtering
  - $\text{Hf}_{0.5}\text{Zr}_{0.5}\text{O}_2$   
2.8 ~ 9.5 nm ALD
  - TiN by sputtering
  - PMA 300 ~ 600°C  
for 30 s
  - Al contact
- TiN/HZO/TiN  
MFM capacitors

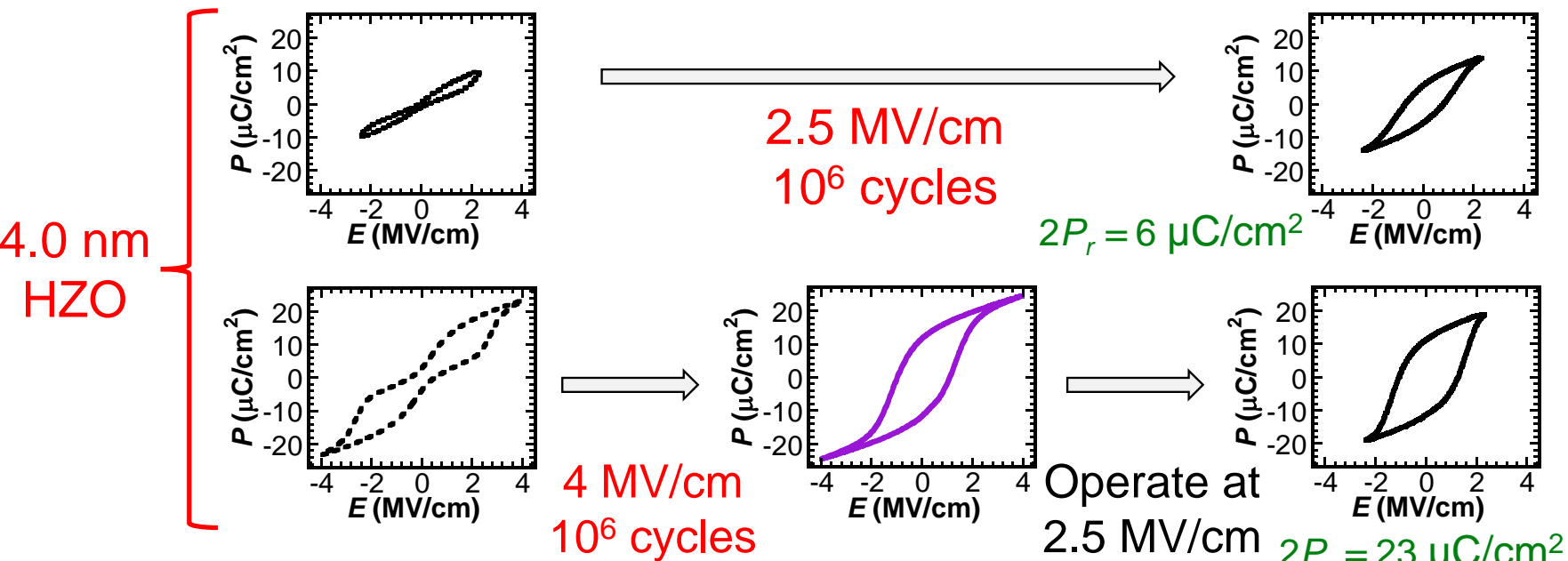


- An annealing temperature of 400 °C is sufficient to obtain  $2P_r$  over  $10 \mu\text{C}/\text{cm}^2$  in HZO films thicker than 6 nm, whereas annealing temperatures of 450, 500, and 600 °C are required for 5, 4, and 3 nm films, respectively, even after  $10^6$  wakeup
- HZO thinning increases the crystallization temperature to ensure sufficient  $2P_r$ , indicating there is a **trade-off between HZO thickness and annealing temperature**

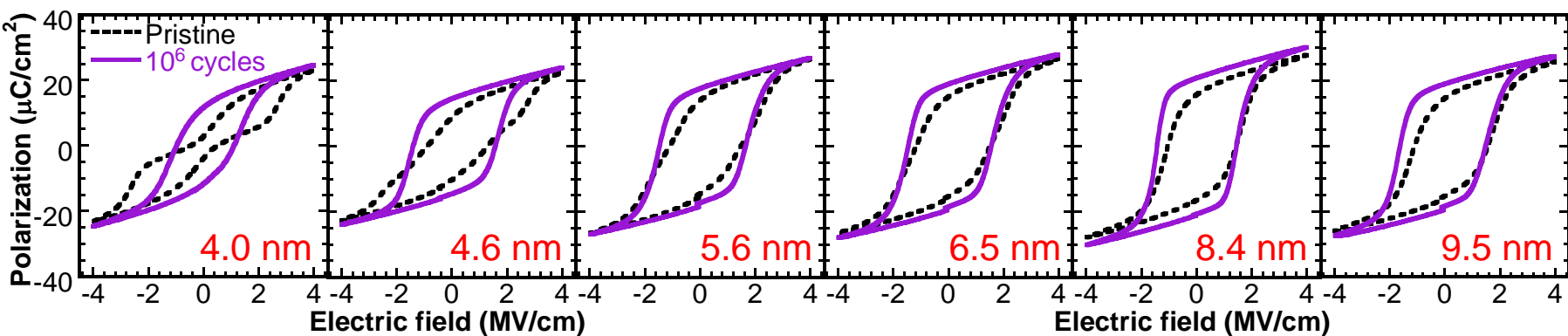


# Necessity of long wakeup for thin HZO capacitor

K. Toprasertpong et al., ACS Appl. Mater. Interfaces **14**, 51137 (2022)

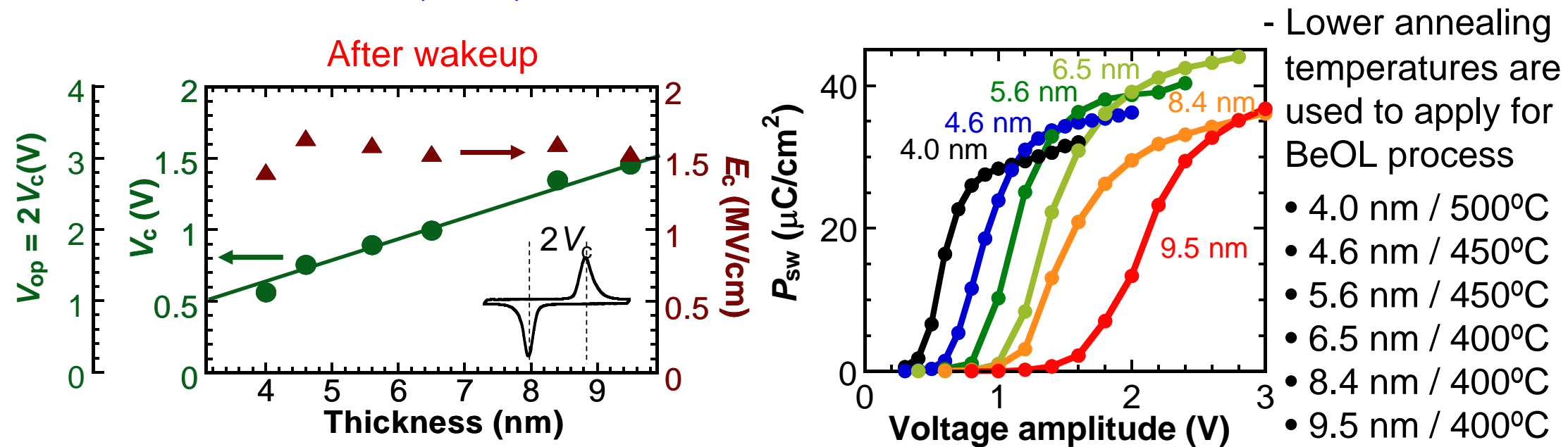


- HZO less than 5 nm exhibits anti-ferroelectric characteristics in pristine condition
- Long wakeup at a high electric field is needed to realize high  $P_r$  ferroelectric characteristics in HZO less than 5 nm



# Low voltage switching in scaled HZO MFM capacitors

K. Tahara et al., VLSI Symp. T7-3 (2021); K. Toprasertpong et al., ACS Appl. Mater. Interfaces **14**, 51137 (2022)



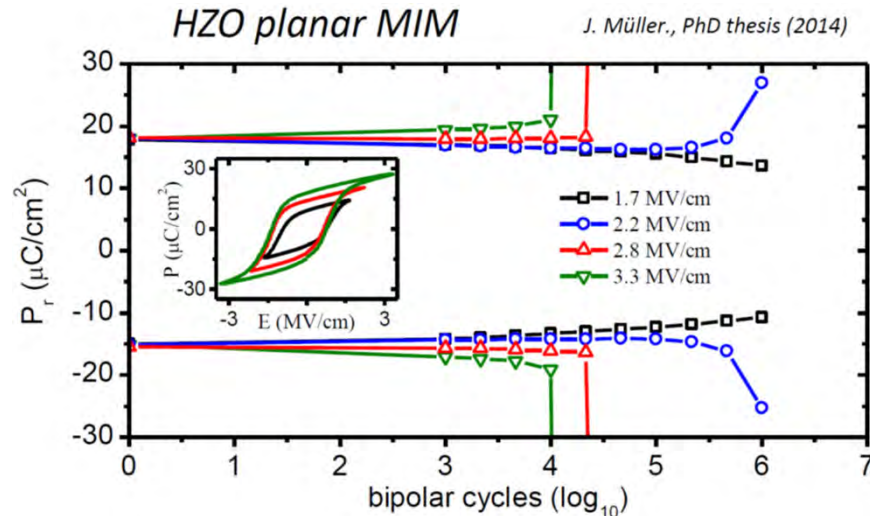
- $E_c$  is found to have only a weak dependency on the thickness and is almost constant in the range of 4.0–9.5 nm
- Operation voltage can be significantly reduced down to less than 1 V ( $\sim 0.8$ V) by thinning HZO down to 5–4 nm

# Reliability of MFM capacitor

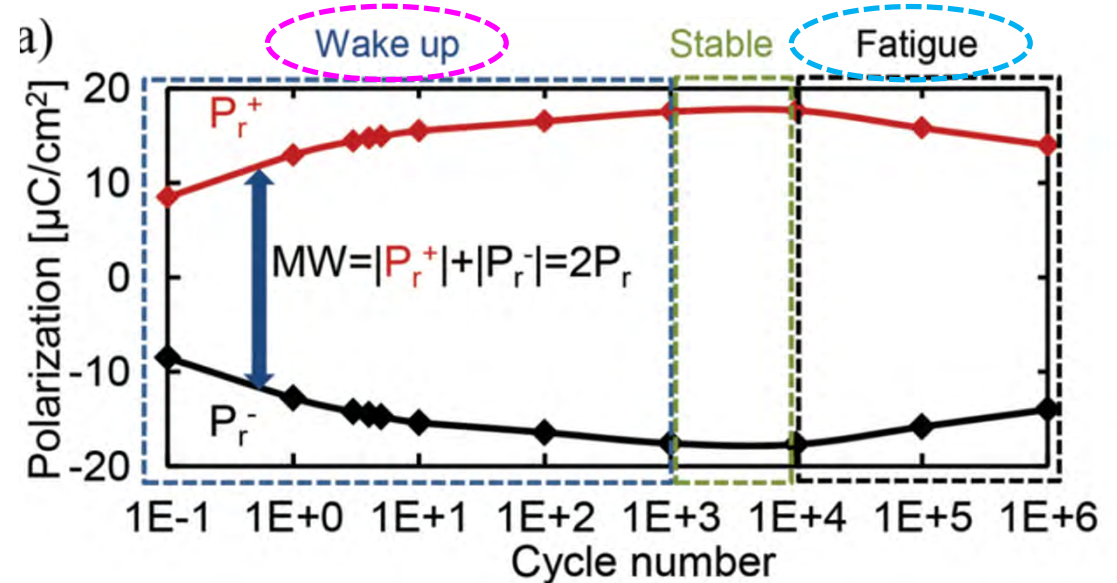


# Reliability issues (1) in HZO MFM ~ breakdown, fatigue and wakeup

J. Muller, IEDM short course (2019)



M. Pesic et al., Adv. Funct. Mater. 26, 4601 (2016)



	SBT (25 nm)	PZT (35 nm)	FE-HfO <sub>2</sub> (10 nm)
$E_{SW}$	~ 300 kV/cm	~ 375 kV/cm	~ 3 MV/cm
$E_{BD}$	~ 1.4 MV/cm	~ 1.2 MV/cm	~ 5 MV/cm
$E_{BD}$ vs. $E_{SW}$	~ 21%	~ 31%	~ 60%

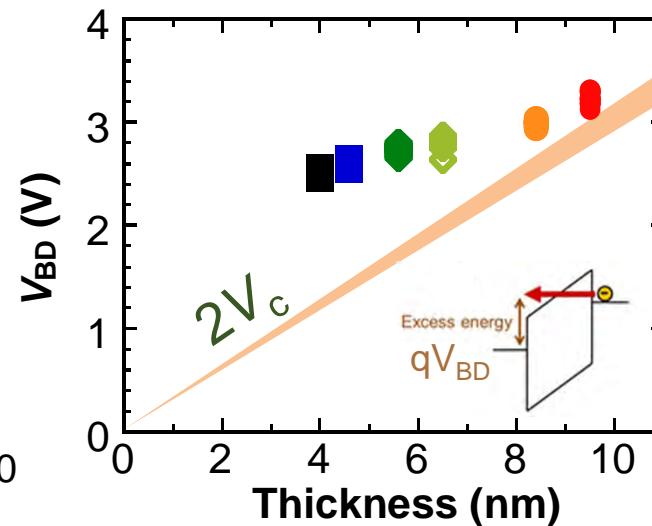
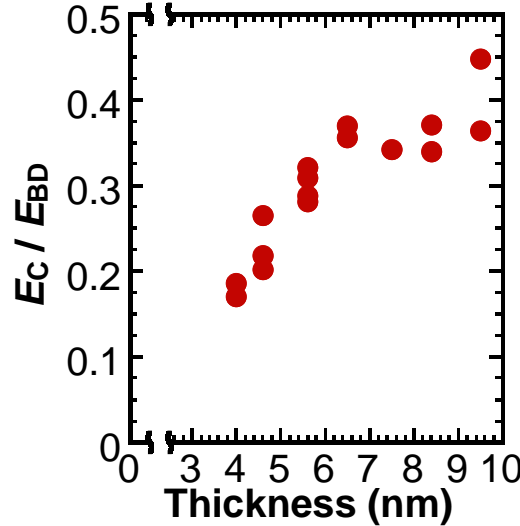
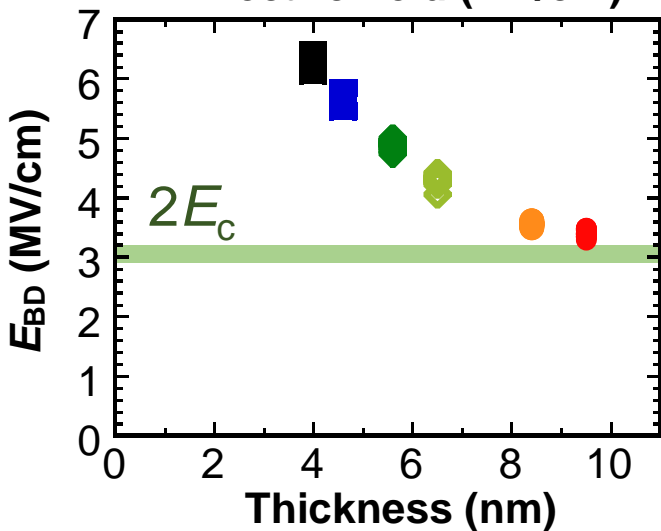
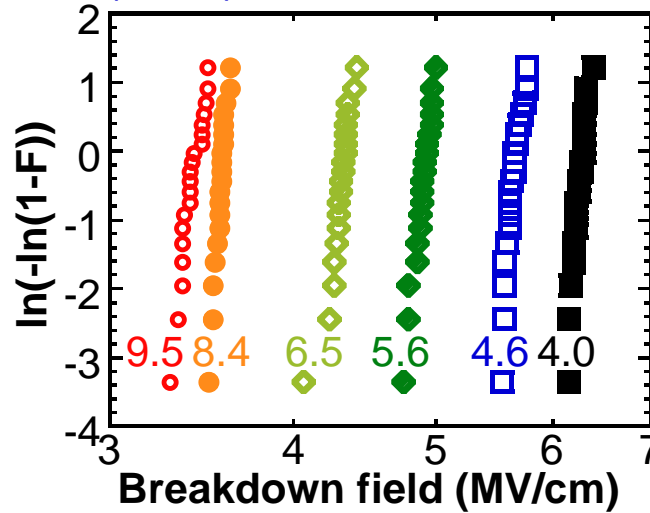
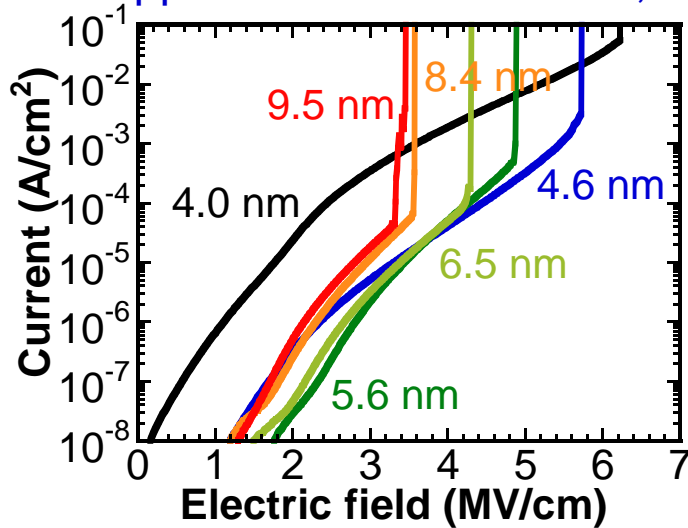
- Compared to other ferroelectrics the high  $E_c$  in FE-HfO<sub>2</sub> leads to an operation point ( $E_{SW} \approx 3E_c$ ) which is close to  $E_{BD}$  (breakdown field)

- Saturated operation endurance is limited mainly by hard dielectric breakdown induced by bipolar cycling stress
- In lower electric field operation, on the other hand, **wakeup**, where  $P_r$  increases with increasing cycle number, and **fatigue**, where  $P_r$  decreases with cycle number, are often observed

# Impact of HZO thickness scaling on breakdown reliability

K. Tahara et al., VLSI Symp. T7-3 (2021); K. Toprasertpong et al., ACS Appl. Mater. Interfaces **14**, 51137 (2022)

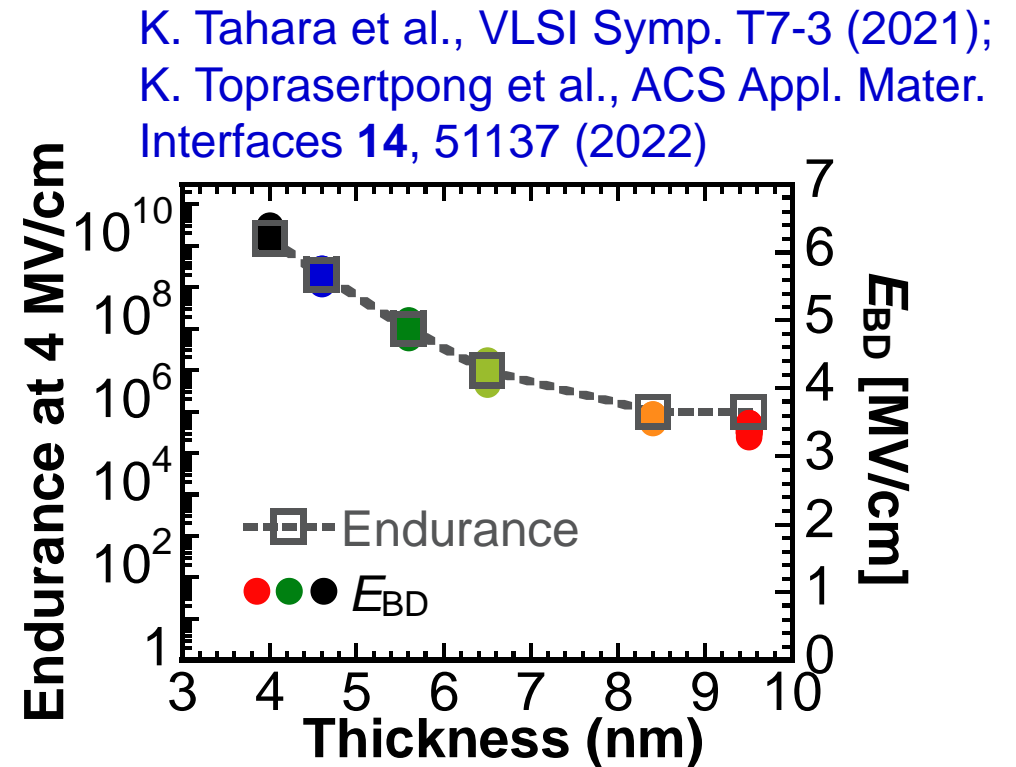
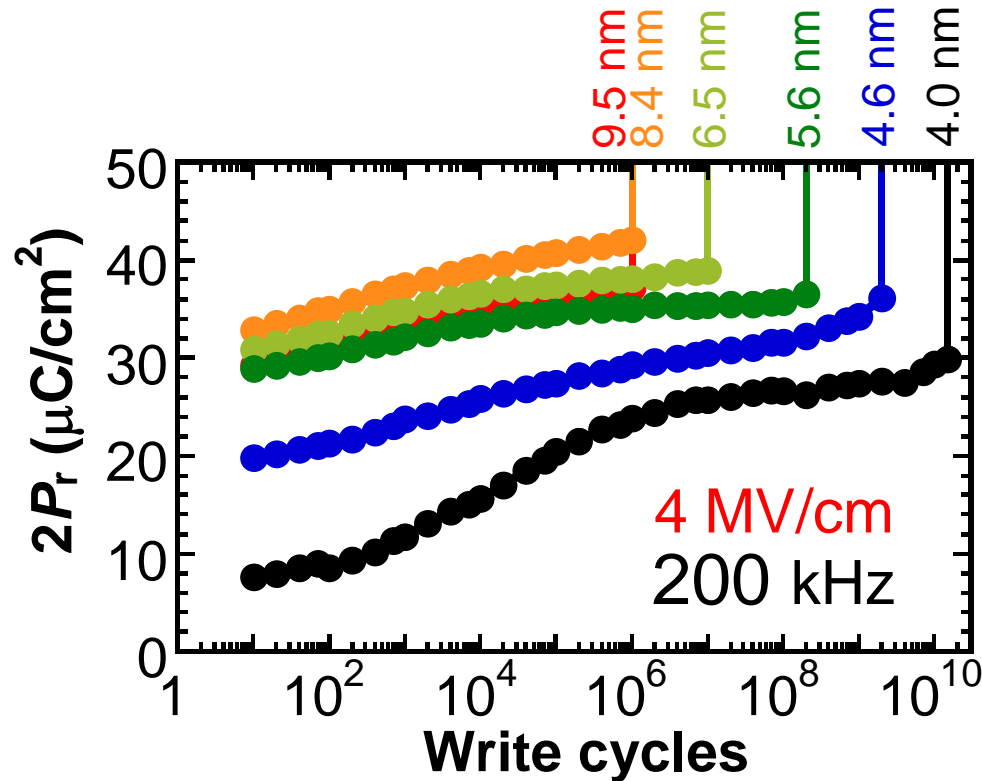
- $E_{BD}$  increases and the ratio of  $E_c/E_{BD}$  decreases with decreasing HZO thickness, indicating improved breakdown reliability
- $V_{BD}$  is almost constant, 3 V, irrespective of HZO thickness, suggesting that the applied voltage is the dominant factor



determining breakdown

- The energy of injected electrons can be critical to damage in HZO films

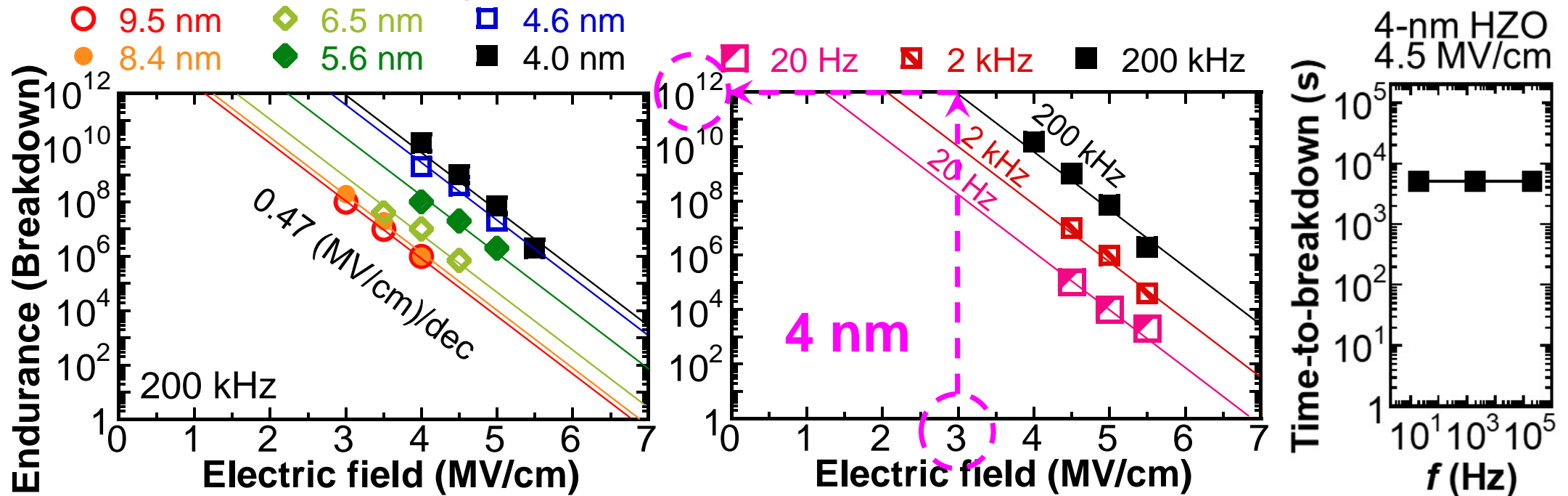
# Write cycle endurance due to breakdown of MFM capacitors



- Significant improvement of endurance, limited by break down under 4 MV/cm cycling, is obtained by greater than 4 orders of magnitude by only thinning HZO films from 9.5 to 4.0 nm, because of the increase of  $E_{BD}$
- Endurance cycle number limited by breakdown increases with a decrease in HZO thickness with the similar HZO thickness dependence of  $E_{BD}$

# Breakdown endurance vs Electric field

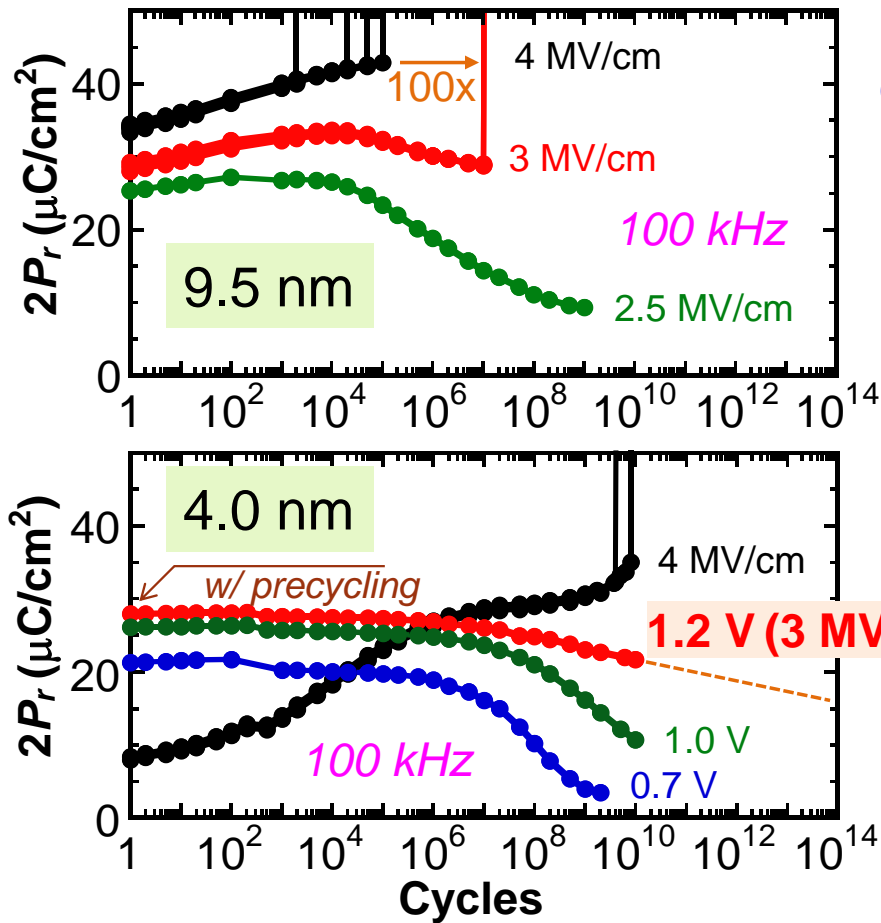
K. Toprasertpong et al., ACS Appl. Mater. Interfaces 14, 51137 (2022)



- Relationship between endurance and operating field is almost the same for all the HZO thicknesses
- The number of endurance cycles decreases by one order for every increasing field of  $0.47 \pm 0.08$  MV/cm, independent of the HZO thickness, resulting in approximately  $1 \times 10^{12}$  cycles for breakdown-limited-endurance of the 4.0 nm HZO capacitor operating at 1.2 V (3 MV/cm)
- The stress frequency does not change the field-acceleration factor
- The number of endurance cycles is proportional to the operating frequency; thus, the total time-to-breakdown is independent of the operating frequency



# Improvement of endurance and reliability with HZO scaling



K. Tahara et al., VLSI Symp. T7-3 (2021); K. Toprasertpong et al., ACS Appl. Mater. Interfaces **14**, 51137 (2022)

## Endurance

10 nm, 4 MV/cm, 100 kHz  $10^4 \sim 10^6$

thickness scaling ↓

4 nm, 4 MV/cm, 100 kHz  $10^{10}$

4 nm, 3 MV/cm, 100 kHz  $10^{12}$  (Projected)

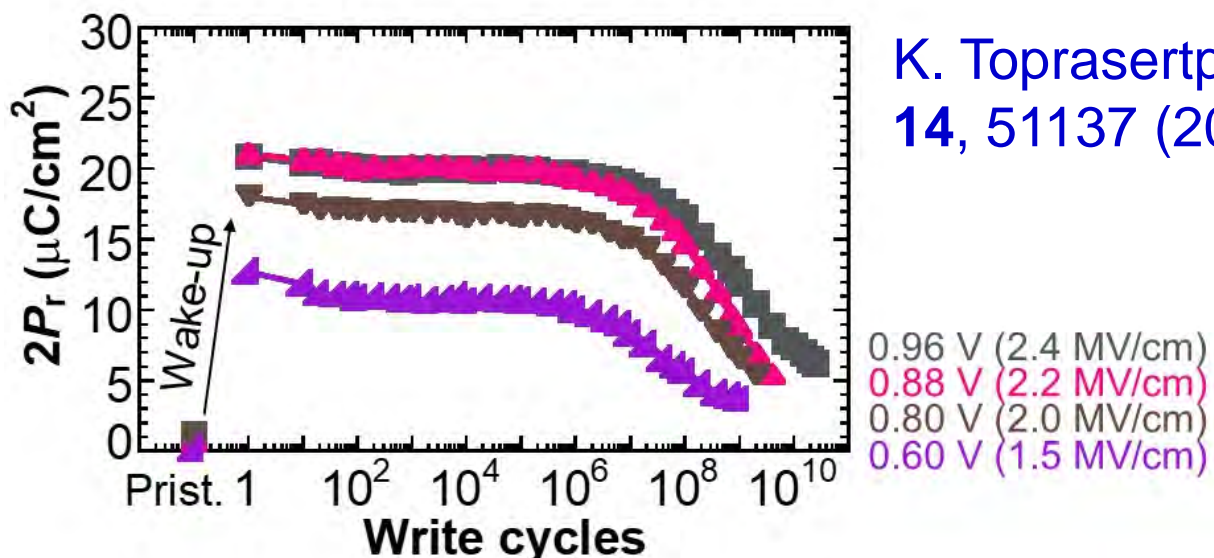
4 nm, 3 MV/cm, 10 MHz  $10^{14}$  (Projected)

Area  $3600 \mu\text{m}^2 \rightarrow \text{sub } \mu\text{m}^2$   $\gg 10^{14}$  (Cell level)

Area scaling : L. Grenouillet et al., VLSI Tech., TF2.4 (2020)

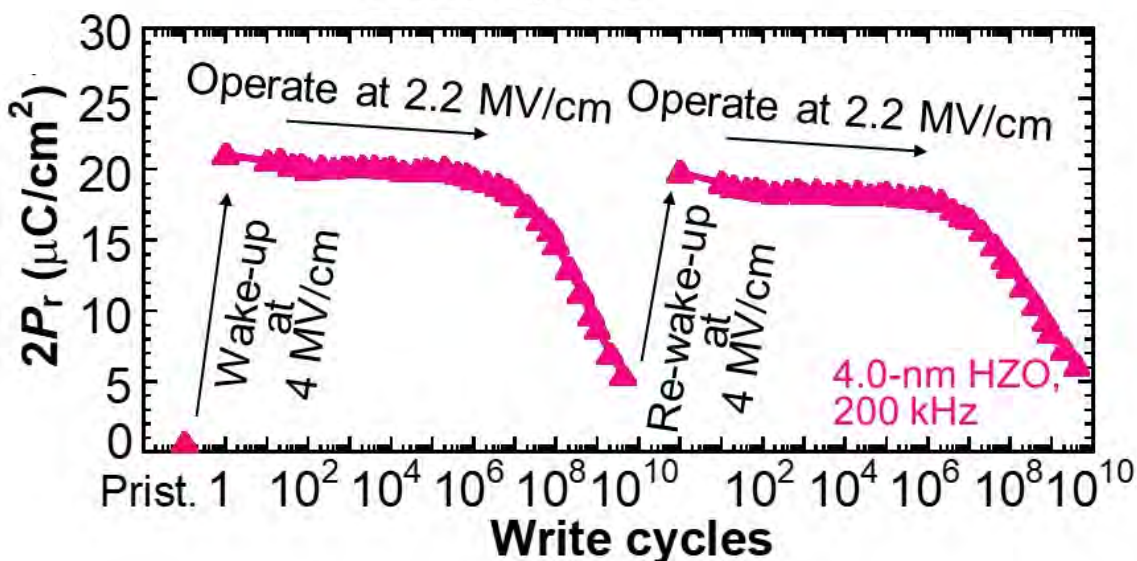
- The endurance cycle of 4-nm-thick HZO is around  $10^{10}$  times at 4 MV/cm, and can be improved up to around  $10^{12}$  times by lowering the electric field down to 3 MV/cm
- The endurance cycle of  $10^{14}$  times or more can be expected at higher operation frequencies

# Fatigue and recovery of HZO MFM capacitors at low electric field

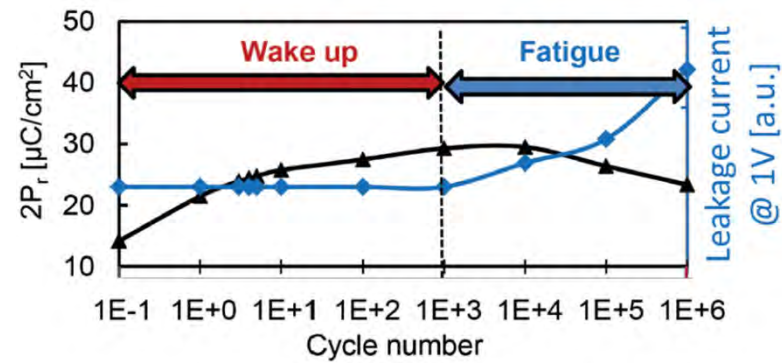


K. Toprasertpong et al., ACS Appl. Mater. Interfaces **14**, 51137 (2022)

- Operating at a low field is found to cause another failure mode caused by fatigue
- At a low operating field,  $2P_r$  values decrease with increasing the number of cycles
- This fatigue can be recovered by applying high operating voltage (electric field)
- This fatigue behavior is attributable to the influence of charge redistribution in the FE-HfO<sub>2</sub> films and eventually results in a read failure

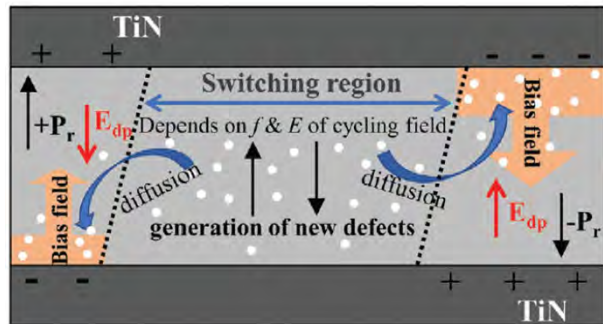
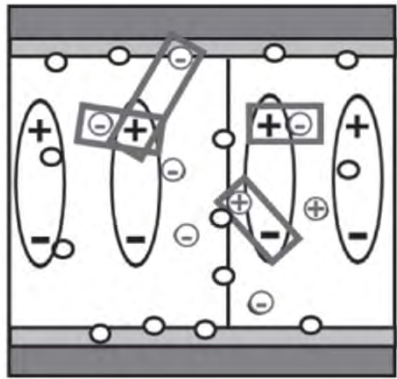


# Possible mechanism of fatigue and recovery of HZO MFM capacitors

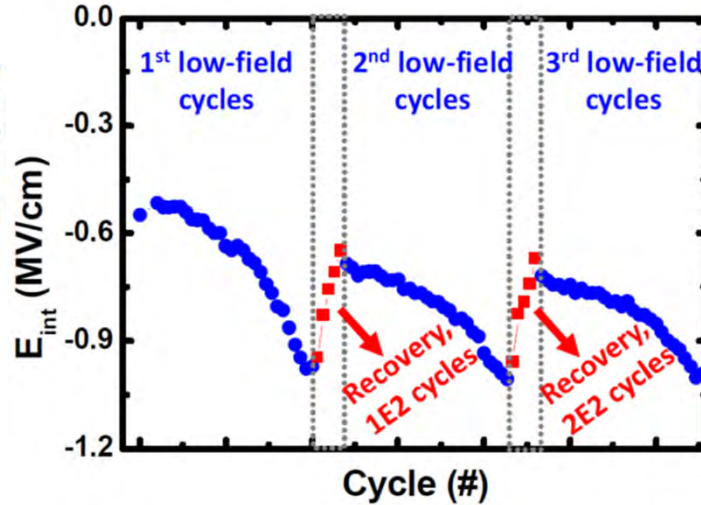


M. Pesic et al., *Adv. Funct. Mater.* **26**, 4601 (2016)

- domain pinning
- local bias field due to charged defects

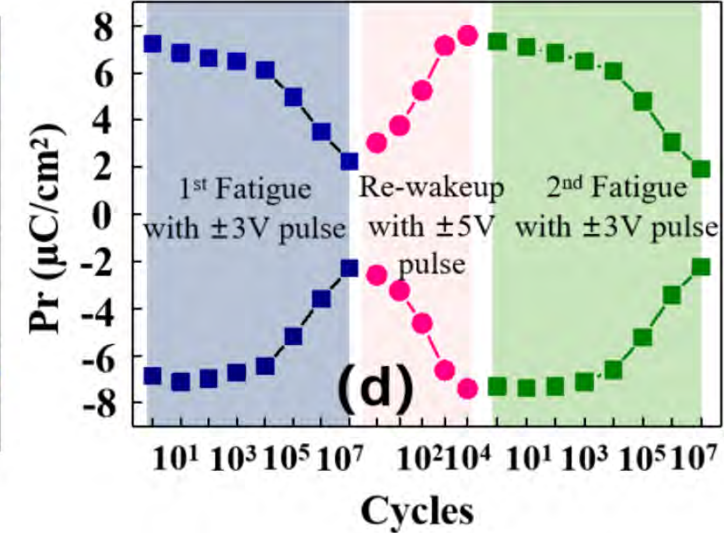
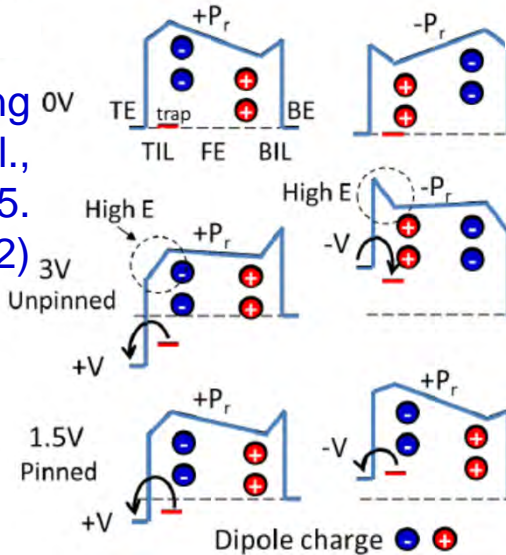


S. Li et al., *Adv. Electron. Mater.* **6**, 2000264 (2020)

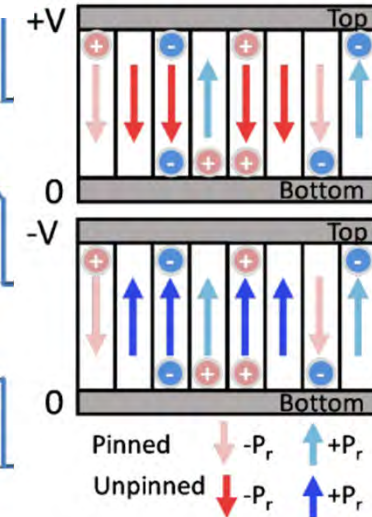


P. J. Liao et al., *VLSI symp.*, T6-3 (2021)

H.-H. Huang et al., *IEDM*, 13.5 (2022)



T. Gong et al., *EDL* **42**, 1288 (2021)



- Fatigue and imprint and recovery are explained by multi-domain switching with local charge trapping and de-trapping

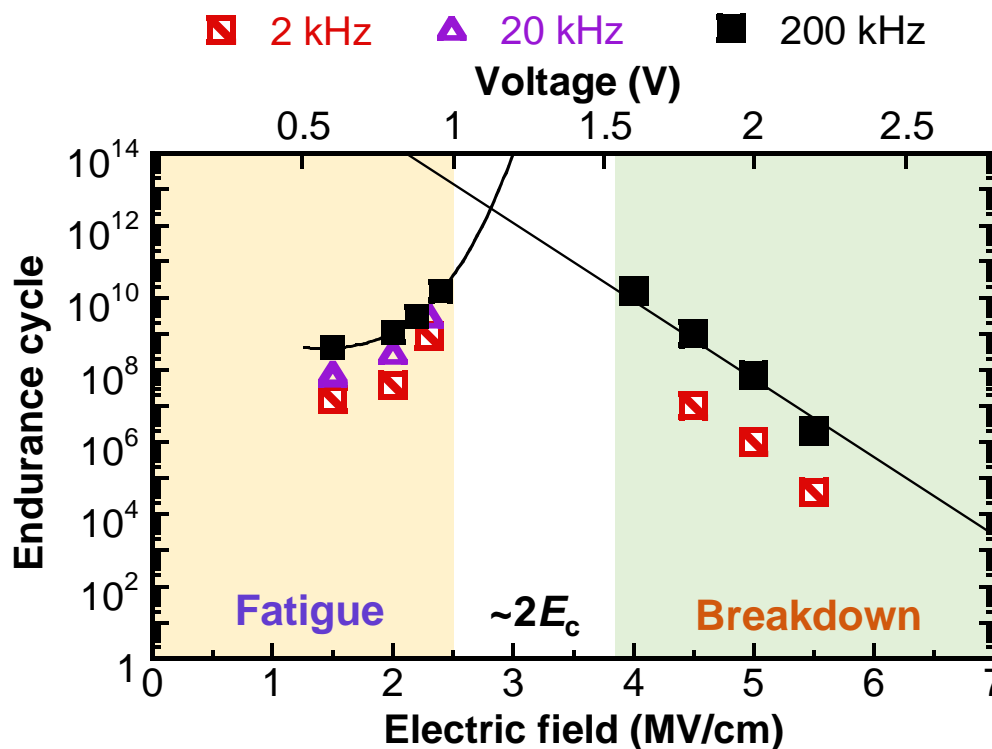
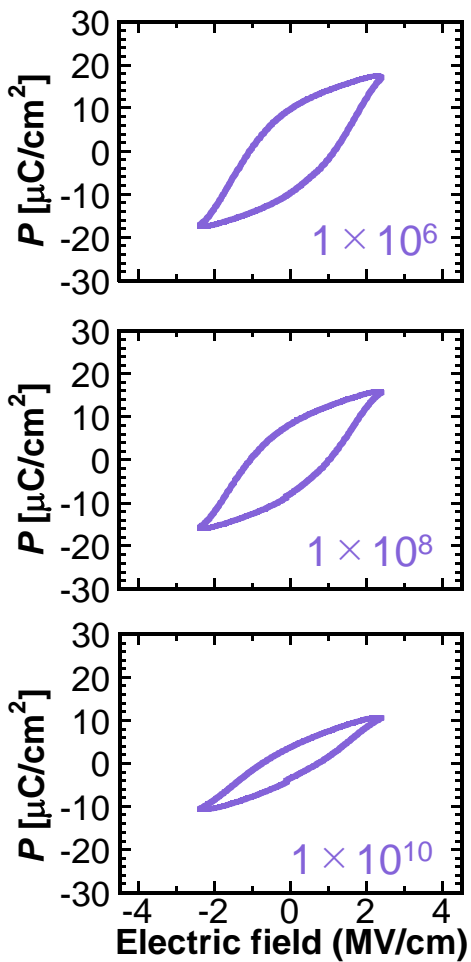


# Optimum electric field of HZO MFM capacitors for endurance

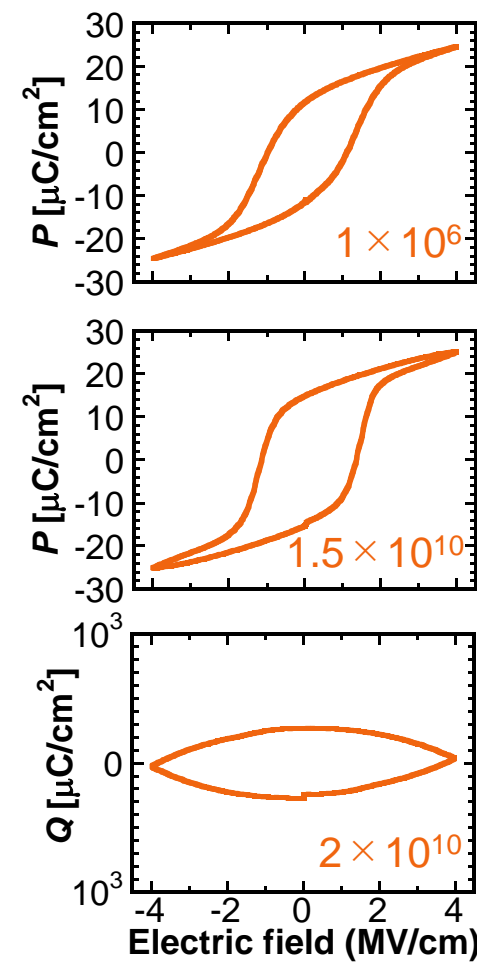
K. Toprasertpong et al., ACS Appl. Mater. Interfaces **14**, 51137 (2022)

Fatigue-limited endurance

Breakdown-limited endurance



- There is an optimum voltage (field) regime for improving the endurance characteristics. The optimum field is around 3 MV/cm or around  $2E_c$ , indicating that the operating voltage of 1.2 V (3 MV/cm) for 4.0 nm HZO films

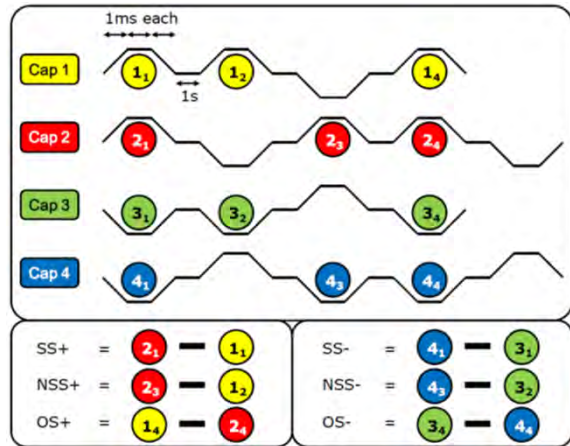




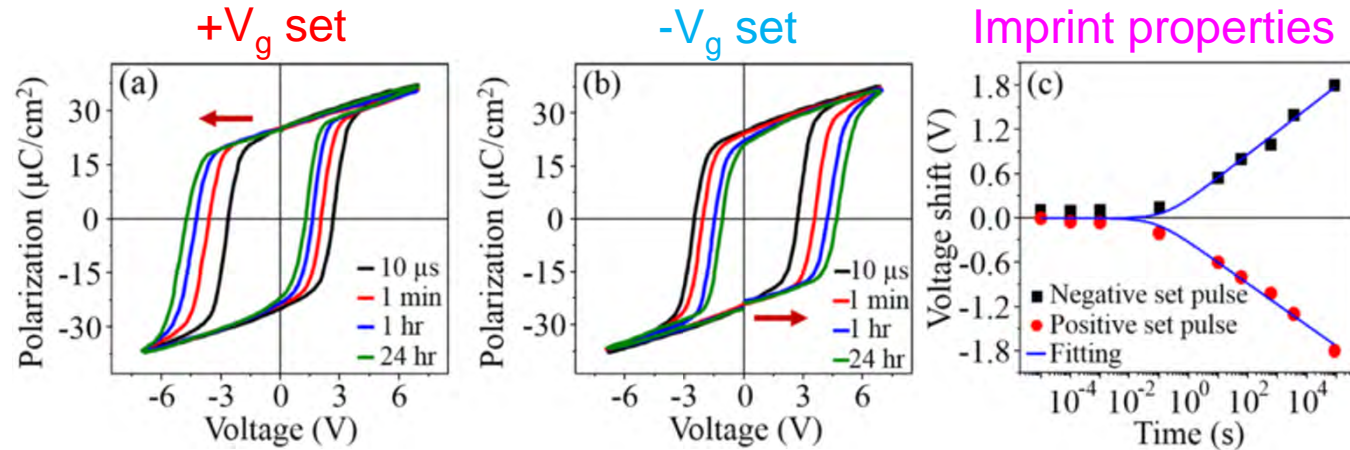
# Reliability issues (2) in HZO MFM ~ retention and imprint

• Complex (FRAM standard) retention test to account for same (SS), new same state (NSS) and opposite state (OS) retention

S. Müller et al., TDMR 99 (2013)



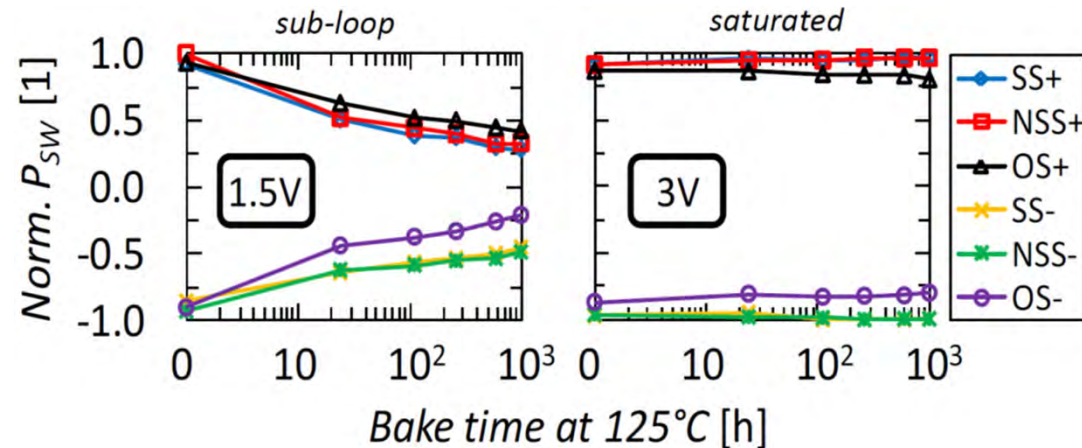
P. Buragohain et al., ACS Applied Mat. & Int. 11, 35115 (2019)



• Good high-T data retention for same and opposite state is commonly observed for FE HfO<sub>2</sub> MFM capacitors

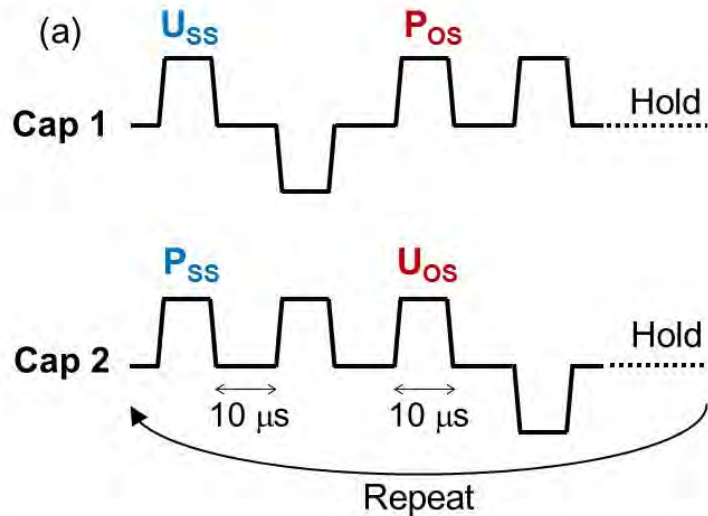
• Sub-loop operation makes retention unstable  
 • Worse retention for opposite state is a problem, which is attributable to imprint properties of HfO<sub>2</sub>-based MFM

• Comparatively large imprint and fully recovery are also commonly observed for HfO<sub>2</sub>-based MFM, which can be one possible critical reliability issue



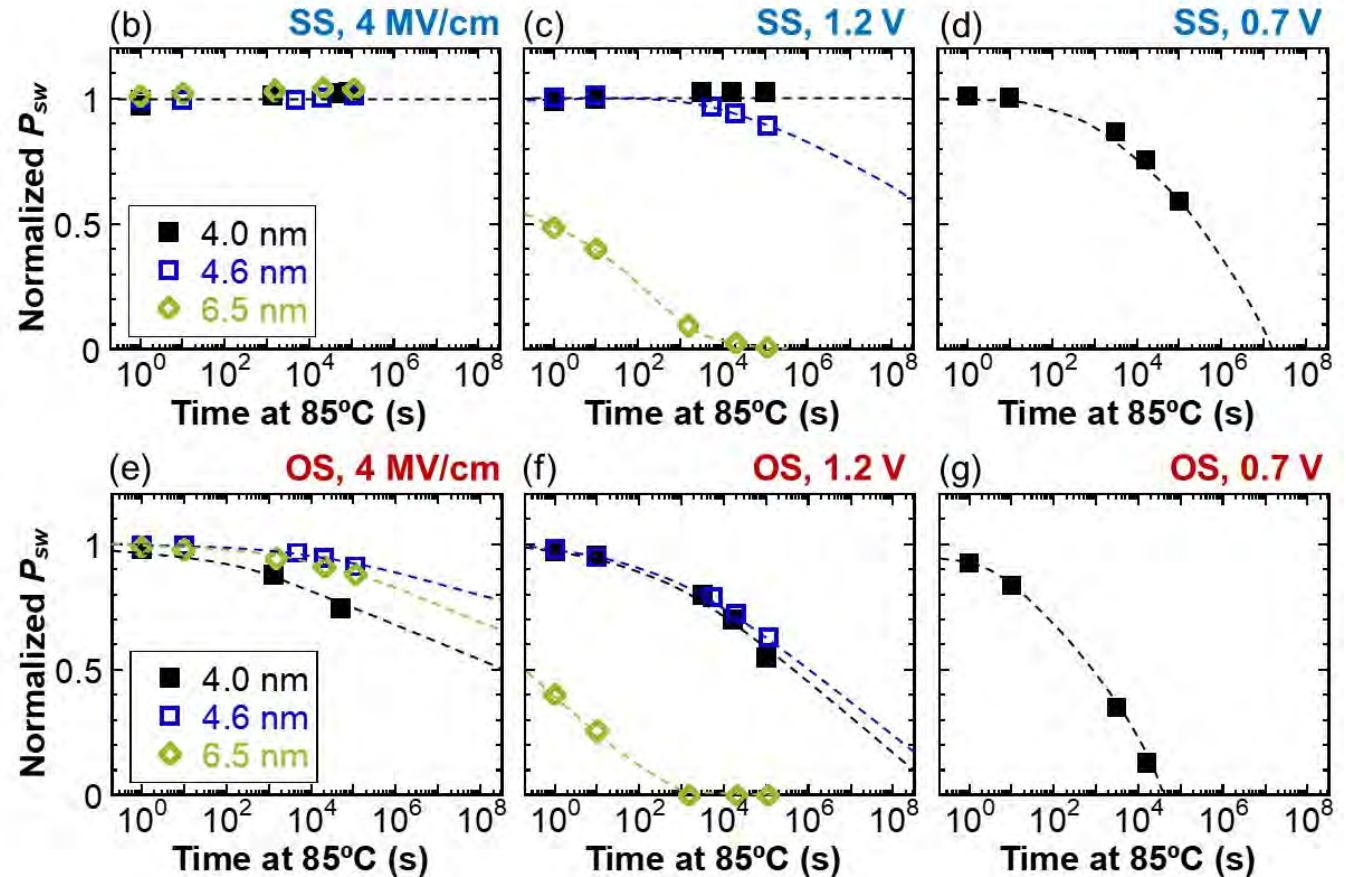
# Retention properties of thin HZO MFM capacitors

K. Toprasertpong et al., ACS Appl. Mater. Interfaces 14, 51137 (2022)



$$P_{sw} \text{ in Same-State (SS)} = P_{ss} - U_{ss}$$

$$P_{sw} \text{ in Opposite-State (OS)} = P_{os} - U_{os}$$

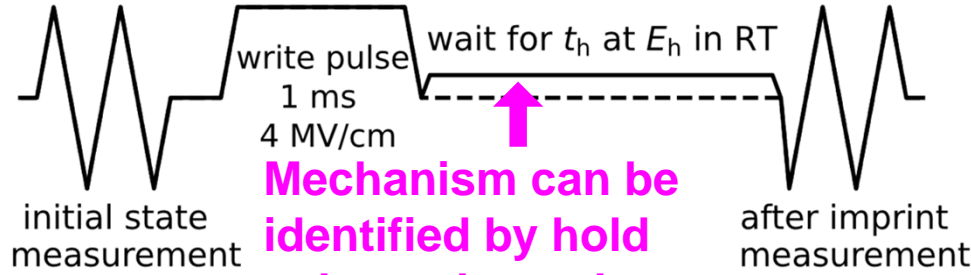
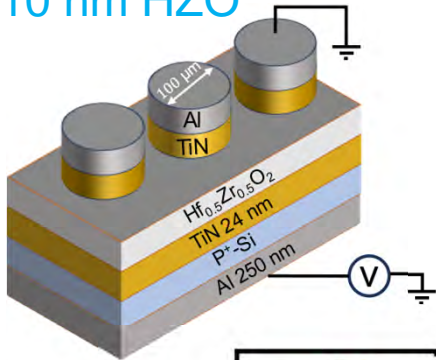


- 4-nm-thick HZO MFM exhibits excellent same state (SS) retention properties even at 1.2 V (3 MV/cm)
- On the other hand, the opposite state (OS) retention is weaker than the SS retention, attribute to imprint properties of HZO films, which need to be further improved

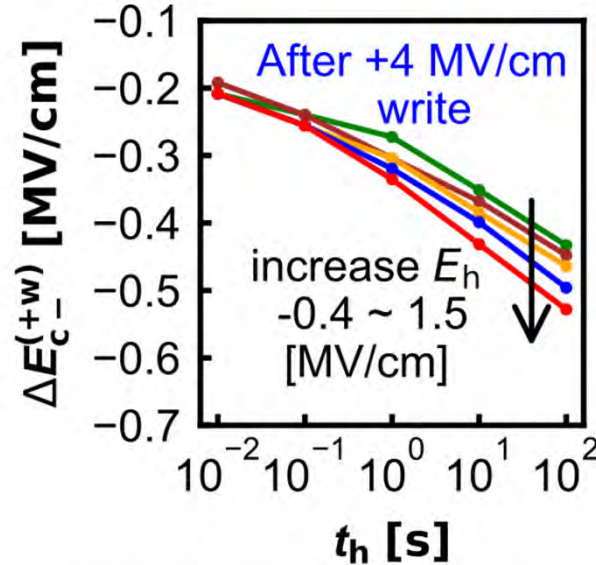
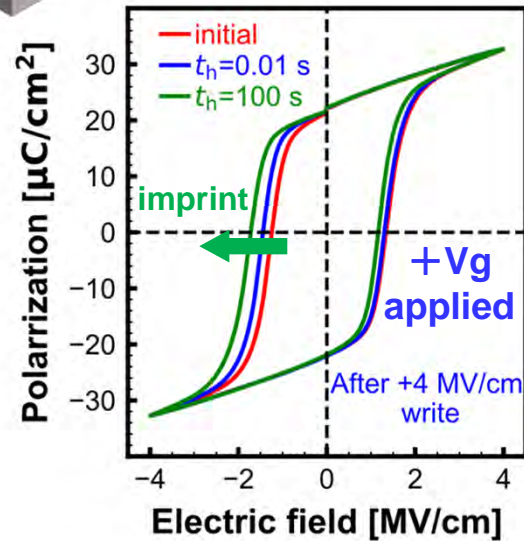


# Physical mechanism of imprint in HZO

10 nm HZO

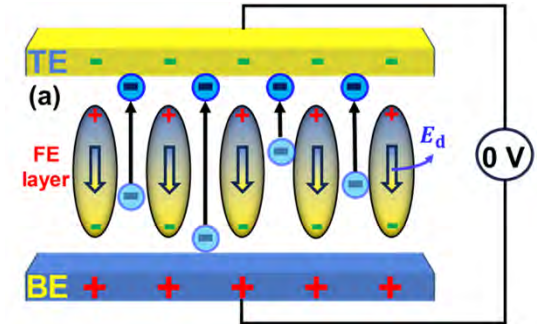


Mechanism can be identified by hold voltage dependence



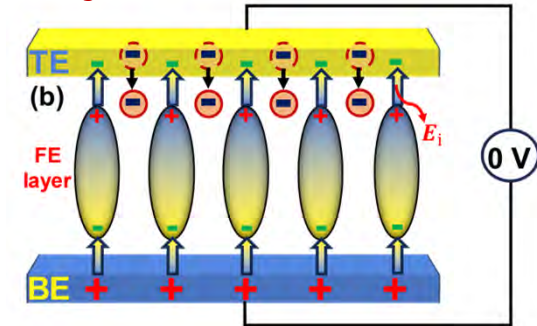
Z. Liu et al., APL 125, 072904 (2024)

Charge drift model



X

Carrier injection model



O

• Imprint in HZO films can be caused by charge generation due to injection (or emission) of carriers (or into) electrodes (**carrier injection model**)

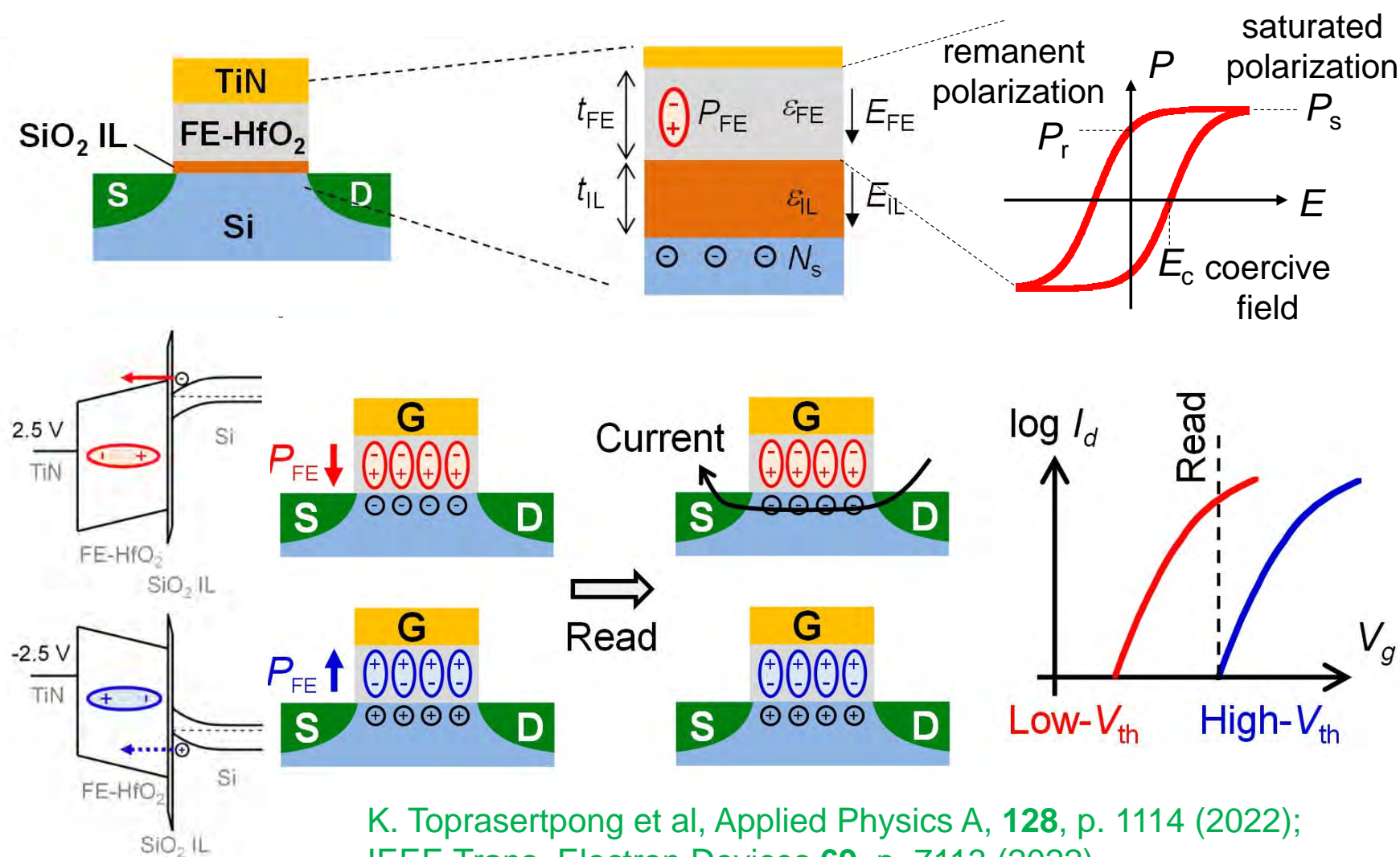
(This model has also been supported by P. Vishnumurthy, IRPS 7A.1 (2024))

# FeFET memory



# FeFET memory operation

# Ferroelectric gate insulator Field-Effect Transistors (FeFET)

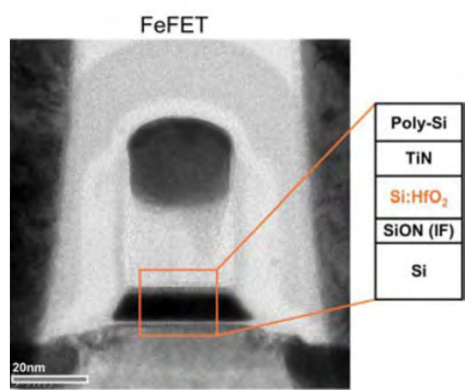


- Polarization condition of FE can control the electric field at MOS interface and resulting  $V_{th}$  of  $I_d$ - $V_g$  characteristics of MOSFETs
- Nonvolatile memory function is obtained by reading out  $V_{th}$  condition with low applied  $V_g$
- Non-destructive readout expected

K. Toprasertpong et al, Applied Physics A, **128**, p. 1114 (2022);  
IEEE Trans. Electron Devices **69**, p. 7113 (2022)

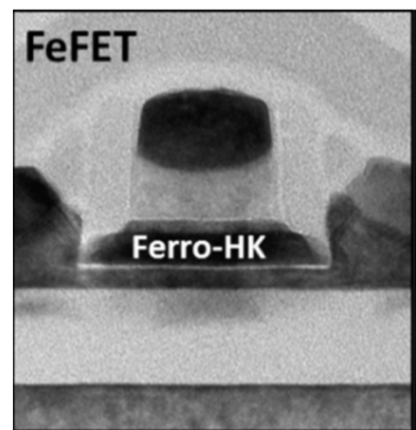
# Recent Progress of HZO devices – scaled FeFETs and advanced structures

28nm node FeFET (GF)



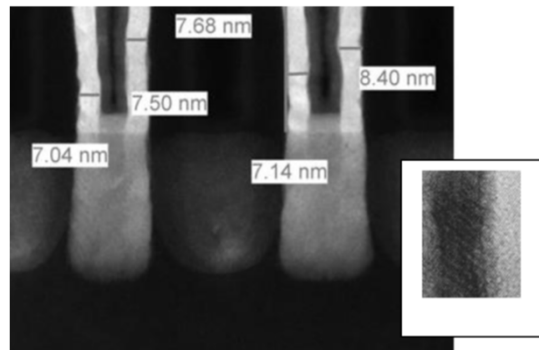
M. Trentzsch, IEDM (2016)

22nm node FDSOI (GF)



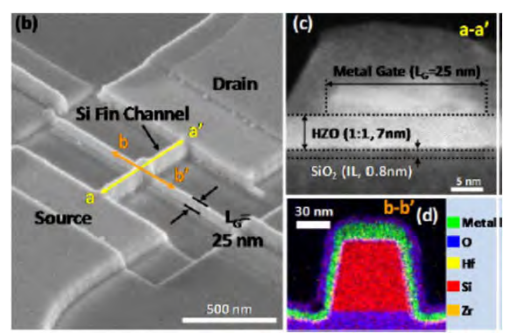
S. Dünkel, IEDM (2017)

14nm node FinFET (GF)



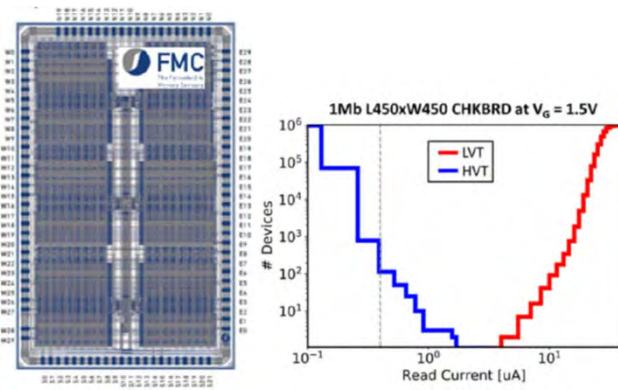
Z. Krivokapic, IEDM (2017)

25nm FinFET (Samsung)



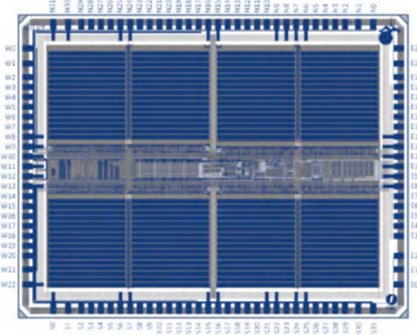
H. Bae, IEDM (2020)

10Mb cell array (GF, FMG)



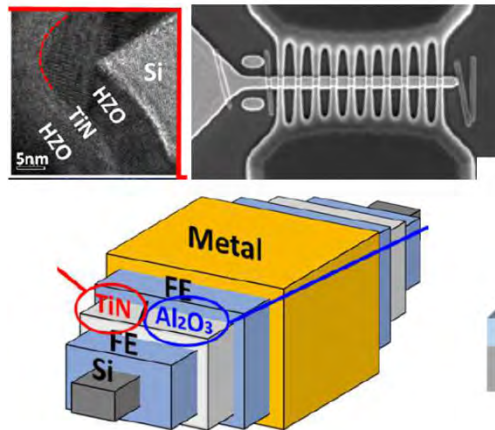
S. Beyer, IMW (2020)

32Mb produce macro (FMG, GF)



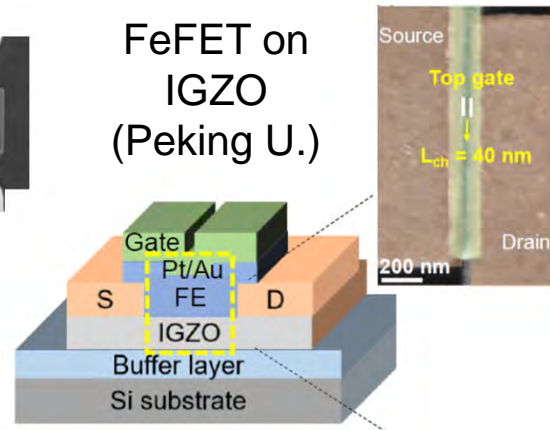
S. Mueller, VL (2021)

GAA FeFET (NTNU)



C.-Y. Liao, VL (2022)

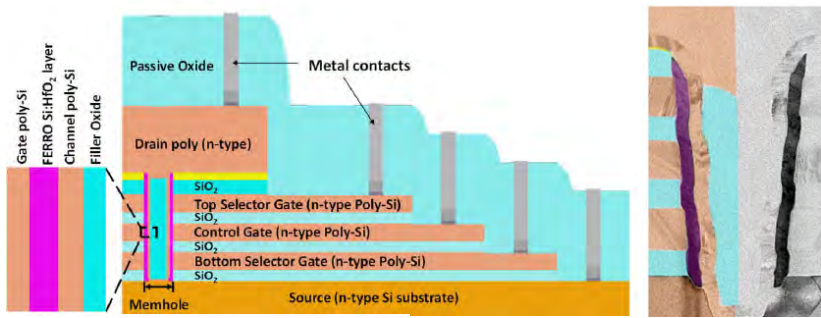
FeFET on IGZO (Peking U.)



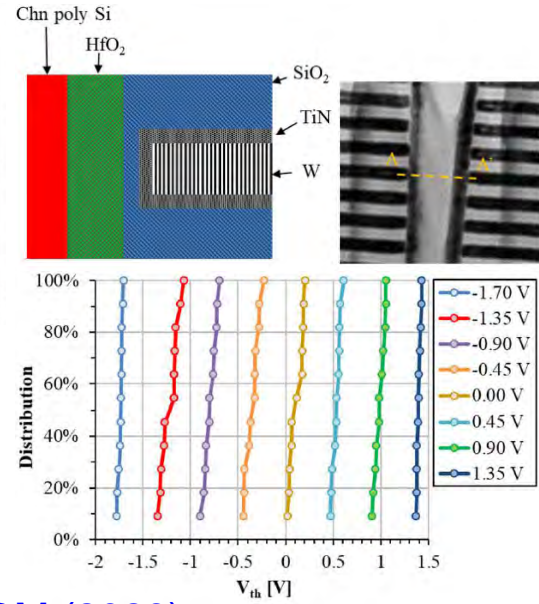
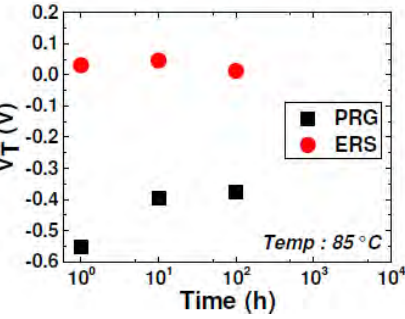
M. Zeng, IEDM (2023)



# Recent Progress of HZO devices – application to FLASH memory cell

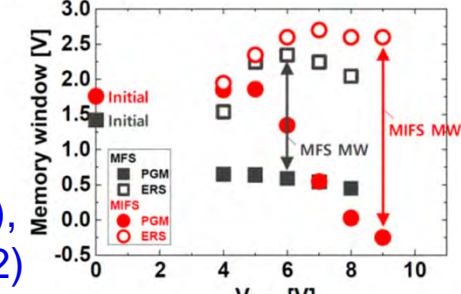
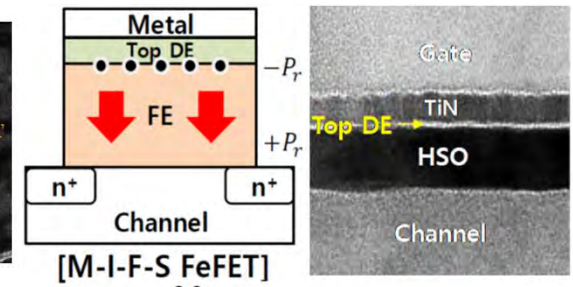


K. Florent (imec), IEDM, 43 (2018)

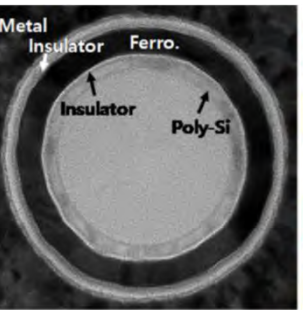


S. Yoon (SK Hynix), IMW (2022)

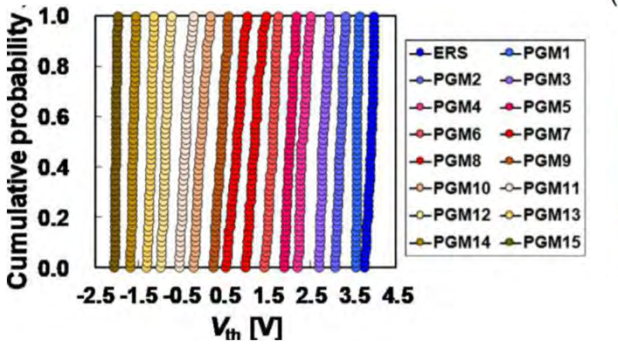
J.-G. Lee (SK Hynix), IMW (2022)



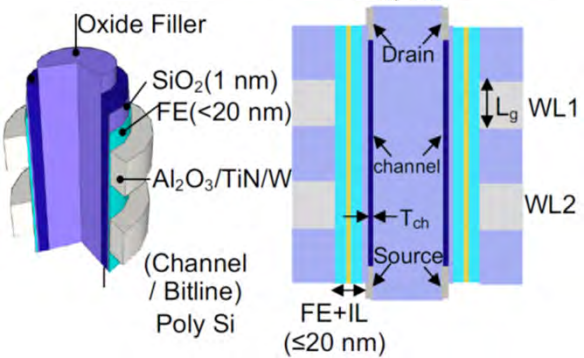
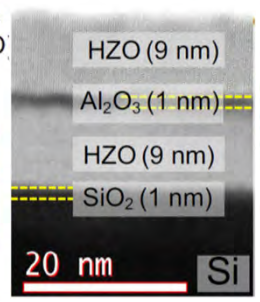
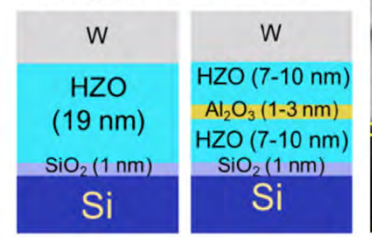
S. Lim (Samsung), IEDM (2023)



Metal
Ferro
Insulator
Silicon
Metal
Insulator
Ferro
Insulator
Silicon



(a) Reference Novel structure (Only HZO) (HZO/Al2O3/HZO)



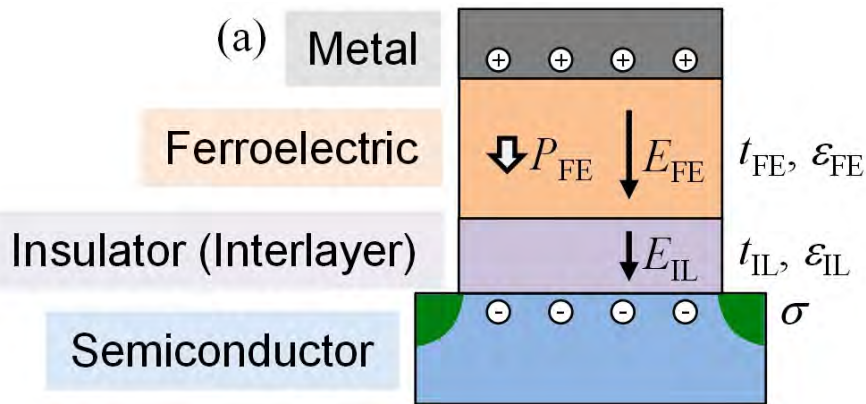
D. Das (Georgia Tech., Samsung), IEDM, 24.1. (2023)

- Application of the FeFET structure to NAND flash memory cell by replacing charge-trap layers by ferroelectric films is actively being studied → one of the most promising and near-term applications

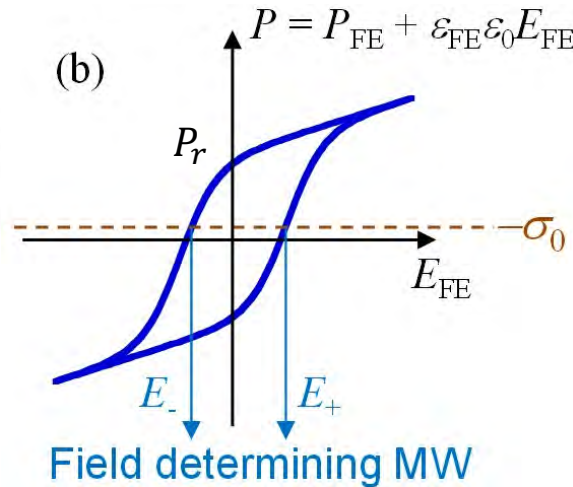


# Idealistic value of memory window in FeFET

K. Toprasertpong et al, IEEE TED **69**, 7113 (2022)



- When sufficient electric field is applied across FE, below  $P_r$  and  $E_c$  match those in major loop P-E curve



$\eta$  : form factor of P-E curve

$$\begin{aligned}
 & P_{FE\pm}(E_{\pm}) + \epsilon_{FE}\epsilon_0 E_{\pm} \\
 &= P_s \tanh\left(\frac{\eta(E_{\pm} \mp E_c)}{E_c}\right) + \epsilon_{FE}\epsilon_0 E_{\pm} \\
 &= \sigma_0 \approx 0 \\
 & \downarrow \\
 & E_{\pm} \approx \pm \frac{E_c}{1 + \frac{\epsilon_{FE}\epsilon_0 E_c \tanh(\eta)}{P_r}}
 \end{aligned}$$

$$MW = (E_+ - E_-)t_{FE} = \frac{\boxed{2E_c t_{FE}}}{1 + \frac{\epsilon_{FE}\epsilon_0 E_c \tanh(\eta)}{P_r}}$$

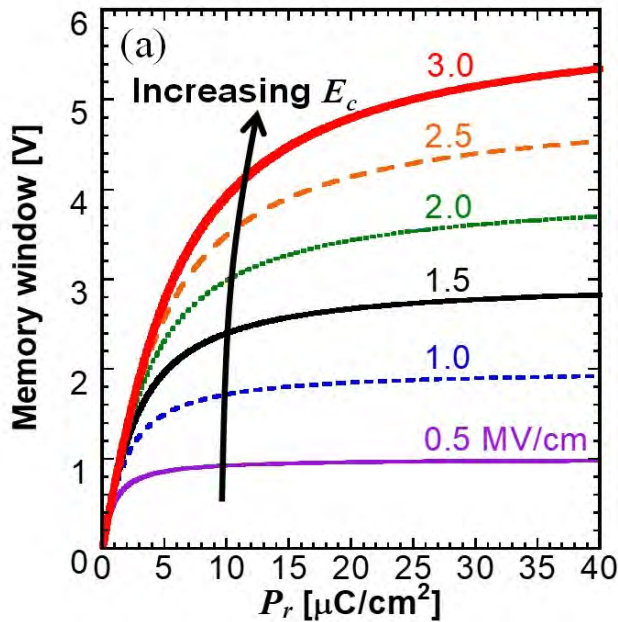
$$\begin{aligned}
 MW &= (E_+ t_{FE} - \frac{\sigma_0 t_{IL}}{\epsilon_{IL}\epsilon_0} + \varphi_s + \Phi_{MS}) \\
 &- (E_- t_{FE} - \frac{\sigma_0 t_{IL}}{\epsilon_{IL}\epsilon_0} + \varphi_s + \Phi_{MS}) \\
 &= (E_+ - E_-)t_{FE}
 \end{aligned}$$

- Under the idealistic condition, maximum memory window is given by  $2E_c t_{FE}$

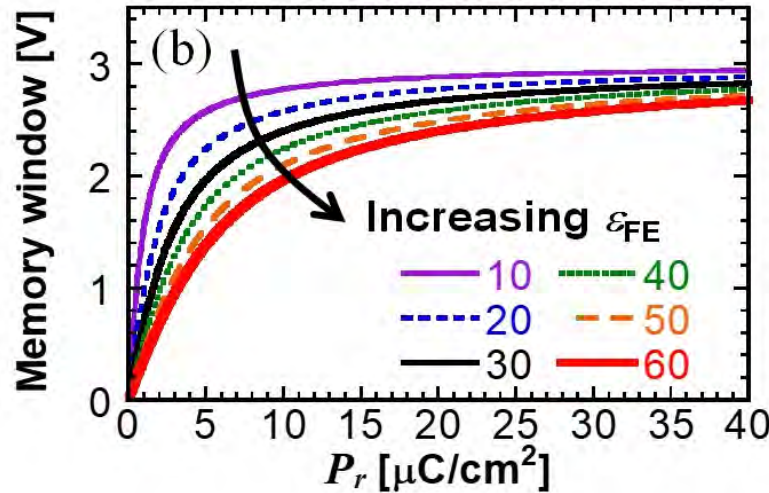
# For increasing memory window of FeFET

K. Toprasertpong et al, IEEE TED **69**, 7113 (2022)

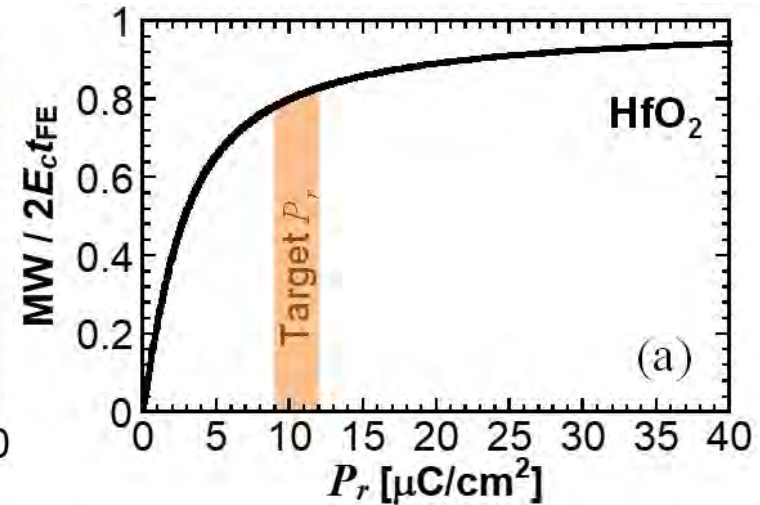
$$MW = (E_+ - E_-)t_{FE} = \frac{2E_c t_{FE}}{1 + \frac{\varepsilon_{FE} \varepsilon_0 E_c \tanh(\eta)}{P_r \eta}}$$



- higher  $E_c$



- lower  $\varepsilon_{FE}$



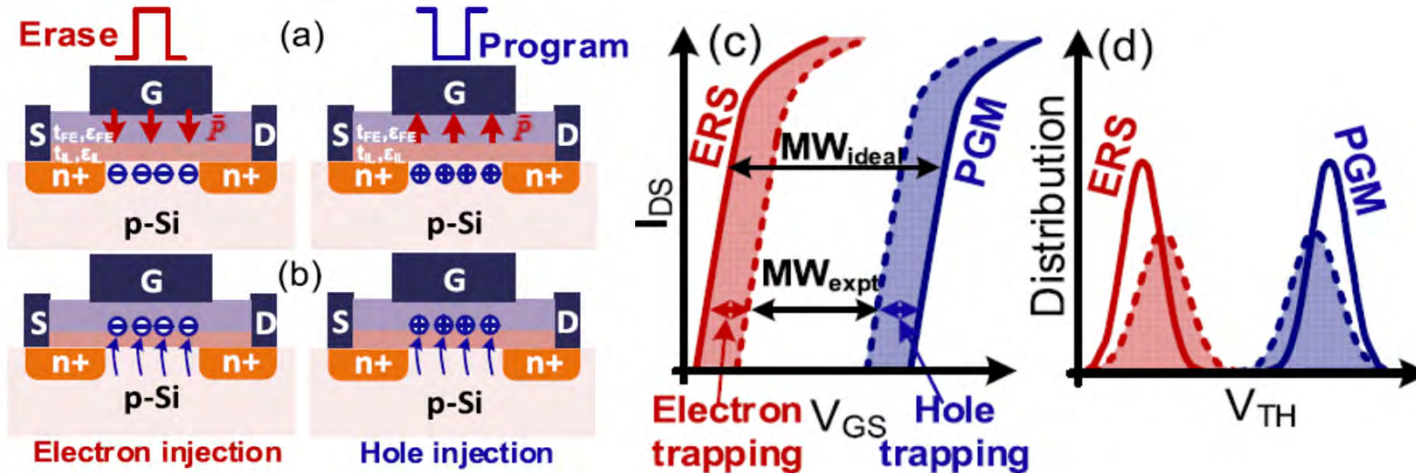
- $P_r > 3 \varepsilon_{FE} \varepsilon_0 E_c$   
 $\sim 10 \mu\text{C}/\text{cm}^2$

- HfO<sub>2</sub>-based ferroelectrics with higher  $E_c$  and lower  $\varepsilon_{FE}$  are suitable materials than conventional Perovskite ferroelectrics such as PZT and SBT

# Importance extrinsic factors to reduce memory window

## (1) Influence of trapped electron and holes

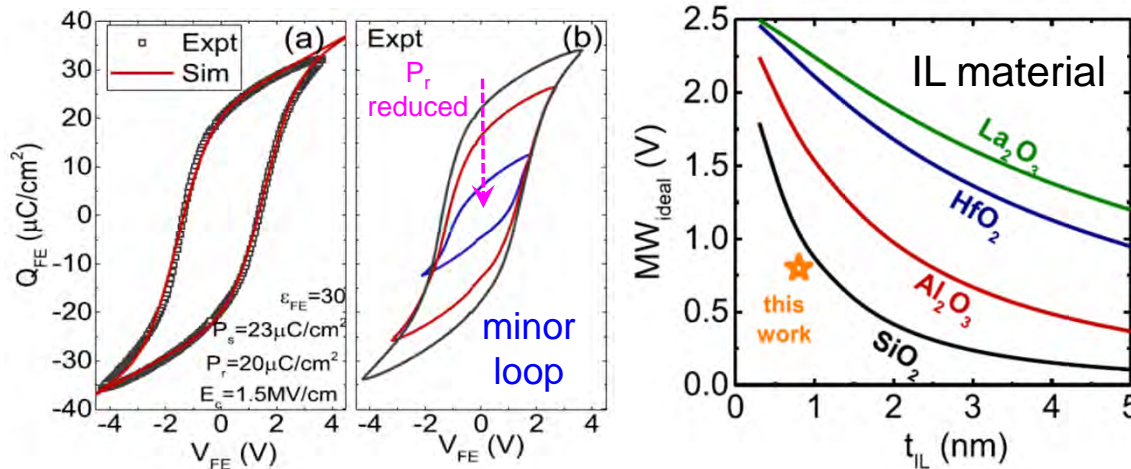
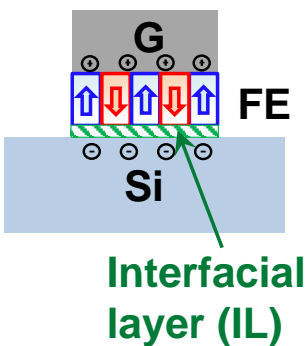
K. Ni et al., TED **65** (2018) 2461



- Electrons and holes trapped during erase and program operation reduce memory window

- Electric field and voltage across FE) and IL are determined by capacitance balance between FE and IL, when amounts of trapped charges are small
- Thicker IL and lower permittivity reduce the memory window

## (2) Reduction in $E_{FE}$ and $P_r$ due to interfacial layer (IL)

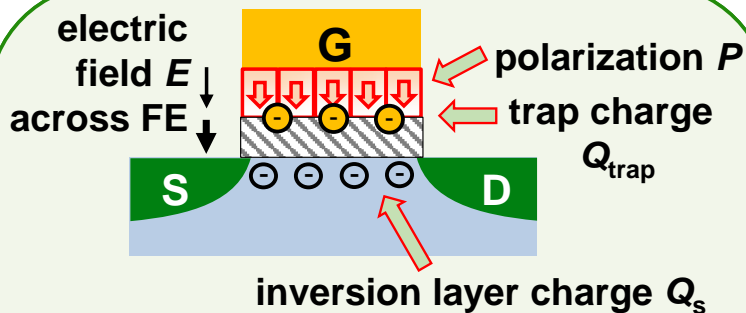


# Understanding of coupling between polarization and carrier traps in FeFET



# Importance of MFIS interfaces for FeFET operation

## Coupling between polarization, traps and inversion charges



$Q_s$  is induced by  $P$   
 $\Rightarrow$  a part of  $Q_s$  is trapped ( $Q_{\text{trap}}$ )  
 $\Rightarrow Q_{\text{trap}}$  changes  $E(x)$  across FE  
 $\Rightarrow P$  changes by  $E(x)$  across FE  
 ✘ **complicated characteristics**

## MFIS interface (MOS interface)

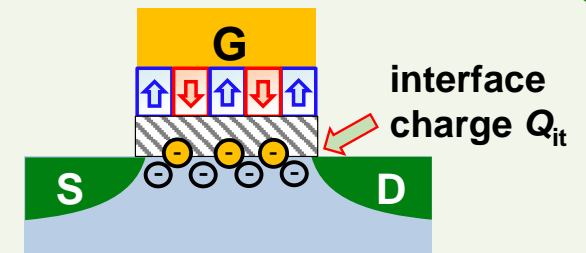
M : Metal  
 F : Ferroelectric  
 I : Insulator  
 S : Semiconductor

Basic question:

- typical  $P \sim 10\sim 20 \mu\text{C}/\text{cm}^2$
- $\rightarrow N_s = \sigma_s / q > 10^{14} \text{ cm}^{-2}$
- $\rightarrow$  too high  $N_s$  (typical  $N_s$  of MOSFET =  $10^{11}\sim 10^{13} \text{ cm}^{-2}$ )
- $\rightarrow E_{\text{IL}} = \sigma_s / \epsilon_{\text{IL}} > 30 \text{ MV}/\text{cm}$
- $\rightarrow$  too high  $E_{\text{IL}}$

K. Toprasertpong et al., Applied Physics A, 128 (2022) 1114

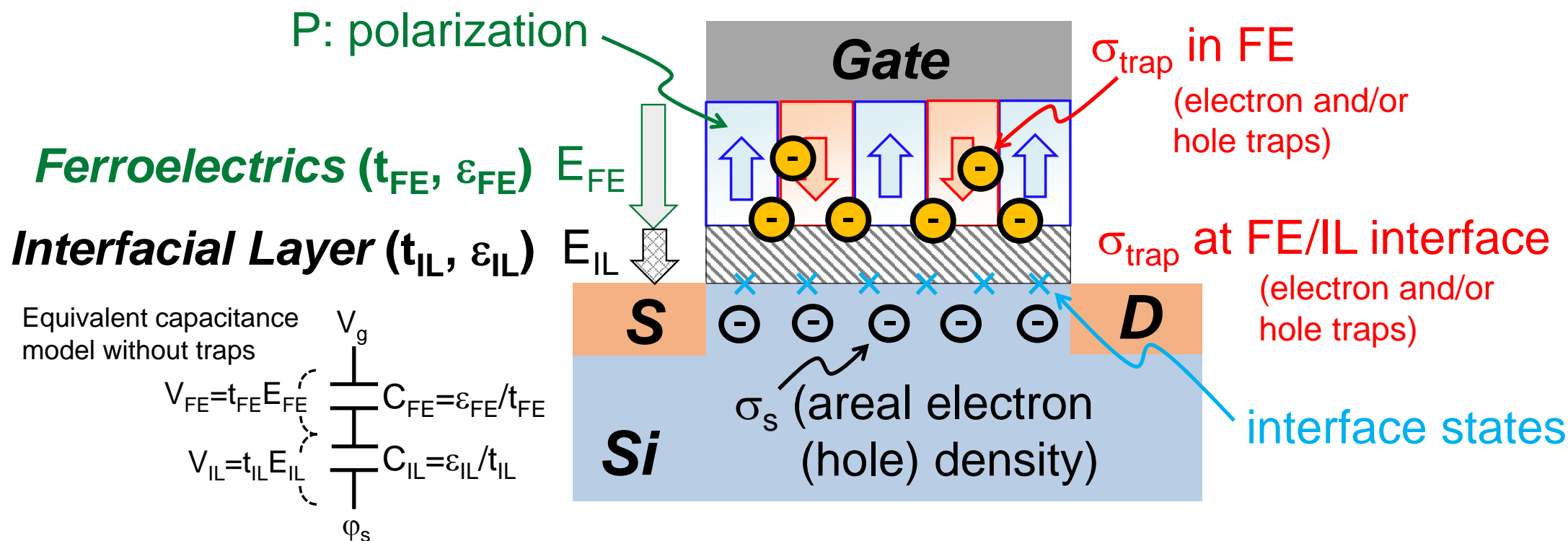
## Interface state $D_{\text{it}}$



- affect SS and mobility
- ✘ **degrade FET performance**
- (However, they do not cause complicated coupling with polarization, because  $E(x)$  across IL does not change at same surface potential with different  $P$ )

Understanding MFIS interface and carrier trapping properties is critical to FeFET operation and characteristics

# Issues of ferroelectric gate stacks and the impact on FeFET

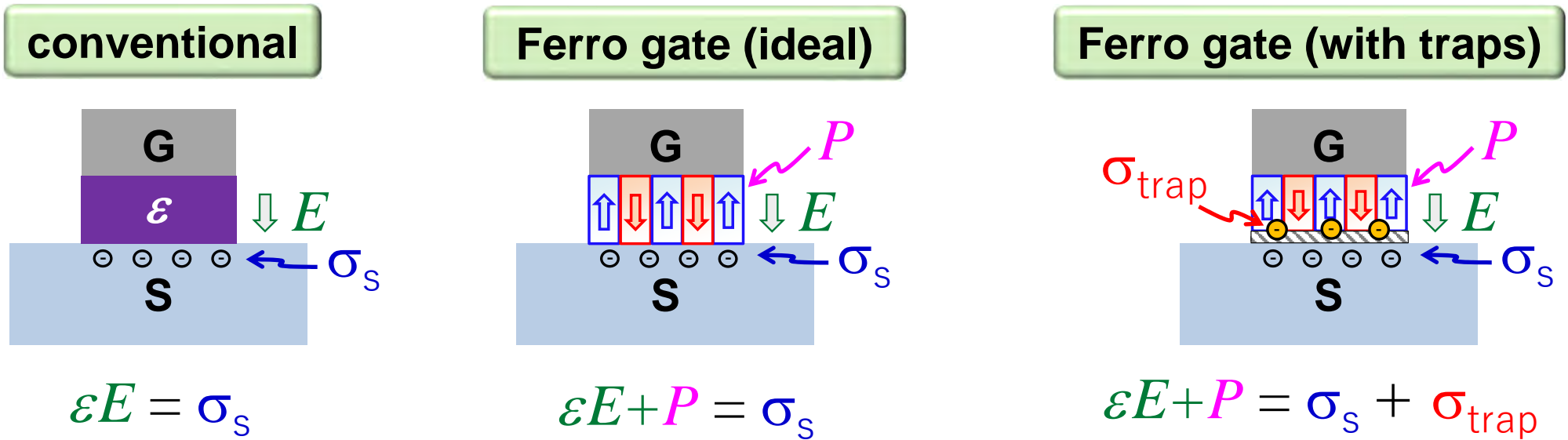


- When traps can be ignored, electric field across ferroelectrics ( $E_{FE}$ ) and electric field across interfacial layers ( $E_{IL}$ ) are determined by the capacitance ratio of FE and interfacial layers (IL)
- Here, thinner thickness and higher permittivity of IL lead to higher  $E_{FE}$
- When a large amount of traps are included, we need to take into account the charge balance between polarization, inversion-layer charges, trap charges and interface state charges, which can strongly affect  $E_{FE}$  and  $E_{IL}$

# Significant influence of traps on FeFET operation

Under inversion condition (MOSFET operation condition)

K. Toprasertpong et al.,  
IEDM (2019) 570



$P$ : polarization

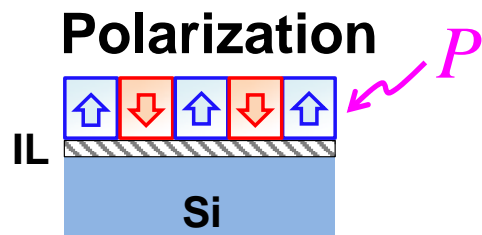
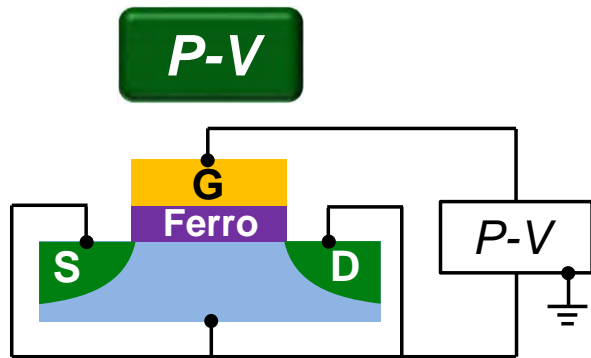
$\sigma_s$  : areal density of inversion charges

$\sigma_{\text{trap}}$  : areal density of trapped charges

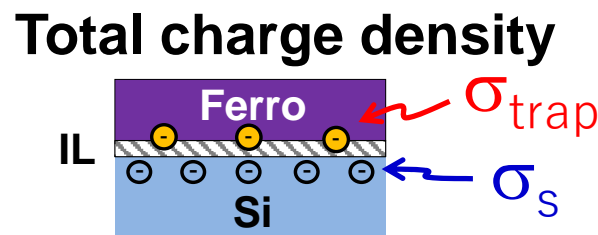
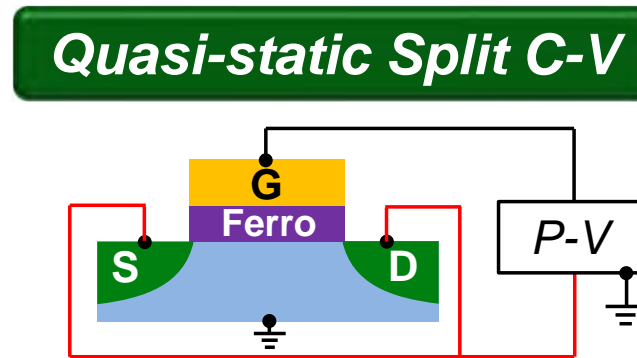
Quantitative discrimination of polarization, inversion charges and trapped charges is quite important to understand FeFET operation

# Evaluation method to quantify each component

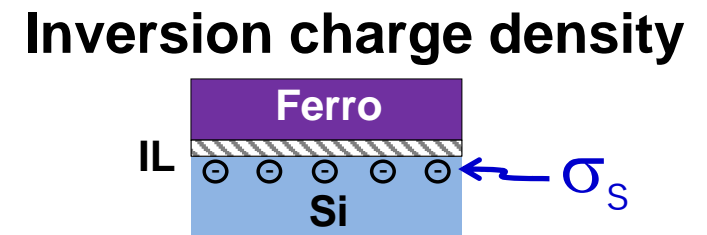
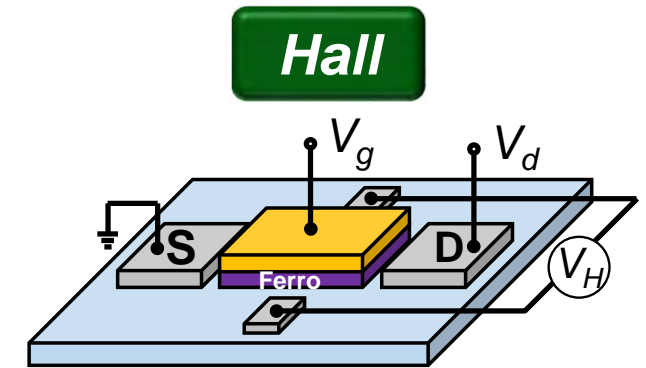
K. Toprasertpong et al., IEDM (2019) 570, VLSI Symp. (2020)TF1.5



$P$  measured



$\sigma_s + \sigma_{\text{trap}}$  measured

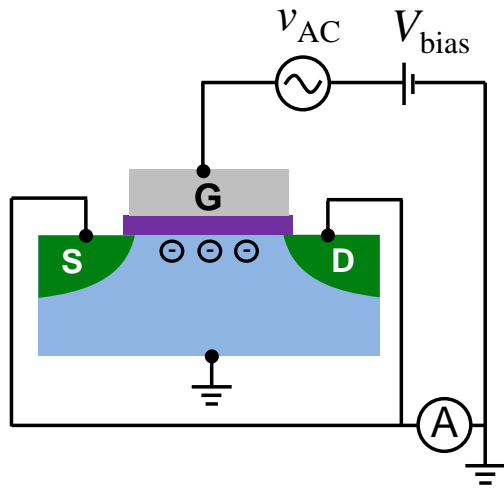


only  $\sigma_s$  measured

- We can independently evaluate  $P$ ,  $\sigma_s$  and  $\sigma_{\text{trap}}$  by using (1) P-V, (2) quasi-static (QS) split C-V, (3) Hall measurements
- The contribution of traps ( $\sigma_{\text{trap}}$ ) on FeFET operation can be quantified



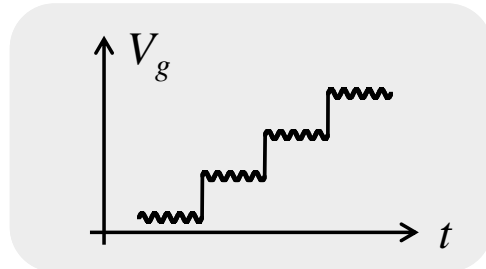
# Evaluation of areal inversion charge density by conventional split C-V



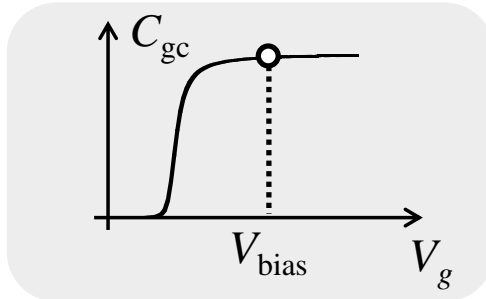
$C_{gc}$ : gate-channel capacitance

$$\sigma_s = qN_s$$

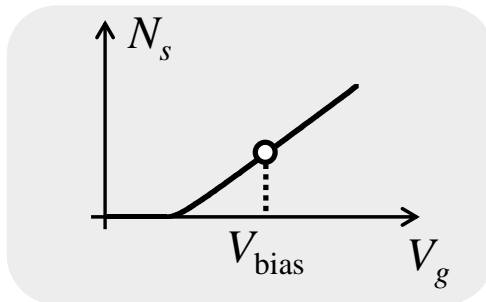
- When traps and interface states can be ignored,  $N_s$  corresponds to areal density of free (mobile) inversion carriers



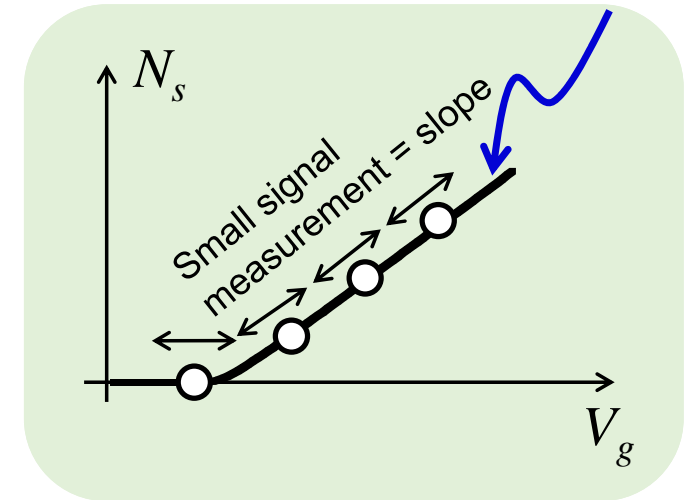
measure capacitance by ac signal



integration of capacitance  $\Rightarrow$  charge density



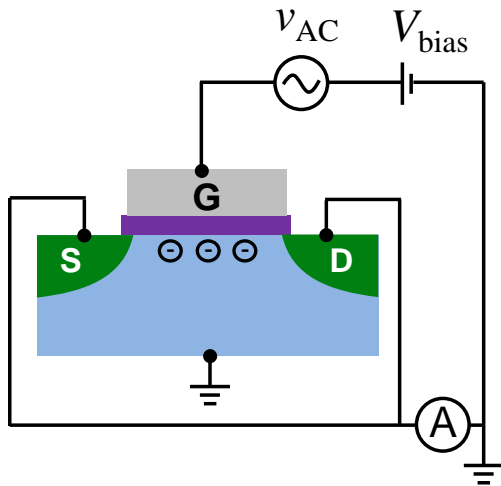
Relationship to be determined



Real procedure for determining relationship between  $N_s$  and  $V_g$

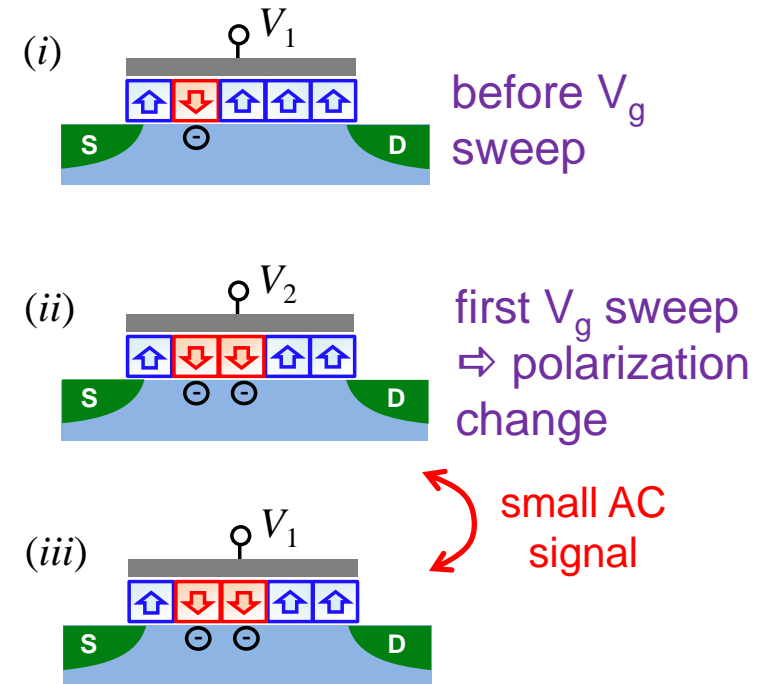
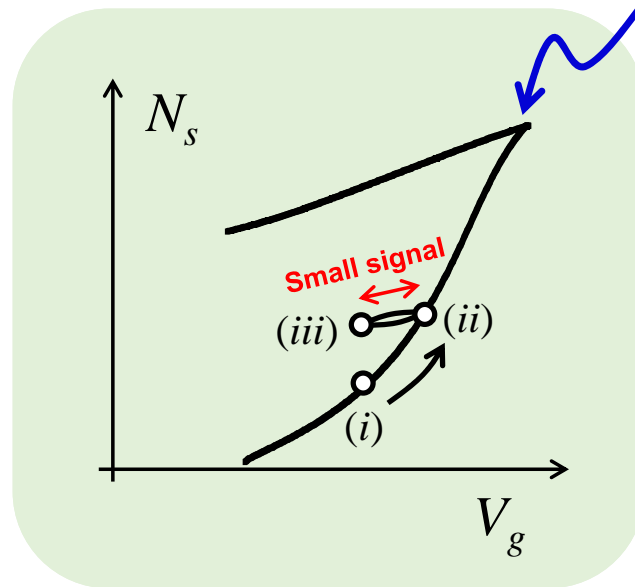
- (1) Evaluate slope of  $N_s$ - $V_g$  characteristics by small signal ac measurement
- (2) Represent  $N_s$ - $V_g$  by connecting the slope at each  $V_g$  point

# Problem of applying conventional split C-V to FeFET



**FeFET**

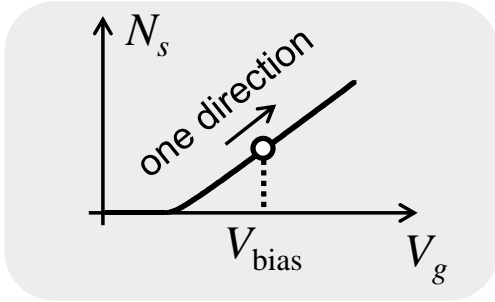
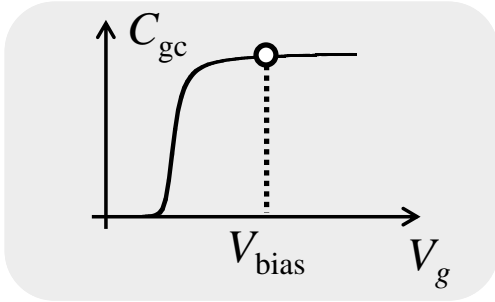
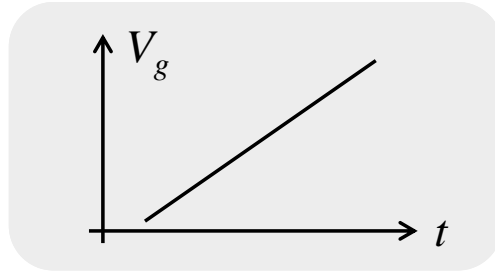
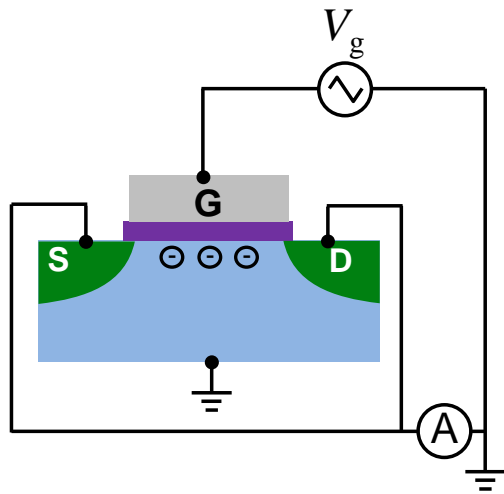
Relationship to be determined



polarization retained  
 ⇒ response of minor-loop  
 ⇒ AC response ≠ slope of  $N_s - V_g$

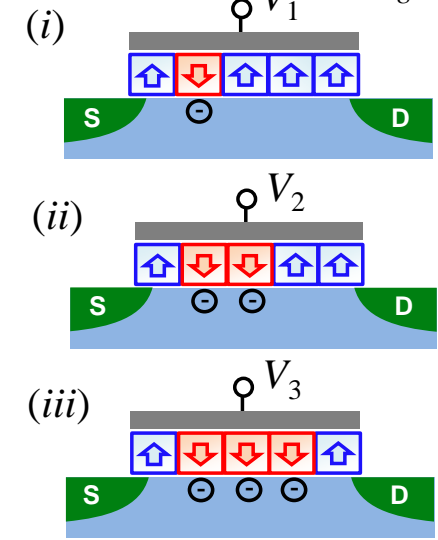
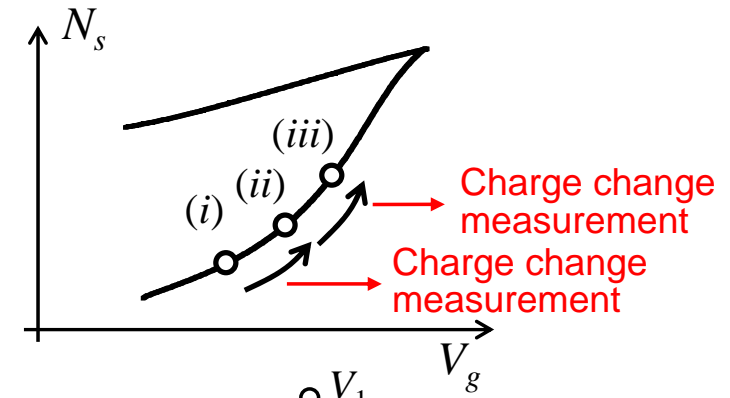
**Conventional split C-V is not applicable to determination of  $N_s$  in FeFET**

# Application of quasi-static split C-V to FeFET



$$C = \frac{dQ}{dV}$$

$$N_s = \frac{1}{q} \int C_{gc} dV_g$$



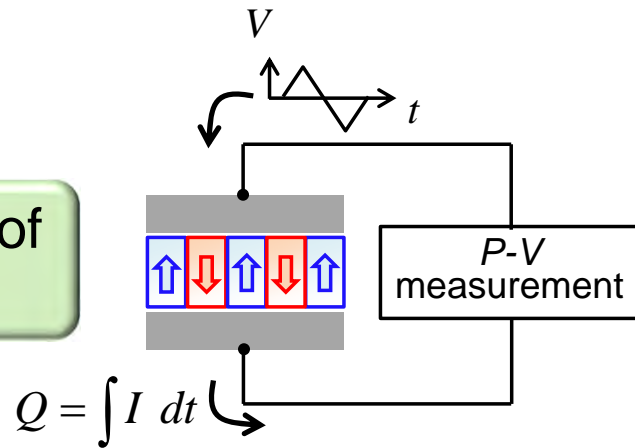
K. Toprasertpong *et al.*,  
IEDM19, 570, 2019

- When a large-signal (one-directional and one-time sweep) C-V measurement is used instead of the small-signal one, the "change in  $N_s$  due to polarization reversal" can be correctly evaluated
- Note that this  $N_s$  includes channel charges, interface charges and injected/trapped charges

# P-V and quasi-static split C-V measurements

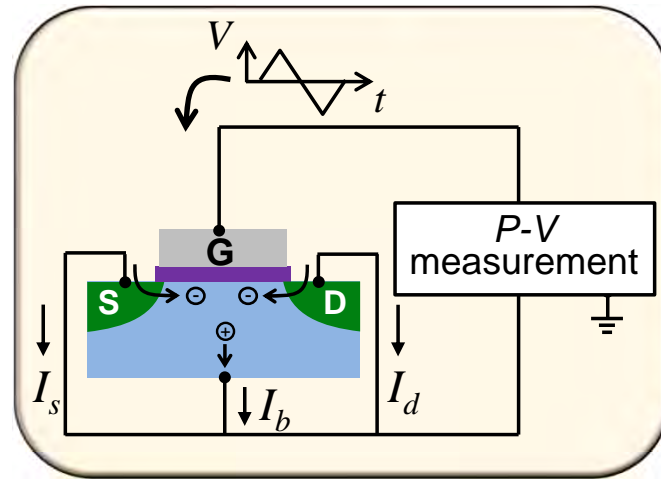
P-V measurement of MFM capacitor

= charge movement during voltage sweep (not P but  $\Delta P$  measured)

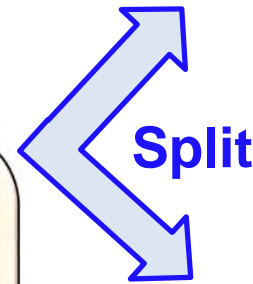


P-V measurement of FeFET

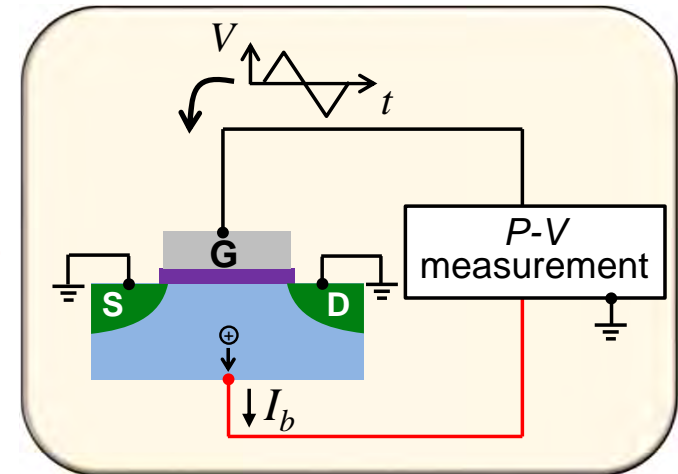
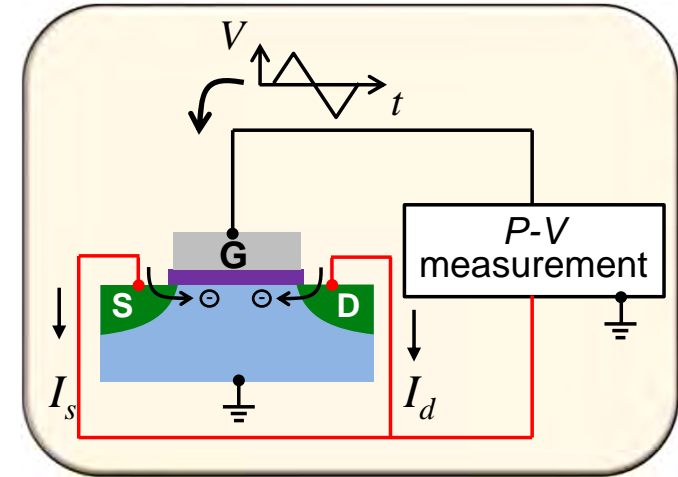
K. Toprasertpong *et al*, Appl. Phys. Lett. **116**, 242903, 2020



S/D current



substrate current



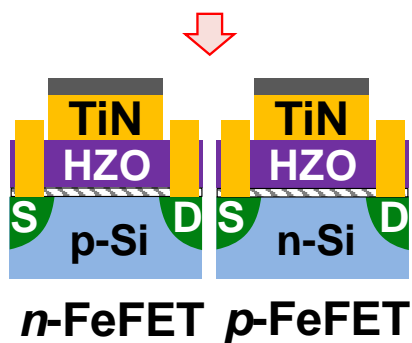
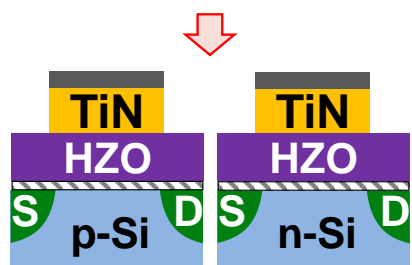
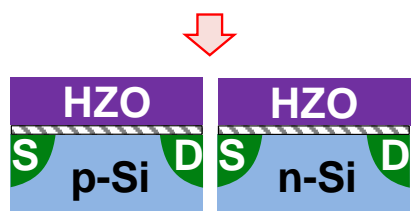
K. Toprasertpong *et al.*, IEDM19, 570, 2019

Measurable by standard P-V evaluation machines



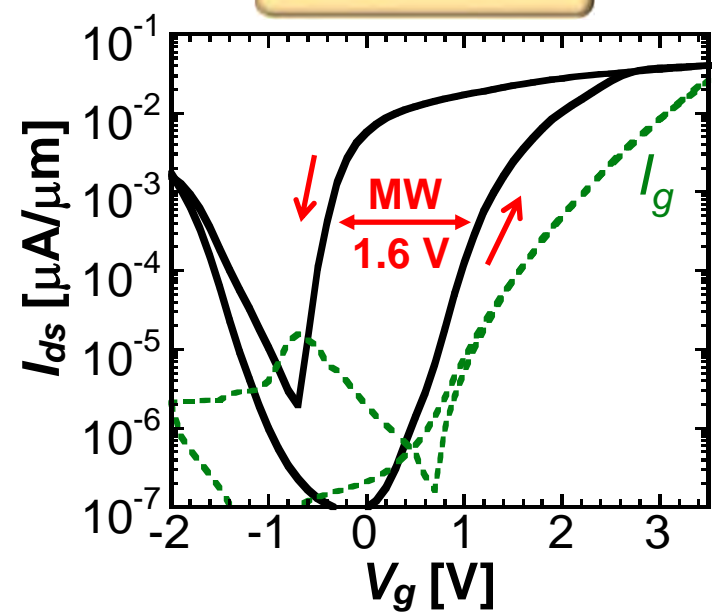
# $I_d$ - $V_g$ characteristics of n- and p-FeFET with same gate stacks

K. Toprasertpong et al., IEDM (2019) 570, VLSI Symp. (2020)TF1.5

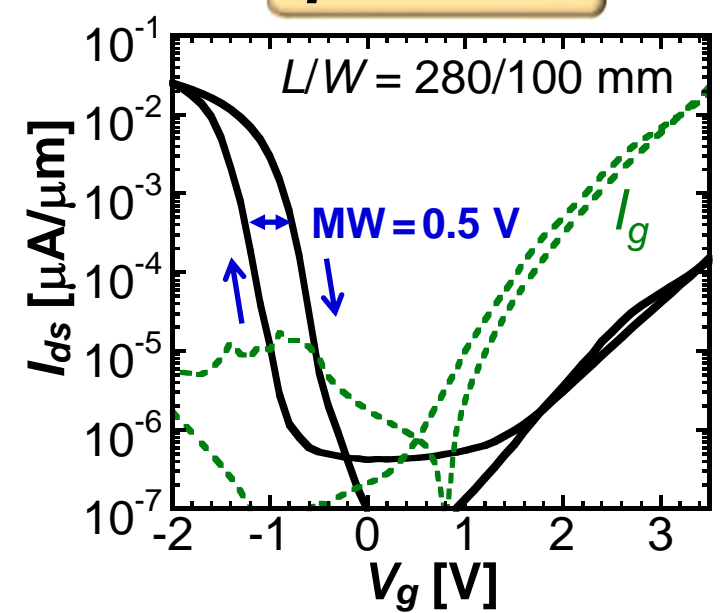


Same HZO and same process

**n-FeFET**



**p-FeFET**



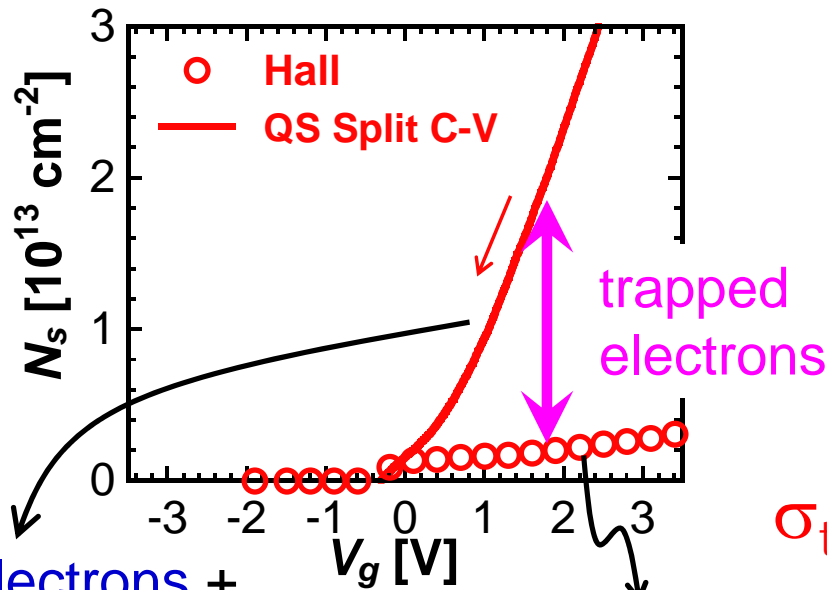
- Under the same HZO and gate stack, memory window of n-FeFET is much higher than that of p-FeFET
- These devices are used for characterization of polarization, inversion carriers and trapped carriers

# Asymmetric carrier trapping in positive and negative gate voltage

## Electron distribution under positive $V_g$

K. Toprasertpong *et al.*, IEDM19 (2019) 570; VLSI Symp. (2020) TF1.5, Appl. Phys. A, 128 (2022) 1114

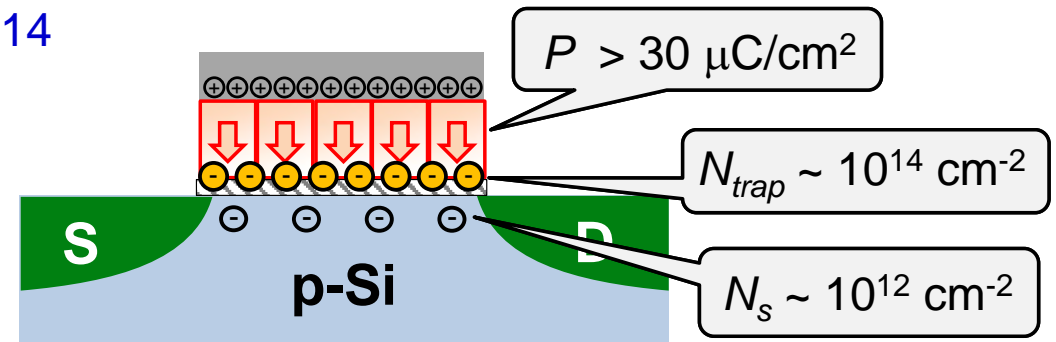
### Electrons in n-FeFET



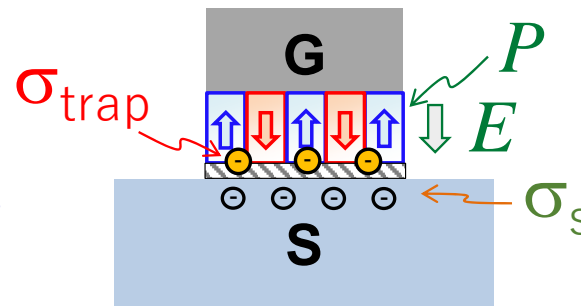
Free electrons +  
trapped electrons  
 $\sim 10^{14} \text{ cm}^{-2}$

Free electrons  
 $\sim 10^{12} \text{ cm}^{-2}$

Similar large trap density at FE/IL interfaces has been reported independently by R. Ichihara *et al.* (Kioxia), VLSI symp. (2020)



• Although ferroelectric polarization induces an areal electron density of around  $10^{14} \text{ cm}^{-2}$ , the induced electrons are mostly trapped in HZO (probably around HZO/IL interface)



Electric field across FE is shielded by large amounts of electron traps

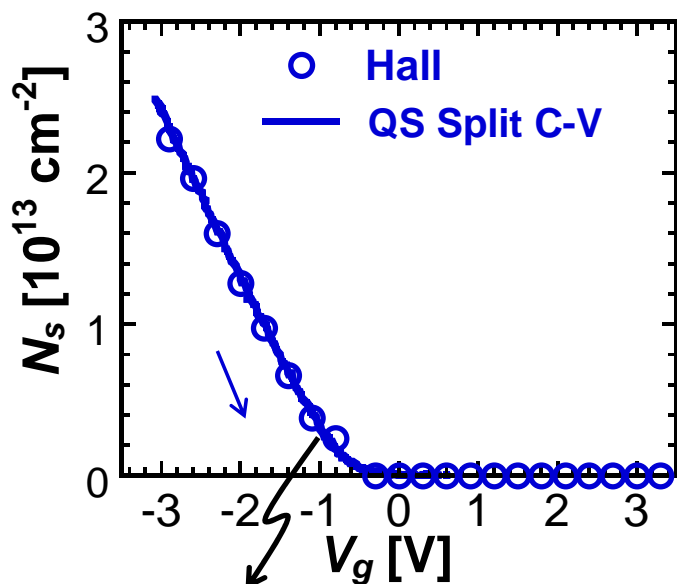
$$\epsilon E + P = \sigma_s + \sigma_{\text{trap}}$$

# Asymmetric carrier trapping in positive and negative gate voltage

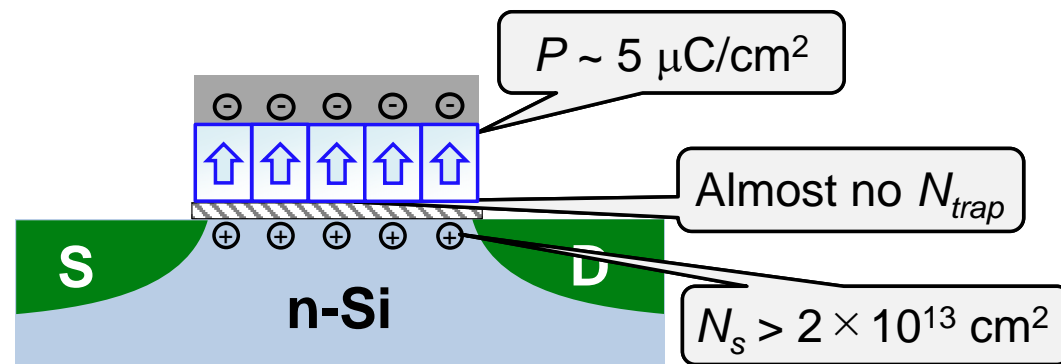
## Hole distribution under negative $V_g$

K. Toprasertpong *et al.*, IEDM19 (2019) 570; VLSI Symp. (2020) TF1.5, Appl. Phys. A, 128 (2022) 1114

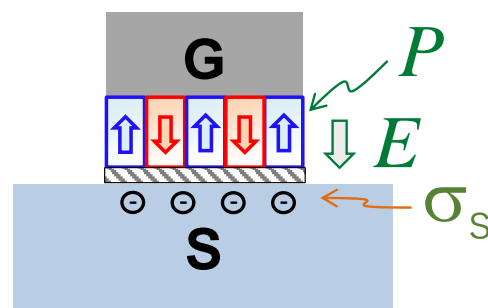
### Holes in p-FeFET



Free holes + trapped holes  $\sim$   
 Free holes  $\rightarrow$  no significant trapping



- Polarization-induced inversion-layer holes are rarely trapped  $\Rightarrow$  Polarization  $P$  = hole areal density  $N_s$ , which is much higher than electron one
- $P$  in p-FeFET is smaller than that in n-FeFET



Electric fields across ferroelectric and IL layers are determined by capacitance ratio

$$\epsilon E + P = \sigma_s$$

# Electron-trap-enhanced polarization in n-FeFET

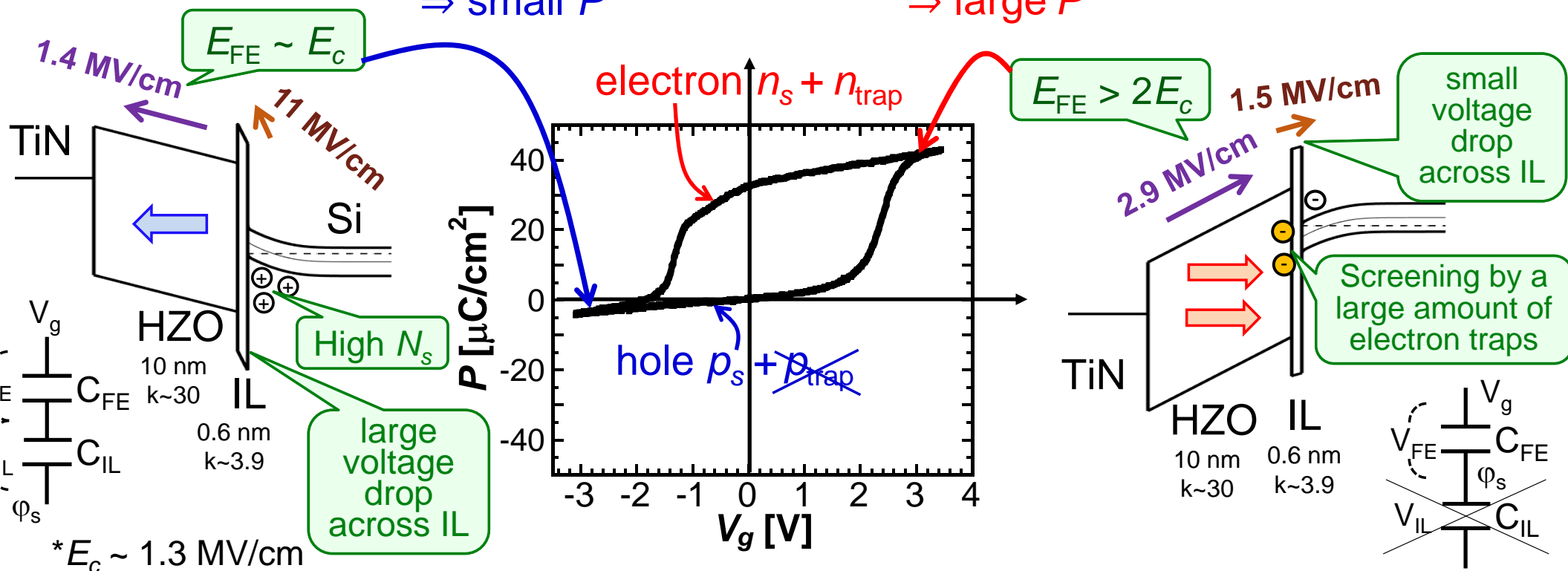
K. Toprasertpong et al., IEDM (2019) 570, VLSI Symp. (2020)TF1.5; Appl. Phys. A, 128 (2022) 1114

negative  $V_g$

High electric field in IL  
 $\Rightarrow$  small  $P$

High electric field in HZO  
 $\Rightarrow$  large  $P$

positive  $V_g$



In  $p$ -FeFET,  
 high  $N_s \Rightarrow$  high  $E_{IL} \Rightarrow$  low  $E_{FE} \Rightarrow$  small  $P$

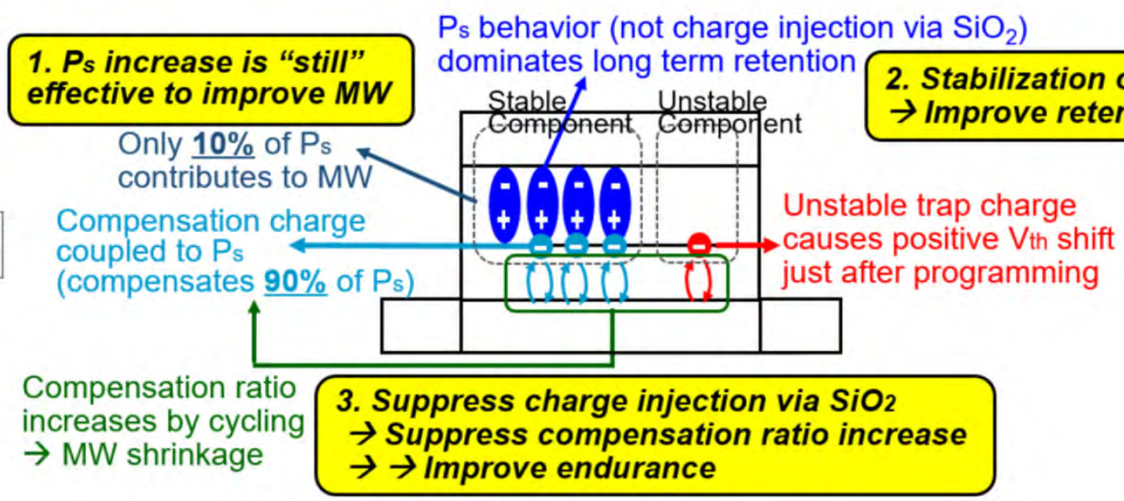
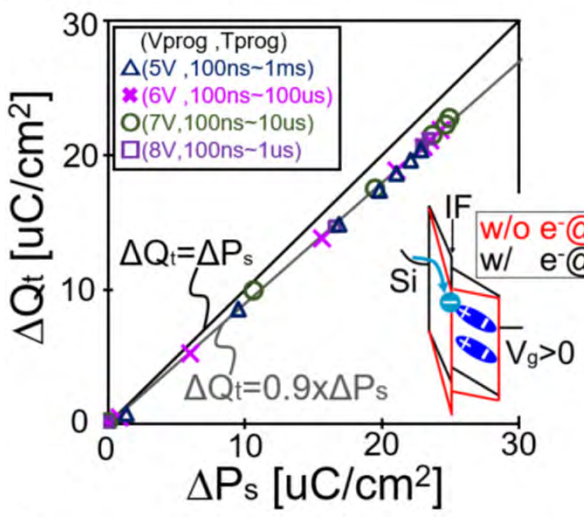
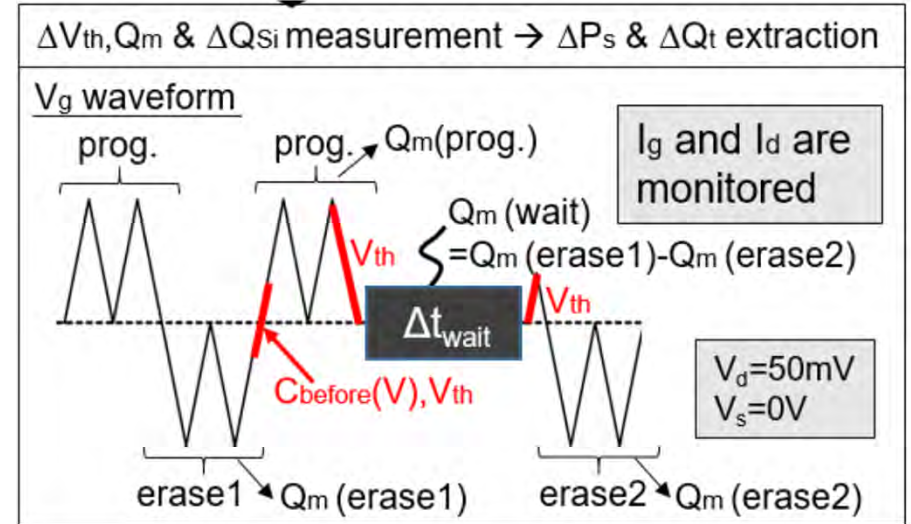
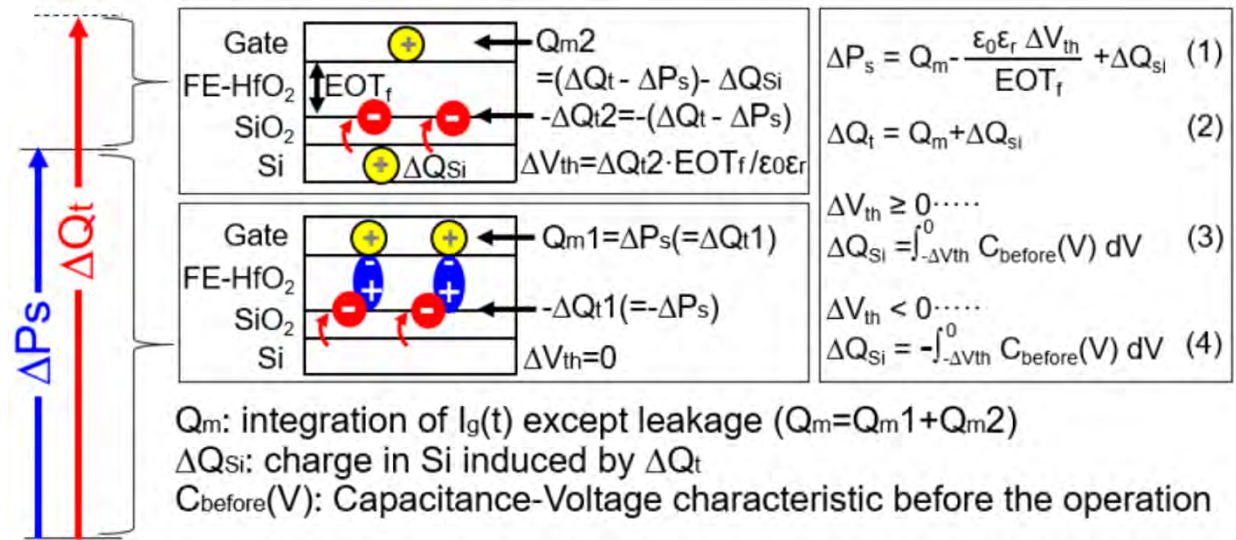
In  $n$ -FeFET, screening by electron trap  $\Rightarrow$   
 high  $E_{FE} \Rightarrow$  large  $P \Rightarrow$  large memory window



# Another report on trap-assisted polarization in FeFET

## FE-HfO<sub>2</sub>/SiO<sub>2</sub>/Si FeFET

R. Ichihara et al., VLSI Symp., (2020), IEDM, 130 (2021)

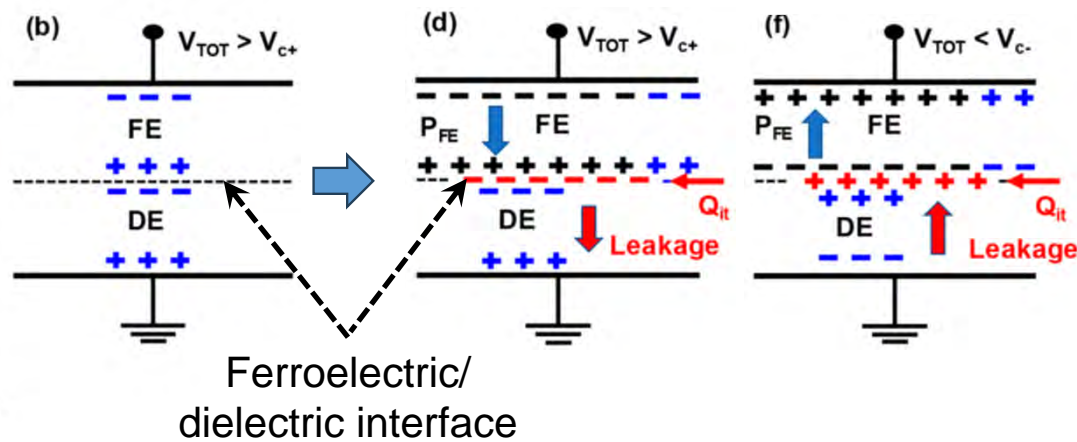
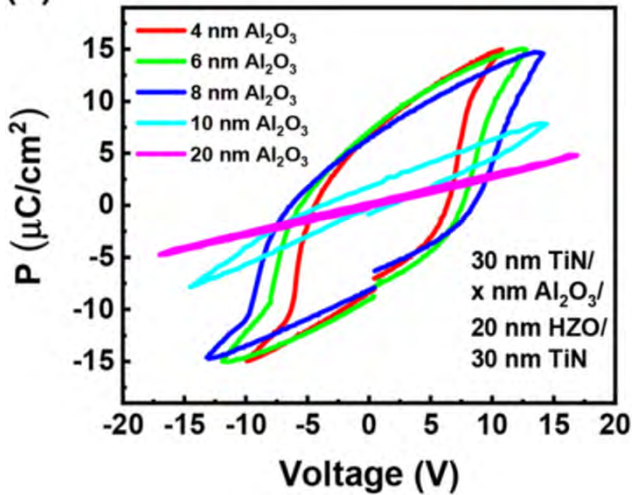


- Polarization and trapped charges are estimated by monitoring  $I_g$  and  $I_d$  separately
- Trapped charges near FE/IL interfaces amount to 90 % of polarization

# Carrier traps at ferroelectric/IL interface

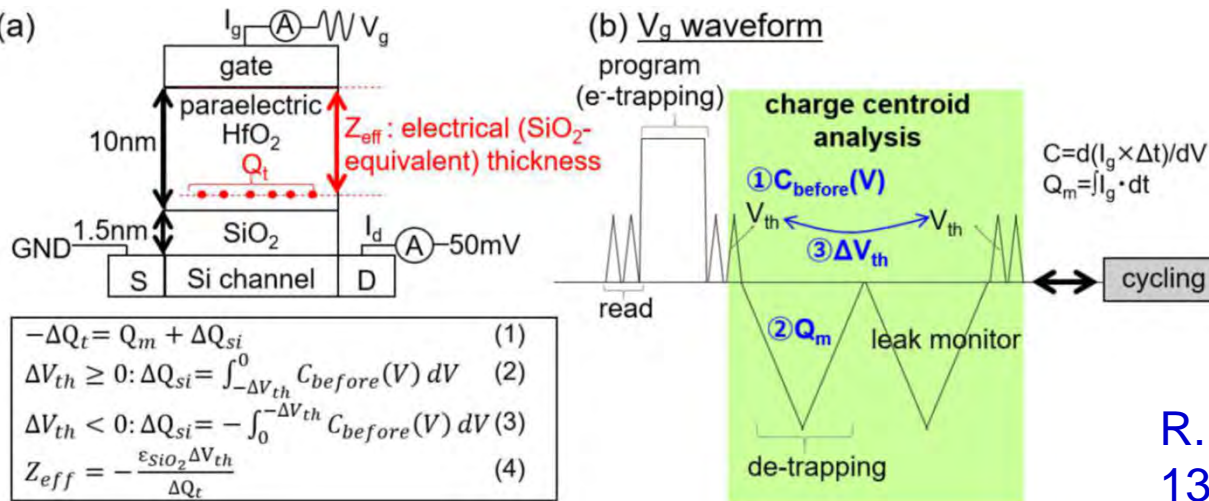
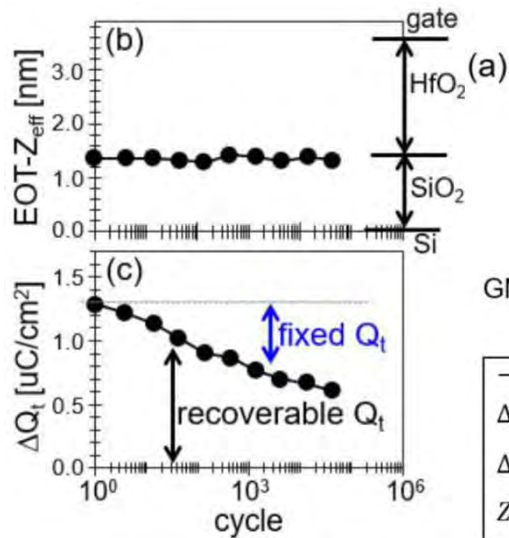
## MFIM capacitors

M. Si et al., ACS Appl. Electron. Mater. 1, 745 (2019)



- Full polarization switching of an FE layer in an MFIS capacitor is obtained by leakage-current-induced charges at the FE/ultrathin-IL interface

## Paraelectric HfO<sub>2</sub>/SiO<sub>2</sub>/Si FET



- The trap position estimated from  $I_g$  and  $I_d$  for similar paraelectric HfO<sub>2</sub>/SiO<sub>2</sub>/Si FETs is almost at the HfO<sub>2</sub>/SiO<sub>2</sub> interface

R. Ichihara et al., IEDM, 130 (2021)



# Pros and cons of large amounts of electron traps in FeFETs

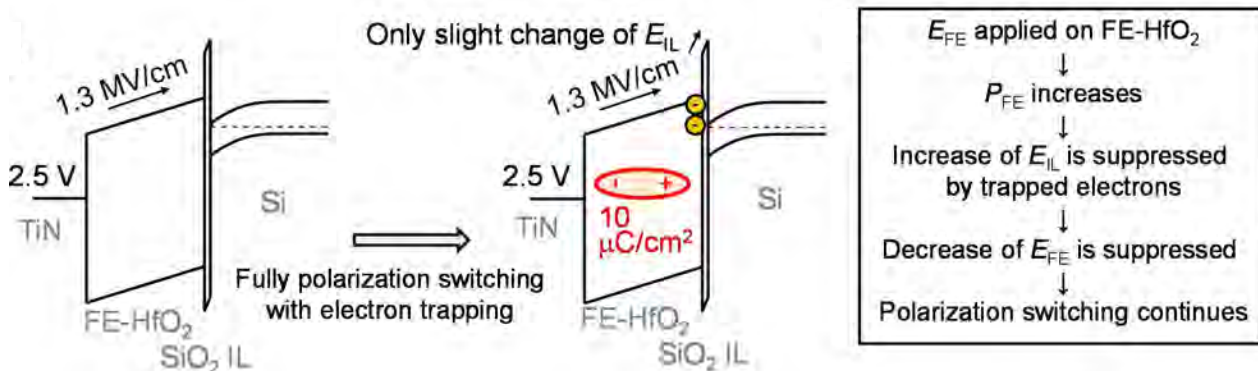
## Impact of large amounts of electron traps around FE/IL interfaces

- Cons

- reduction in memory window due to existing traps
- memory window narrowing due to generated traps
- necessity of long read delay time after write

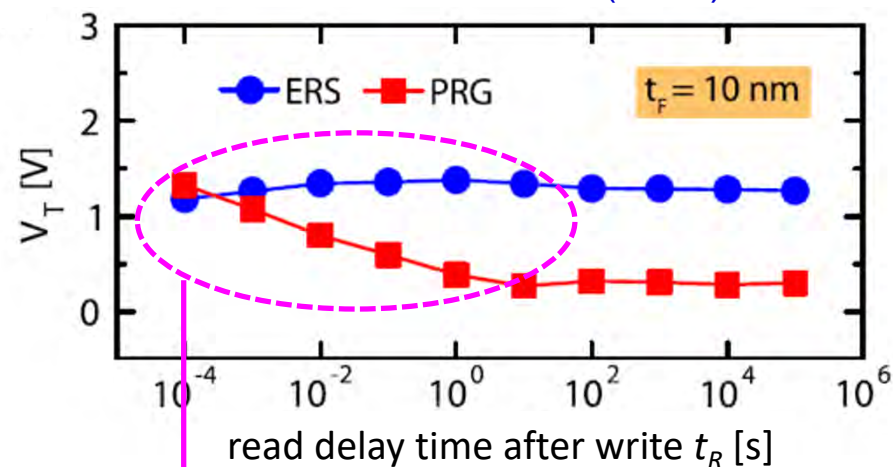
- Pros

- increased electric field across FE (trap-assisted polarization switching)
- mitigation of depolarization field



K. Toprasertpong et al, Appl. Phys. A 128, 1114 (2022)

Mulaosmanovic et al, TED 66 (2019) 3828



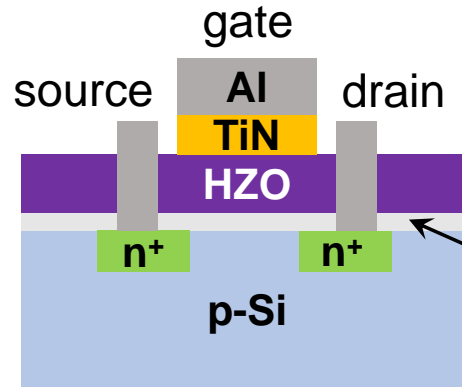
lower PRG  $V_{th}$  after positive  $V_g$  pulse is obtained after sufficient read delay time to induce **electron de-trapping** (explained later)

# Impact of annealing temperature on structure and FeFET characteristics

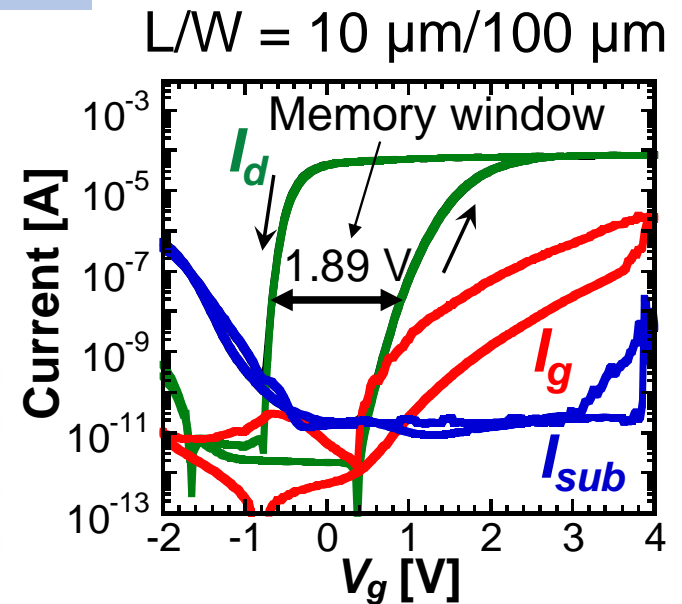
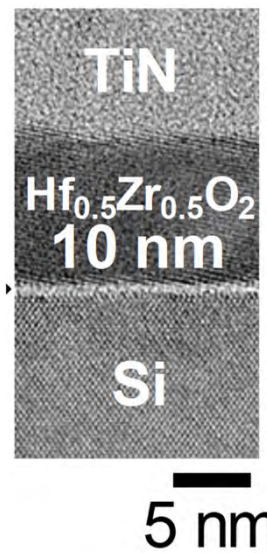
- Si sub cleaning
- SiO<sub>2</sub> oxidation 208nm
- Marking 400nm
- Active area definition by BHF
- SiO<sub>2</sub> re-oxidation 25nm
- S/D patterning by photoresist
- Ion implantation
  - P 30keV 2x10<sup>14</sup> cm<sup>-2</sup>
- Thermal activation @ 1000 °C
- SiO<sub>x</sub> 0.6 nm with SC2
- ALD Hf<sub>0.5</sub>Zr<sub>0.5</sub>O<sub>2</sub> 10nm
- TiN 16 nm by EB evaporation
- Al 650 nm
- Gate patterning
- Contact etching BHF
- Al:Si(2%) 350nm for S/D Contact
- Al 500 nm for back contact

PMA 300 ~ 700 °C 30s → annealing for crystallization of HZO  
→ critical process parameter

K. Toprasertpong et al., IEDM (2019) 570, VLSI Symp. (2020)TF1.5, APL 116 (2020) 242903, EDL 41 (2020) 1588

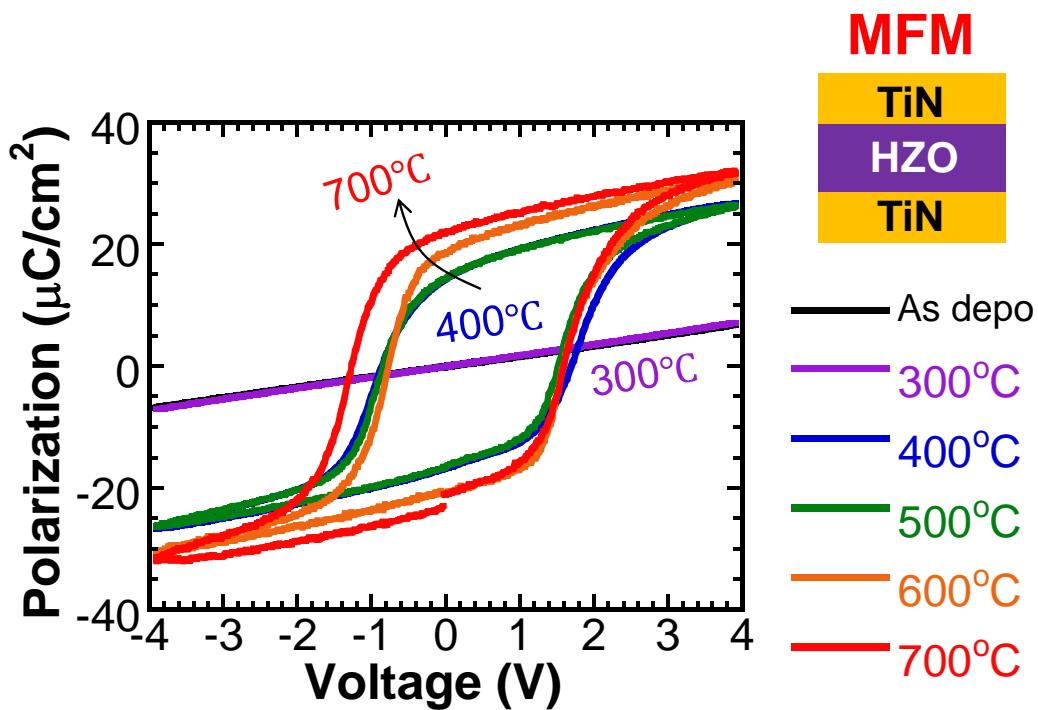


Al: 650nm  
TiN: 16nm  
HZO: 10nm  
Interfacial SiO<sub>x</sub>: 0.6nm

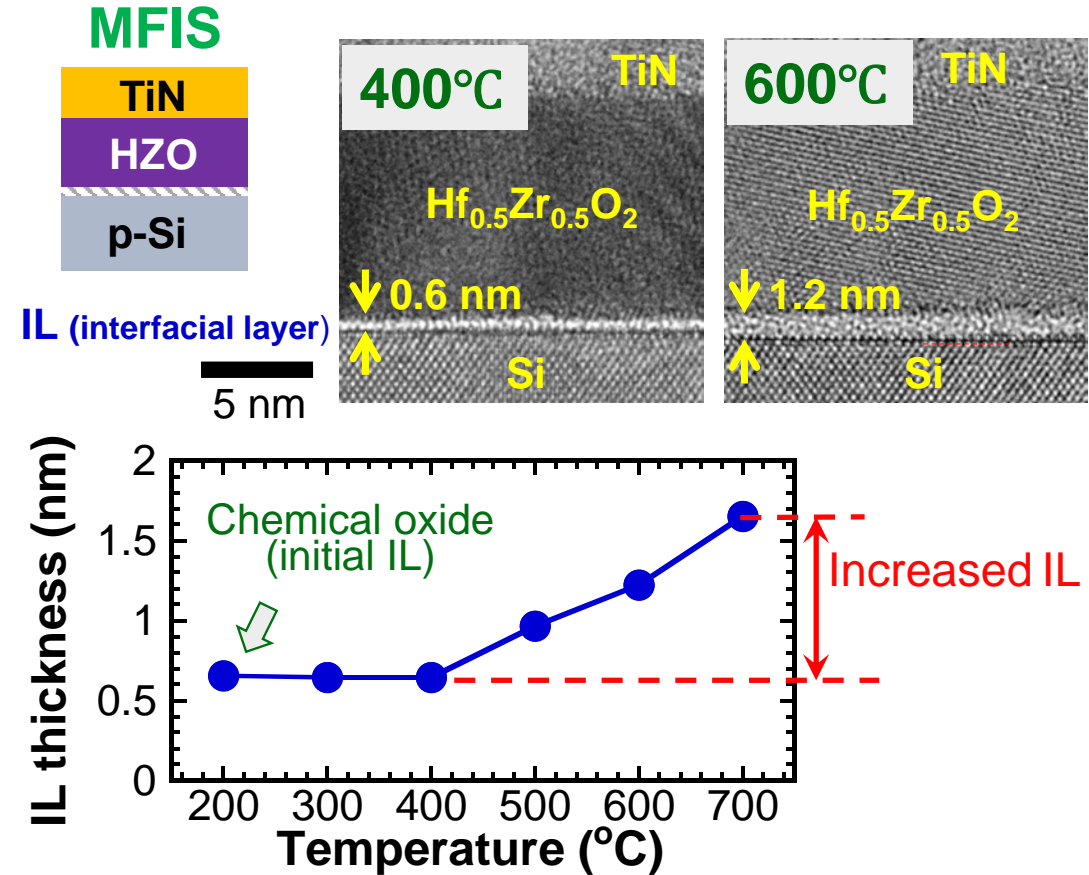




# Impact of annealing condition on ferroelectric and MFIS interface properties



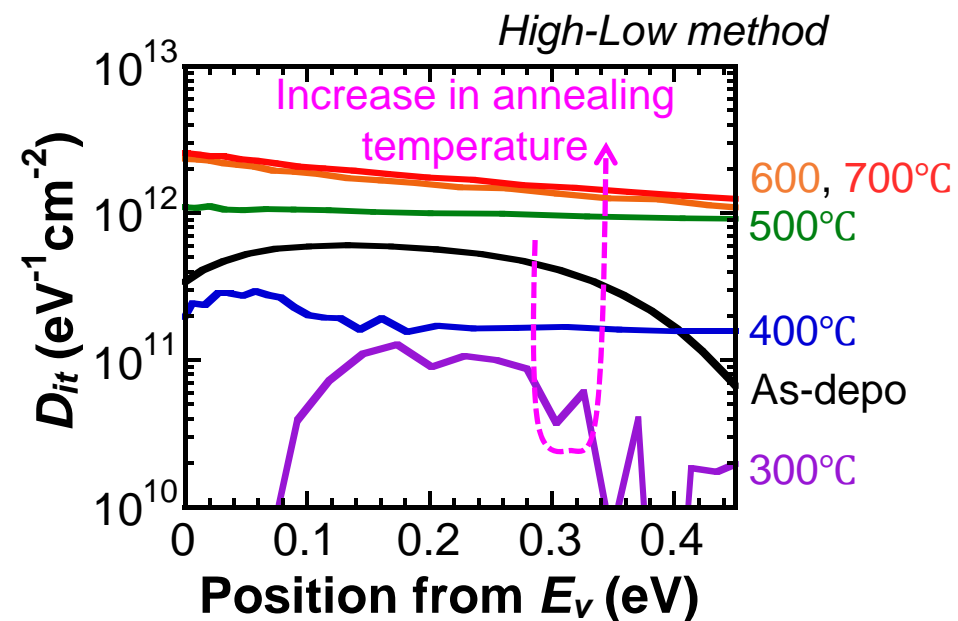
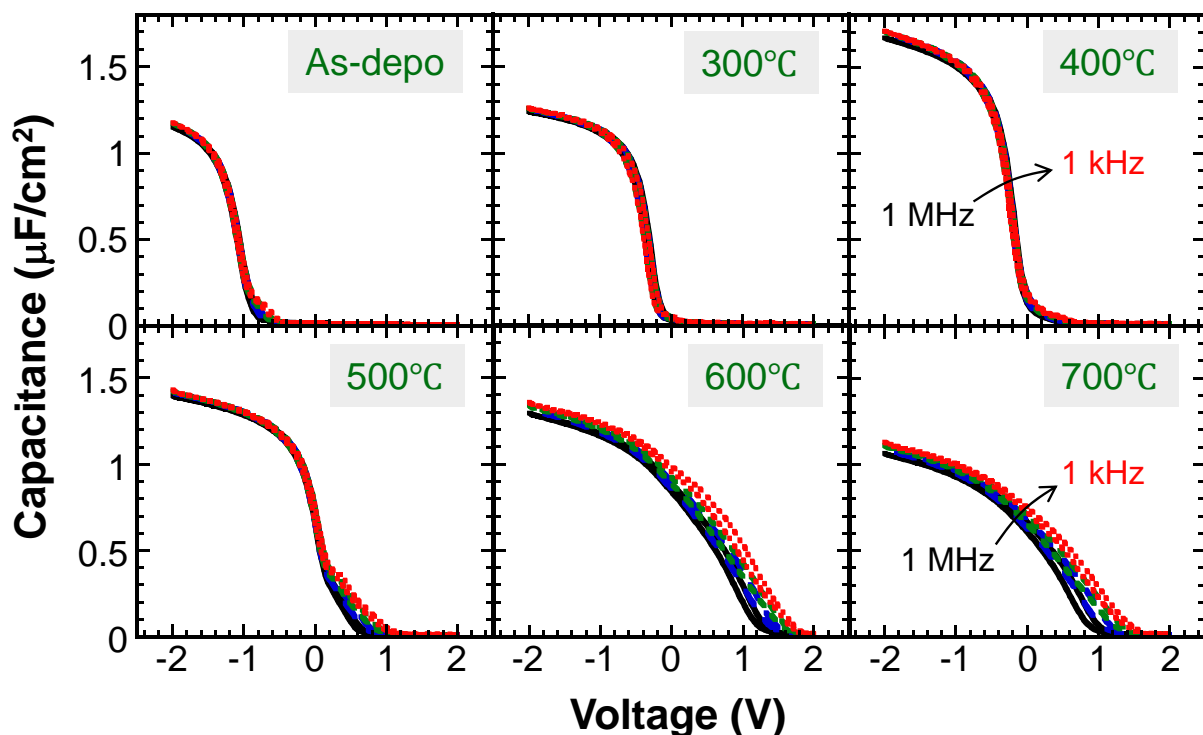
- Ferroelectric characteristics appear at annealing temperatures higher than 400 °C
- Gradual increase in polarization with an increase in annealing temperature



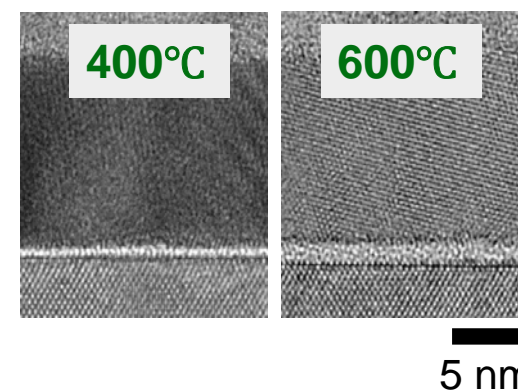
- Annealing temperature higher than 400 °C → Increase in IL thickness

# Evaluation of MFIS interface properties by C-V characteristics

K. Toprasertpong *et al*, IEEE Electron. Dev. Lett. **41**, 1588 (2020)

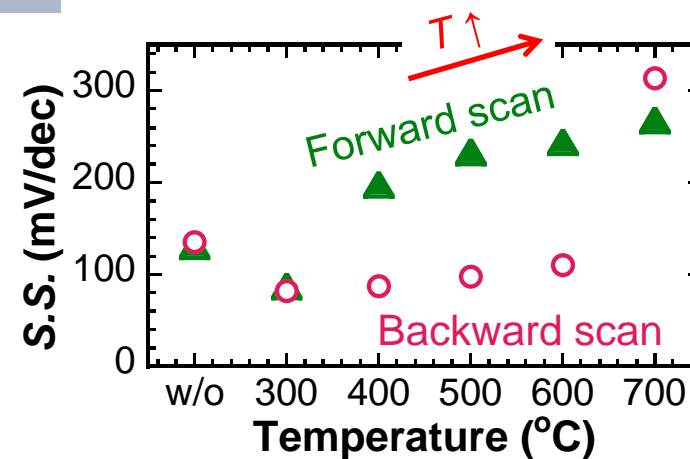
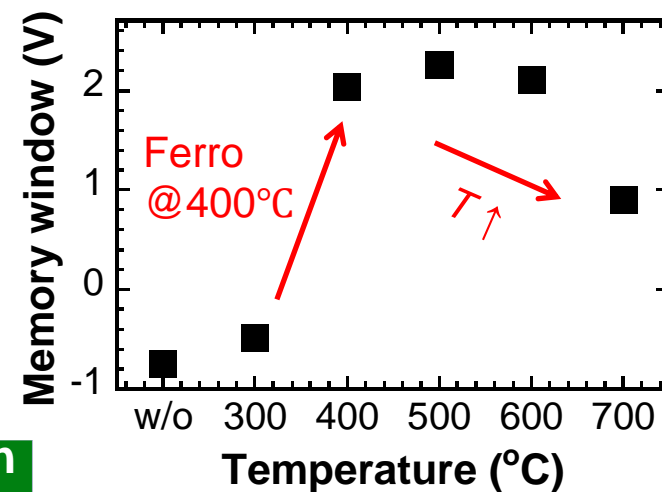
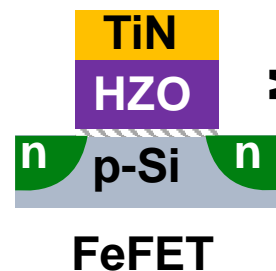
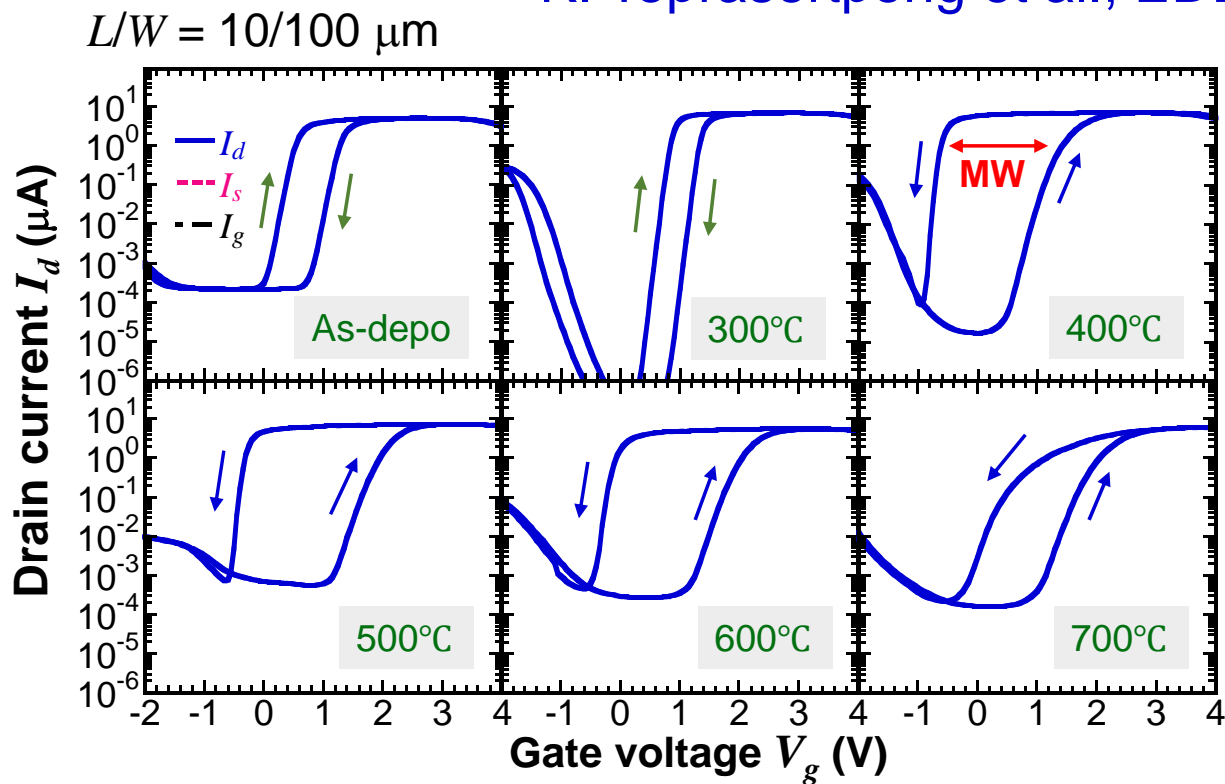


High annealing temperature degrades MFIS interface  
⇒ Interfacial properties of IL grown during annealing may not be good



# Impact of annealing condition on FeFET characteristics

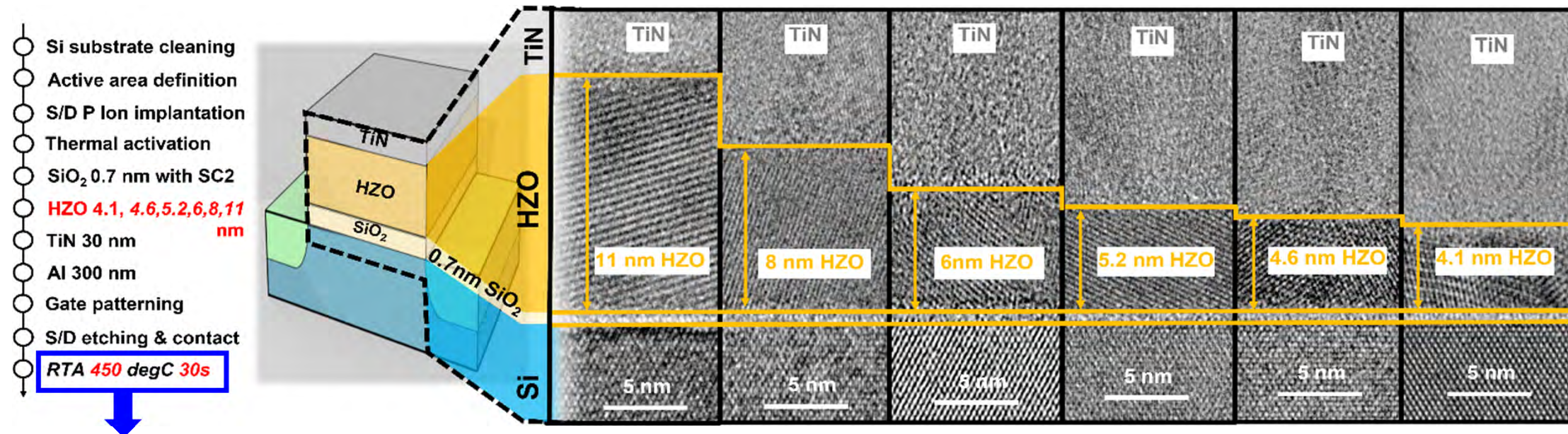
K. Toprasertpong et al., EDL 41 (2020) 1588



- Annealing is necessary for crystallization of ferroelectric phase, while annealing at too high temperature degrades MFIS interfaces (high  $D_{it}$ , high S.S., high  $I_{off}$  and narrow memory window)
- ⇒ Optimum annealing temperature exists (400°C in this study)

# HZO FeFETs with different HZO thickness

Z. Cai et al., VLSI Tech. and Circ., T5-2 (2023); published in IEEE TED (2024)



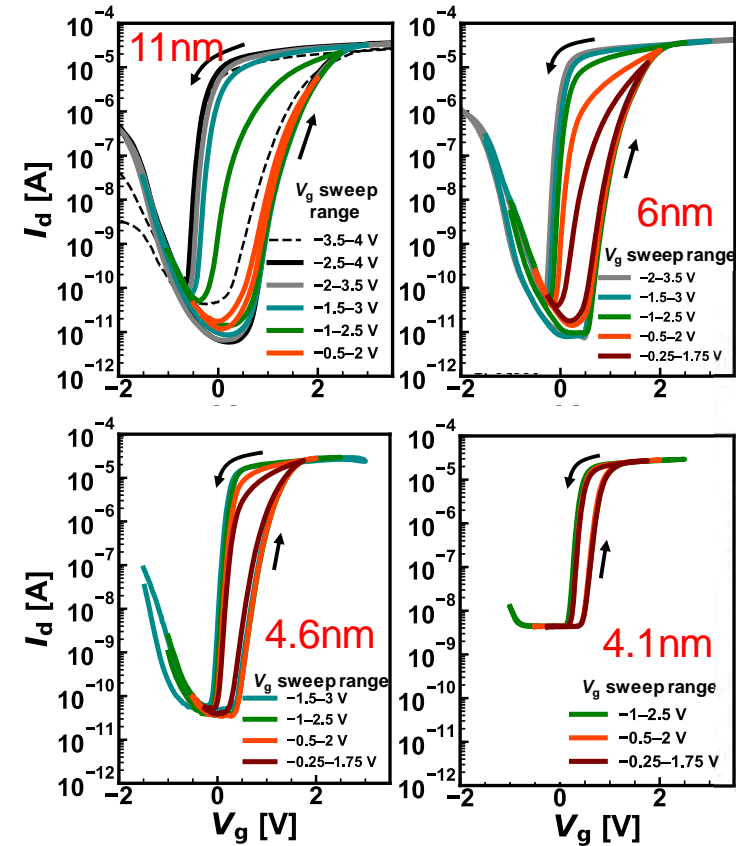
✓ Enough ferro-electric property and good interface quality

- ❑ Impact of HZO film thickness scaling on FeFET characteristics and reliability is also systematically examined for low voltage operation and better reliability in FeFETs
- ❑ ALD Hf<sub>0.5</sub>Zr<sub>0.5</sub>O<sub>2</sub> films with 0.7-nm-thick SiO<sub>2</sub> interfacial layers show good crystallinity from 11 nm to 4.1 nm after 450°C annealing

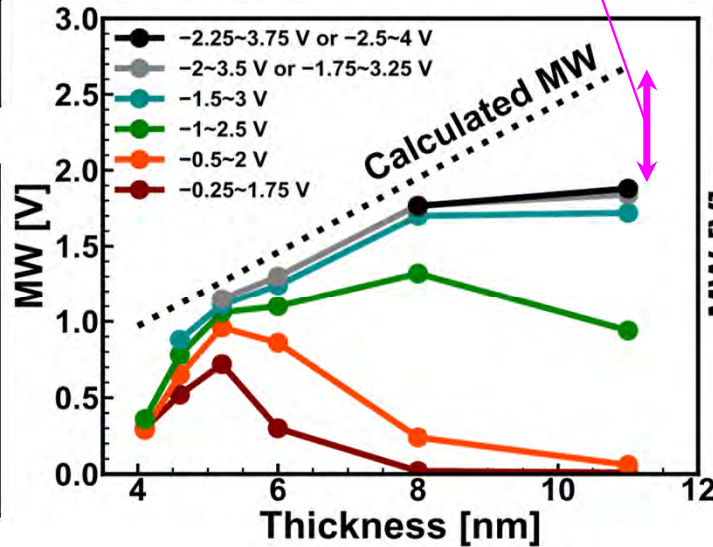


# Memory window evaluated by DC and pulse measurements

Z. Cai et al., VLSI Tech. and Circ., T5-2 (2023);  
published in IEEE TED (2024)

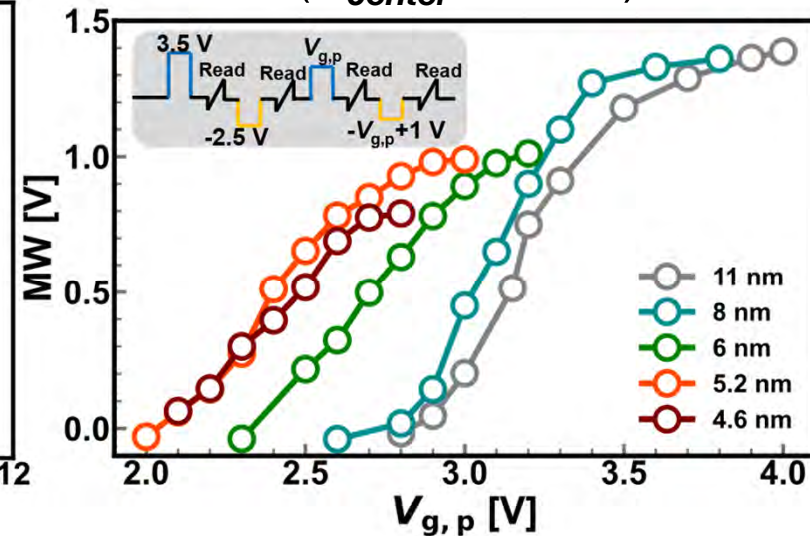


due to higher density of traps



$$V_{g,n} = 1 \text{ V} - V_{g,p}$$

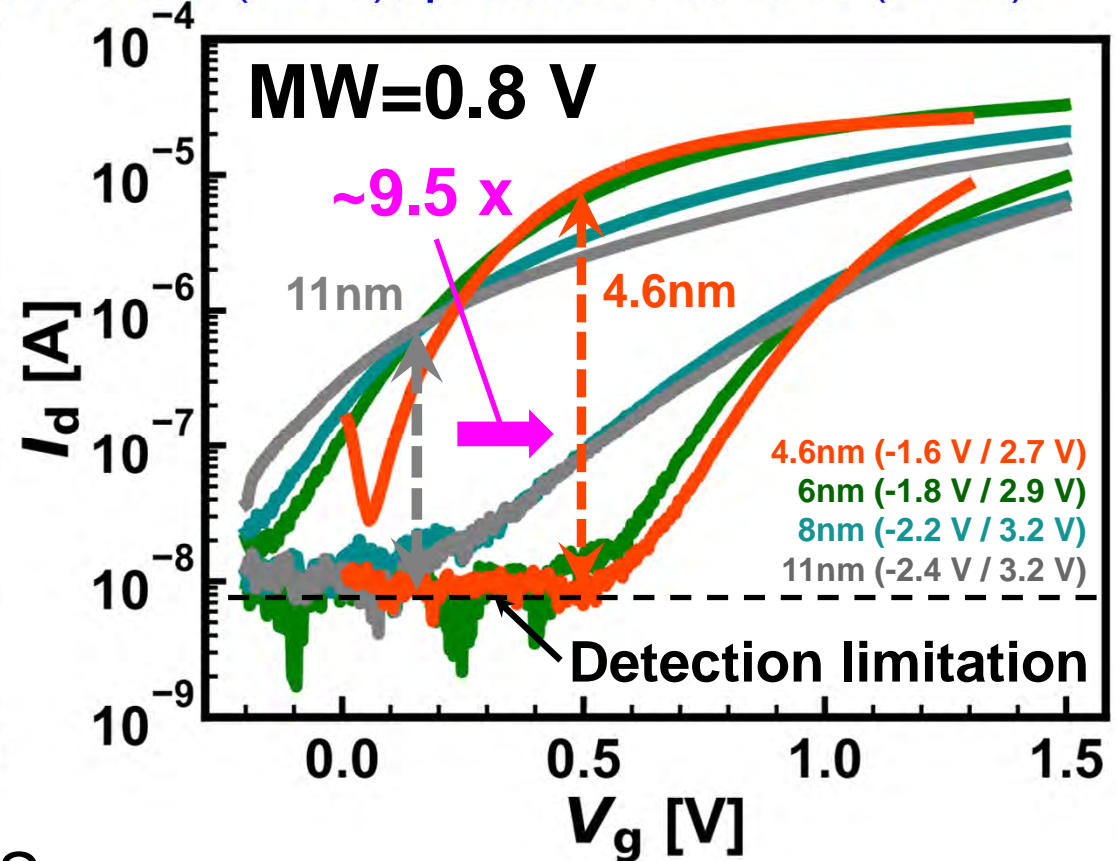
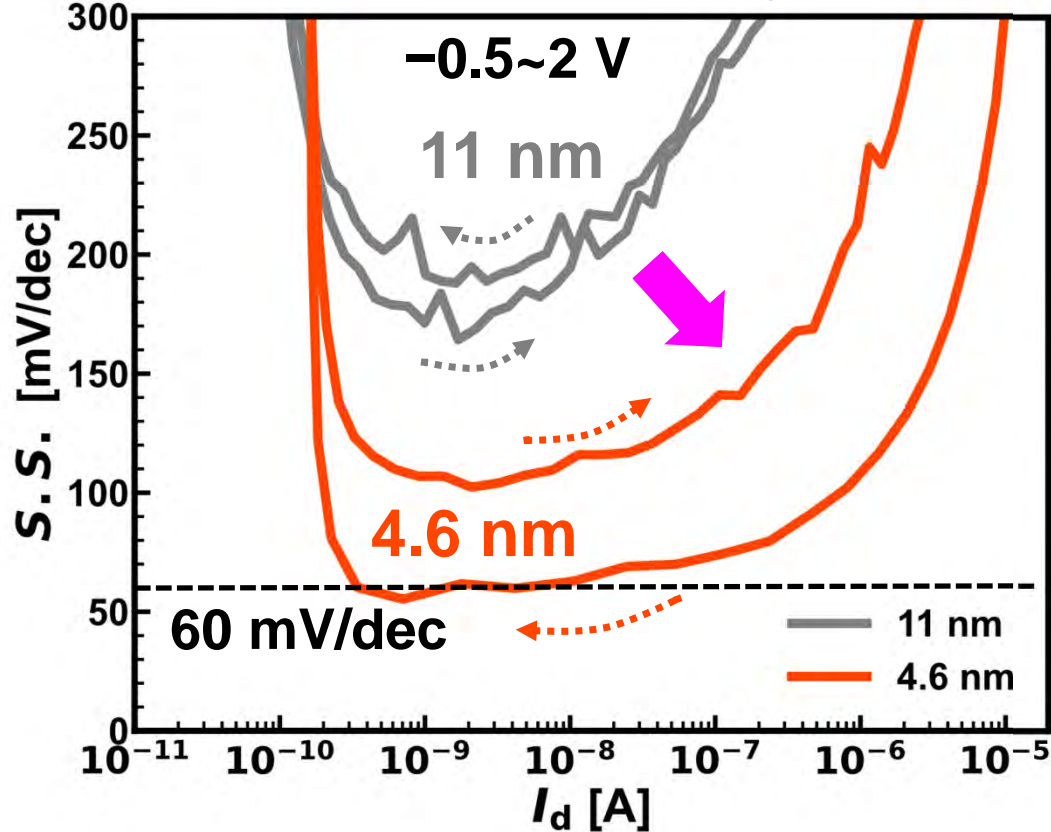
$$(V_{center} = 0.5 \text{ V})$$



- ❑ Saturated memory window (MW) is higher with thicker HZO (saturated MW ~  $2E_C t_{FE}$  → decrease in saturated MW is a drawback of thinner HZO)
- ❑ Under low-voltage operation, larger MW is obtained in an optimum thin HZO
- ❑ Sufficient MW in low voltages can be obtained by appropriate HZO scaling

# Impact of HZO scaling on sub-threshold swing and $I_{on}/I_{off}$ ratio

Z. Cai et al., VLSI Technology and Circuits, T5-2 (2023), published in TED (2024)

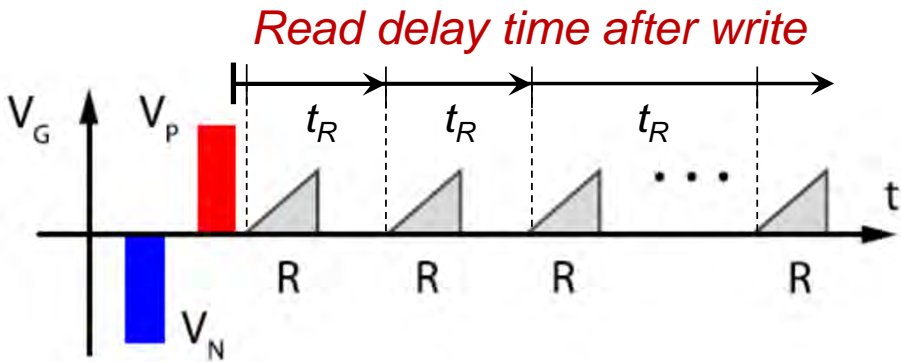


- ❑ HZO scaling leads to low S.S.
- ❑  $I_{on}/I_{off}$  ratio at a given  $V_g$  (index in current readout operation) is improved by HZO thickness scaling

# Issues related FeFET memory operation

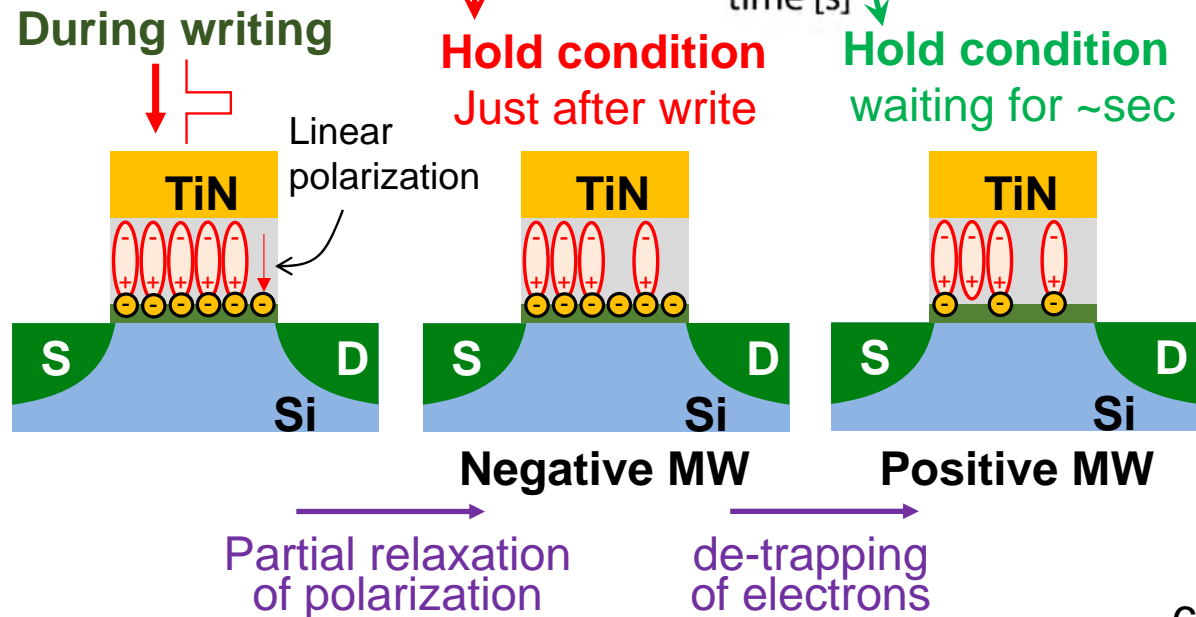
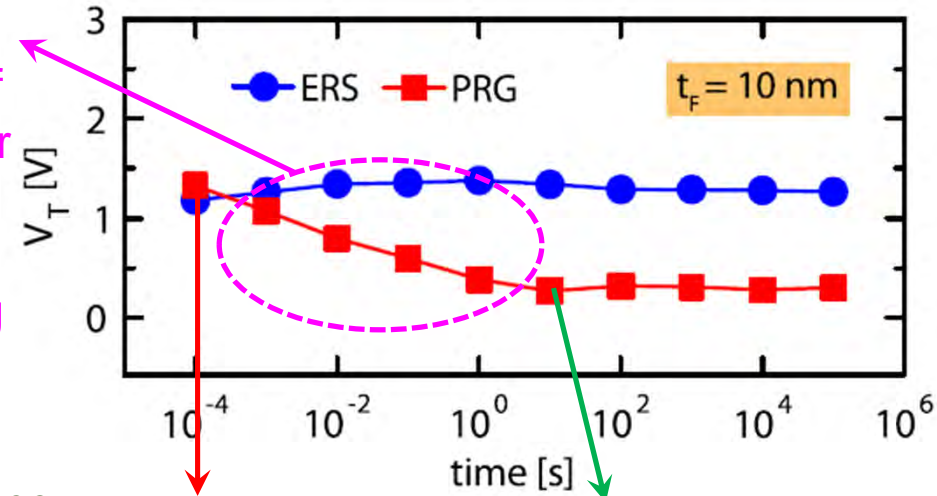
# Necessity of long read-after-write time

Mulaosmanovic et al, TED 66 (2019) 3828



- Memory window does not open at short read-after-write time
- Sufficient read delay time after positive  $V_g$  pulse to induce **electron de-trapping** is necessary for the readout of low  $V_{th}$  (program: PGM) condition

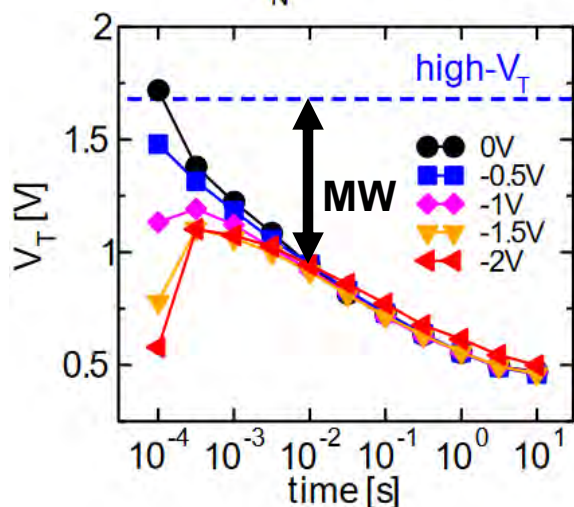
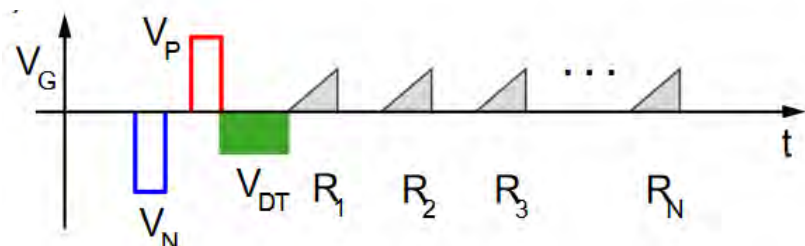
Continuous de-trapping of electrons after writing lowers PRG  $V_{th}$  with longer waiting time





# For improving long read-after-write time issue

## Introducing de-trapping pulse



- Short negative pulse just after write operation can enhance de-trapping of trapped electrons, which can increase memory window in short term

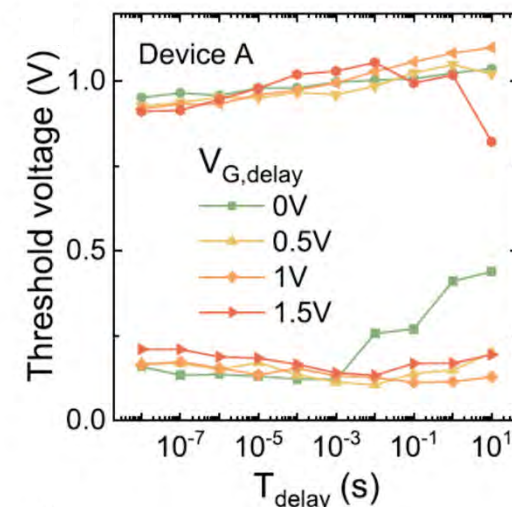
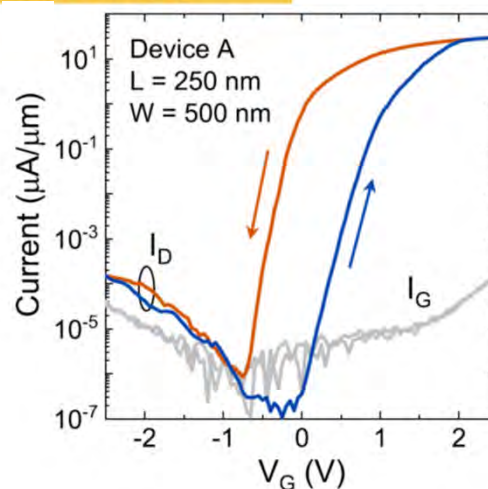
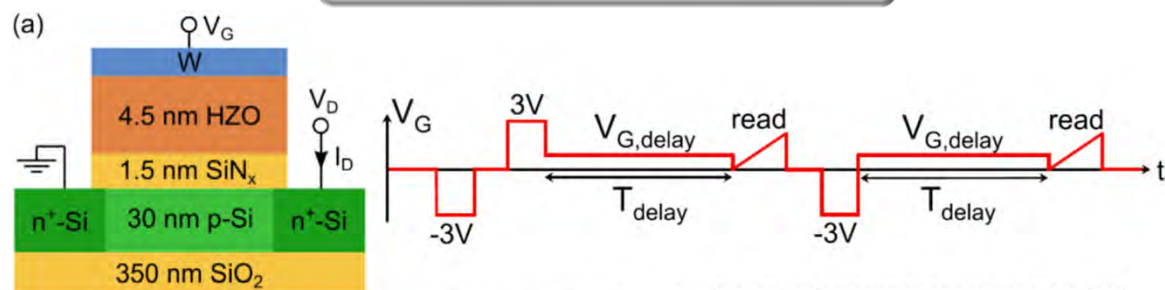
H. Mulaosmanovic et al, EDTM, 7C-4 (2020)

H. Zhou et al, IEDM, 395 (2020)

N. Tasneem et al, IEDM, 122 (2021)

Z. Wang et al, IEDM, 430 (2021)

## IL engineering

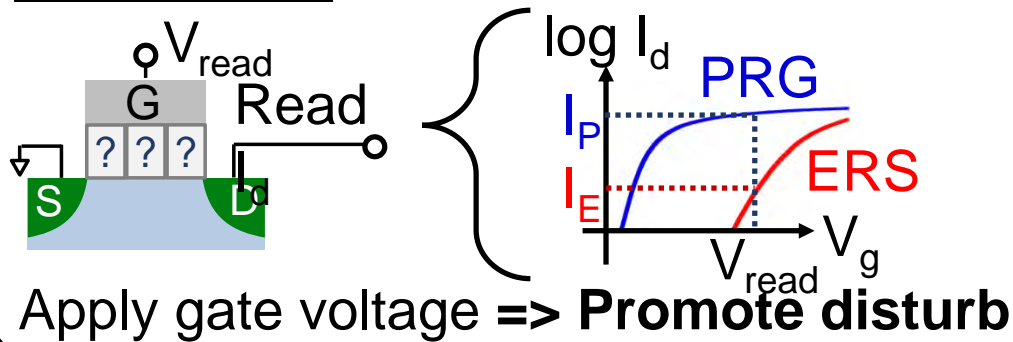


- IL engineering, allowing fast de-trapping of electrons or reducing electron traps, is expected to realize fast read-after-write time

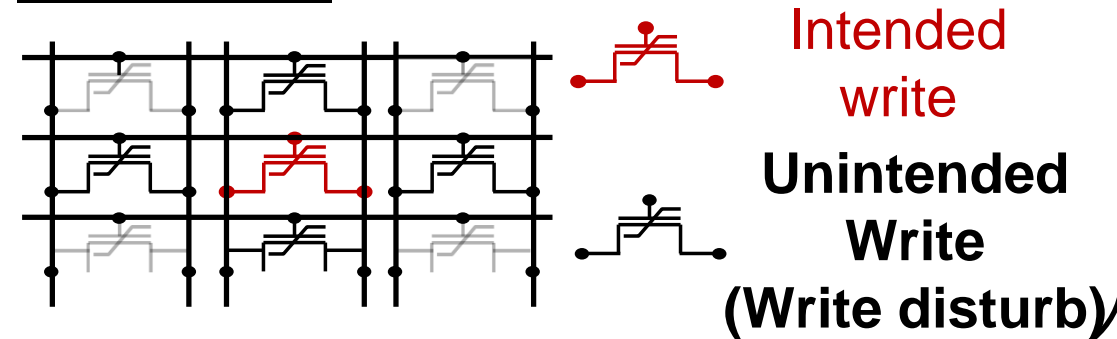
M. Hoffmann et al., *IEEE EDL* **43**, 717 (2022)

# Read/write disturb characteristics of FeFET memory

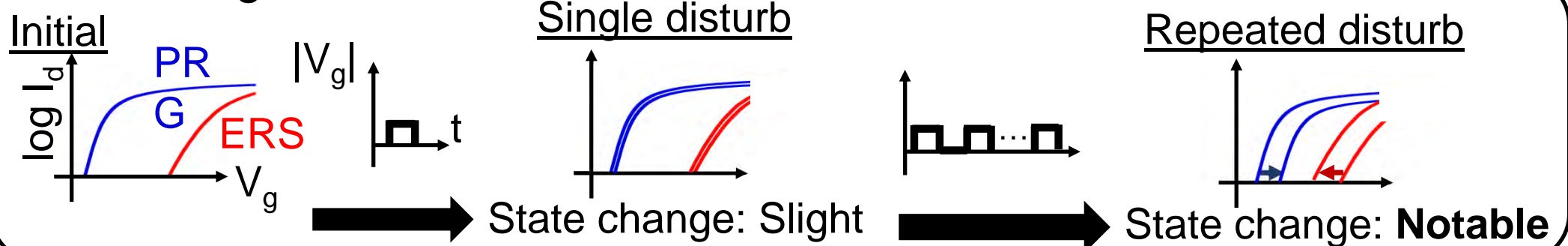
## Read disturb



## Write disturb

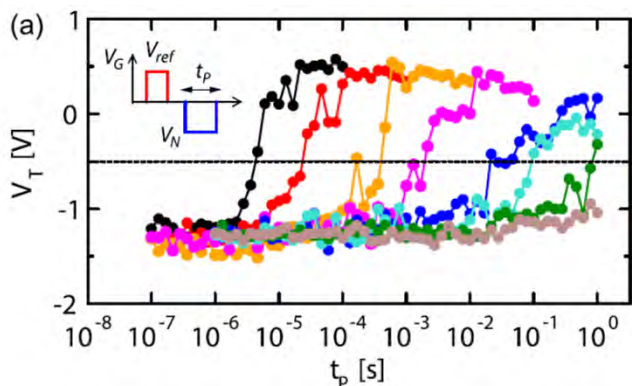


## Low-voltage disturb



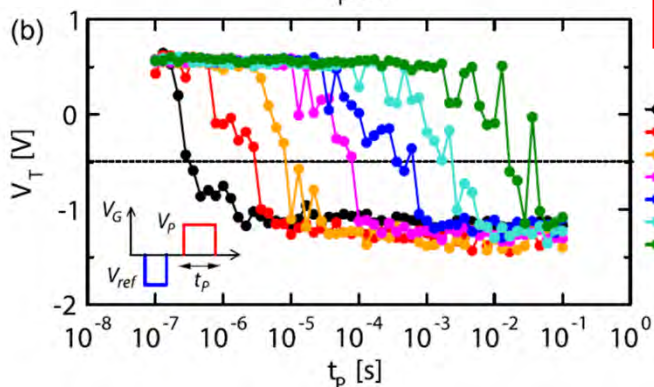
- One advantage in FeFET memory is non-destructive readout
- Read disturb characteristics can determine non-destructive readout time
- Write disturb characteristics are critical for memory array operation

# Dependence of polarization switching on ulse voltage and time

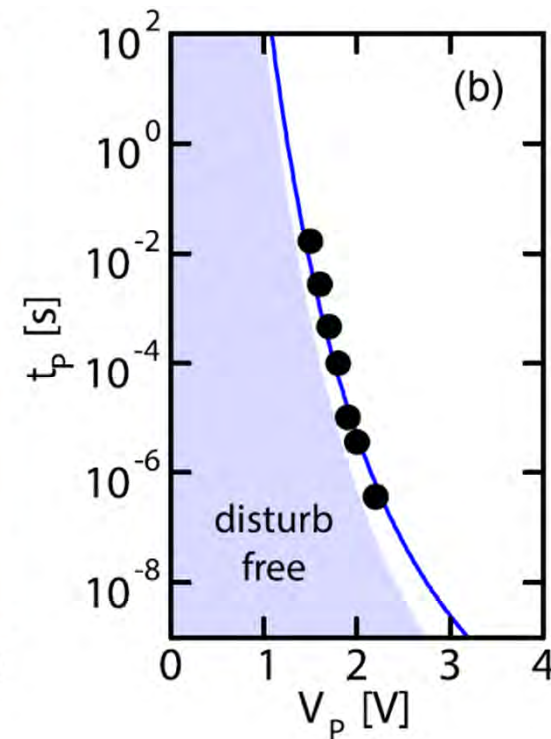
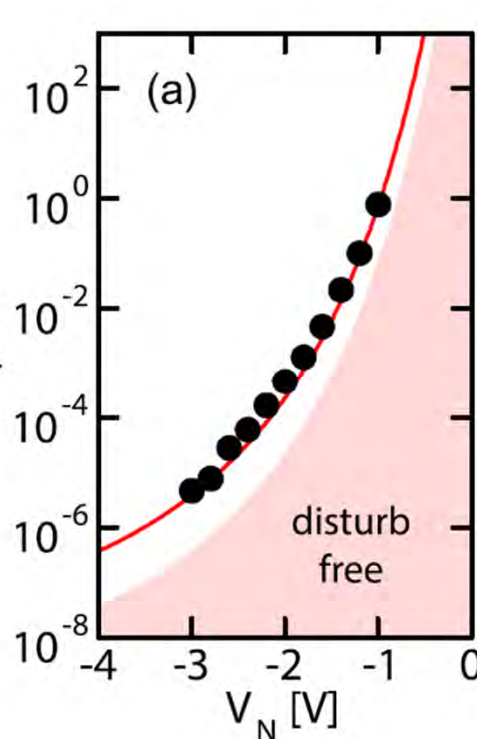


H. Mulaosmanovic et al., EDL, 41 (2020) 1420

$$t_P \sim \exp\left(\frac{\alpha}{k_B T} \cdot \frac{1}{V_G^2}\right)$$



$L/W = 24 \text{ nm}/170 \text{ nm}$

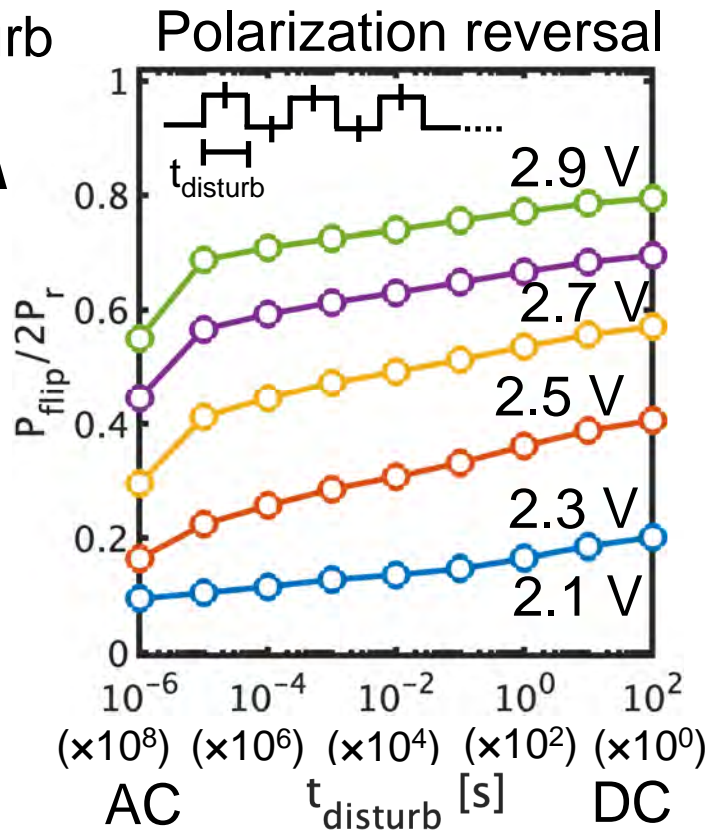
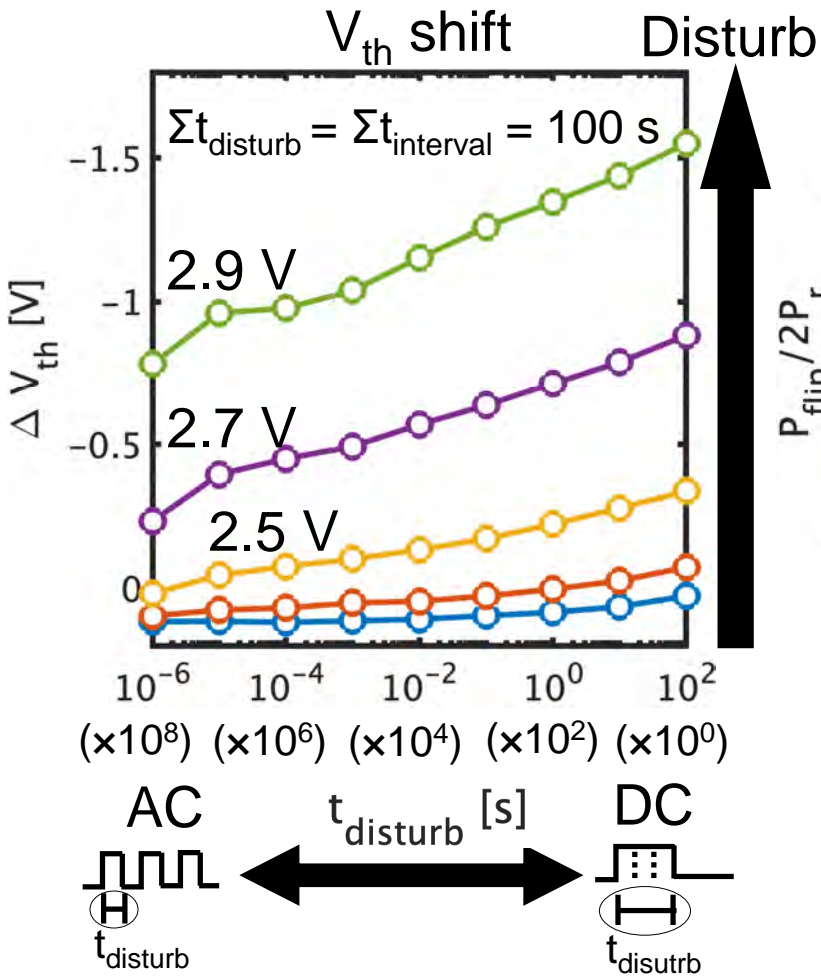


- Ferroelectric switching is strongly dependent on voltage (electric field) and time during read operation, indicating that the readout voltage and time are critical to non-destructive readout
- The disturb time can be well represented as a function of the gate voltage, which can provide guidelines for a disturb-free operation of FeFETs

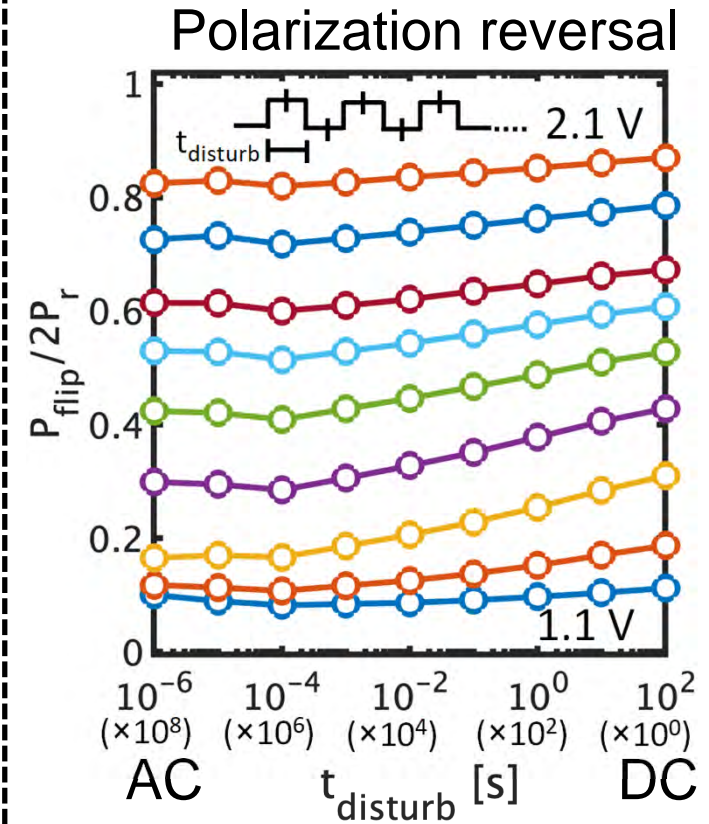


# Experimental disturb characteristics of FeFET and MFM capacitor

## FeFET



## MFM capacitor

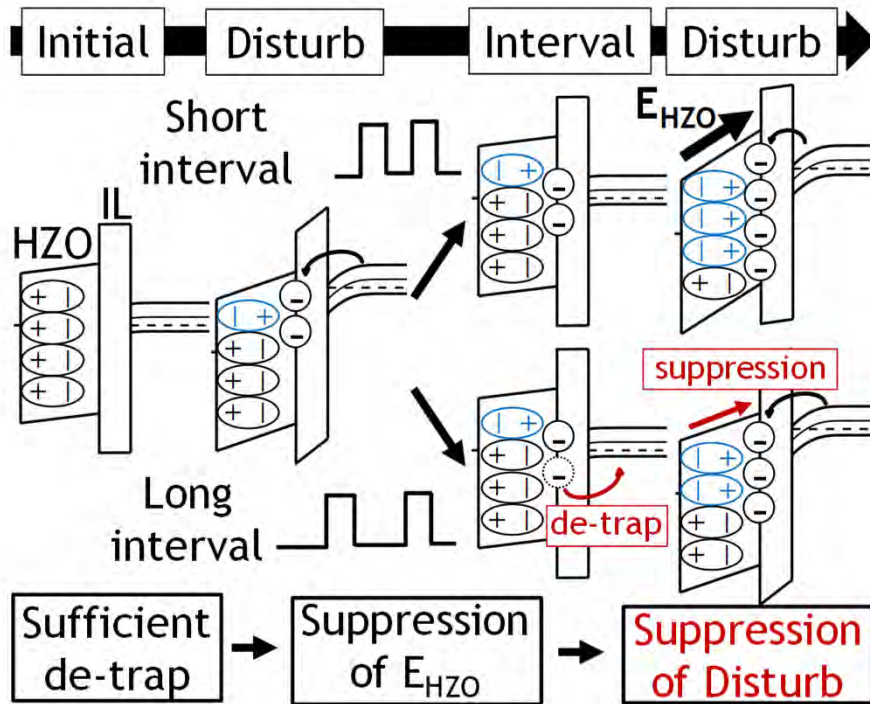


- “Disturb” is not simply summed up
- Shorter disturb time leads to more relaxation of both threshold and polarization, resulting in less disturb

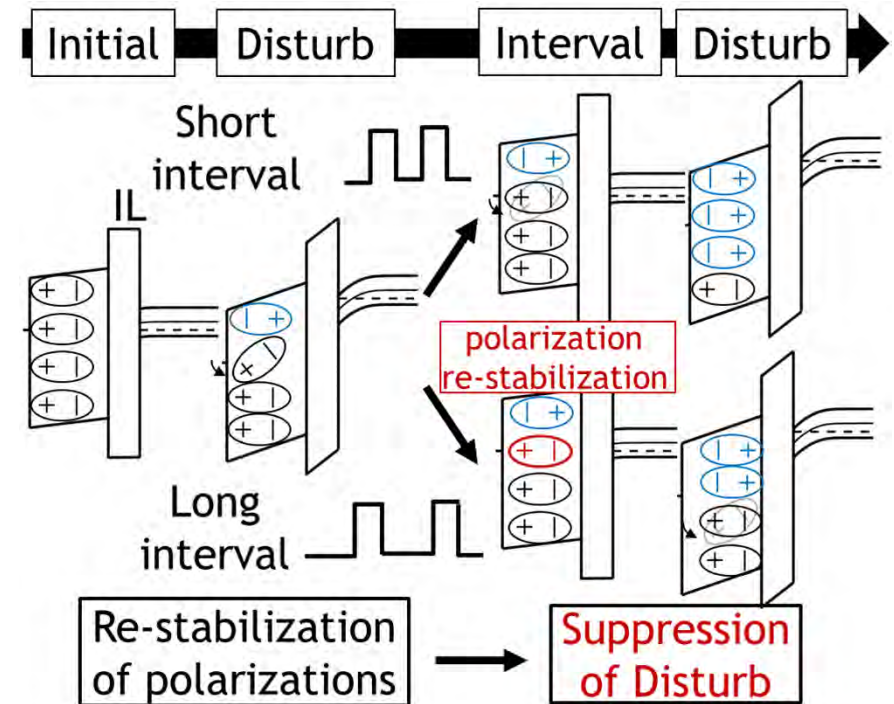


# Physical model of non-accumulative characteristics of FeFET

## Trap dynamics model



## Polarization dynamics model



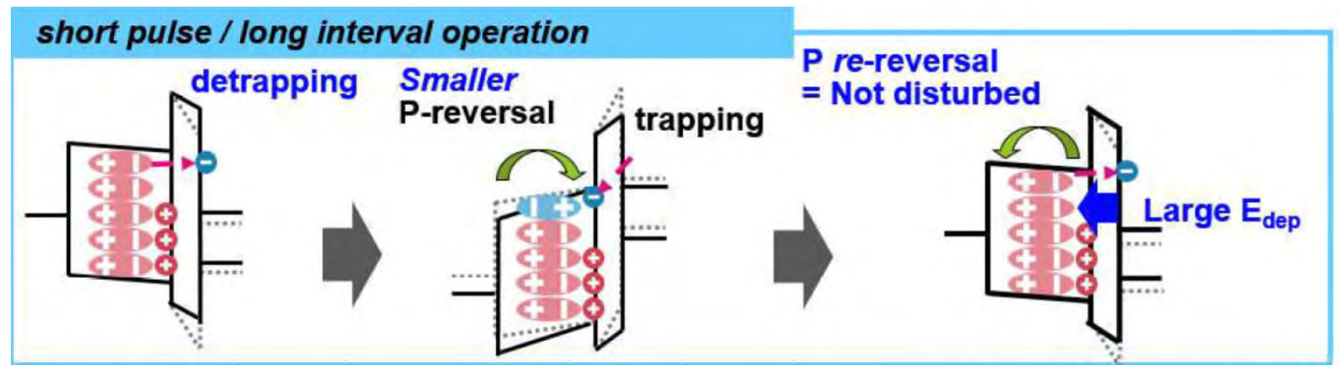
- The non-accumulation effect that can improve the disturbance characteristics can be explained by two mechanisms: the electrons are detrapped during the hold, weakening the electric field for the next disturbance, and the polarization that is nearly reversed by the disturbance is restabilized during the hold.

# Importance of trap-property-aware device operation for FeFETs

- Amounts of trapped/de-trapped electrons can be modulated by bias conditions → **electric field across FE can be intentionally controlled**  
 → **write/read disturb can be mitigated by trap control**

(1) long interval/short  $V_g$  pulse operation

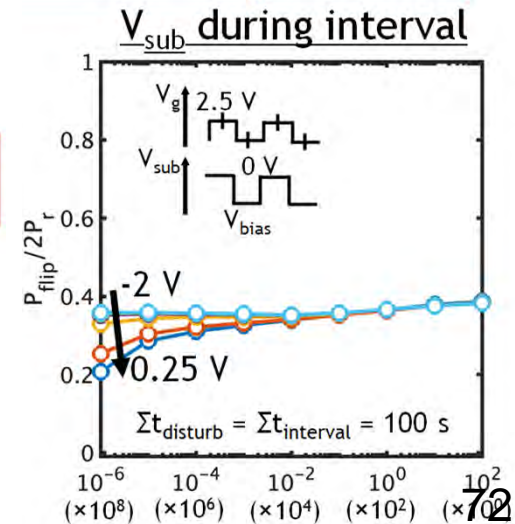
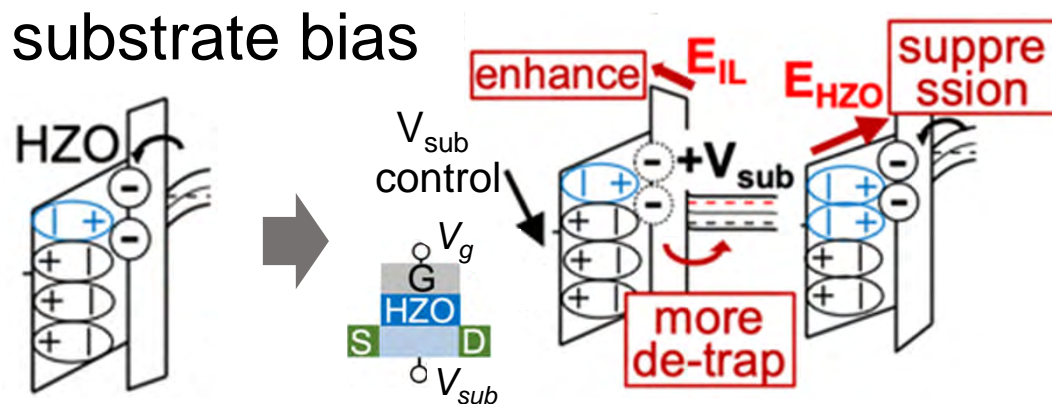
T. Hamai (Kioxia) et al.,  
IRPS 6A.1-2 (2023)



(2) short/low negative  $V_g$  pulse during interval

(3) short/low positive substrate bias during interval

M. Otomo et al.,  
VLSI symp, 2024

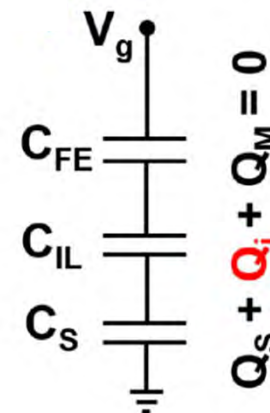
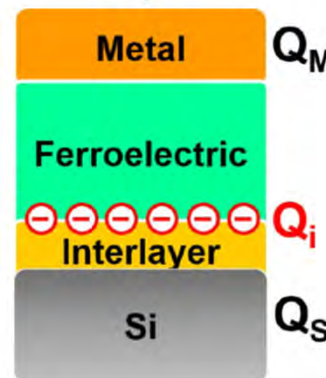
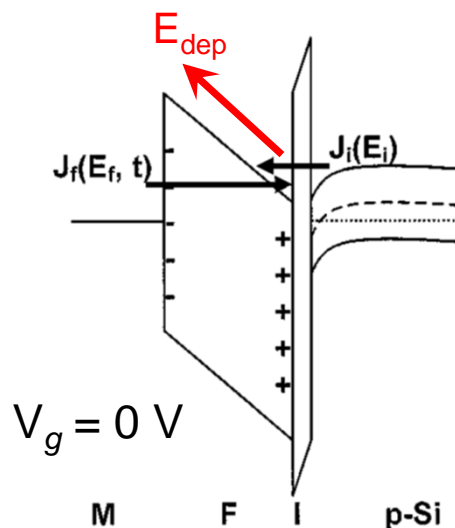
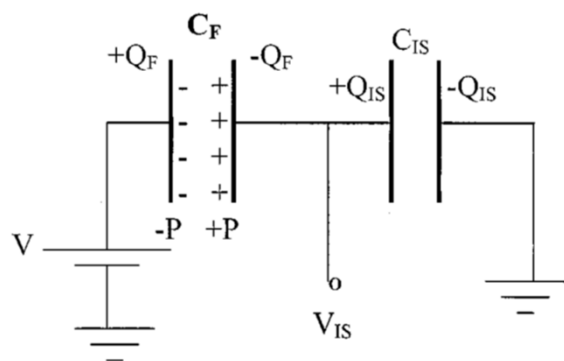
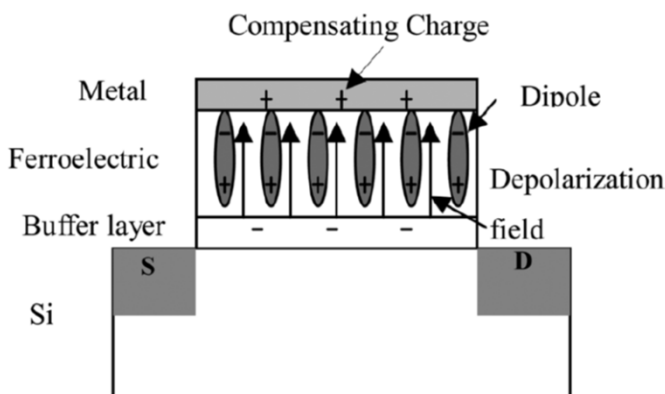


# FeFET reliability

# Depolarization field in FeFET gate stack

X. Pan et al., APL **99**, 013505 (2011);  
T.-P. Ma et al., EDL **23**, 386 (2002)

X. Wang et al., TED **67**, 4500 (2020)



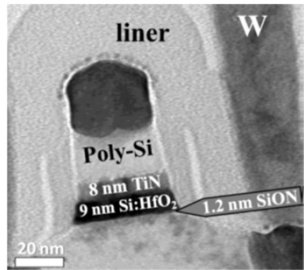
$$E_{\text{dep}} = \frac{V_{\text{FE}}}{t_{\text{FE}}} \Big|_{V_g=0} = - \frac{P_0(Q_i) + Q_i}{(C_{\text{FE}} + C_{\text{IS}})t_{\text{FE}}}$$

- $Q_i$ : electron or hole trap density. The sign is opposite to that of  $P_0$

- Interfacial layers of FeFETs introduce depolarization field across FE in the direction of reducing the polarization at  $V_g = 0$  V, tending to reduce the memory retention time
- Trapped charges at FE/IL interfaces can reduce  $E_{\text{dep}}$ , which is expected to improve retention characteristics

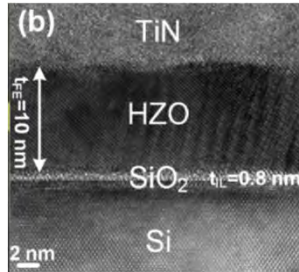
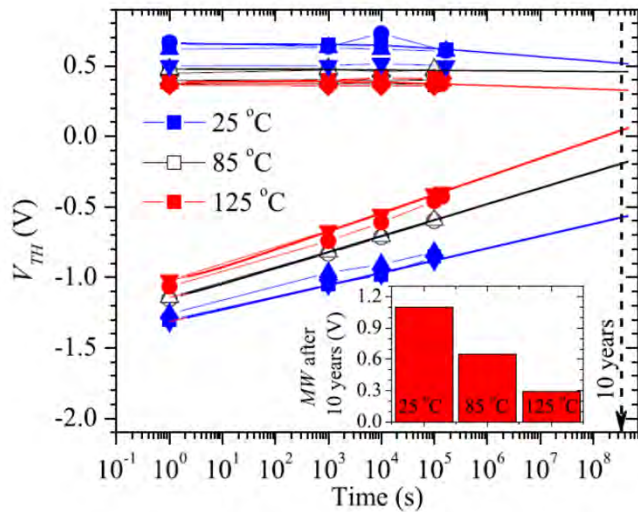


# Typical retention characteristics of FeFET



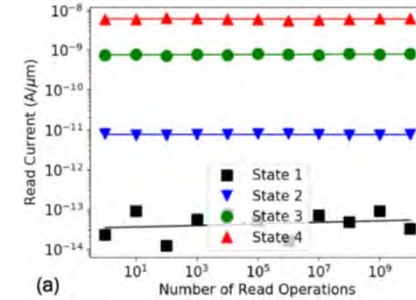
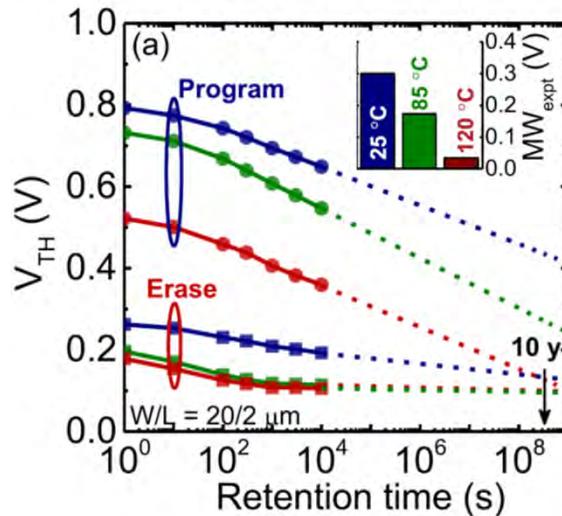
E. Yurchuk et al., TED 61, 3699 (2014)

$L_g = 32\text{nm}$



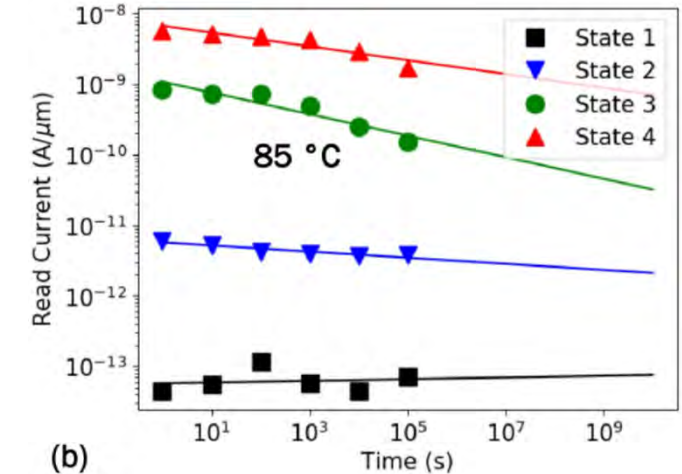
K. Ni et al., TED 65, 2461 (2018)

$L_g = 2\ \mu\text{m}$



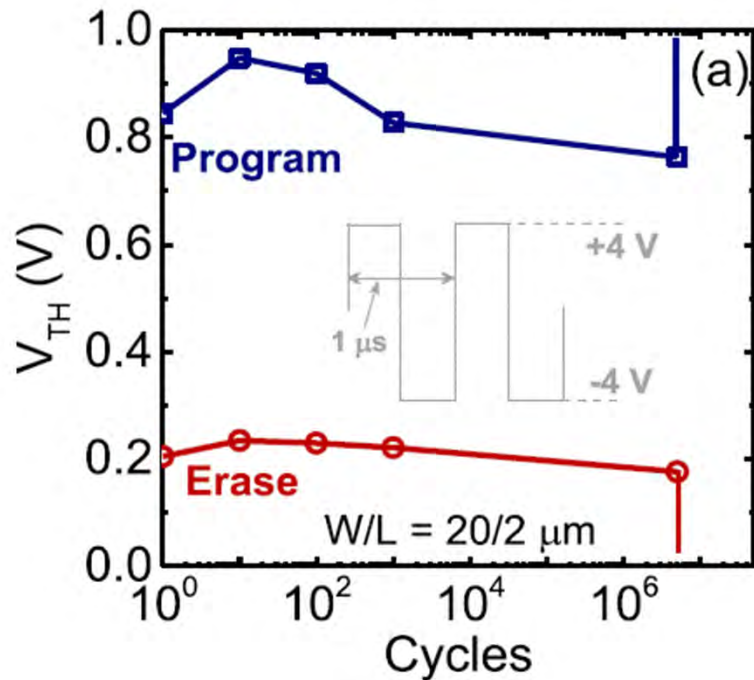
K. Chatterjee et al., EDL 40, 1423 (2019)

$L_g = 350\ \text{nm}$

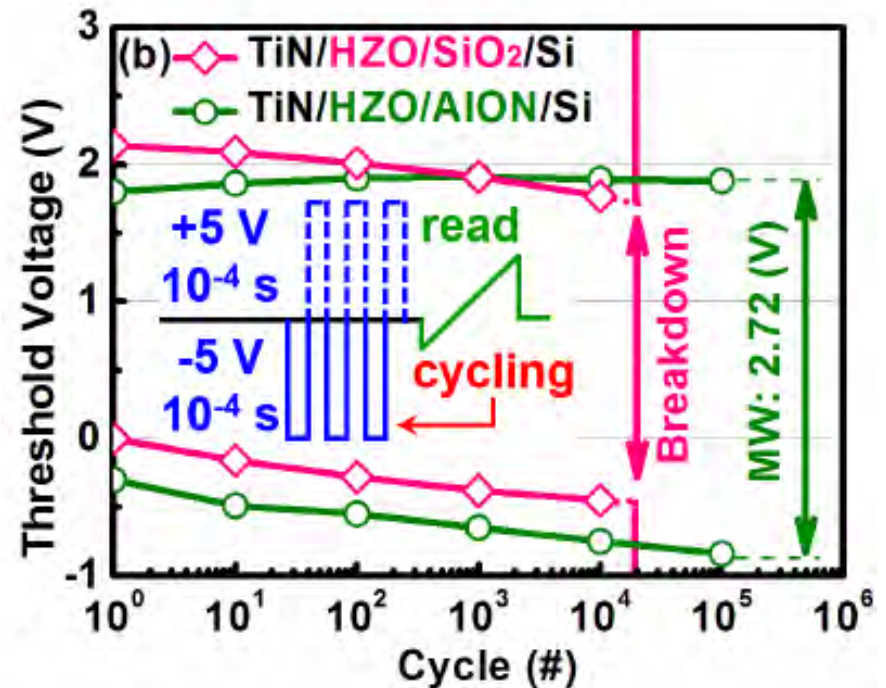


- Since early stage of studies on FeFETs, good retention characteristics over 10 year have been often reported
- Superior retention characteristics of HfO<sub>2</sub>-based FeFETs to perovskite FeFETs are attributable to higher  $E_c$  of HfO<sub>2</sub>-based FE and higher carrier trapping

# Endurance of FeFET ~ gate stack breakdown



K. Ni et al, TED 65, 2461 (2018)

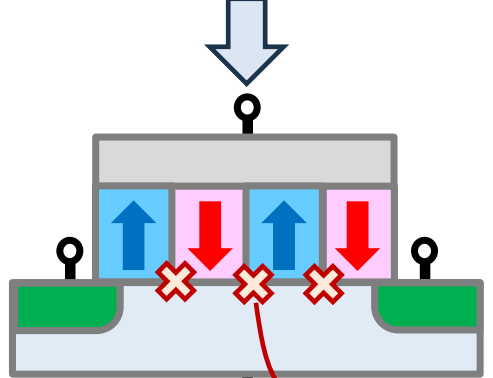
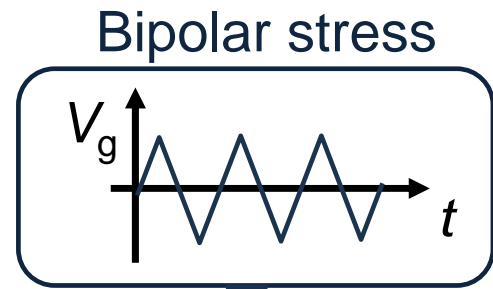


C.-Y. Chan et al, VLSI, TF2.5 (2020)

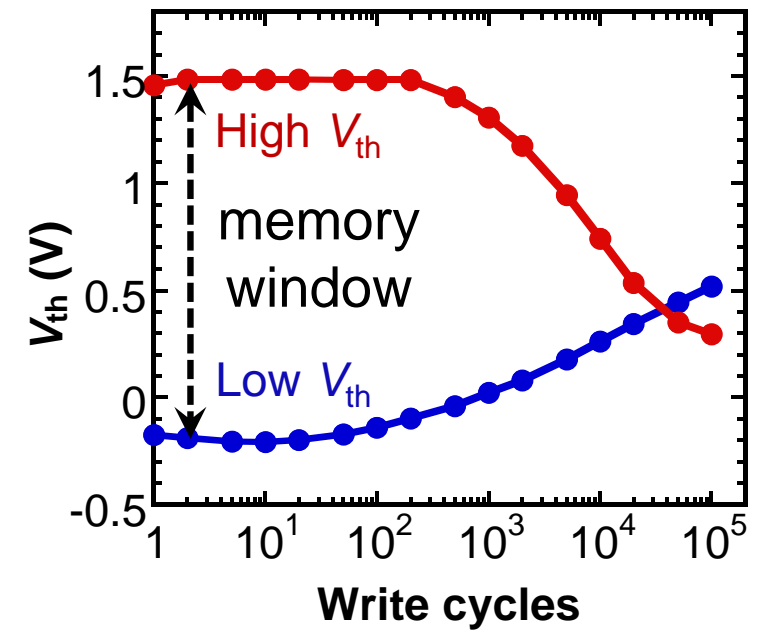
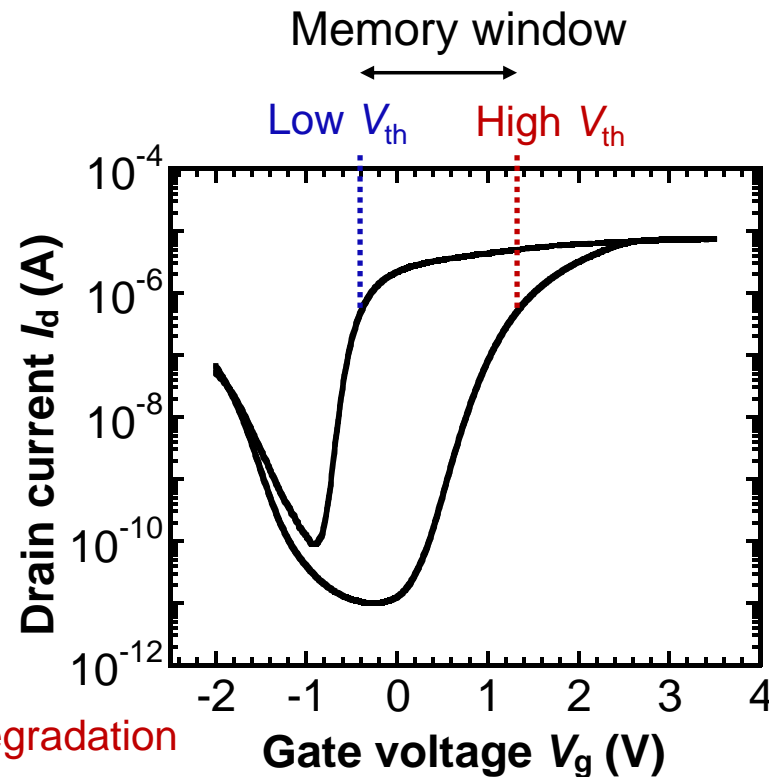
- Some cases have been reported in which endurance properties are determined by dielectric breakdown of gate stacks, attributable to too high operation voltage

# Endurance of FeFET ~ window narrowing

K. Toprasertpong *et al.*, *Appl Phys A*  
**128**, 1114 (2022)



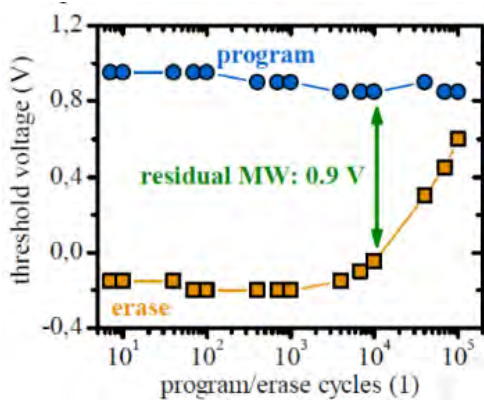
Interface degradation



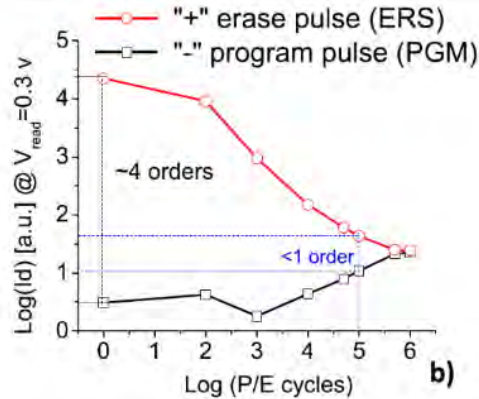
In FeFET memory, bipolar stress results in failure of memory operation  
 $\Rightarrow$  How about bipolar stress in reservoir computing?



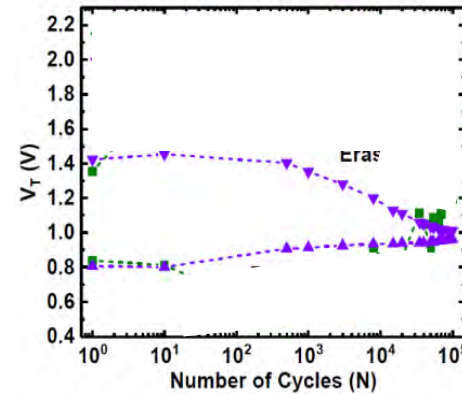
# Many reports on endurance properties



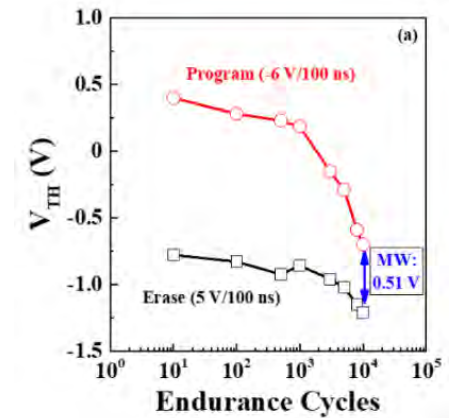
J. Müller et al, IEDM, 280 (2013)



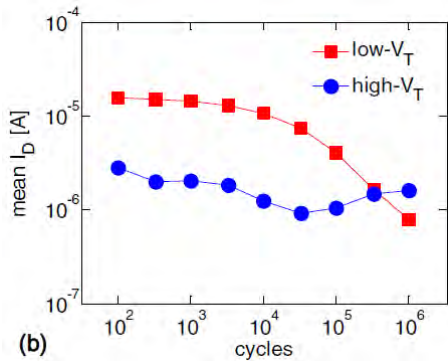
N. Gong, T-P Ma, EDL 39, 15 (2018)



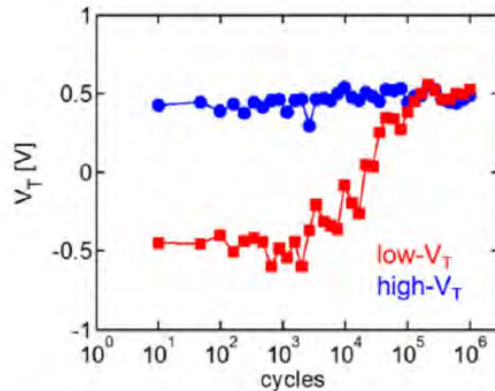
T. Ali et al, VLSI, TF2.2 (2020)



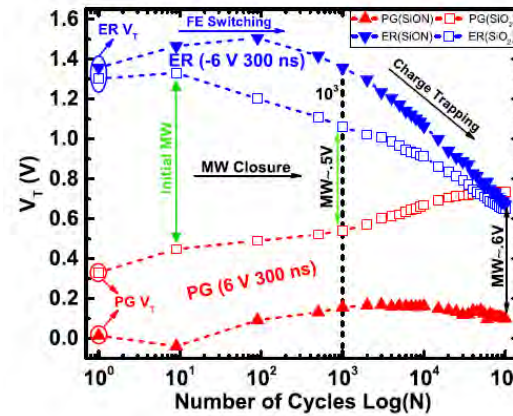
B. Zeng et al, EDL 39, 1508 (2018)



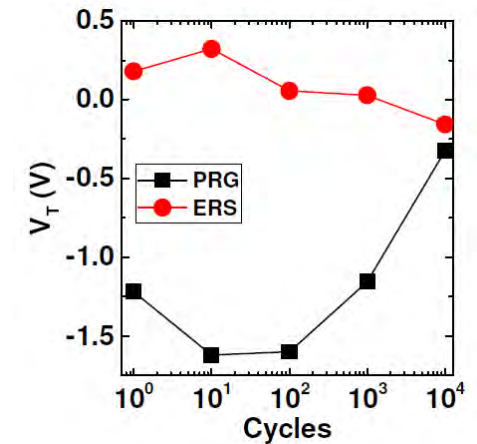
M. Trentzsch et al, IEDM, 294 (2016)



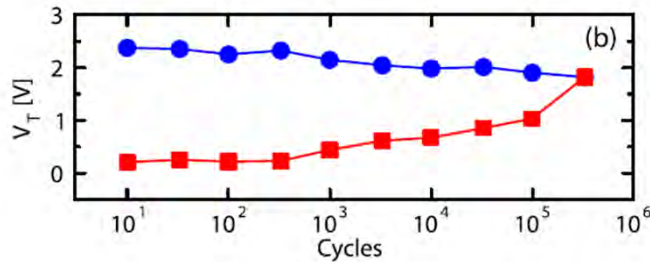
S. Dünkel et al, IEDM, 485 (2017)



T. Ali et al, TED 65, 3769 (2018)



K. Florent et al, IEDM, 43 (2018)

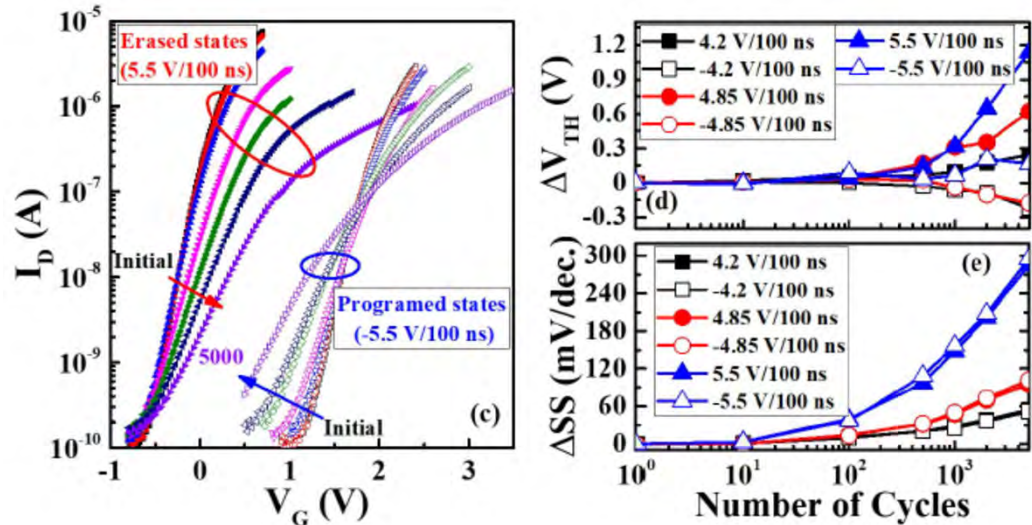


H. Mulaosmanovic et al, TED 66, 3838 (2019)

- Endurance properties of low  $V_{th}$  and high  $V_{th}$  have some variations among reports, though window narrowing is the common characteristic

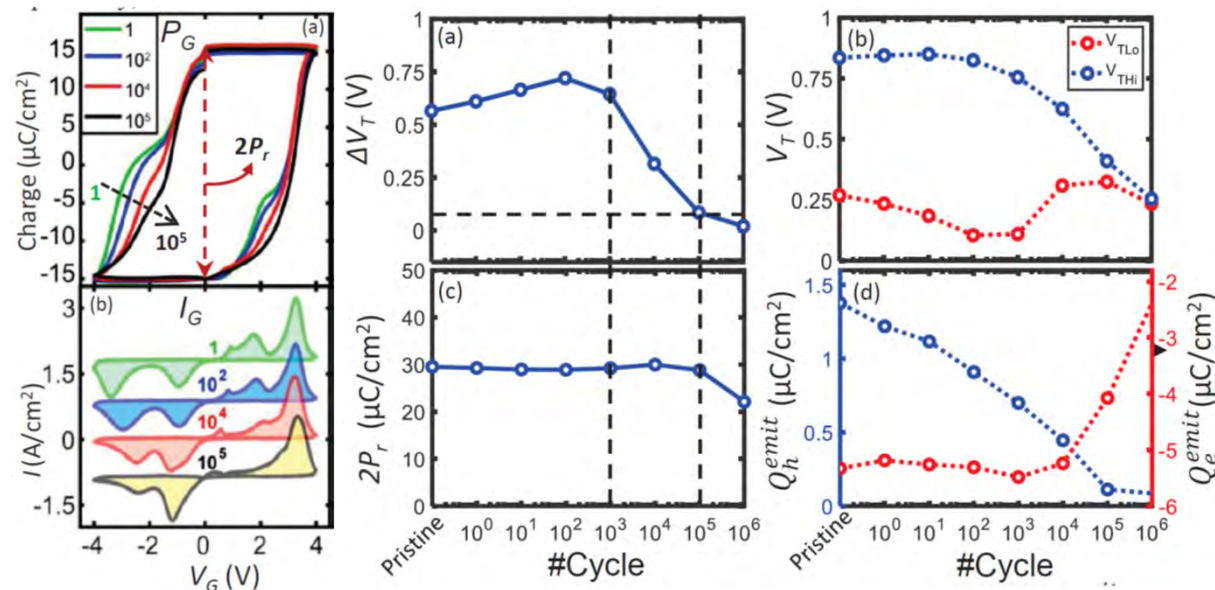


# Typical I-V and p-V characteristics of FeFET with write/erase cycling stress



B. Zeng et al., IEEE EDL 98, 40, 2019

- Repeated cycling stress causes not only a voltage shift but also a significant degradation of sub-threshold swing (S factor) of I-V characteristics → generation of interface traps and degradation of interface properties



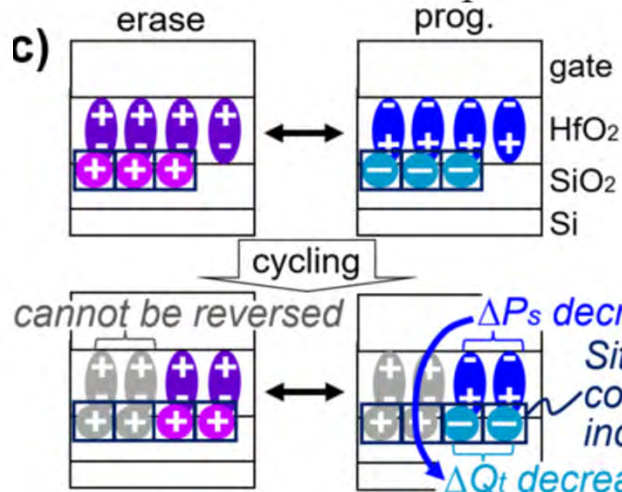
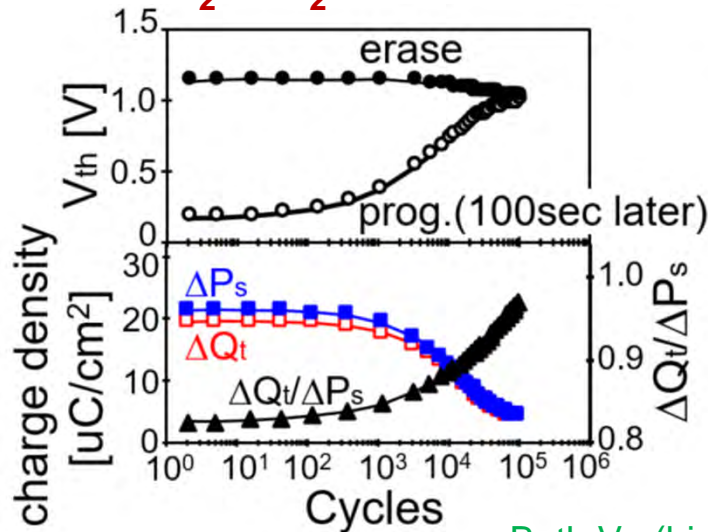
N. Tasneem et al., IEDM, p. 122, 2021

- Some papers reports no degradation in polarization even after cycling stress causing a significant reduction in memory window
- Polarization degradation in FE films might not be a dominant factor for memory window narrowing

# Another report on trap-assisted polarization in FeFET

FE-HfO<sub>2</sub>/SiO<sub>2</sub>/Si FeFET

R. Ichihara et al., VLSI Symp., (2020), IEDM, 130 (2021)



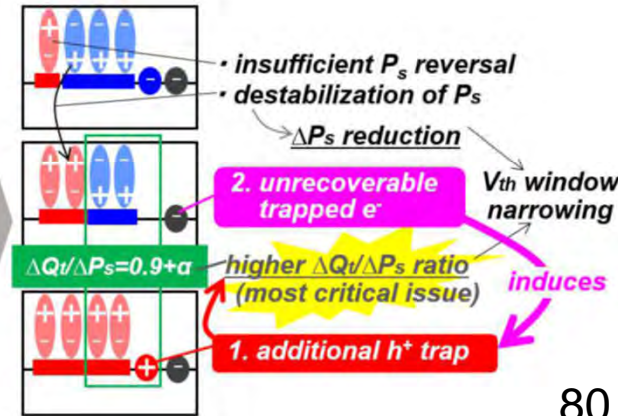
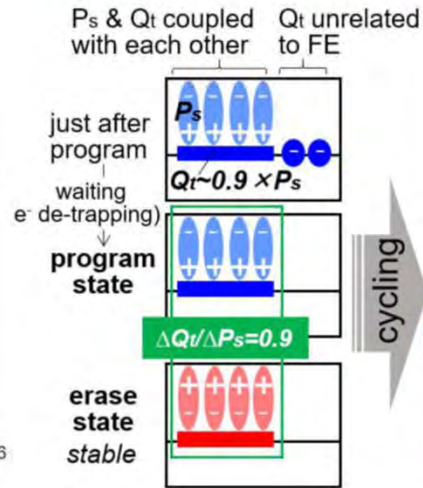
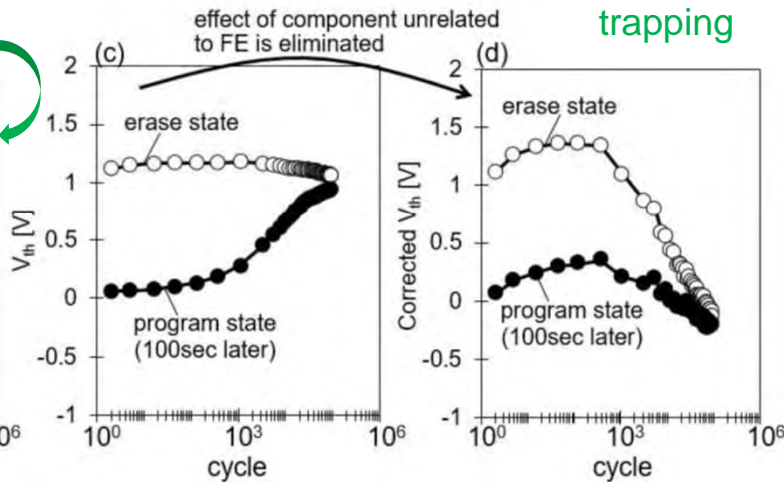
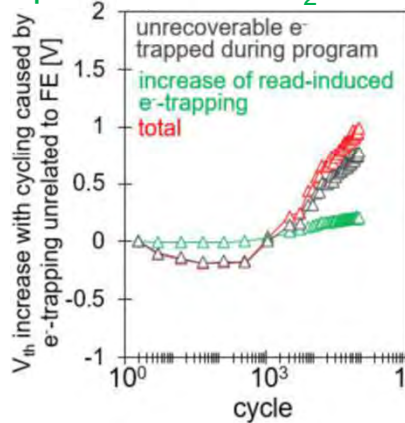
- Ratio of trapped charges to polarization increases with an increase in cycle number, leading to memory window narrowing

- Increase in electron trapping leads to decrease in  $\Delta P_s$  and increase in hole trapping, leading higher  $\Delta Q_t/\Delta P_s$  ratio  $\rightarrow$  memory window narrowing

Increase in fixed charges, estimated by paraelectric HfO<sub>2</sub> FET

Both  $V_{th}$  (high) and  $V_{th}$  (low) decrease with cycling number due to hole trapping

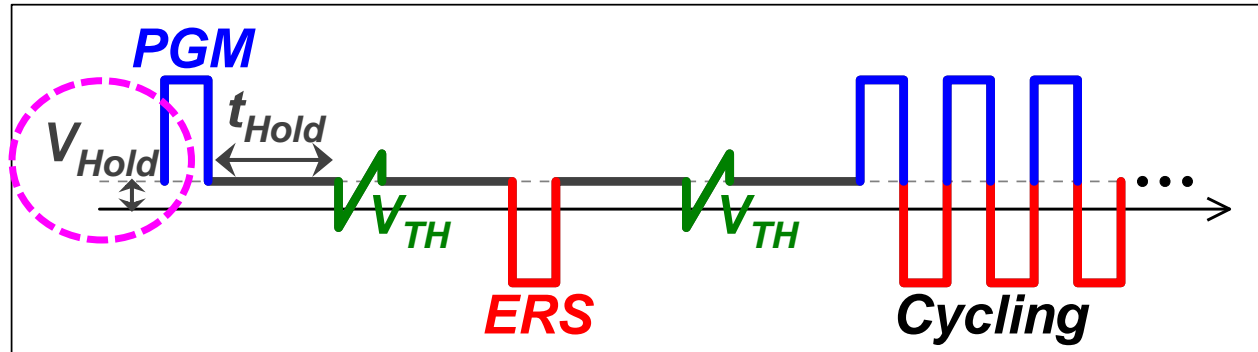
$\Delta P_s$  decreases  
Sites that can compensate  $P_s$  increase  
 $\Delta Q_t$  decreases but the ratio to  $\Delta P_s$  increases





# Effect of hold voltage on memory window narrowing of FeFET

S.-K. Cho et al., IEDM, 4-7 (2024)

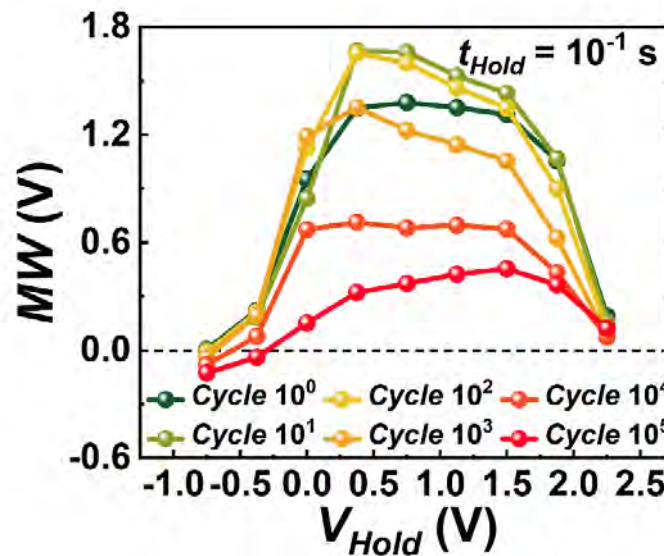
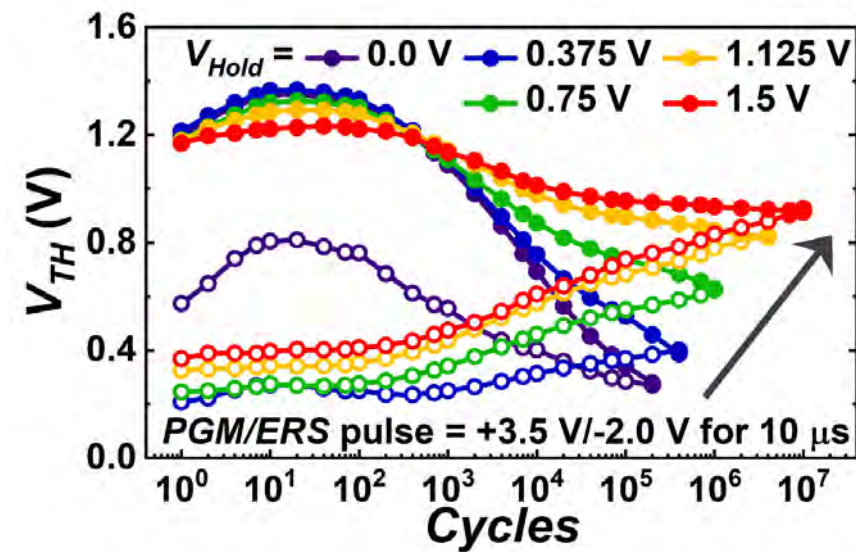


11 nm HZO/SiO<sub>2</sub>(0.6 nm)/Si FeFET

□ It is found that endurance characteristics and memory window after stress are dependent on hold voltage

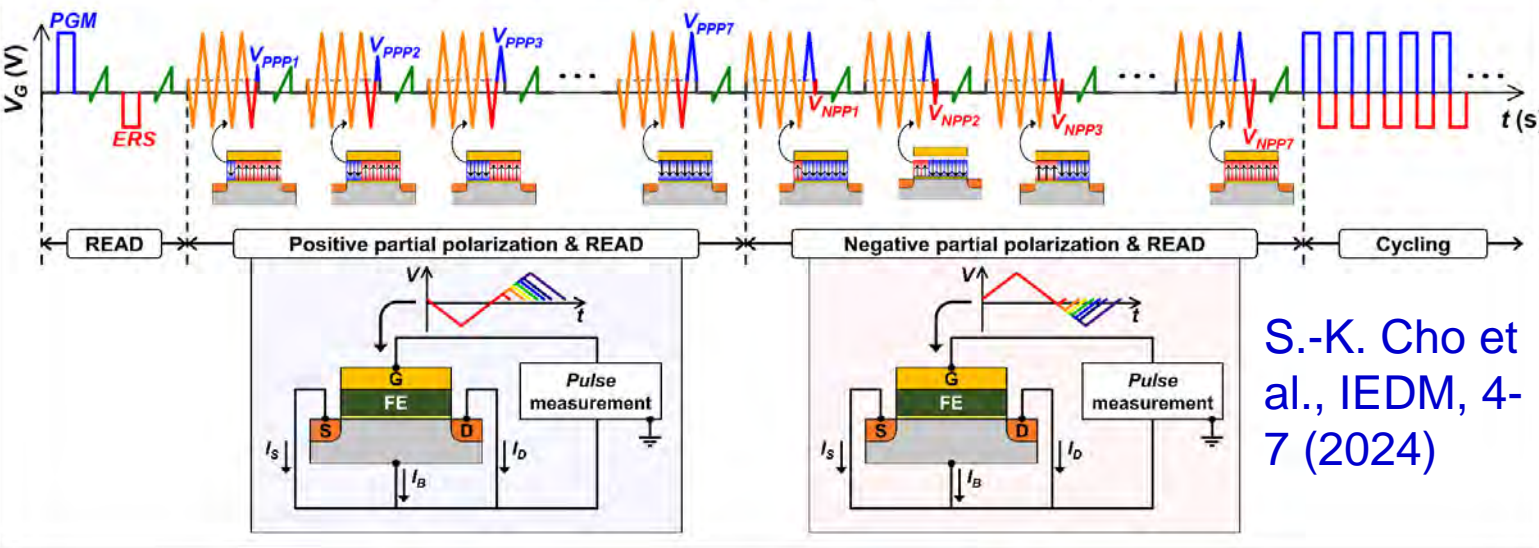
□ Memory window appears for degraded FeFETs without memory window by applying positive hold voltage

□ Optimum hold voltage is shifted to positive direction with increasing cycle numbers, indicating influence of hole traps



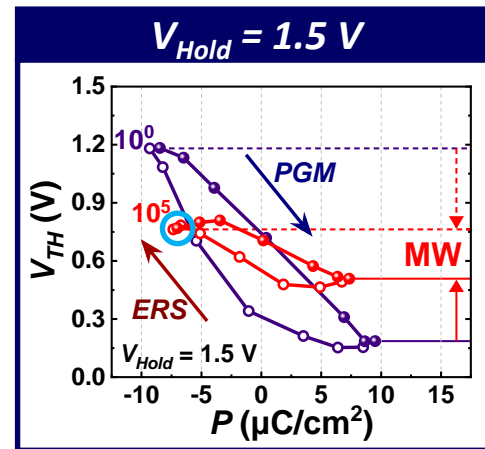
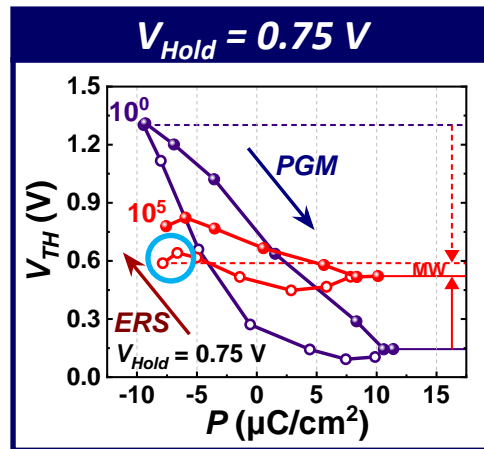
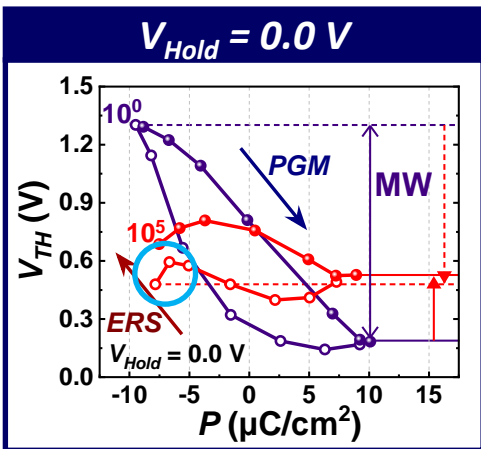
# New method for evaluating $P-V_{th}$ relation

Measurement method for  $V_{TH}$ - $P$  relationship



S.-K. Cho et al., IEDM, 4-7 (2024)

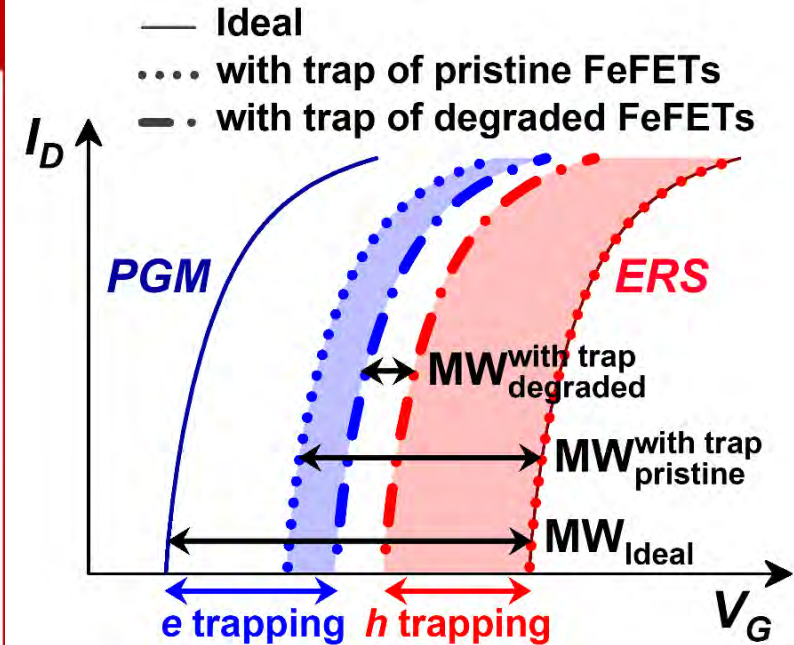
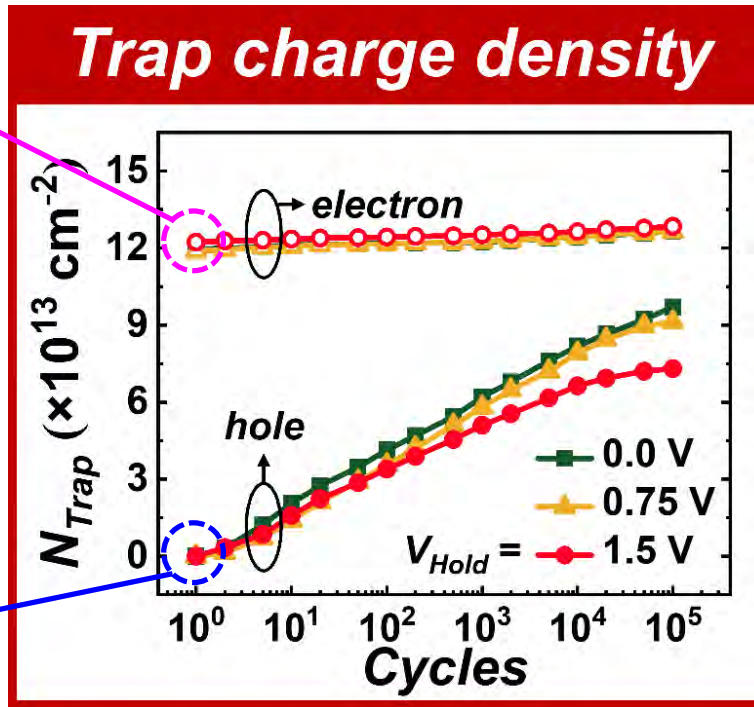
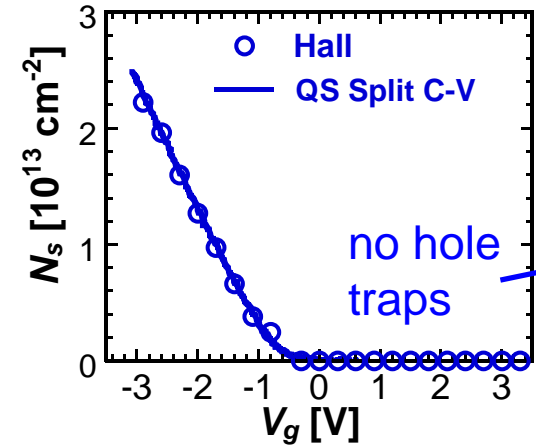
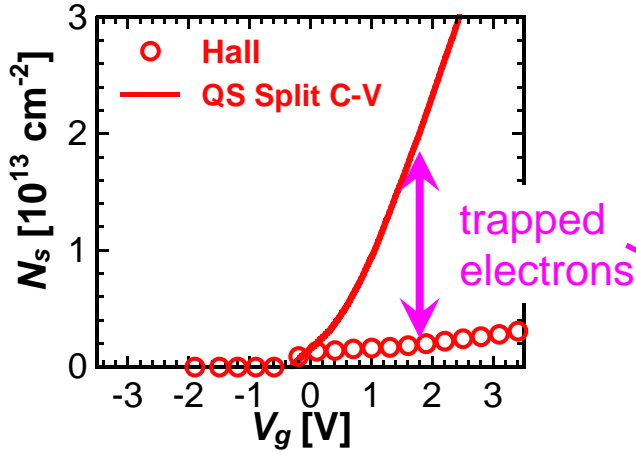
- We have proposed and demonstrated a method to evaluate  $P-V_{th}$  characteristics to identify the physical origin of memory window reduction
- No degradation in polarization is observed for FeFETs with no memory window
- Positive  $V_{hold}$  changes  $V_{th}$  after erase under the same polarization, indicating importance of hole de-trapping





# Physical understanding of memory window narrowing mechanism

K. Toprasertpong et al. JJAP 63, 02SP47 (2024);  
S.-K. Cho et al., IEDM, 4-7 (2024)

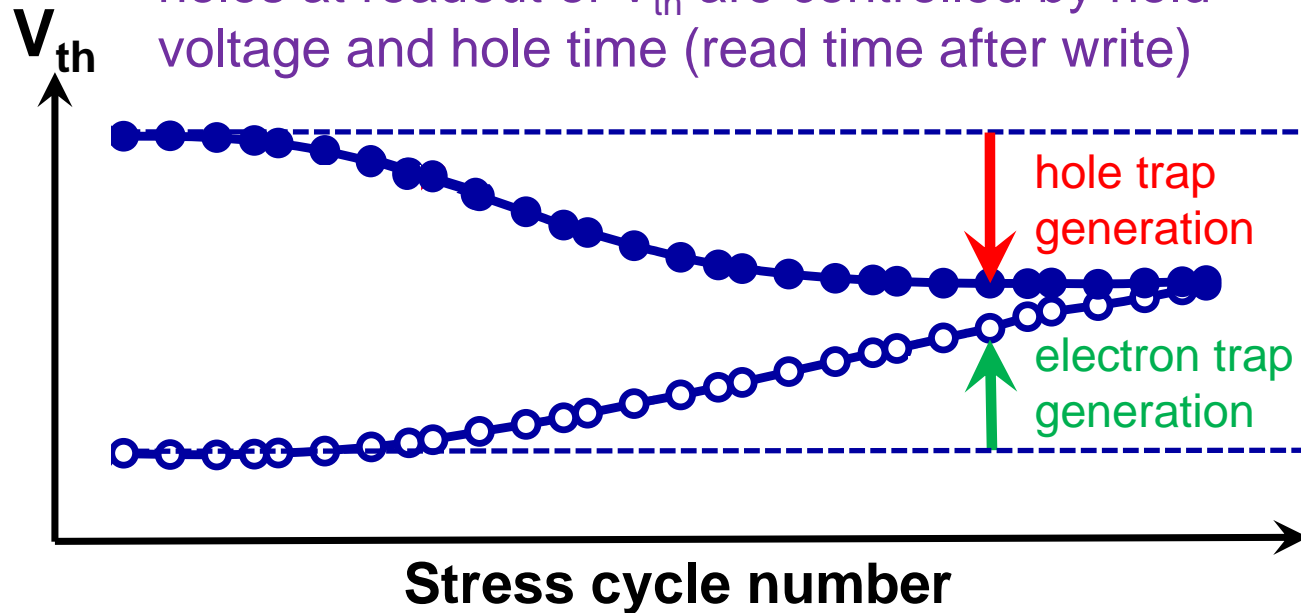


**Pristine condition  
(Hall measurement)**

It is found from an analysis of  $V_{th}$  shift that memory window reduction is mainly caused by hole trap generation

# Interpretation of memory window narrowing of FeFET

- Amounts of trapped electrons and trapped holes at readout of  $V_{th}$  are controlled by hold voltage and hole time (read time after write)



- Note that no fixed charge generation is assumed in this figure

Insufficient hole de-trapping  
⇒ more holes trapped at  $V_{hold}$   
⇒  $V_{th}$  becomes lower with cycling

Insufficient electron de-trapping  
⇒ more electrons trapped at  $V_{hold}$   
⇒  $V_{th}$  becomes higher with cycling

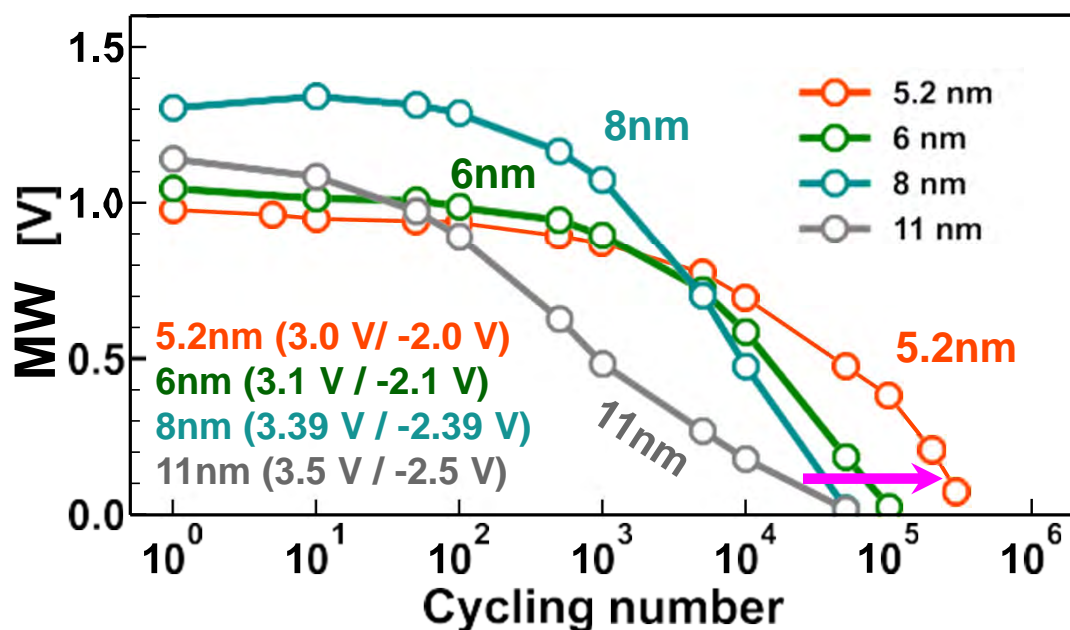
S.-K. Cho et al., IEDM, 4-7 (2024)

- FeFETs have two aspects in memory operation: polarization switching memory function and trap memory function, both of which compete in terms of memory window
- The physical origin of memory window narrowing is that trapped charges increases with increasing cycle number and that these charges, which have the opposite impact to polarization, are not de-trapped at the  $V_{th}$  readout time

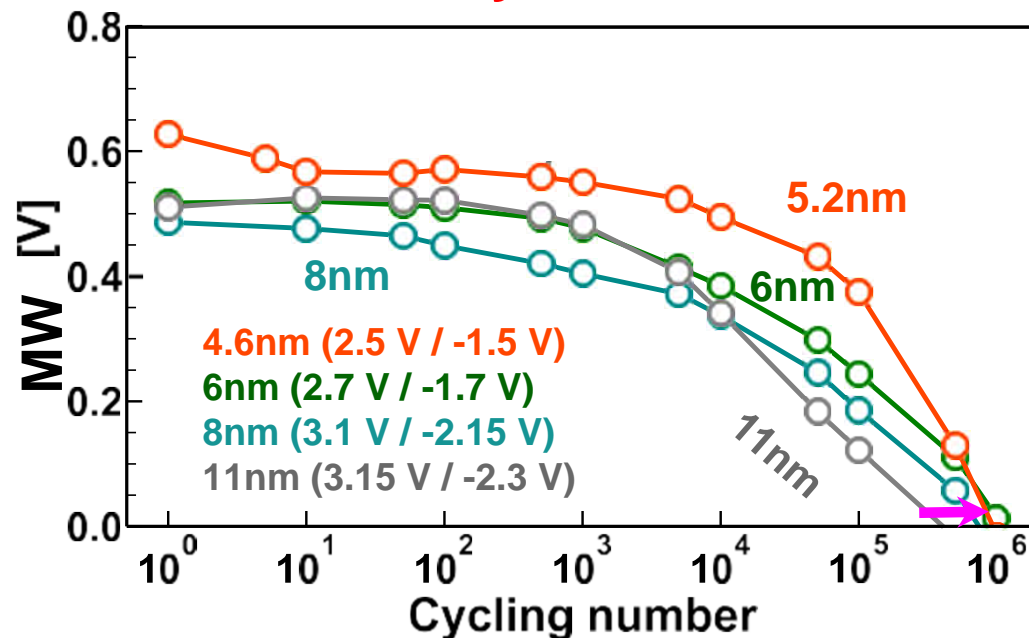
# Endurance with different HZO thickness

Z. Cai et al., VLSI Technology and Circuits, T5-2 (2023): published in TED (2025)

**Same electric field across HZO**



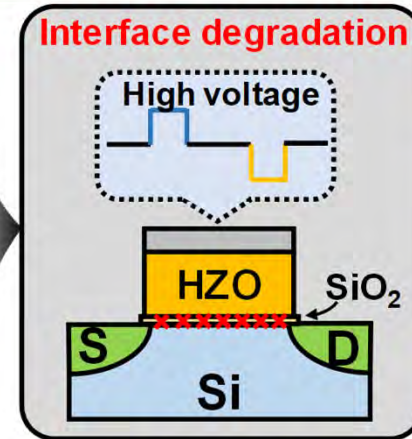
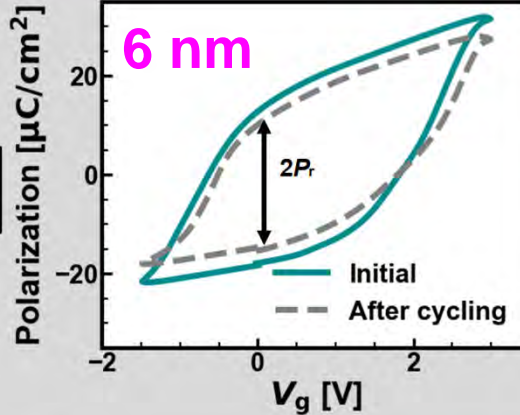
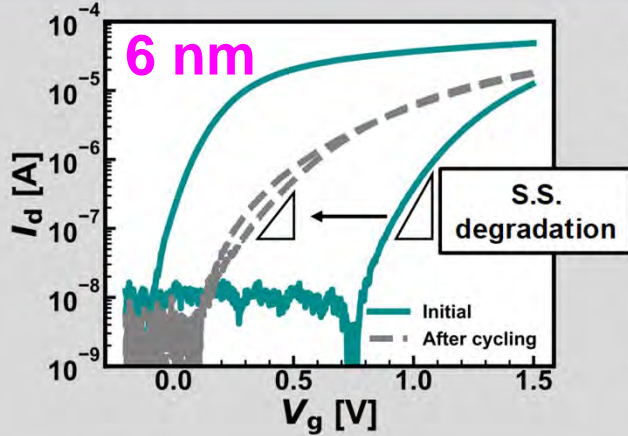
**Same memory window of ~ 0.5 V**



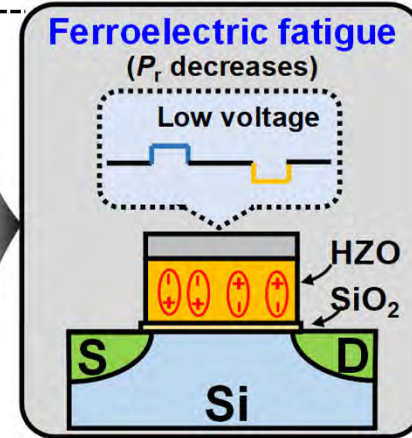
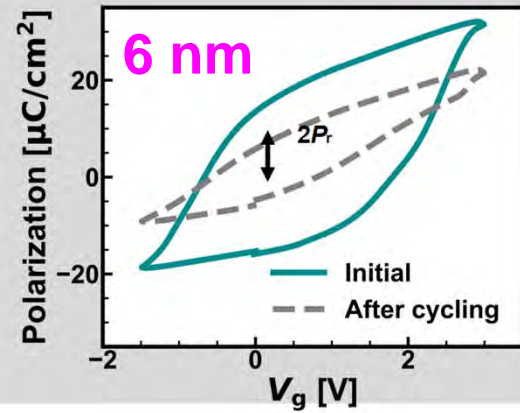
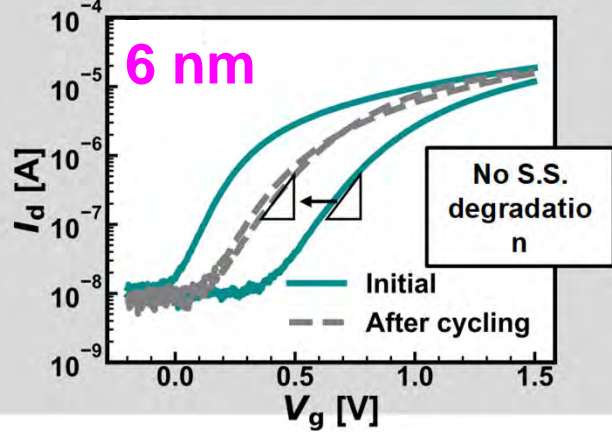
- ❑ Dominant failure in endurance of FeFETs is known to be fatigue (memory window narrowing), rather than gate stack breakdown
- ❑ **HZO scaling and lower voltage operation lead to smaller fatigue**
- ❑ Improvement in endurance due to HZO scaling is still limited, implying **the existence of degradation mechanism under low voltage**

# Difference in MW narrowing in high and low voltage operations

High voltage  
(3.1 V / -2.1 V)



Low voltage  
(2.7 V / -1.7 V)



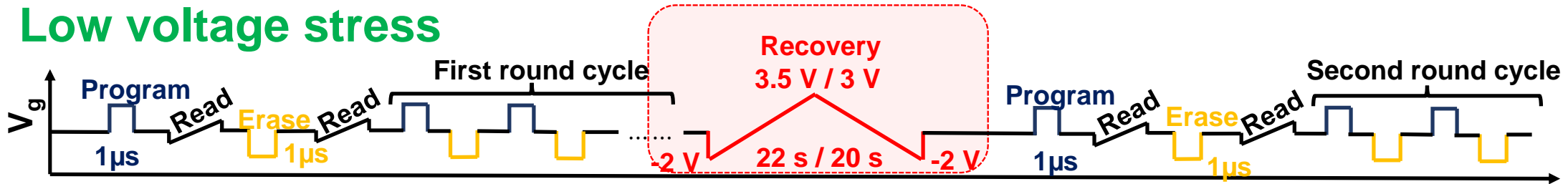
Z. Cai et al.,  
VLSI  
Technology  
and Circuits,  
T5-2 (2023);  
IEEE TED  
(2025)

- ❑ Fatigue under low voltage is found to be caused by  $P_r$  degradation
- ❑  $P_r$  degradation is not observed for fatigue under high voltage, which is caused by MOS interface degradation

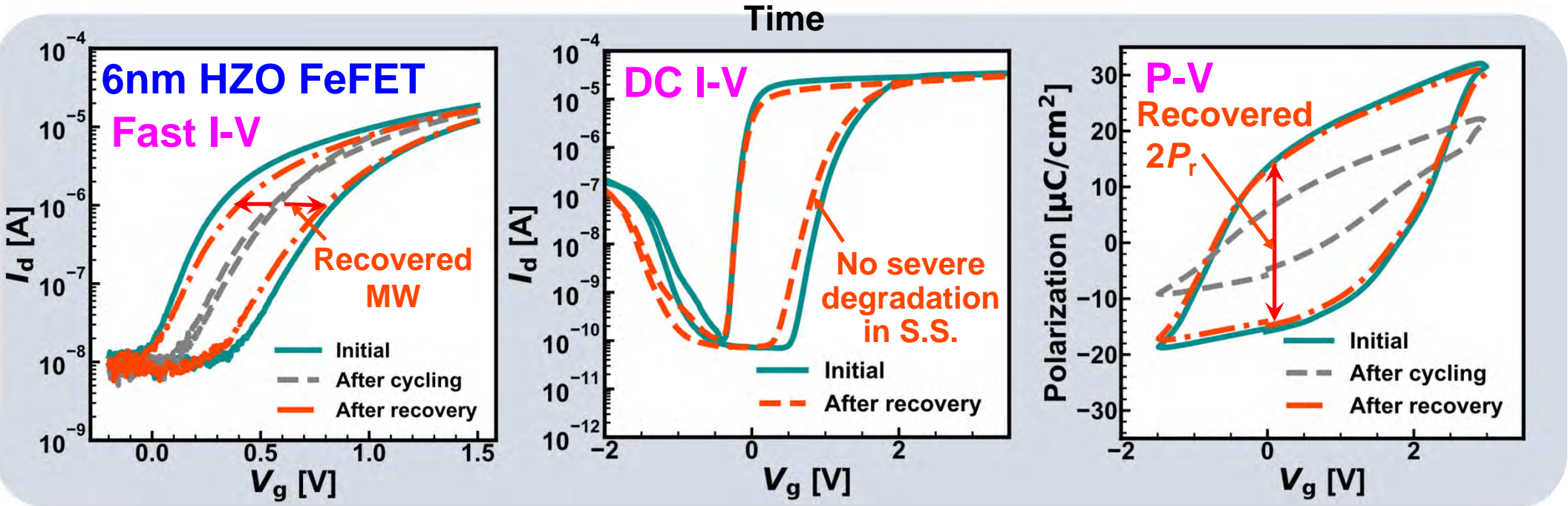


# Recovery of fatigue after low voltage operation

## Low voltage stress



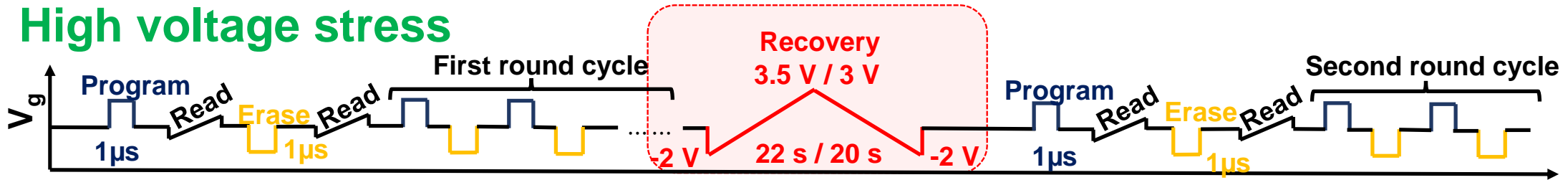
Low voltage



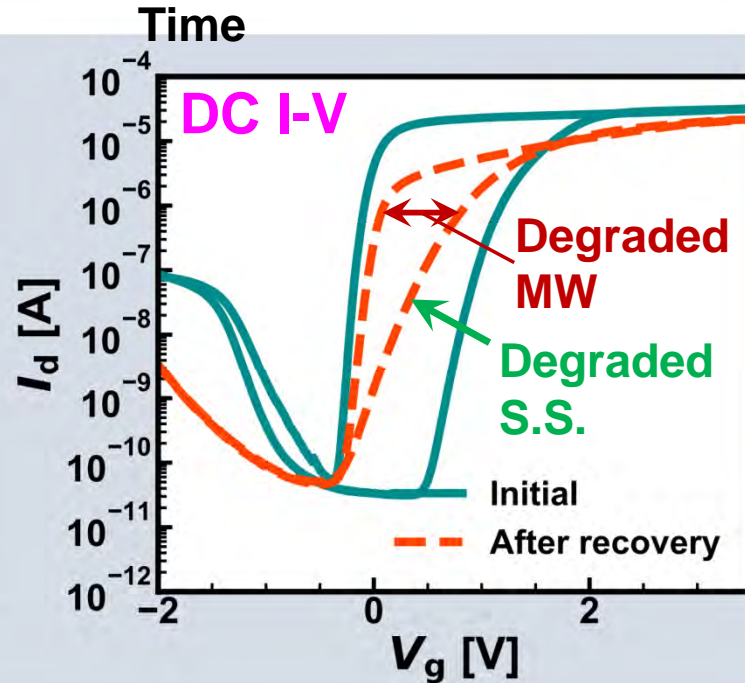
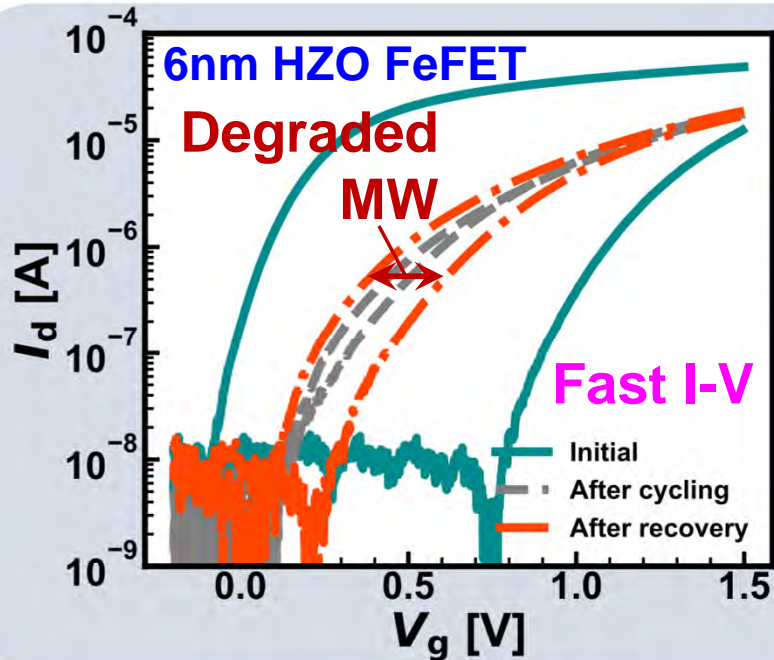
□  $P_r$  degradation and resulting MW narrowing under low voltage operation can be recovered by applying a high voltage pulse

# Recovery of fatigue after high voltage operation

## High voltage stress



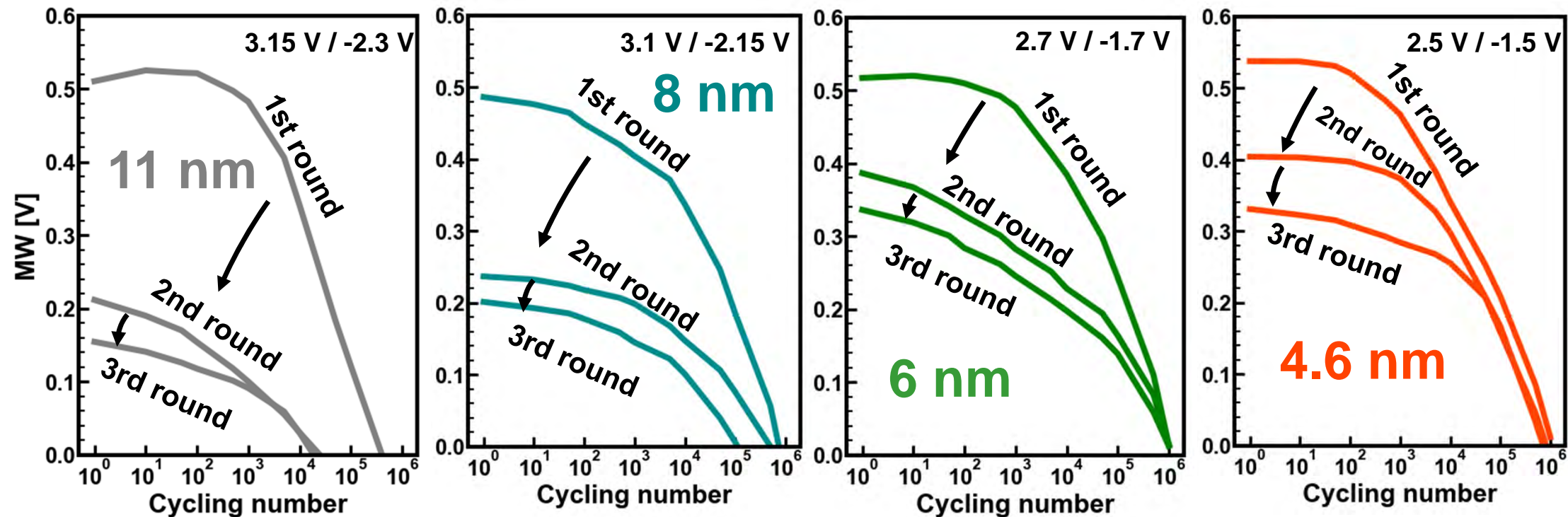
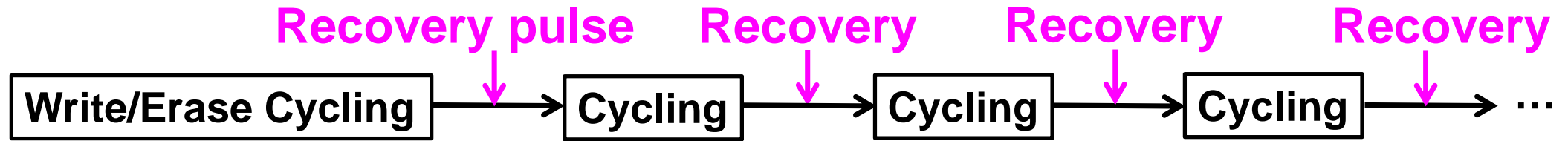
High voltage



Z. Cai et al.,  
VLSI  
Technology and Circuits,  
T5-2 (2023);  
IEEE TED  
(2025)

- MW narrowing under high voltage operation, which is caused by interface degradation, cannot be recovered by a high voltage pulse 88

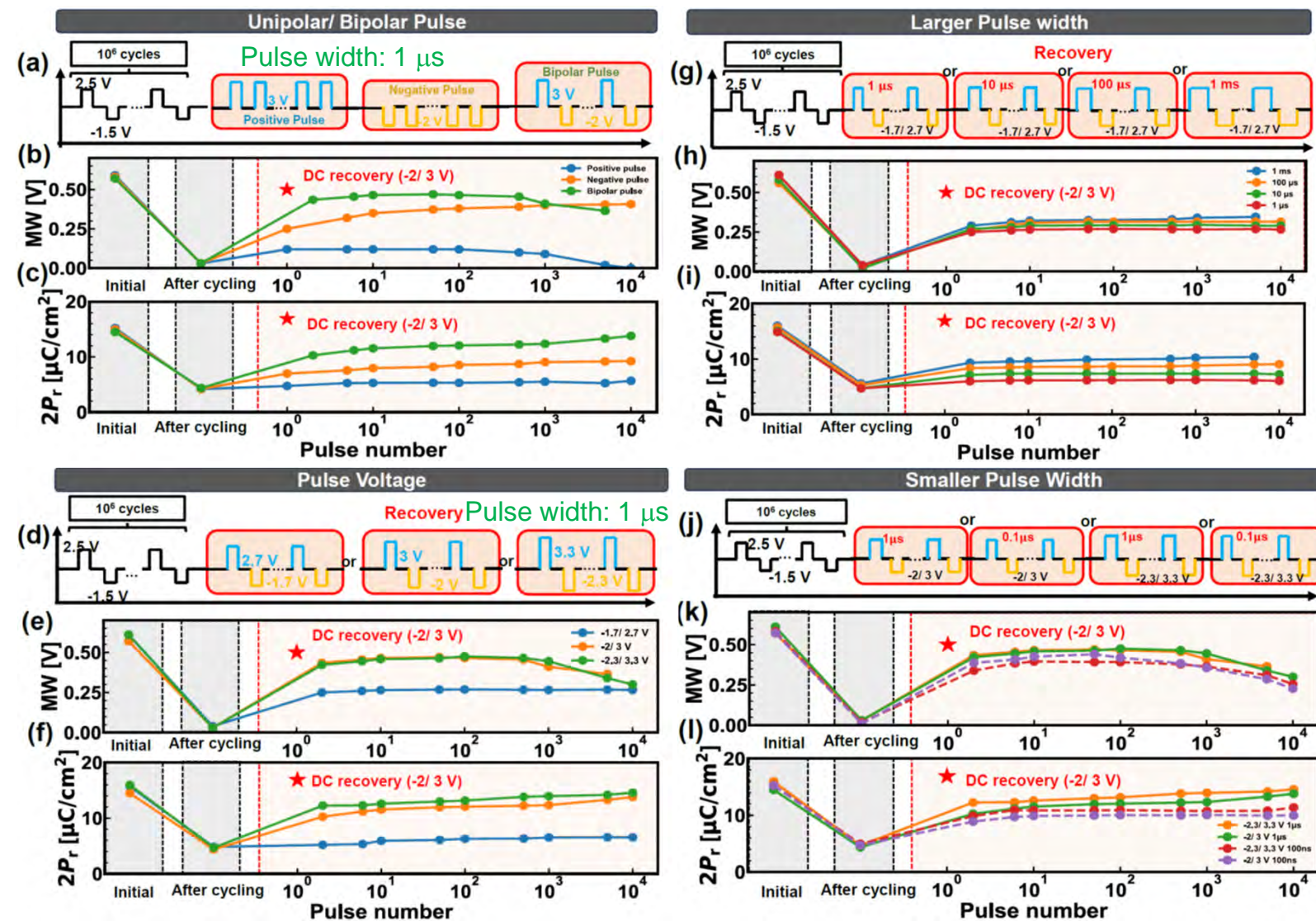
# Multiple recovery scheme of FeFETs with different HZO thickness



- A multiple recovery scheme is more effective in improving endurance of **thinner HZO** FeFETs under **lower-voltage** operation Cai, VLSI (2023) 89



# Effect of recovery pulse condition on recovery characteristics

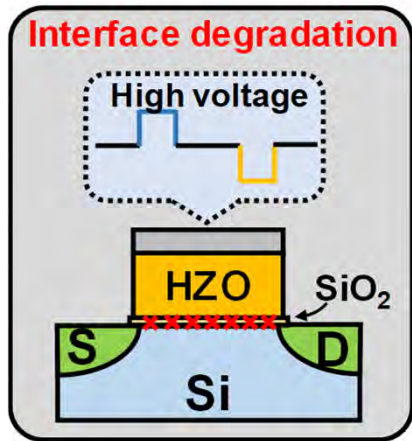


- ❑ Bipolar pulse is most effective for recovery
- ❑ Recovery pulse width of 1  $\mu\text{s}$  is enough for recovery
- ❑ Pulse voltage is critical
- ❑ Longer pulse with lower voltage does not work well
- ⇒ these results are included in the patent

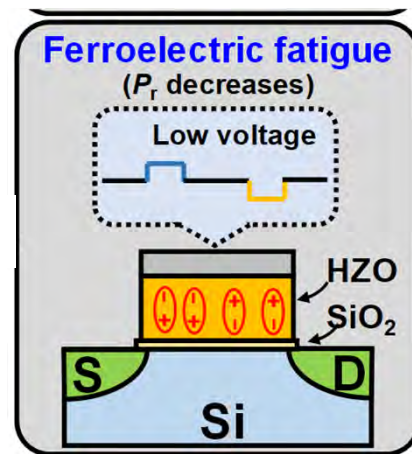


# Summary of impact of HZO thickness scaling on FeFET endurance

Memory window narrowing → Mixture of two mechanisms



Interface degradation  
→ high  $V_g$  driven (hot carrier induced)  
→ permanent degradation



Ferroelectric fatigue ( $P_r$  degradation)  
→ low  $E_{FE}$  driven (domain pinning)  
→ recoverable degradation

Endurance improvement strategy:

- Thinner HZO film (HZO thickness scaling)
- Use lower  $V_g$
- Reduce interface permanent degradation
- +
- Use recovery pulse for recovering remaining  $P_r$  degradation

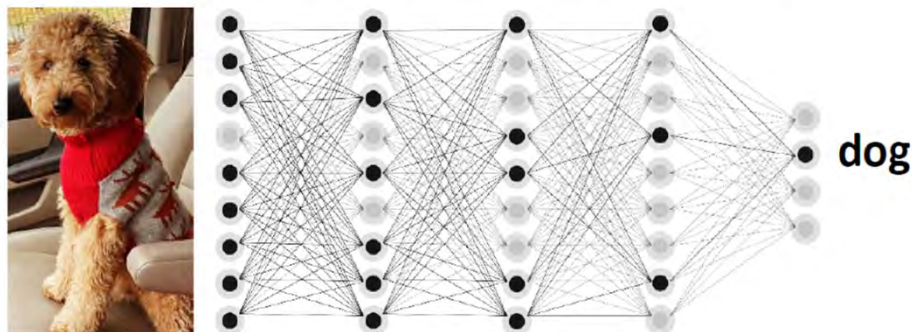
# AI applications

# Expectation of FeFETs for AI applications

# AI revolution by deep neural networks

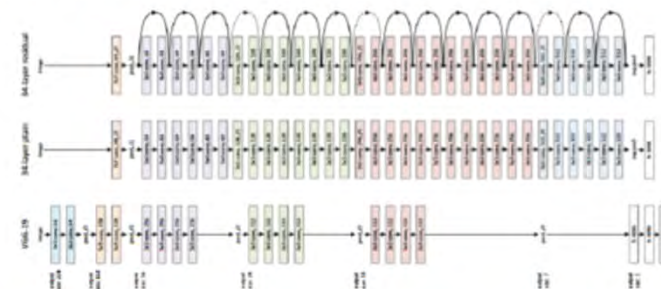
A. Sebastian, IEDM short course, 2.3. (2023)

## Artificial deep neural networks



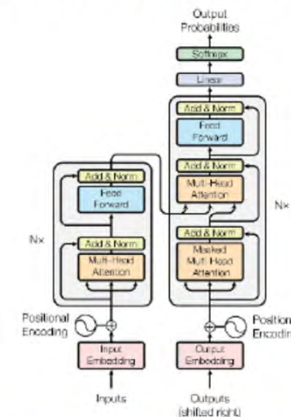
- The machine learning paradigm of artificial deep neural networks (DNNs) has revolutionized AI in recent years
- Powerful tool to learn representations from unstructured data
- Recent consolidation of DNN architectures around **convolutional neural networks (CNNs)**, long-short term memory (LSTM) networks and **transformers**

## Convolutional neural networks



He et al., "Deep Residual Learning for Image Recognition", CVPR (2016)

## Transformers

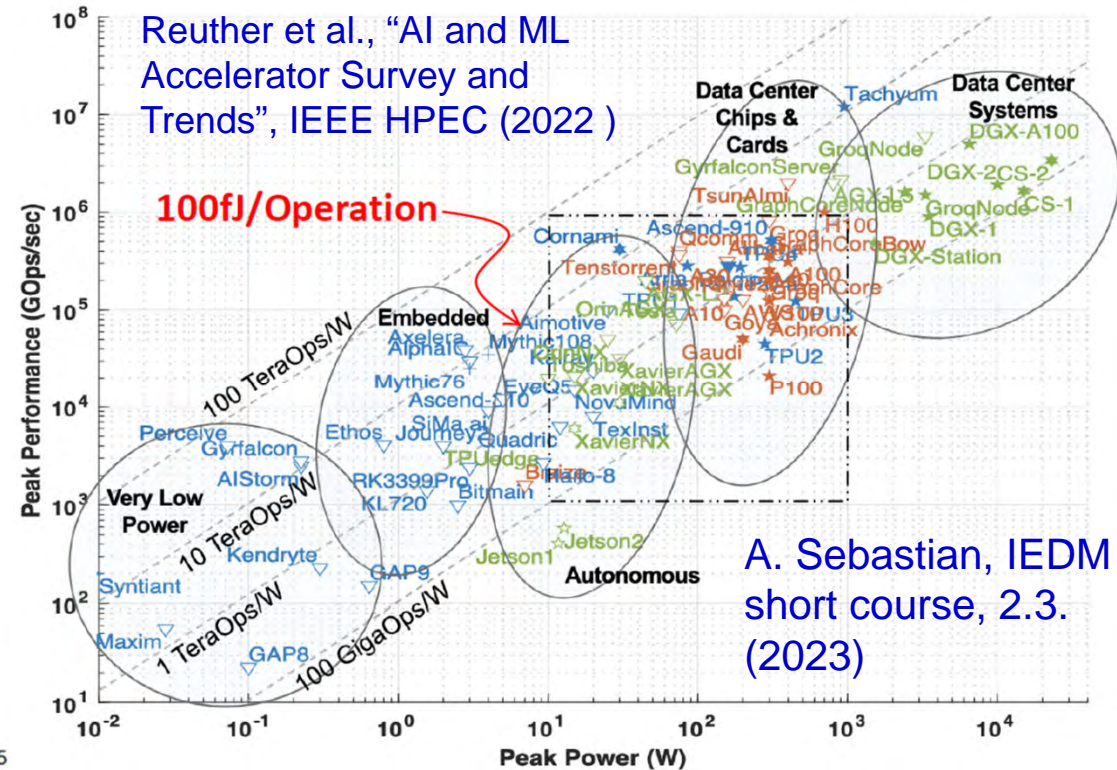
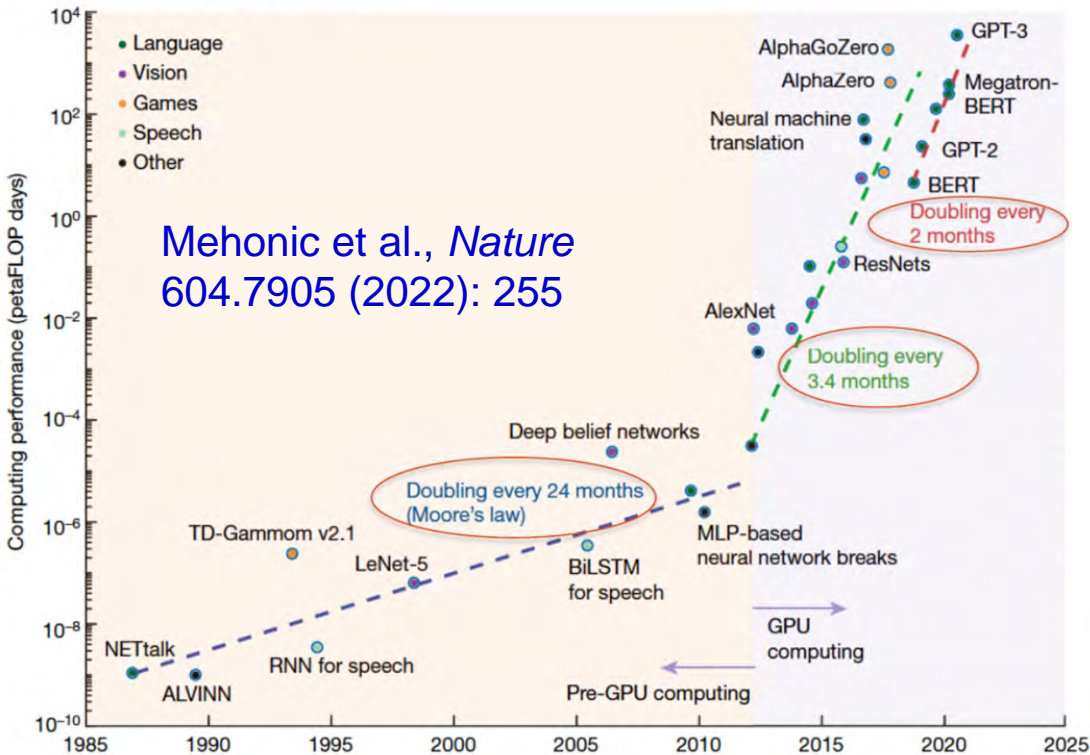


Vaswani et al., "Attention is all you need", NeurIPS (2017)



# Power crisis of AI system

a Computing power demands



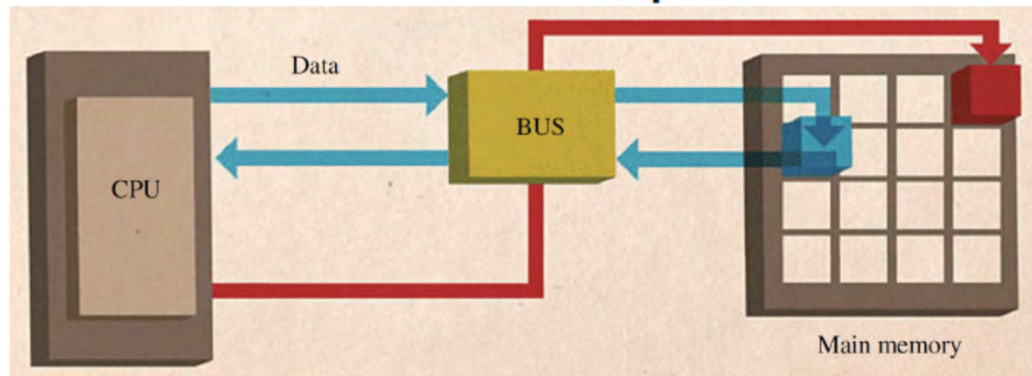
A. Sebastian, IEDM short course, 2.3. (2023)

- Software for ML/AI strongly demands rapid growth computing power
- Peak performance vs. power plot, based on present CMOS system, suggests that achieving energy efficiencies better than **100 fJ/Operation** is challenging
- **Innovation of AI software/hardware is mandatory, particularly for edge AI**

# Possible innovation for mitigating power issues of AI system

J. J. Yang, VLSI symp. short course, T-5 (2023)

## Classical computer



1. Separate processor and storage (**Von Neumann bottleneck**)
2. Sequential process
3. Analog/Digital conversion

Q. Xia, J. Joshua Yang, *Nature Materials* **18**, 309 (2019)

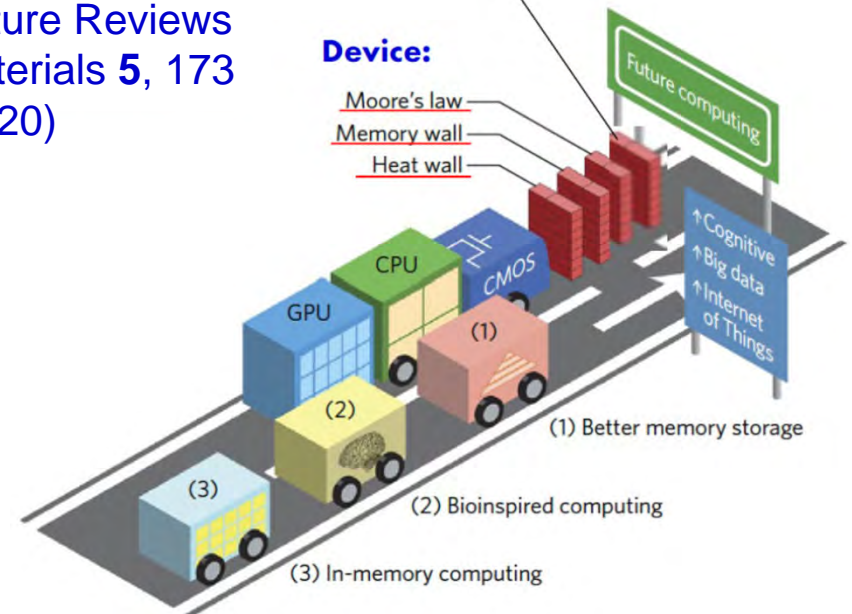
*Nature Electronics* **1**, 22–29 (2018)  
*Nature Reviews Materials* **5**, 173 (2020)

Architecture:

**von Neumann Bottleneck**

Device:

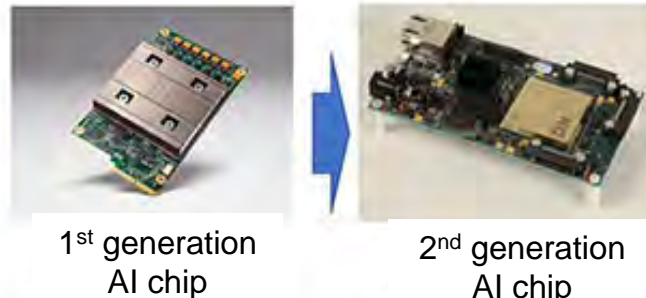
Moore's law  
Memory wall  
Heat wall



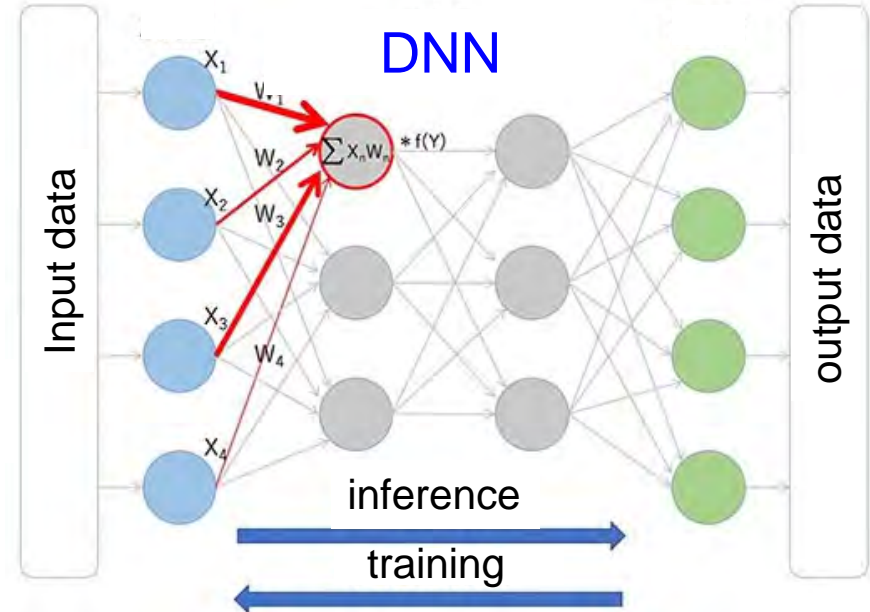
- In hardware level, **AI-specific hardware design, in-memory computing and utilization of analog computing** are key technologies
- In architecture level, new algorithm with **low computational power and high energy efficiency** is strongly expected for edge AI applications



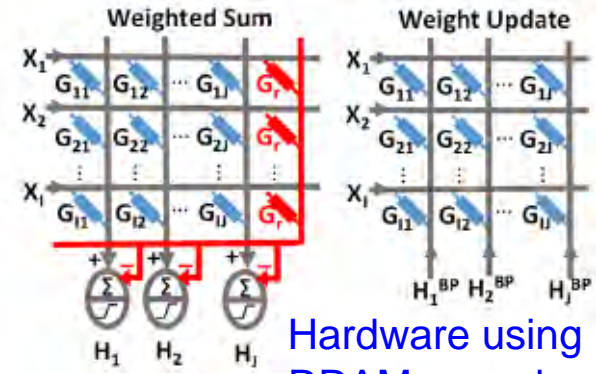
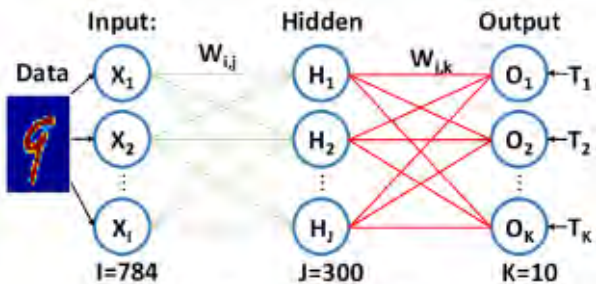
# Expectation of AI-specific hardware and AI chip



Chip specialized for AI processing      Chip mimicing computation in brain



Heavy multiply-add calculation needed

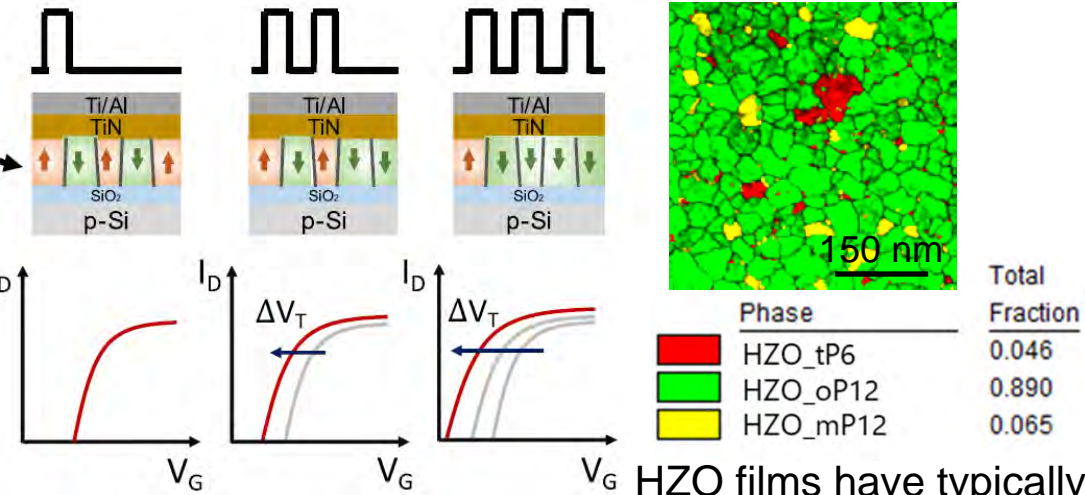


Hardware using RRAM cross bar

- Demands of AI applications are expanding rapidly
- A variety of deep neural network (DNN)-based

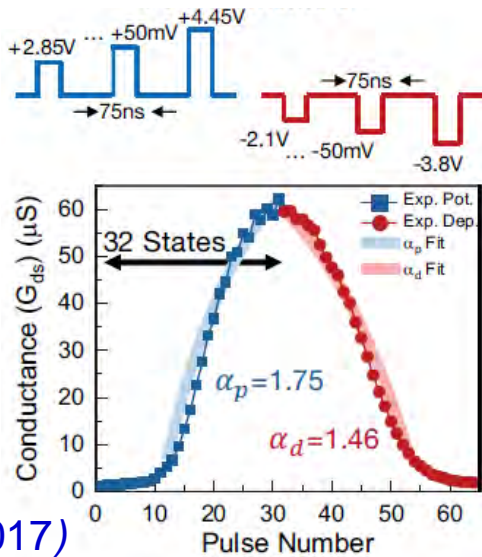
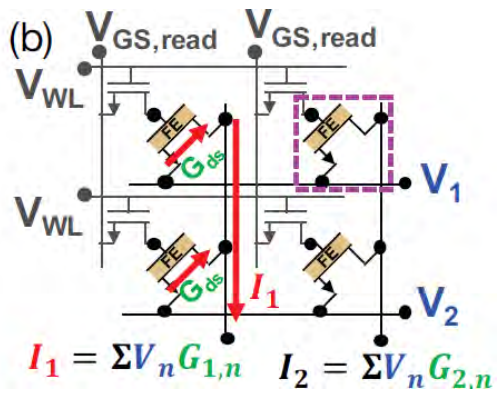
- information processing are mainly performed by software at present
- **Von-Neumann bottleneck** between logic and memory functions is critical
- Implementation of **hardware to perform NN-based calculations** is expected, in terms of **low power consumption and computation efficiency**
- Devices with both memory and switch functions are promising
- **Cross-bar arrays using non-volatile memories** like RRAM, PCRAM, MRAM and FeRAM etc. are promising for this application

# FeFET analog memory (synaptic nature)



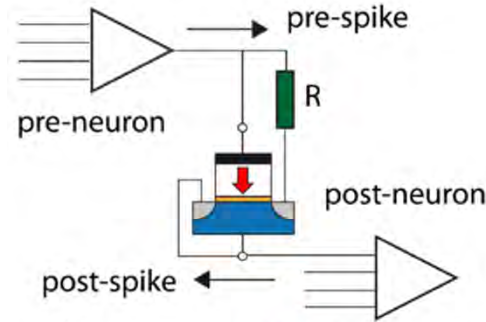
HZO films have typically many small grains

M. Jerry et al., *J. Phys. D: Appl. Phys.* **51**, 434001 (2018)

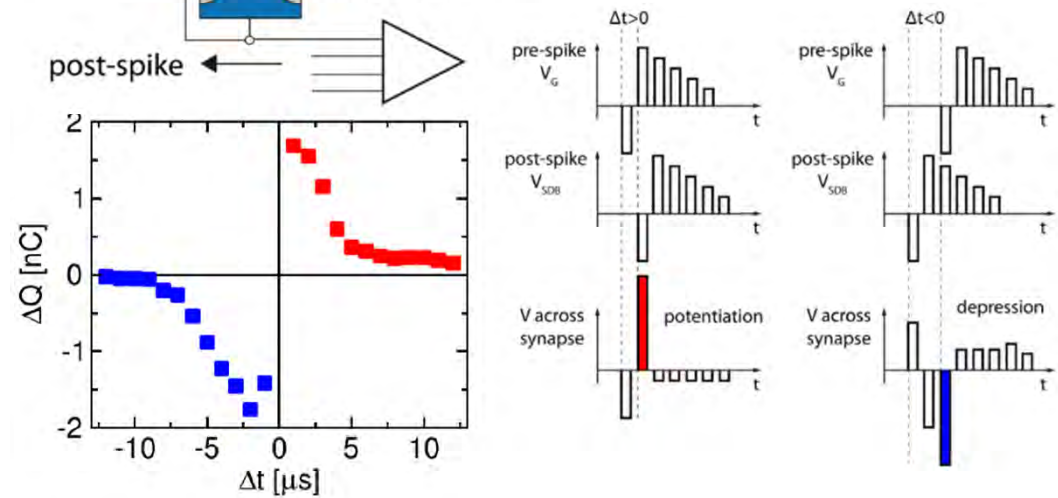


M. Jerry et al., *IEDM*, 139 (2017)

## Spike timing dependent plasticity (STDP)



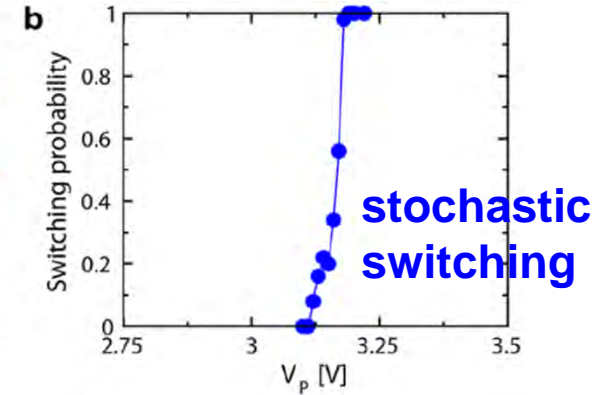
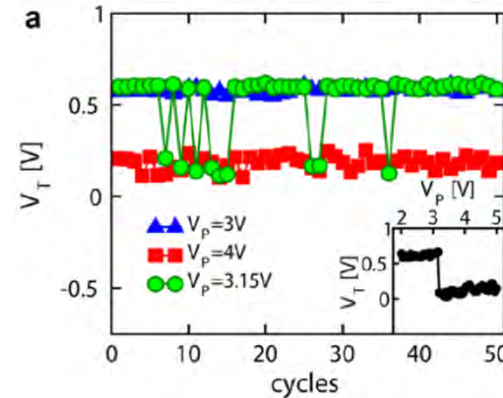
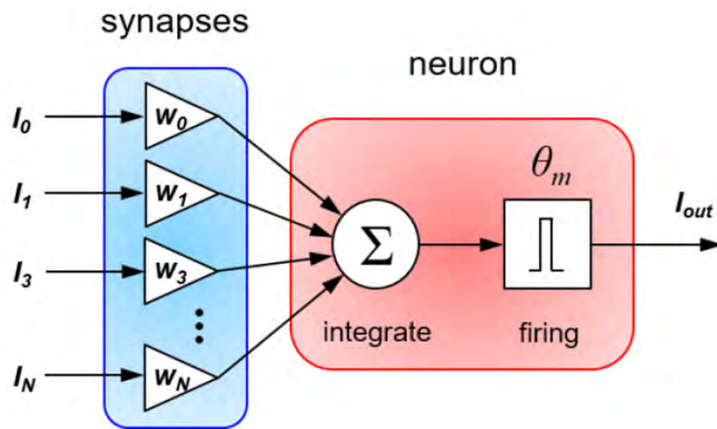
H. Mulaosmanovic et al., *VLSI symp.*, T176 (2017)



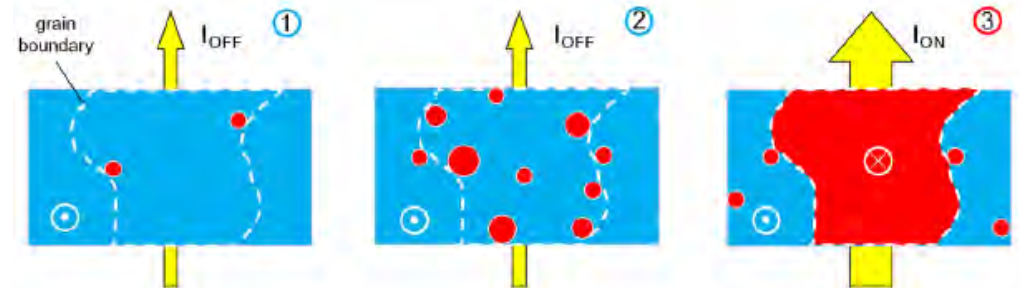
- FeFETs with large areas shows analog memory characteristics, attributable to many localized polarization domains  
→ FeFETs can be employed for artificial synapse



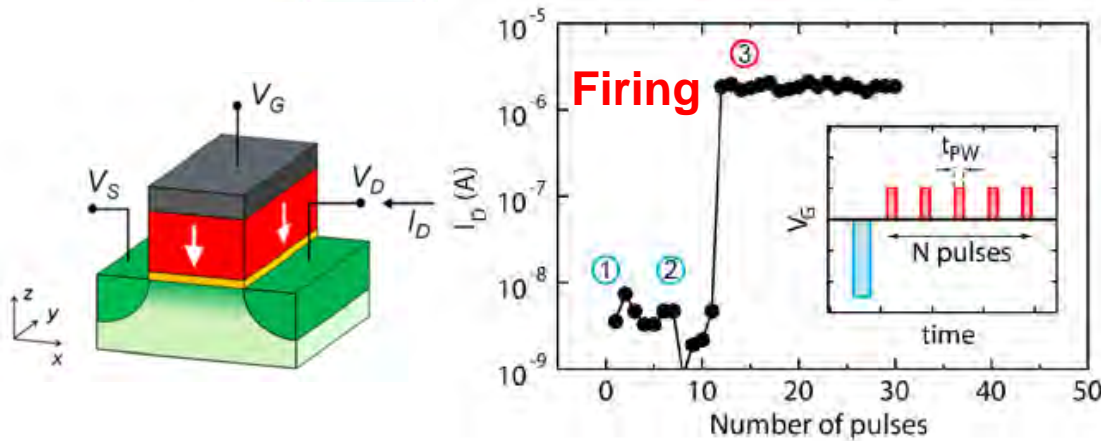
# Accumulative and stochastic polarization (neuron-like nature)



Schematic view of accumulative polarization switching



- Polarization reversal occurs through an invisible “polarization domain nucleation” process, resulting in accumulative and stochastic behavior
- utilized as artificial neurons



H. Mulaosmanovic et al, ACS Appl. Mater. Interfaces 2017 **9**, 3792 (2017); ACS Appl. Mat. Interfaces **10**, 23997 (2018)

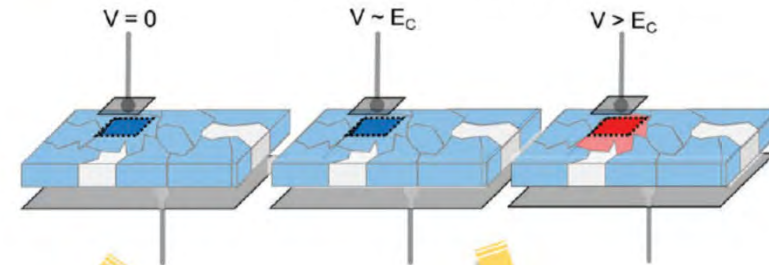
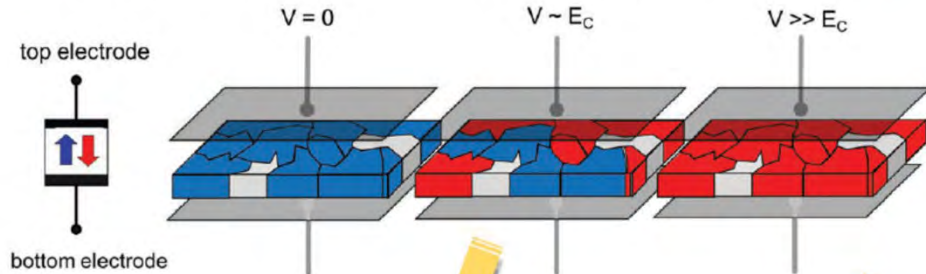
# Different natures of FeFET and their applications to neuromorphic computing

M. Mikolajick et al., Adv. Mater. **35**, 2206042 (2023)

-  polarization up
-  polarization down
-  no polarization / non-ferroelectric

Large area device

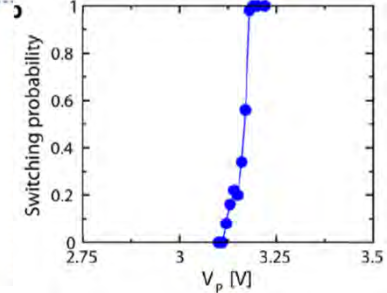
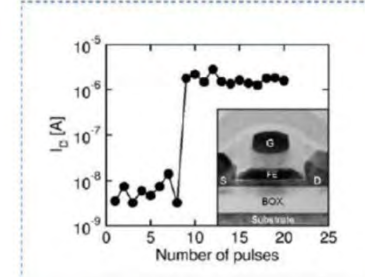
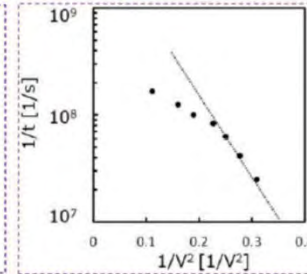
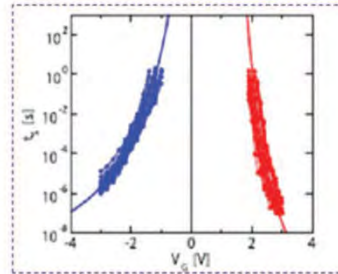
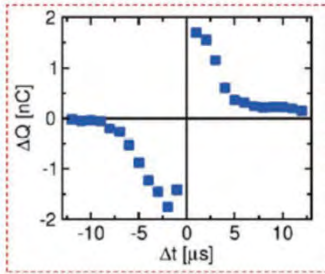
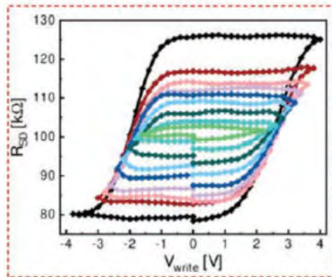
Small area device



Gradual switching

Digital switching

Accumulative switching



analog memory

STDP

neuron-like firing

stochastic firing

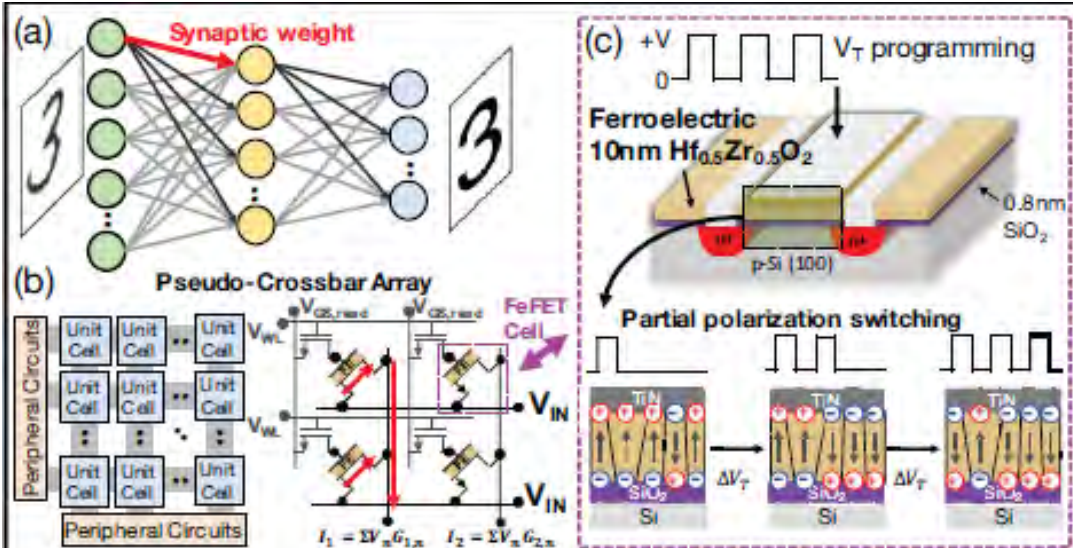
Deep neural network

Spiking neural network



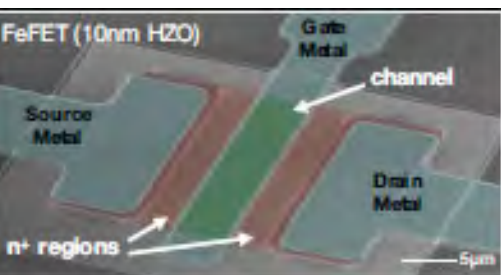
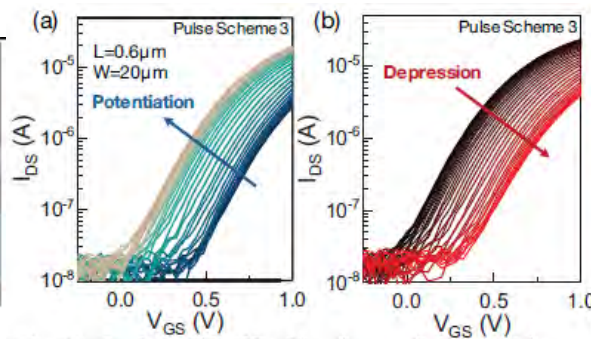
# Application of FeFET to cross-bar array for DNN calculation

M. Jerry et al., IEDM 139 (2017)



Analog Synapse Devices			
Type	Filamentary RRAM	Interfacial RRAM	Ferroelectric
Mechanism	current + field assist	current + field assist	electric-field
Prototypical behavior	identical pulses 	identical pulses 	non-identical pulses 
Symmetry	Low	High	High ✓
Accuracy	Low	High	High ✓
Speed	ns	ms	ns ✓

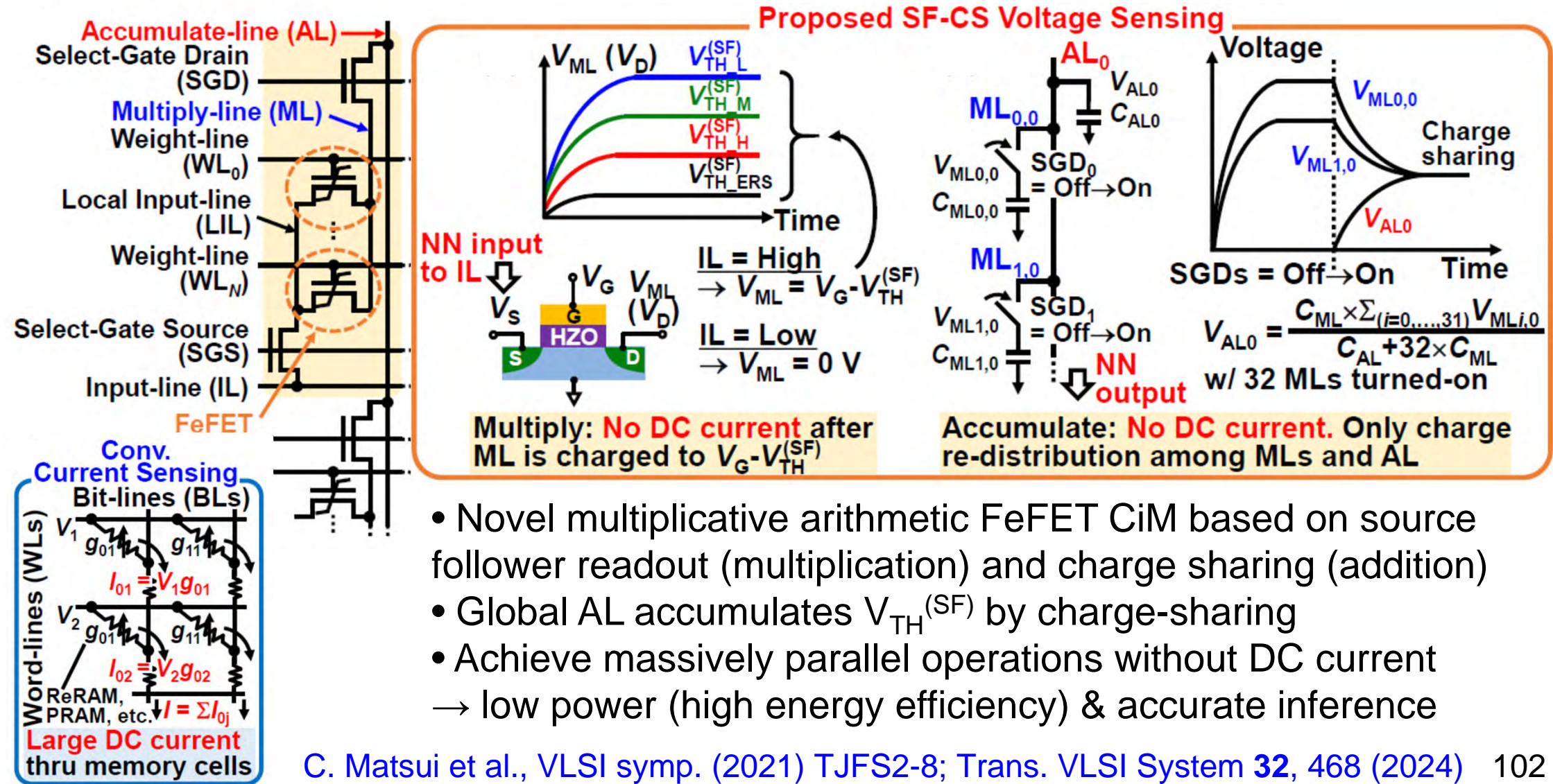
Analog eNVM type	TaO <sub>x</sub> /TiO <sub>2</sub> [3]	PCMO [4]	Ag:a-Si [5]	AlO <sub>x</sub> /HfO <sub>2</sub> [2]	FeFET (This Work)	6-bit SRAM
# of conductance states	102	50	97	40	32	--
Nonlinearity (weight increase/decrease)	0.66/-0.69	3.68/-6.76	2.4/-4.88	1.94/-0.61	1.75/1.46	--
Asymmetry	1.35	10.44	7.28	2.55	0.29	--
R <sub>ON</sub>	5 MΩ	23 MΩ	26 MΩ	16.9 kΩ	559.28 kΩ	--
ON/OFF ratio	2	6.84	12.5	4.43	45	--
Weight increase pulse	3V/40ms	-2V/1ms	3.2V/300μs	0.9V/100μs	3.65V (avg.)/75ns	--
Weight decrease pulse	-3V/10ms	2V/1ms	-2.8V/300μs	-1V/100μs	-2.95V (avg.)/75ns	--
Weight update cycle-to-cycle variation (σ)	<1%	<1%	3.5%	5%	<0.5%	--
Accuracy for online learning	~10%	~10%	~73%	~41%	~90%	~94%
Area	1,071.3 μm <sup>2</sup>	1,071.3 μm <sup>2</sup>	1,072.0 μm <sup>2</sup>	3,657.2 μm <sup>2</sup>	1,190.4 μm <sup>2</sup>	10,311 μm <sup>2</sup>
Latency for online learning (1M images)	1132 years (3.57x10 <sup>10</sup> s)	22.19 years (7.00x10 <sup>8</sup> s)	13.3 years (4.20x10 <sup>8</sup> s)	1.77 years (5.60x10 <sup>7</sup> s)	9.33 hours (3.36E4 s)	7.76 s
Energy for online learning (1M images)	65.86 mJ	29.4 mJ	87.94 mJ	150 mJ	98.01 mJ	6.98 mJ
Leakage power	35.29 μW	35.29 μW	35.29 μW	35.29 μW	35.29 μW	1.1 mW



- Early demonstration of application of FeFET analog memory to synaptic weights in cross-bar array for deep neural network calculations with emphasis on high symmetry and fast writing speed



# High energy efficiency FeFET CiM with source follower readout

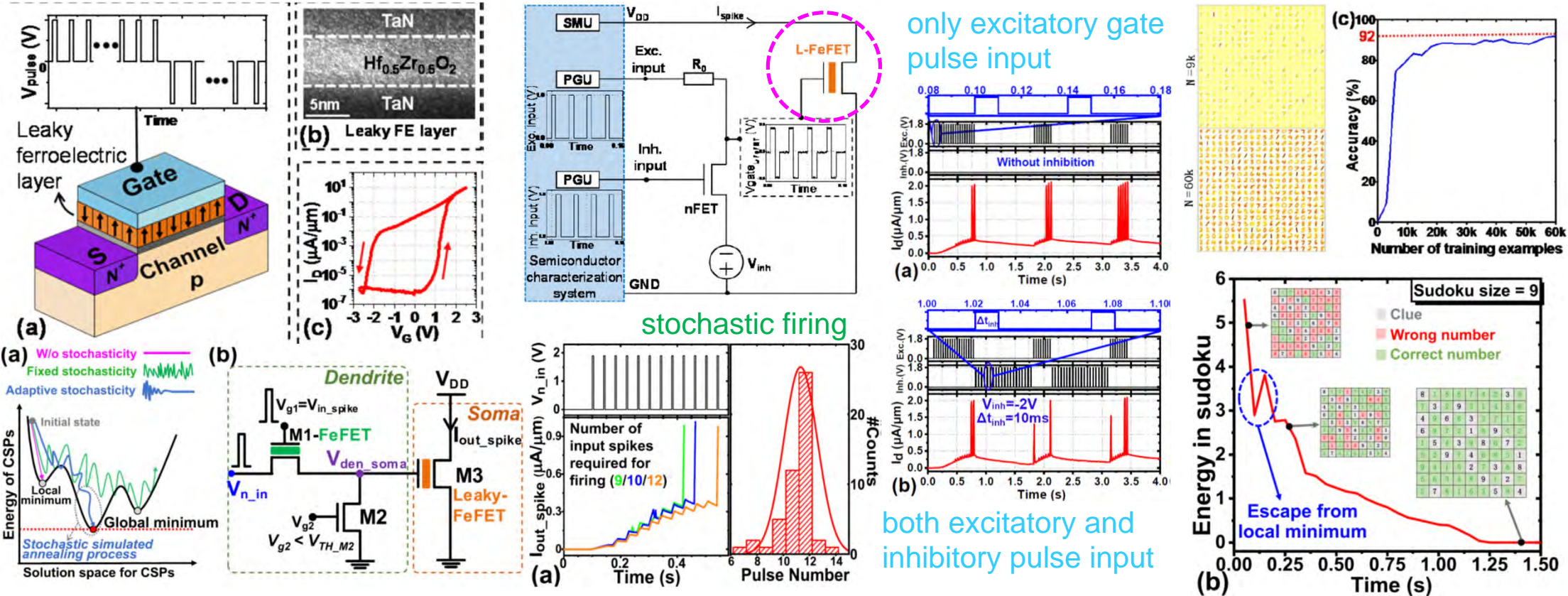


- Novel multiplicative arithmetic FeFET CiM based on source follower readout (multiplication) and charge sharing (addition)
- Global AL accumulates  $V_{TH}^{(SF)}$  by charge-sharing
- Achieve massively parallel operations without DC current → low power (high energy efficiency) & accurate inference



# Application of Leaky-FeFET to spiking neural network

C. Chen et al., VLSI symp., T136 (2019), J. Luo et al., IEDM 122 (2019); EDL 43, 308 (2022)

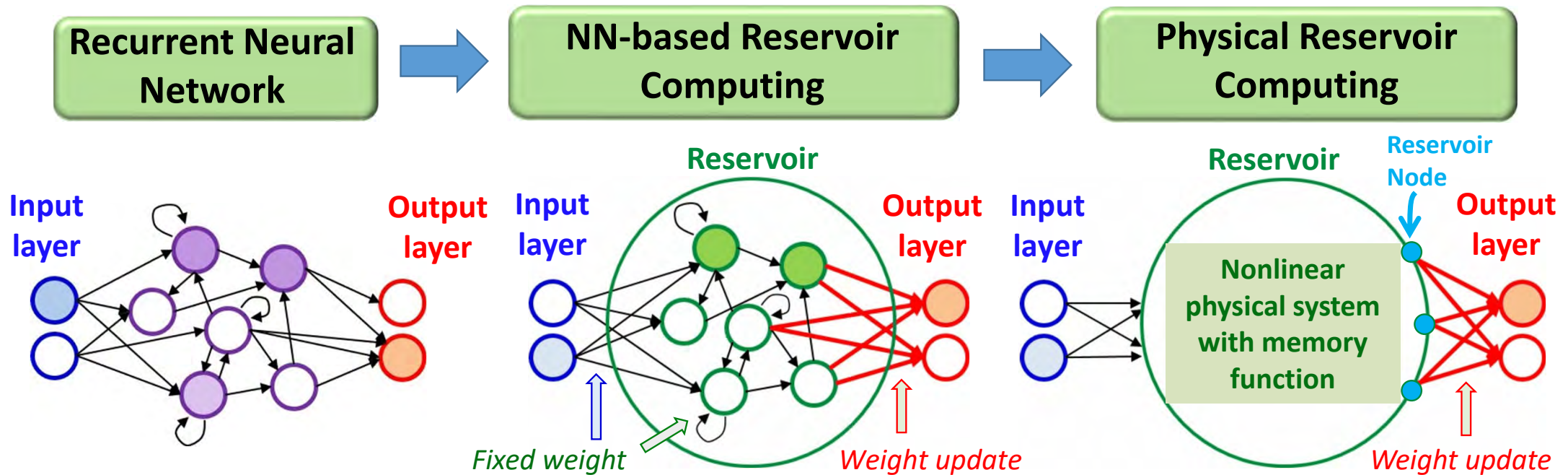


- Leaky-FeFET with thin HZO and larger gate leakage current was demonstrated to show the leaky integrate-and-fire (LIF) function, which was utilized spiking-neural network
- Neuron firing due to polarization switching is controlled by excitatory and inhibitory gate pulse input
- Stochastic polarization function of FeFET is utilized for SNN-based inference and optimization problem

# Physical reservoir computing using FeFETs

# Physical reservoir computing

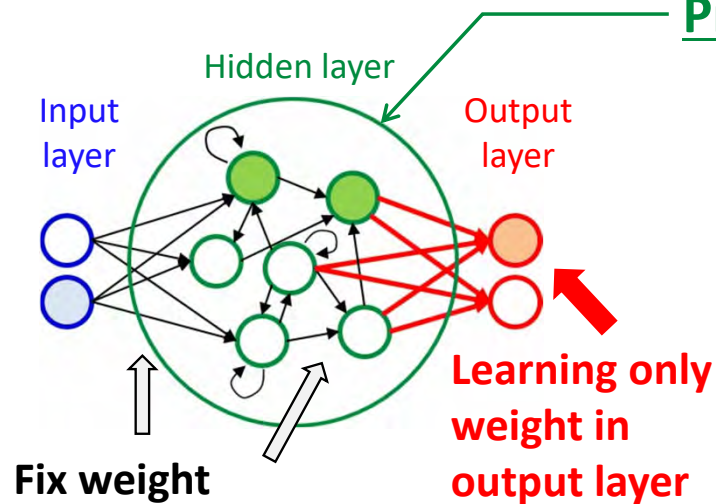
G. Tanaka et al., Neural Networks 115, 100 (2019)



- Recurrent neural network  $\Rightarrow$  suitable for processing time-series data
- Reservoir computing  $\Rightarrow$  Only weights of a single output layer are trained (other weights are fixed)  $\Rightarrow$  Training with high speed and low energy consumption
- Reservoir can be implemented by a nonlinear physical system (hardware)  $\Rightarrow$  Further reduces computational and hardware cost  $\Rightarrow$  promising for edge AI applications

# Requirements for physical reservoir

## Properties needed for reservoirs

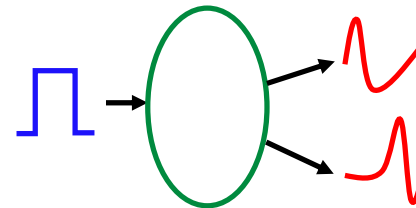


**Short term memory**

⇒ Next state is dependent on present state and input

**Non linearity**

⇒ Non-linear mapping from input to output data

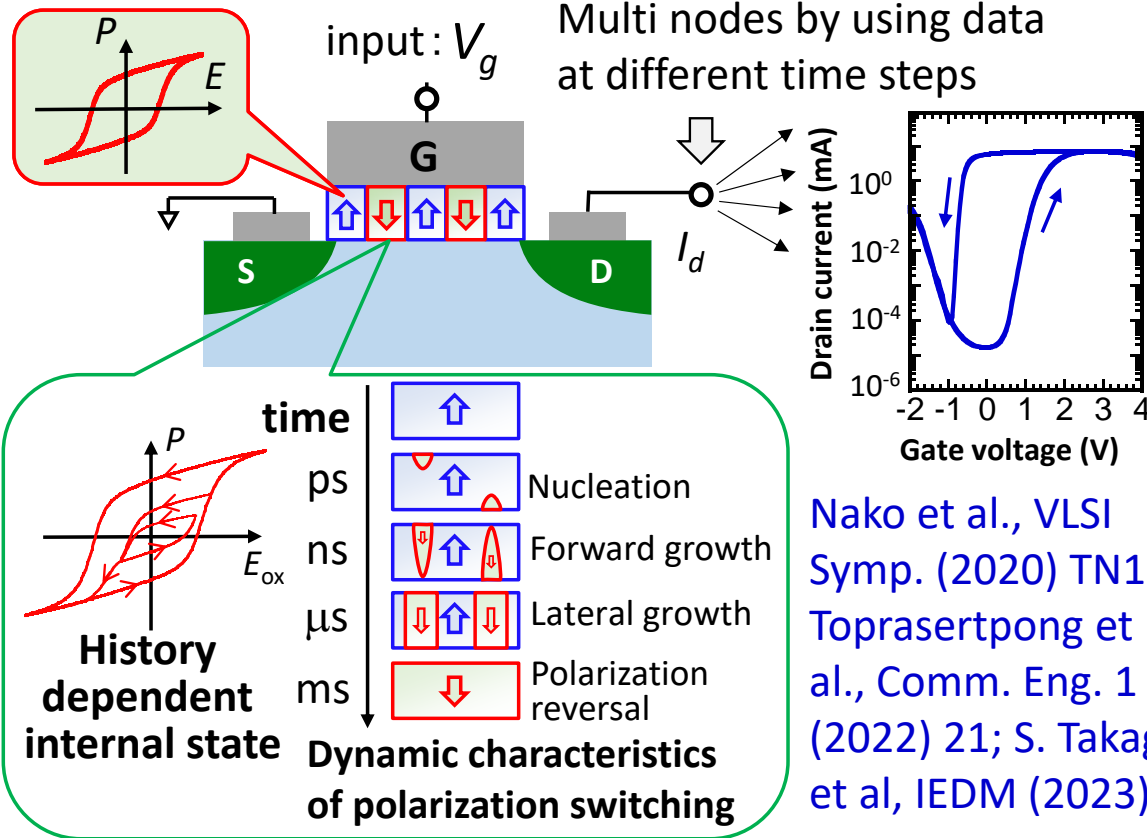


Mapping into higher dimensional space

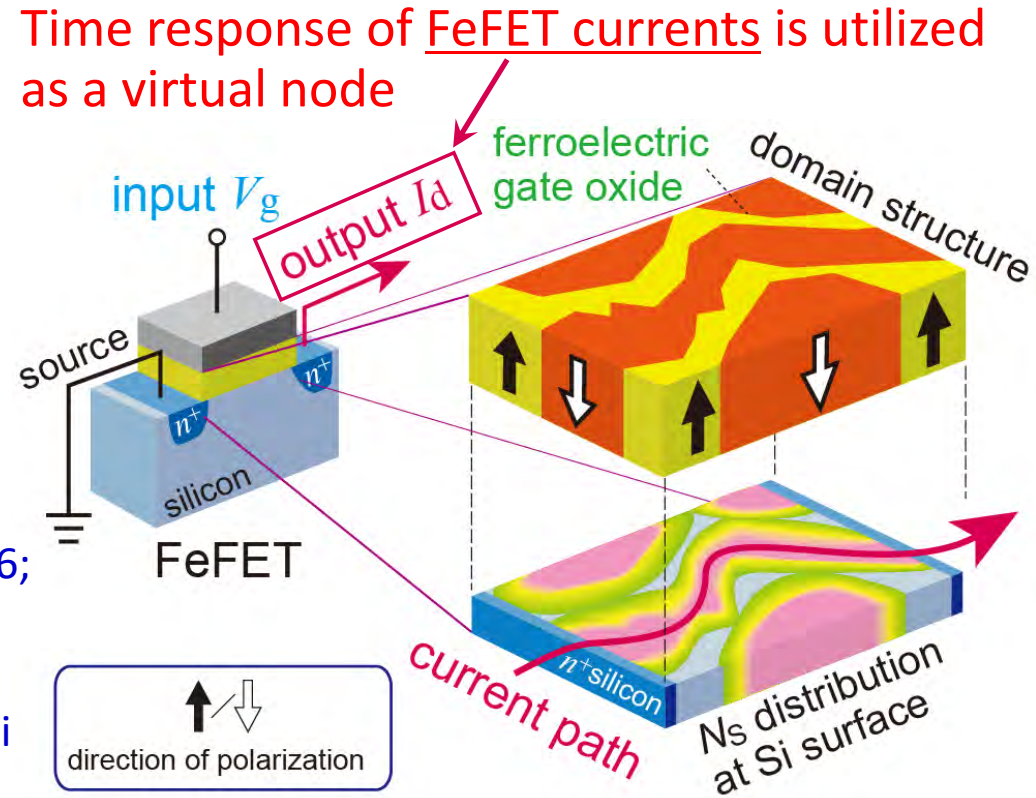
- Reservoir can be implemented by a physical system with short-term memory and rich non-linear functions through dynamics
- We propose FeFET as a reservoir  
⇒ realize CMOS-friendly reservoir computing system (high compatibility with Si standard process and easy integration with CMOS circuitry)



# Expectation for FeFET reservoir computing



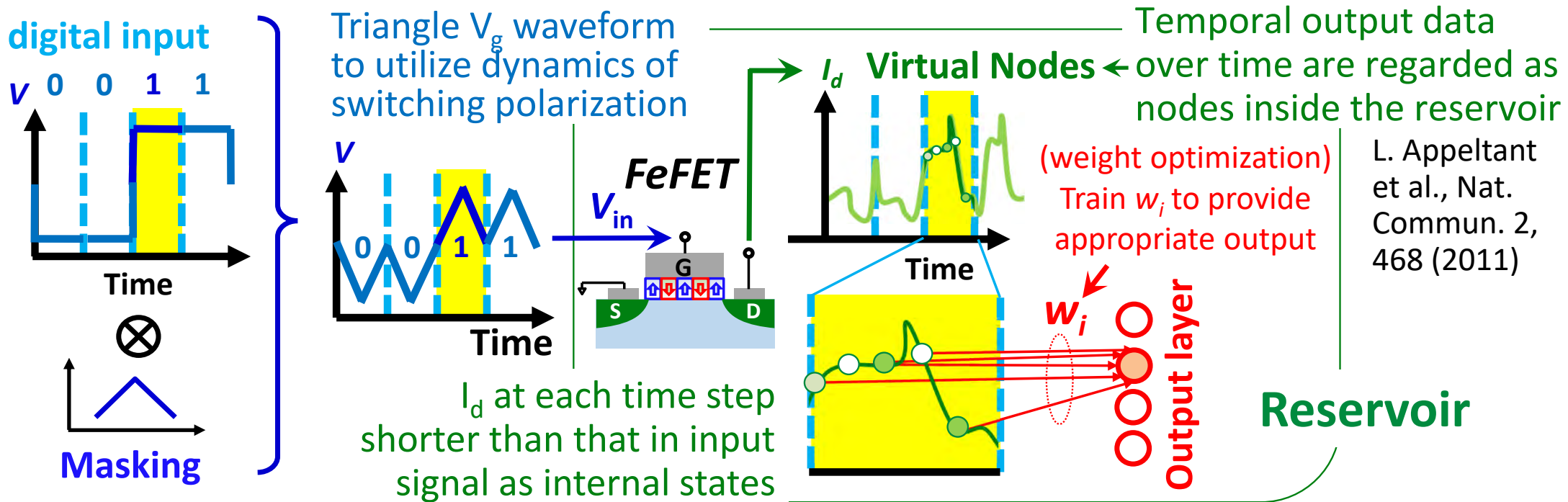
Nako et al., VLSI Symp. (2020) TN1.6; Toprasertpong et al., Comm. Eng. 1 (2022) 21; S. Takagi et al, IEDM (2023)



- Memory function due to polarization and rich non-linearity due to complex time responses of polarization domains
- Enhancing these functions is critical to computing performance improvement

# Operation of reservoir computing using FeFET

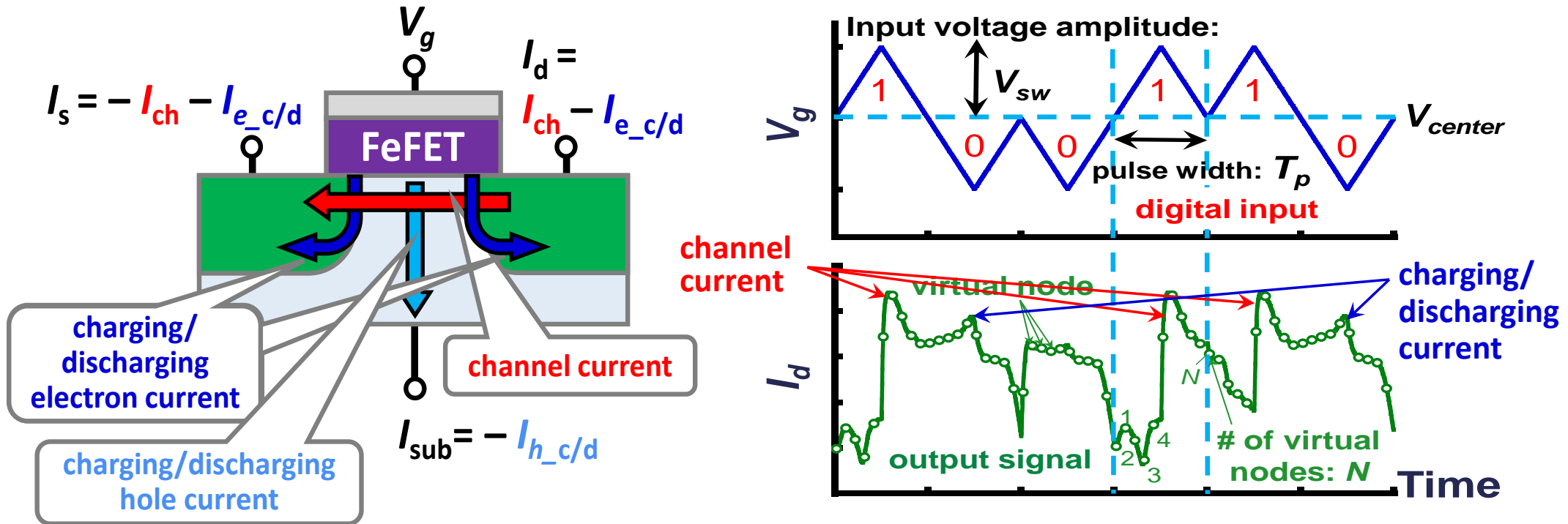
Nako et al., VLSI Symp. (2020) TN1.6; Toprasertpong et al., Comm. Eng. 1 (2022) 21



- How to extract rich information from output signal is a key to successful reservoir computing
- It is essential to design and optimize the operating scheme to maximize the performance of the reservoir computing system with FeFETs

# Pattern recognition with current waveform

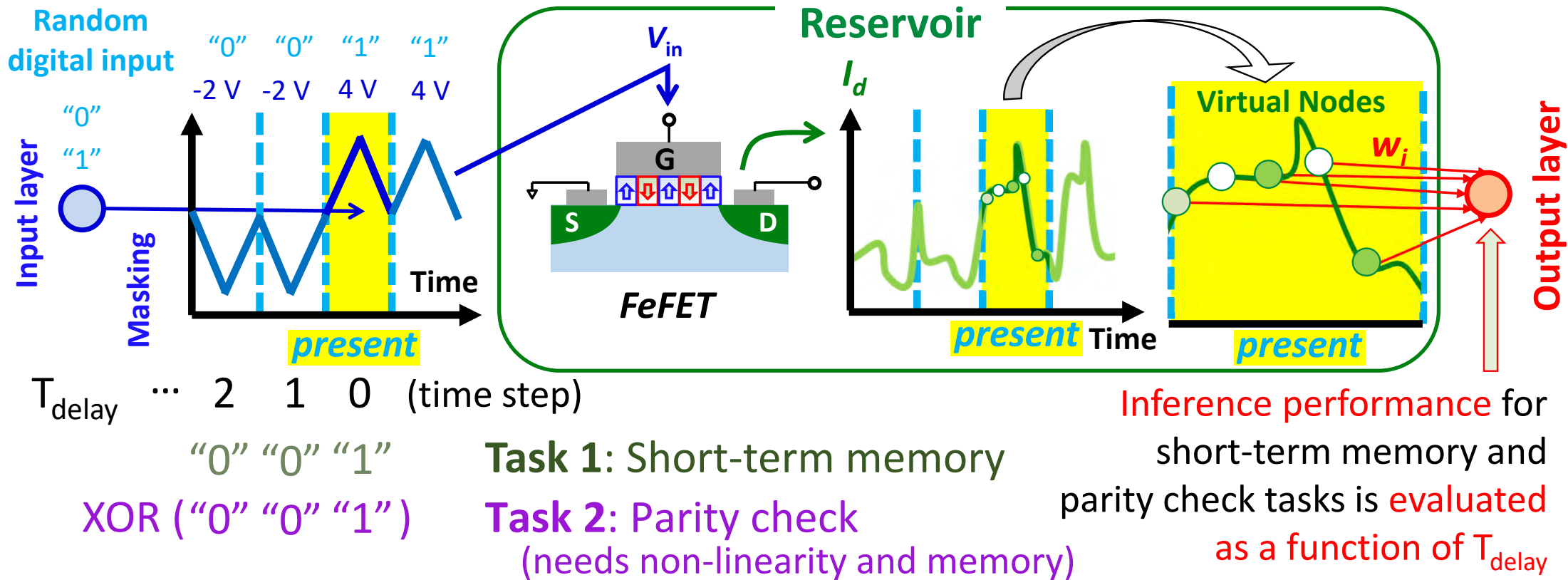
Nako et al., VLSI Symp. (2020) TN1.6; Toprasertpong et al., Comm. Eng. 1 (2022) 21



- Polarization switching can affect both channel current and charging/discharging current
- The time-series current waveform patterns of FeFETs, which depend on the input history, are utilized for inference

# Evaluation of computing performance by basic tasks

Nako et al., VLSI Symp. (2020) TN1.6; Toprasertpong et al., Comm. Eng. 1 (2022) 21

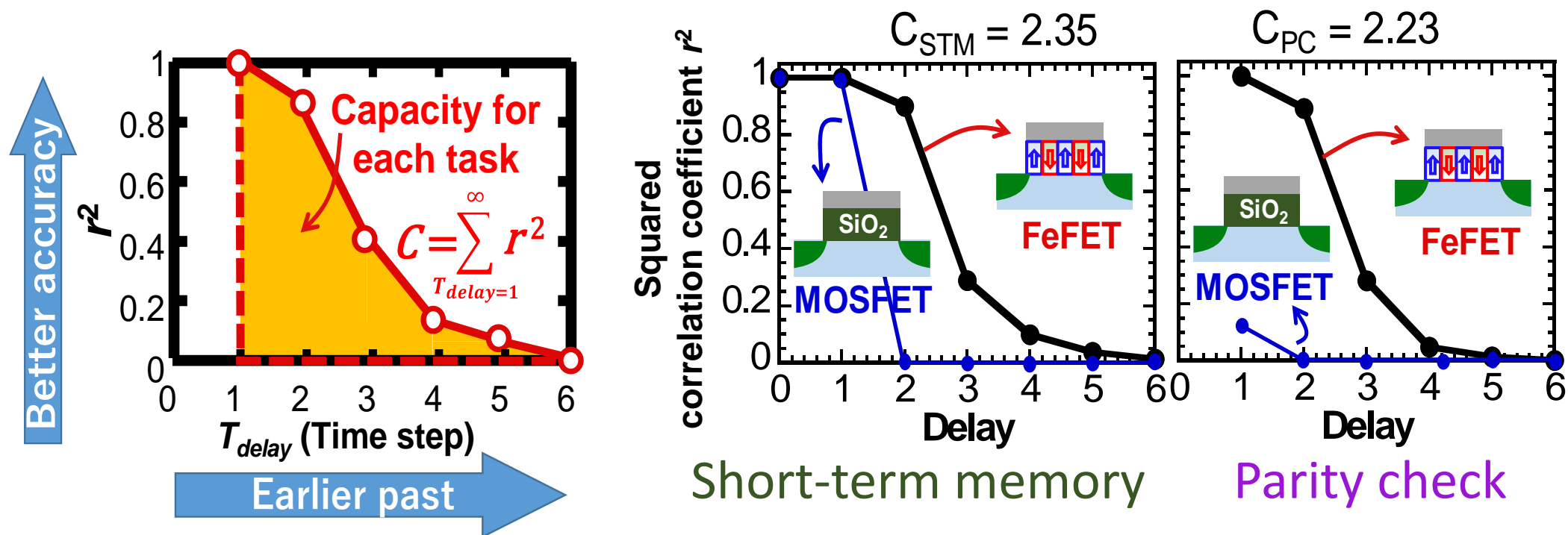


- Two basic tasks are performed to evaluate the "short-term memory" and "non-linearity" of the FeFET reservoir as a function of the time delay step



# Basic task performance of a single FeFET reservoir

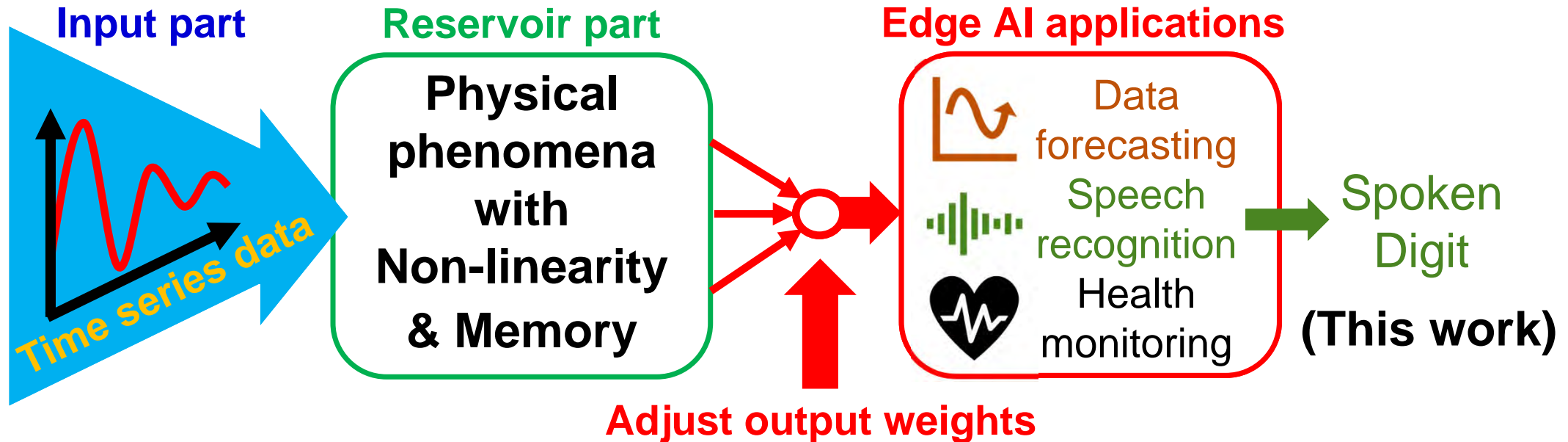
Nako et al., VLSI Symp. (2020) TN1.6; Toprasertpong et al., Comm. Eng. 1 (2022) 21



- Reservoir computing performance is estimated by correlation coefficient as a function of the time delay step and the integrated value (capacity)
- MOSFETs have no reservoir computing performance
- FeFETs exhibit much higher performance, attributed to polarization in HZO

# Application of physical reservoir computing

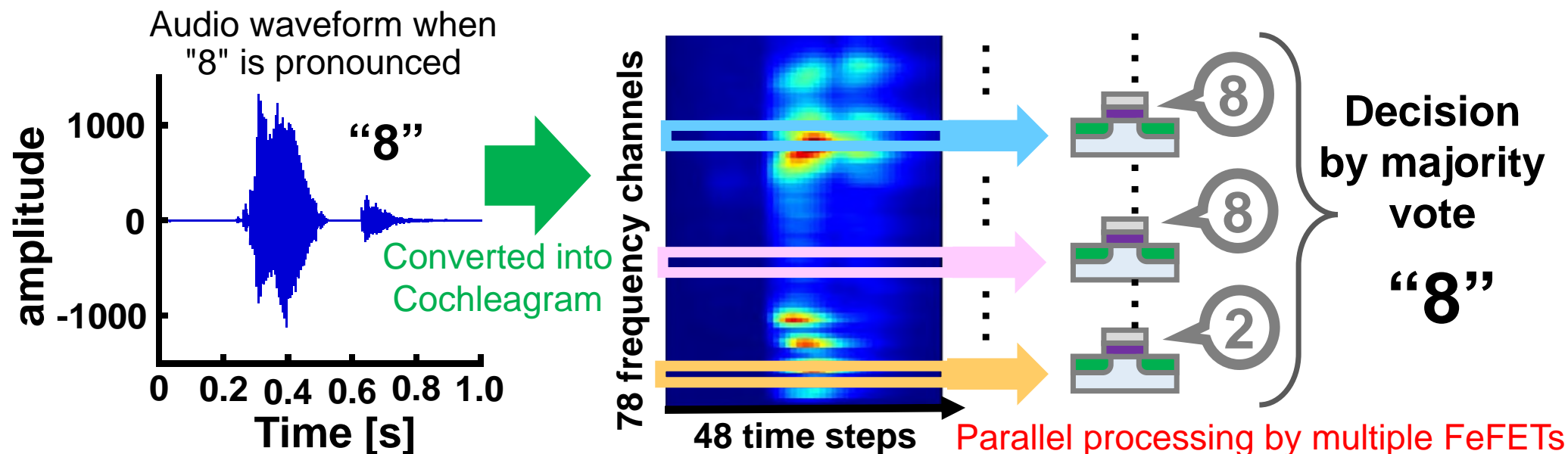
G. Tanaka et al., Neural Networks 115, 100 (2019)



- Potentially important edge AI applications include data forecasting, speech recognition, and health monitoring
- In this study, we apply FeFET reservoir computing to two applications, NARMA as a data forecasting application and spoken digit as a speech recognition application

# Spoken digit recognition by FeFET reservoir computing

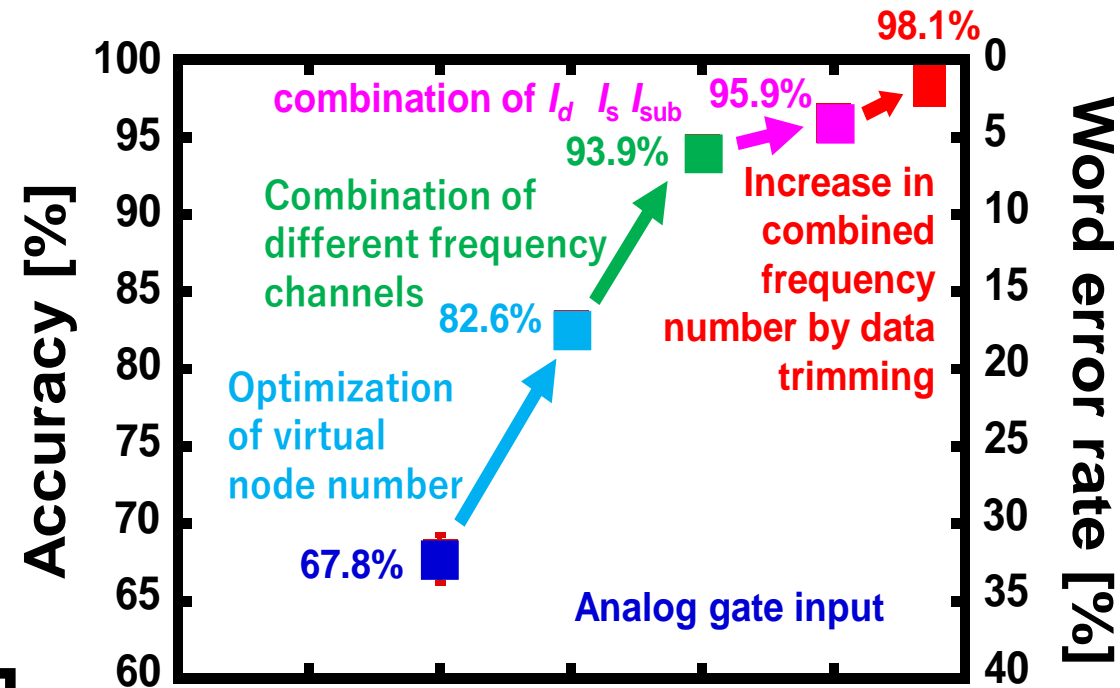
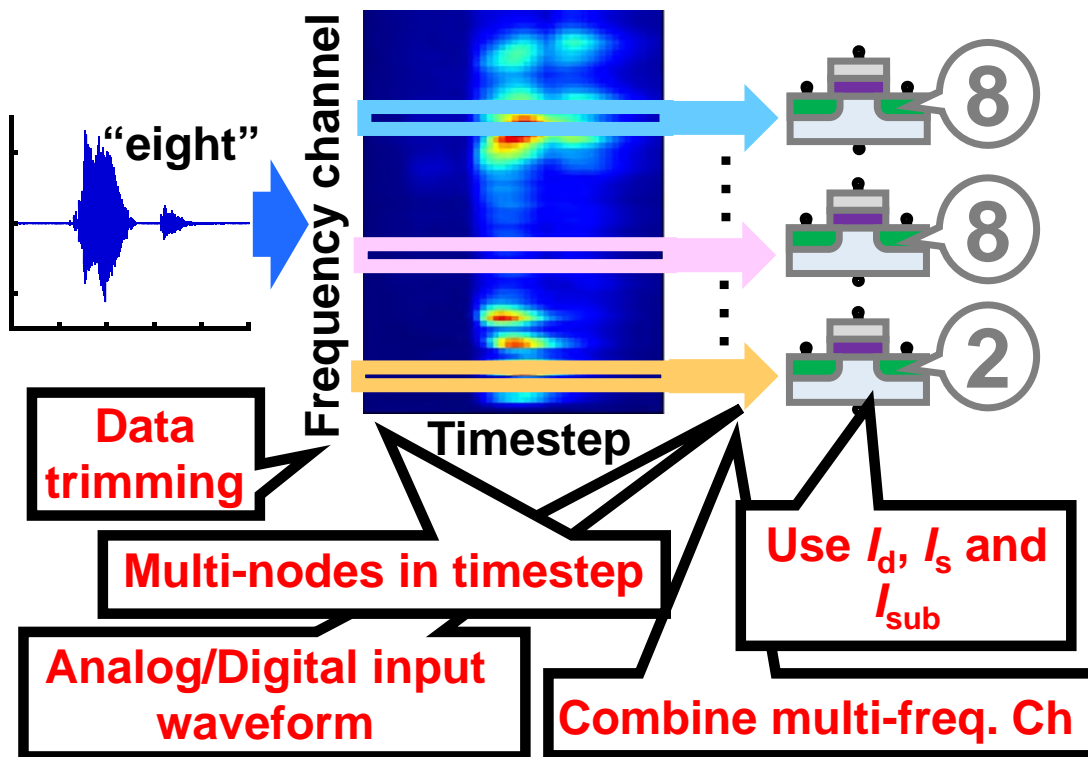
Nako et al., VLSI Symp., 220 (2022) TN1.6; IEEE TED, 70, 5657 (2023)



- Spoken 0-9 digit speech data are converted into cochleagram, which is composed of time series data with multi-frequency channels
- We have proposed a new reservoir computing scheme using parallel processing by multiple FeFETs for spoken digit recognition
- Final decision is made by a majority vote of inference by multiple FeFETs

# Improvement of accuracy in FeFET reservoir computing

E. Nako et al., Symp. VLSI Tech., 220 (2022); S. Takagi et al., IEDM (2023)



- Optimization of virtual node number, an adaptation of analog input, and the optimum combination of multi-frequency channel data additively contribute to an increase in recognition accuracy
- FeFET reservoir computing achieves 98.1% classification accuracy



# Acknowledgement

This work was supported by JST CREST (JPMJCR20C3) and JSPS KAKENHI (21H01359).

I have appreciated Kasidit Toprasertpong, Zuo Cheng Cai, Zhenhong Liu, Seong-Kun Cho, Masaki Otomo, Kento Tahara, Ryosho Nakane, Eishin Nako, Koichiro Iwashige, Tsung-En Lee, Shin-Yi Min, Rikuo Suzuki, Koshuke Ito, Xuan Luo, Makoto Kawano, Zeyu Wang, Zaoyang Lin, Mingxia Wan, Mitsuru Takenaka in the University of Tokyo, and Yukinobu Hikosaka, Ko Nakamura, and Hitoshi Saito in Fujitsu Semiconductor Memory Solution for their cooperations and technical supports

**Thank you very much  
for your kind attention !**

